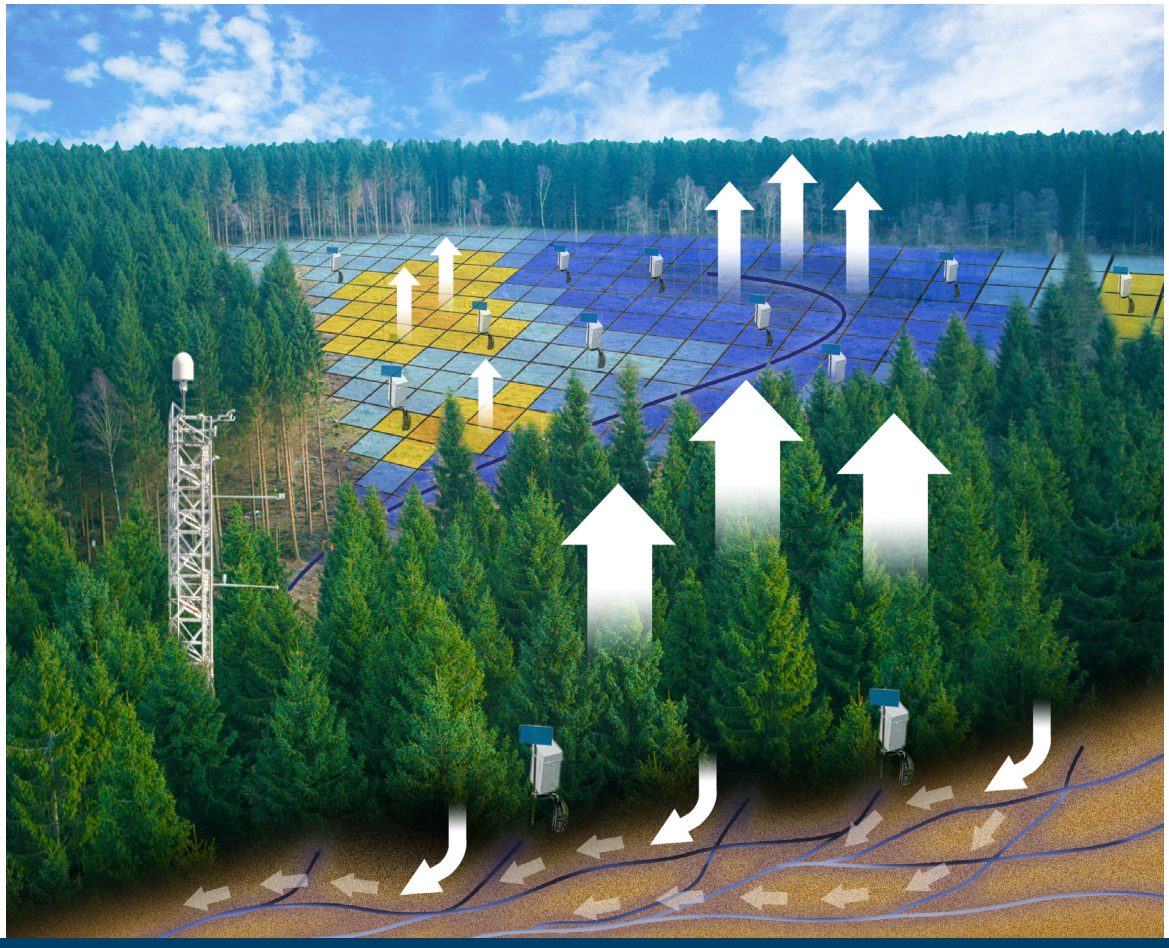

Measuring and modelling spatiotemporal changes in hydrological response after partial deforestation

Inge Wiekenkamp

Energie & Umwelt / Energy & Environment
Band / Volume 519
ISBN 978-3-95806-512-3

Mitglied der Helmholtz-Gemeinschaft

JÜLICH
Forschungszentrum

Schriften des Forschungszentrums Jülich
Reihe Energie & Umwelt / Energy & Environment Band / Volume 519

Forschungszentrum Jülich GmbH
Institut für Bio- und Geowissenschaften
Agrosphäre (IBG-3)

Measuring and modelling spatiotemporal changes in hydrological response after partial deforestation

Inge Wiekenkamp

Schriften des Forschungszentrums Jülich
Reihe Energie & Umwelt / Energy & Environment Band / Volume 519

ISSN 1866-1793 ISBN 978-3-95806-512-3

Bibliografische Information der Deutschen Nationalbibliothek.
Die Deutsche Nationalbibliothek verzeichnet diese Publikation in der
Deutschen Nationalbibliografie; detaillierte Bibliografische Daten
sind im Internet über http://dnb.d-nb.de abrufbar.

Herausgeber und Vertrieb:	Forschungszentrum Jülich GmbH Zentralbibliothek, Verlag 52425 Jülich Tel.: +49 2461 61-5368 Fax: +49 2461 61-6103 zb-publikation@fz-juelich.de www.fz-juelich.de/zb
Umschlaggestaltung:	Grafische Medien, Forschungszentrum Jülich GmbH
Druck:	Grafische Medien, Forschungszentrum Jülich GmbH
Copyright:	Forschungszentrum Jülich 2020

Schriften des Forschungszentrums Jülich
Reihe Energie & Umwelt / Energy & Environment, Band / Volume 519

D 93 (Diss. Stuttgart, Univ., 2020)

ISSN 1866-1793
ISBN 978-3-95806-512-3

Vollständig frei verfügbar über das Publikationsportal des Forschungszentrums Jülich (JuSER)
unter www.fz-juelich.de/zb/openaccess.

Declaration of Authorship

I, Inge WIEKENKAMP, declare that this thesis titled, "Measuring and modelling spatiotemporal changes in hydrological response after partial deforestation" and the work presented in it are my own. Due acknowledgement has been made in the text to all the other works and materials that were used.

Hiermit erkläre ich, Inge WIEKENKAMP, dass diese Arbeit nur meine Originalarbeit umfasst und dass ich die vorliegende Dissertation"Measuring and modelling spatiotemporal changes in hydrological response after partial deforestation"unabhängig geschrieben habe. Alle anderen verwendeten Quellen und Materialien wurden im Text entsprechend anerkannt.

Signed:

Date:

"The matter with human beans,' the big friendly giant went on, 'is that they is absolutely refusing to believe anything unless they is actually seeing it right in front of their own schnozzles."

Roald Dahl - The Big Friendly Giant

Abstract

Vegetation plays an important role in the hydrological cycle, as it governs the partitioning of water fluxes and therewith affects the functioning of the system. Deforestation can cause a highly non-linear response of the natural system and may change the interaction between the land surface and the atmosphere, flow conditions, groundwater recharge and soil moisture storage, which in turn affects the quality and amount of available water resources. To be able to predict changes of deforestation and other land use management activities, there is a need for comprehensive understanding of the hydrological effects of such activities. Although the effects of land use change on hydrology have been studied intensively, predicting the effects of land use change on hydrological states and fluxes remains challenging. Existing paired catchment studies mostly focus on yearly discharge, often do not consider changes in subsurface storage and evapotranspiration, and lack information at the intra-annual time scale. Additionally, soil hydrological processes are often not considered. Thus, only few datasets are available to accurately describe, model, and predict detailed changes in spatiotemporal patterns of hydrological fluxes and states due to land use change.

The aim of this thesis is to improve understanding of the rapid system changes related to deforestation by analysing an innovative dataset and evaluating the predictive ability of a distributed hydrological model. In order to achieve this aim, four steps that represent the individual sub-aims of this project were followed. In the first step, hydrological changes in spatiotemporal fluxes related to partial deforestation measures were defined with a focus on discharge, actual evapotranspiration, and soil moisture. In a second step, the spatial and temporal characteristics of water movement in the vadose zone (piston flow, preferential flow) and the factors that control these processes were assessed. In a third step, changes in spatial and temporal characteristics of water movement in the vadose zone related to partial deforestation were defined. In a final step, the effects of partial deforestation were simulated with a distributed hydrological model (ParFlow-CLM) and were compared with the observed changes to test the predictive ability of the model. For this thesis, data from the Wüstebach catchment established within the TERENO (TERrestrial Environmental Observatories) network in Germany have been used. This catchment provides an unique monitoring setup to investigate the major components of the water balance (evapotranspiration, discharge, precipitation) and the spatiotemporal distribution of

soil moisture before and after a partial deforestation. Given the large amount of previous work, the thesis starts with an overview of the state-of-the-art for investigating the hydrological impact of deforestation and other land use changes with a focus on the impacts on discharge, actual evapotranspiration and soil moisture storage. After evaluating data-driven studies, existing modelling studies are evaluated by comparing the study area characteristics, the applied hydrological models, and the calibration and validation procedures. Next, the study area is introduced and the measurement setup in the Wüstebach catchment is explained in detail. To put this thesis in the context of previous work, the main insights about this catchment obtained in previous studies is also briefly reviewed.

To analyse the hydrological impact of deforestation, five years of measured hydrological data from the Wüstebach catchment were analysed, including all major water budget components three years before and two years after a partial deforestation. A data-driven approach was used to understand changes and related feedback mechanisms in spatiotemporal hydrological response patterns. As expected from earlier studies, it was found that partial deforestation caused a decrease in evapotranspiration and an increase in discharge. A closer look at the high-resolution datasets revealed new insights into the intra-annual variability and relationships between the water balance components. The overall decrease in evapotranspiration caused a large increase in soil water storage in the deforested region, especially during the summer period, which in turn caused an increase in the frequency of high discharge in the same period. Although the evapotranspiration in the forested region was larger on average, the deforested region showed a higher evapotranspiration during part of the summer period on several occasions. This was related to the wetter conditions in the deforested area accompanied with the emergence of grass vegetation. At the same time, wetter soil moisture conditions in the deforested area increased the spatial variance of soil moisture in the summer and therewith altered the relationship between spatial mean and variance. Altogether, this data-based analysis illustrates that detailed spatiotemporal monitoring can provide new insights into the hydrological effects of partial deforestation.

Next, soil moisture sensor response time analysis was used on the 5-year soil moisture monitoring dataset to identify factors that control preferential

and sequential flow before and after partial deforestation. For this, the sensor response times at 5, 20 and 50 cm depth were classified into one of four classes: (1) non-sequential preferential flow, (2) velocity-based preferential flow, (3) sequential flow, and (4) no response. For the three years before deforestation, it was found that the spatial occurrence of preferential flow was governed by small-scale soil and biological features and local processes, and showed no obvious relationship with any of the selected catchment-wide spatial attributes. Event-based occurrence of preferential flow was highly affected by precipitation amount, with a nearly catchment-wide preferential response during large storm events. During intermediate events, preferential flow was controlled by small-scale heterogeneity, instead of showing catchment-wide patterns. The effect of antecedent catchment wetness on the occurrence of preferential flow was generally less profound, although a clear negative relationship between the mean soil moisture content and the percentage of preferential flow was found for precipitation events larger than 25 mm. Overall, the results of this analysis before deforestation demonstrate that sensor response time analysis can offer insights into the spatio-temporal interrelationships of preferential flow occurrence.

In a next step, sensor response time analysis was also applied to the 2-year soil moisture monitoring dataset obtained after partial deforestation to analyse the effects of the partial deforestation on flow conditions in the vadose zone of the Wüstebach catchment. Results of this analysis showed that partial deforestation increased sequential flow occurrence and decreased the occurrence of no flow in the deforested area. Similar precipitation conditions after deforestation caused more sequential flow in the deforested area, which was related to higher antecedent moisture and missing interception. Results of this analysis demonstrated that the combination of a sensor response time analysis and a soil moisture dataset that includes pre- and post-deforestation conditions can offer new insights in preferential and sequential flow conditions after land use change.

In a final step, the five-year long hydrological dataset was used to evaluate the ability of the ParFlow-CLM model to predict hydrological effects of partial deforestation. ParFlow-CLM simulations in the Wüstebach catchment were performed for a three year spin-up period, a three year control period where the entire catchment was forested and a two year post-treatment period, where the hydrological effects of partial deforestation were simulated.

The results showed that ParFlow-CLM did not only capture low and intermediate discharge conditions, but was also able to correctly predict evapotranspiration fluxes in the catchment before and after partial deforestation. Also, observed spatiotemporal soil moisture patterns and post-deforestation related changes were fairly well represented. At the same time, this model evaluation informed about current model limitations that could be improved to obtain even better predictions. Modelling results have shown that the global plant parameterization strategy within CLM 3.5 may not always be directly transferrable to small catchments. Peak flow conditions and observed soil wetness increases after deforestation were underestimated by the model. This could be addressed by improving the soil parameterization and the soil process description (preferential and lateral flow). Overall, the results of this model application in non-stationary conditions clearly illustrate the potential of distributed hydrological models to forecast non-linear system changes.

The thesis concludes with a synthesis of the main outcomes and a discussion of possible future research activities. Overall, the combination of the Wüstebach dataset and the ParFlow-CLM model simulations have provided new hydrological insights in spatiotemporal system changes related to deforestation. Extrapolation of this study to other research areas and other modelling platforms could provide new understanding on the hydrological effects of deforestation and other land use change related activities.

Zusammenfassung

Die Vegetation spielt eine wichtige Rolle im Wasserkreislauf. Sie steuert die Verteilung von Wasserflüssen und wirkt damit auf die Funktionsweise des hydrologischen Systems ein. Abholzung kann zu einer stark nichtlinearen Reaktion des natürlichen Systems führen und damit Veränderungen der Land-Atmosphäre Interaktionen, Fließbedingungen, Grundwasserneubildung und Speicherung von Bodenfeuchtigkeit bedingen. Dies wirkt sich wiederum auf die Qualität und Menge der verfügbaren Wasserressourcen aus. Um hydrologische Veränderungen im Zuge der Entwaldung und anderer Landnutzungsaktivitäten vorhersagen zu können, ist ein umfassendes Verständnis hydrologischer Prozesse erforderlich. Obwohl die Auswirkungen von Landnutzungsänderungen auf die Hydrologie intensiv untersucht wurden, bleibt die Vorhersage der Auswirkungen von Landnutzungsänderungen auf hydrologische Zustände und Flüsse eine Herausforderung. Bisher konzentrieren sich vergleichende Einzugsgebietsstudien vordergründlich auf jährliche Abflüsse, berücksichtigen jedoch keine Veränderungen der unterirdischen Speicher und der Evapotranspiration und können keine Erkenntnisse zu innerjährlichen Abflüssen liefern. Zudem werden bodenhydrologische Prozesse häufig nicht berücksichtigt. Aktuell sind nur wenige Datensätze verfügbar, die Veränderungen der zeitlichen und räumlichen Muster hydrologischer Flüsse und Zustände im Zuge von Landnutzungsänderungen genau beschreiben, modellieren und vorhersagen können.

Das Ziel dieser Arbeit ist es, das Verständnis schneller Systemänderungen im Zusammenhang mit der Entwaldung zu verbessern. Dazu wurde ein innovativer Datensatz analysiert und die Vorhersagefähigkeit eines räumlich verteilten hydrologischen Modells bewertet. Zur Zielerreichung wurden vier Schritte formuliert, welche zugleich die einzelnen Teilziele der Arbeit repräsentieren. Im ersten Schritt wurden hydrologische Veränderungen der raumzeitlichen Flüsse im Zusammenhang mit Teilentwaldungsmaßnahmen definiert. Dabei wurden Schwerpunkte in den Bereichen Abfluss, reale Evapotranspiration und Bodenfeuchtigkeit gesetzt. In einem zweiten Schritt wurden die räumlichen und zeitlichen Eigenschaften der Wasserbewegung in der Vadosen Zone (Piston-Abfluss, präferentieller Abfluss) sowie die damit verbundenen steuernden Faktoren bewertet. In einem dritten Schritt wurden die mit der Teilentwaldung im Zusammenhang stehenden Veränderungen der räumlichen und zeitlichen Eigenschaften des Wasserdurchflusses

in der Vadosen Zone definiert. Im letzten Schritt wurden die Auswirkungen der Teilentwaldung mit einem räumlich verteilten hydrologischen Modell (ParFlow-CLM) simuliert und mit den beobachteten Veränderungen verglichen, um so die Vorhersagefähigkeit des Modells zu testen. Für diese Arbeit wurden Daten aus dem Wüstebach Einzugsgebiet des TERENO-Netzwerks (TERrestrial Environmental Observatories) in Deutschland verwendet. Das Wüstebach Einzugsgebiet bietet ein einzigartiges Messgerät-Setup zur Untersuchung der Hauptkomponenten des Wasserhaushalts (Evapotranspiration, Abfluss, Niederschlag) und der raumzeitlichen Verteilung der Bodenfeuchtigkeit vor und nach der Teilentwaldung. In Anbetracht des großen Umfangs bisheriger Arbeiten wird zunächst ein Überblick über den aktuellen Stand der Forschung bezüglich der hydrologischen Auswirkungen der Entwaldung und anderer Landnutzungsänderungen gegeben, wobei die Effekte auf Abfluss, reale Evapotranspiration und Speicherung der Bodenfeuchte im Fokus stehen. Nach der Auswertung der datengetriebener Studien werden vorhandene Modellierungsstudien über die Eigenschaften der Untersuchungsgebiete, angewandte hydrologische Modelle sowie Kalibrierungs- und Validierungsverfahren miteinander verglichen. Anschließend wird sowohl das Untersuchungsgebiet vorgestellt als auch der Aufbau der Messstationen im Wüstebach Einzugsgebiet erläutert. Die vorliegende Arbeit wird zudem in den Kontext früherer Arbeiten aus dem Wüstebach Einzugsgebiet gesetzt, indem die wichtigsten Erkenntnisse vergangener Studien betrachtet werden.

Die Analyse der hydrologischen Auswirkungen der Entwaldung wurde mittels hydrologischer Daten aus fünf Jahren Messung im Wüstebach Einzugsgebiet durchgeführt. Darin einbezogen sind sowohl alle wichtigen Wasserhaushaltskomponenten drei Jahre vor und zwei Jahre nach der Teilentwaldung. Zur Erlangung eines Verständnisses bezüglich der hydrologischen Veränderungen und der damit verbundenen Rückkopplungsmechanismen in raumzeitlichen hydrologischen Reaktionsmustern wurde ein datengetriebener Ansatz verwendet. In Übereinstimmung mit den Ergebnissen früherer Studien wurde festgestellt, dass eine Teilentwaldung zu einer Abnahme der Evapotranspiration und zu einer Zunahme des Abflusses führt. Ein genauerer Blick auf die hochauflösenden Datensätze ergab neue Erkenntnisse über die innerjährliche Variabilität und die Beziehungen zwischen den einzelnen Komponenten des Wasserhaushalts. Die insgesamt geringere Evapotranspiration

bewirkte einen starken Anstieg der Bodenwasserspeicherung in der abgeholzten Region, insbesondere in den Sommermonaten, was wiederum zu einer Zunahme der Häufigkeit hoher Abflüsse im selben Zeitraum führte. Obwohl die Evapotranspiration in der bewaldeten Region im Durchschnitt höher war, wies die abgeholzte Region mehrmals eine höhere Evapotranspiration während eines Teils der Sommerperiode auf. Dies hing mit den feuchteren Bedingungen im abgeholzten Gebiet zusammen, einhergehend mit der Entstehung von Grasvegetation. Gleichzeitig erhöhten feuchtere Bodenverhältnisse im abgeholzten Gebiet im Sommer die räumliche Varianz der Bodenfeuchtigkeit und veränderten damit das Verhältnis zwischen räumlichem Mittelwert und Varianz. Insgesamt zeigt datenbasierte Analyse, dass eine detaillierte raumzeitliche Überwachung neue Erkenntnisse über die hydrologischen Auswirkungen der Teilentwaldung liefern kann.

Danach wurde eine Analyse zur Reaktionszeit der Bodenfeuchtigkeitssensoren für den zugehörigen Fünf-Jahres-Datensatz durchgeführt. Die Analyse zielte darauf ab, Faktoren zu identifizieren, die den präferentiellen und sequenziellen Abfluss vor und nach der Teilentwaldung steuern. Dazu wurden die Sensorreaktionszeiten in 5, 20 und 50 cm Tiefe in eine von vier Klassen eingeteilt: (1) nicht sequentieller präferentieller Abfluss, (2) geschwindigkeitsbezogener präferentieller Abfluss, (3) sequentieller Abfluss und (4) keine Reaktion. In den drei Jahren vor der Entwaldung wurde festgestellt, dass das räumliche Vorkommen des präferentiellen Abflusses von kleinräumigen Boden- und biologischen Merkmalen sowie lokalen Prozessen abhängt und keine eindeutige Beziehung zu den ausgewählten räumlichen Attributen aufweist. Das ereignisbasierte Auftreten von präferentiellem Abfluss wurde im hohen Maße von der Niederschlagsmenge beeinflusst. Dabei war bei hohen Niederschlagsereignissen fast im gesamten Einzugsgebiet eine präferentielle Reaktion zu verzeichnen. Während mittlerer Niederschlagsereignisse wurde der präferentielle Abfluss dahingegen durch kleinräumige Heterogenität gesteuert und wies keine großräumigen Muster im Einzugsgebiet auf. Die Auswirkung des bereits bestehenden Bodenfeuchtegehalts auf das Auftreten des präferentiellen Abflusses war im Allgemeinen weniger ausgeprägt. Trotzdem wurde ein eindeutiger negativer Zusammenhang zwischen dem mittleren Bodenfeuchtegehalt und dem Prozentsatz des präferentiellen Abflusses bei Niederschlagsereignissen größer als 25 mm festgestellt. Insgesamt zeigen die Ergebnisse vor der Entwaldung, dass die Analyse der

Sensorreaktionszeit Einblicke in die raumzeitlichen Zusammenhänge des Auftretens präferentiellen Abflusses bieten kann.

In einem nächsten Schritt wurde die Analyse der Sensorreaktionszeit auch auf den 2-Jahres-Datensatz nach der Teilentwaldung angewendet. Die Analyse hatte zum Ziel die Auswirkungen der Teilentwaldung auf die Abflussbedingungen in der Vadosen Zone des Wüstebach Einzugsgebiets zu analysieren. Die Ergebnisse zeigten, dass die Teilentwaldung das Auftreten von sequentiellem Abfluss erhöhte und das Auftreten von keiner Reaktion im abgeholzten Gebiet verringerte. Vergleichbare Niederschlagsbedingungen nach der Entwaldung bewirkten mehr sequentiellen Abfluss im abgeholzten Gebiet. Dies hängt mit einer höheren vorausgehenden Bodenfeuchtigkeit und der fehlenden Interzeption zusammen. Die Ergebnisse zeigten, dass die Kombination aus einer Analyse von Sensorreaktionszeiten und Bodenfeuchtedatensatz, der die Bedingungen vor und nach der Entwaldung umfasst, neue Erkenntnisse über präferentiellen und sequentiellen Abfluss im Zuge von Landnutzungsänderungen liefern kann.

Im letzten Schritt wurde der Fünf-Jahres-Datensatz verwendet, um die Fähigkeit des ParFlow-CLM-Modells zu bewerten, die hydrologischen Auswirkungen der Teilentwaldung im Wüstebach Einzugsgebiet vorherzusagen. Für das Einschwingen des ParFlow-CLM Models wurde eine Simulation von drei Jahren durchgeführt. Danach wurde sowohl eine dreijährige Simulation für den Zeitraum des vollständig bewaldeten Einzugsgebiets als auch eine zweijährige Simulation für den Zeitraum nach der Teilentwaldung durchgeführt. Die Ergebnisse zeigten, dass ParFlow-CLM nicht nur realistische niedrige und mittlere Abflussbedingungen abbilden kann, sondern auch die Evapotranspiration im Einzugsgebiet vor und nach der Teilentwaldung genau vorhersagen kann. Daneben konnte das Modell die beobachteten raumzeitlichen Bodenfeuchtemuster sowie die entwaldungsbedingten Veränderungen gut reproduzieren. Gleichzeitig offenbarte die Auswertung des Modells einige Einschränkungen, deren Überbrückung die Vorhersagen weiter verbessern könnten. In CLM 3.5 ist die globale Strategie der Pflanzenparametrisierung möglicherweise nicht immer direkt auf kleine Einzugsgebiete übertragbar. Die maximalen Abflussbedingungen und die beobachtete Zunahme der Bodenfeuchte nach der Entwaldung wurden vom Modell unterschätzt. Dies könnte durch die Verbesserung der Bodenparametrisierung und der

Beschreibung der Bodenprozesse (präferentieller und lateraler Abfluss) erreicht werden. Insgesamt zeigen die Ergebnisse unter nicht-stationären Bedingungen ein deutliches Potential verteilter hydrologischer Modelle zur Vorhersage nichtlinearer Systemänderungen.

Die Arbeit schließt mit einer Synthese der zentralen Ergebnisse sowie einer Diskussion über mögliche zukünftige Forschungsaktivitäten. Insgesamt hat die Kombination aus Wüstbach Datensatz und ParFlow-CLM-Modellsimulationen neue hydrologische Erkenntnisse zu raumzeitlichen Systemveränderungen im Zusammenhang mit der Entwaldung geliefert. Die Extrapolation dieser Studie auf andere Forschungsbereiche und andere Modellierungsplattformen könnte neue Erkenntnisse über die hydrologischen Auswirkungen der Entwaldung und anderer Landnutzungsänderungen hervorbringen.

Acknowledgements

The last note has been played. My thesis is finally finished. Clearly, no symphony can be played alone, and therefore I would like to express my gratitude to all people that have been involved in my work during the last years.

This thesis has been like the performance of a symphony, including its staccatos and allegros, and could not have been played without the help of two experienced conductors, a concertmaster, and a handful of important solo players. First and foremost, I would like to thank my direct supervisors Prof. Huisman and Dr. Bogena for their time, discussions, guidance, encouragement and patience during the last years. Thank you so much for all that you have done for me! I would furthermore like to extend my sincere thanks to Harry Vereecken, the director of the IBG-3, for all his support he has provided in the last years. I'd also like to extend my gratitude to Prof. Henry Lin for his discussions on hydropedology-related topics, and for his support during my stay at Penn State University. I would also like to thank Dr. Alexander Graf, Dr. Clemens Drüe and Marius Schmidt, who have provided a lot of assistance with the preparation and evaluation of the climate station and eddy covariance data. I also very much appreciate the support that Dr. Roland Bol has provided during the different stages of my thesis. I have enjoyed our collaboration. I also would like to express my deepest appreciation to the two additional committee members, Prof. Breuer and Prof Bárdossy for their time and effort in reviewing my PhD thesis.

Any symphony to be played requires instruments and musicians from all different orchestra sections, with each section providing an essential contribution to the symphony. This research presented in this thesis could not have been possible without the support of TERENO (Terrestrial ENvironmental Observatories), who provided the measurement infrastructure required to obtain the Wüstebach dataset that is presented in this thesis. Clearly, this thesis would have not been possible without any the IBG-3 technicians that have worked in the Wüstebach catchment. I'm deeply indebted to all of them and wish to give my special gratitude to Ansgar Weuthen, Bernd Schilling, Rainer Harms, Ferdinand Engels, Odilia Esser, Daniel Dolfus and Normen Hermes. Thanks should also go to Ralf Kunkel, who provided support for the online TEODOOR portal, where all (quality-checked) Wüstebach datasets are stored. Valuable advice and contributions to the presented Parflow-CLM simulations were made by Prof. Kollet, Dr. Sebastian Gebler, Fabian Gasper,

Horst Hardelauf and Dorina Baatz. I also want to thank all people involved in the Wüstebach soil sampling campaigns, who have helped to obtained a very large soil dataset for the Wüstebach research area. I would like to extend my sincere thanks to my main room-mates in the institute Dr. Christian von Hebel, Dr. Laura Gangi for the extesive Matlab and R discussions, but mostly for being my true friends. I also wish to thank Martine Kettler, Dr. Youri Rothfuss, Dr. Anna Missong, Marius Schmidt, Dr. Christian von Hebel, Dr. Frank Hermann and Ferdinand Engels for offering me a seat in their car and for having lots of conversations on the road to the research center. Special thanks go to all my collegues that joined me for lunch, walks, talks and many other activities that have made my time at the institute more colourfull. I furthermore wish to thank all other IBG-3 staff members, summer school and seminar participants and organizers, and all conference participants and organizers, that I have been connected to in the last years.

Music is not only made inside the concert hall. Every note that is played requires years of practice and a heart full of emotions. With all my heart, I want to thank my friends and family in Germany and the Netherlands for their moral support, patience and for playing a vital role in my life. Ronald en Janet en Melchior: zonder jullie was ik nooit zo ver gekomen. Finally, my dearest Daniel and Yuna: you give colour to the music in my life.

Contents

List of Figures

List of Tables

List of Abbreviations

ACW	antecedent catchment wetness
A.D.	after the (partial) deforestation
ANN	Artificial Neural Networks
BACI	Before-After-Control-Impact
B.D.	before the (partial) deforestation
CAOS	Catchments As Organized Systems
CET	Central European Time
CLM	Community Land Model
COSMO	Consortium for Small Scale Modelling (DWD)
CRNP	Cosmic-Ray Neutron Probe
CZO	Critical Zone Observatories
DEM	Digital Elevation Model
DOC	Dissolved Organic Carbon
DWD	Deutscher Wetterdienst (German Weather Service)
EC	Eddy Covariance
EC_a	actual Electrical Conductivity
Emb	error(s) in the mass balance
EMI	Electro- Magnetic Induction
Ev	error in the volume
Ewb	error(s) in the water balance
ERT	Electrical Resistivity Tomography
ET	evapotranspiration
FAO	Food and Agriculture Organization of the United Nations
FDC	Flow Duration Curve
GPR	Ground Penetrating Radar
GW	groundwater
HOBE	Hydrological Observatory—Skjern Catchment
HRU	hydrological response unit
HY	hydrological year
KGE	Kling-Gupta Efficiency
KGE_{np}	non-parametric Kling-Gupta Efficiency
IST	Index of Time Stability

LAI	Leaf Area Index
LTER	Long-Term Ecosystem Research
MAE	mean absolute error
MAP	mean annual precipitation
MBE	mean bias error
MSE	mean squared error
MGCG	multigrid preconditioned conjugate gradient (method)
MRD	mean relative difference
NCAR	National Center for Atmospheric Research
NSE	Nash–Sutcliffe efficiency
Pearson R	Pearson correlation coefficient
PFT	Plant Fuctional Type
PR	performance rating
RMSE	root mean square error
SAI	Stem Area Index
SM	Soil Moisture
SDRD	standard deviation of the relative difference
SSWR	squared sum of weighted residuals
Spearman R	Spearman rank correlation coefficient
TDR	Time Domain Reflectometry
TERENO	TERestrial ENvironmental Observatories
TerrSysMP	Terrestrial System Modelling Platform

List of Symbols

A	leaf photosynthesis	$\mu molCO_2 m^2/s$
b_p	minimal stomatal conductance	μmol m^{-2} s^{-1}
$C.I.$	confidence interval	
C_v	turbulent transfer coefficient	0.01 $m/s^{-1/2}$
Cv_θ	coefficient of variation in soil moisture	vol. %
c_s	leaf surface's CO_2 concentration	Pa
c_p	air specific heat capacity (constant P)	$1.013 \cdot 10^3 JK^{-1}kg^{-1}$
d_{leaf}	leaf dimension (wind flow direction)	m
e_{ls}	vapour pressure at leaf surface	Pa
e_{li}	saturation vapour pressure inside leaf	Pa
e_s	saturation vapour pressure	Pa
e	actual vapour pressure	Pa
E_g	ground evaporation	m/s
E_i	evaporation of intercepted water	m/s
ET_0	potential evapotranspiration	m/s
ET_a	actual evapotranspiration	m/s
ET_ad	actual evapotranspiration (deforested area)	m/s
ET_af	actual evapotranspiration (forested area)	m/s
ET_am	actual evapotranspiration (area averaged)	m/s
f_d	fraction of dry leaves	-
f_{sno}	fraction of snow covered soil	-
f_w	fraction of wet leaves	-
G	ground heat flux	W/m^2
h	lag distance (semivariance equation)	-
K_s	hydraulic conductivity	m/s
K_r	relative permeability	-
LAI	leaf area index	-
LAI_{sha}	leaf area index of shaded leaves	-
LAI_{sun}	leaf area index of sunlit leaves	-
m'	interfacial thickness (ParFlow model)	m
m_p	empirical parameter slope of Ball-Berry eq.	-

N	amount of measurements	-
n_c	curvature of Choudhury's function	-
n_m	Manning's coefficient	$(s/m)^{-1/3}$
n_{mvg}	n parameter - Mualem - van Genuchten eq.	-
Obs	observed data	[unit of obs. data]
P	precipitation	m/s
P_{rain}	incoming precipitation from rainfall	m/s
P_{sno}	incoming precipitation from snow	m/s
Q	discharge	m/s
q	volume specific Darcy flux	m^3/s
q_{atm}	specific air humidity (atmoshpere)	kg (vapor)/kg (air)
q_e	water flux (surface - subsurface)	m/s
q_c	spec. humidity within the canopy	kg (vapor)/kg (air)
$q_{csat,T}$	satur. specific humidity at veg. Temp.	kg (vapor)/kg (air)
q_g	specific air humidity (surface)	kg (vapor)/kg (air)
q_r	general sink term ParFlow (e.g P/ ET)	s^{-1}
q_s	source/ sink term (pumping/injection)	s^{-1}
R^2	coefficient of determination	-
R_n	net radiation	W/m^2
R_s	Spearman rank correlation coefficient	-
r_a	aerodynamic resistance	s/m
r_b	leaf boundary layer resistance	s/m
r_i	fraction of roots in layer i	-
r_d''	actual T_{pot} fract. (to calc. T in CLM 3.5)	-
r_s	stomatal resistance	s/m *or* s m^2 μmol $^{-1}$
$r_{s,sha}$	stomatal resistance of shaded leaves	s m^2 μmol $^{-1}$
$r_{s,sun}$	stomatal resistance of sunlit leaves	s m^2 μmol $^{-1}$
r_{soil}	soil resistance	s/m
SAI	stem area index	-
Sim	simulated data	[unit of sim. data]
S_s	specific storage coefficient	m^{-1}
S_{snow}	snow storage	m^3
S_w	relative saturation	-
s_1	soil moisture term	-
T	transpiration	mm
T_a	minimum amount of precipitation	m/s
T_p	period without rain	h
T_{pot}	potential transpiration	m/s

U_{av}	leaf friction velocity	m/s
t	time (step)	s
$\vec{v}$	depth averaged velocity vector	m/s
w	plant available water coefficient	-
w_i	plant wilting factor for layer i (CLM 3.5)	-
wv	vertical wind component	m/s
z	vertical downward position	m
α	inverse air entry suction (Mualem-van Genuchten)	m-1
α_{np}	the absolute error of the flow duration curve	m-1
β_{np}	bias in the discharge volume	[unit of variable]
β_t	soil wetness index	-
γ	psychrometric constant	P/K
γ_s	semivariance	[unit of variable]^2
Δ	saturation vapour pressure curve over Temp.	Pa/K
ΔGW	change in groundwater	mm
ΔS	change in storage	m/s
λ	latent heat vapourization	$2.45 \cdot 10^6 J/kg$
θ	soil moisture content	vol. %
θ_{sat}	saturated water content	vol. %
θ_{ice}	volumetric water content of the ice fraction	vol. %
θ_{liq}	volumentric water content of the water fraction	vol. %
$< \theta >$	mean soil moisture content	vol. %
ρ_{atm}	air density (atmosphere)	kg/m^3
σ_θ	standard deviation of soil moisture content	vol. %
ϕ	porosity	-
Ψ_m	matrix potential (pressure head unsat. soil)	m
ψ	surface pressure head	m
ψ_{open}	soil matric potential (opened stomata)	m
ψ_{closed}	soil matric potential (closed stomata)	m
ψ_p	subsurface pressure head	m
∇	nabla operator	m^{-1}

Chapter 1

Introduction

"The hydrological cycle is increasingly affected by changes, many of them triggered by humans, which extend from the local to global scales, act on short to decadal timescales, affect all characteristics of water-related dynamics (mean, variability, extremes), and extend over the atmosphere, critical zone (boundary layer), groundwater, lakes, rivers and oceans" (Ehret et al., 2014).

Hydrology studies the movement of water in our terrestrial system. It is a highly complex research field with a manifold of challenges that are rooted in the high variability of hydrological processes in time and space and the resulting difficulty to capture these processes quantitatively. In our modern era, we are faced with additional complexity, as climate change and rapid land use conversion are increasingly affecting hydrological systems (Wagener et al., 2010; Sivapalan et al., 2012; Ehret et al., 2014). This has further increased the need to provide high-quality predictions on the direction and magnitude of the hydrological impacts of such changes. One of the main challenges related to this need is that the future states and fluxes of such non-stationary systems are not described by past observations. In hydrology, understanding the impacts of such drastic changes can be complex, as the interdependent system dynamics (e.g. discharge, evapotranspiration) and storages (e.g. soil water storage, groundwater storage) are affected simultaneously.

One of such drastic system changes is the removal of forest (deforestation), which can highly disturb the functioning of hydrological systems (e.g. Hewlett, 1961; Bosch and Hewlett, 1982; Brown et al., 2005; Brown et al., 2013). Important forest-related processes, such as plant transpiration, root water uptake, and infiltration affect the water fluxes aboveground and beneath the subsurface (Figure 1.1). The canopy redistributes incoming precipitation via interception, crown drip, stem flow and direct throughfall. Trees

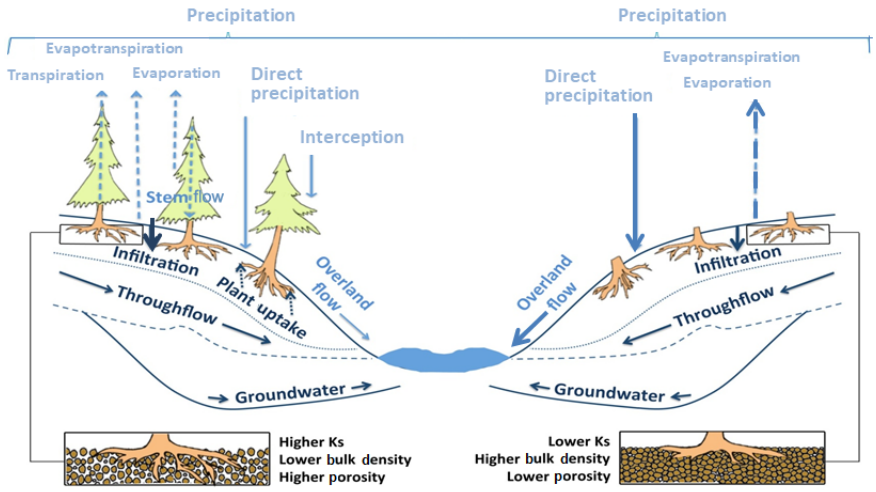

FIGURE 1.1: Expected hydrological changes (fluxes and properties) related to deforestation activities. The left side of the figure shows the original hydrological system for a forested catchment (with interception, transpiration, stemflow, root water uptake). The right side of the figure shows the deforested conditions, with altered fluxes (overland flow, infiltration, evapotranspiration). On the bottom of the figure, potential changes in soil properties are shown.

can additionally re-enrich the atmosphere with water vapor via transpiration, where water is evaporated via the leaves into the atmosphere (Jasechko et al., 2013). The water required for transpiration is provided by root water uptake, which in turn affects the total storage and the spatial distribution of water in the vadose zone (Bouten et al., 1992; Bouten, 1995; Vereecken et al., 2008; Rosenbaum et al., 2012).

Deforestation can significantly affect the hydrological regime of a system by altering or removing part of the processes that are steered by the vegetation (such as interception, transpiration and root water uptake; Figure 1.1). At the same time, deforestation can also affect soil properties, which in turn affect the general movement of water through the subsurface. Current knowledge on the hydrological effects of deforestation originates largely from paired catchment studies, and is mainly focused on the influence of deforestation and afforestation on the annual water balance (Bosch and Hewlett, 1982; Best et al., 2003; Andréassian, 2004; Oudin et al., 2008). The most important findings of these studies can be summarized by the following seven statements:

1. A reduction in forest cover generally increases the water yield whereas afforestation of a sparsely vegetated area decreases the water yield (Hibbert, 1967; Bosch and Hewlett, 1982).

2. A reduction in forest cover of less than 20 % will not lead to detectable changes in measured streamflow (Bosch and Hewlett, 1982; Stednick, 1996).

3. Changes in discharge related to deforestation depend on the precipitation characteristics of a catchment. The largest changes in streamflow that were caused by deforestation occurred in areas with a large amount of precipitation (Bosch and Hewlett, 1982)

4. Changes in forest cover affect the volume and timing of flood events, but the magnitude of change is highly variable (McGuinness and Harrold, 1971; Troendle and King, 1985; Hornbeck et al., 1993; Rogger et al., 2017).

5. Afforestation decreases low flows and deforestation increases low flows (Johnson, 1998)

6. The resilience of a hydrological system to deforestation practices depends on species composition and climate conditions (Jones and Post, 2004; Brown et al., 2005)

7. The type and severity of processes affected by deforestation are highly dependent on the considered time scale (Andréassian, 2004; Nijzink et al., 2016).

These statements illustrate the current state of research in this field, where generalizations can only be made up to a certain degree (e.g. statement 1) and large uncertainties and gaps remain (e.g. statement 4, 6 and 7). Therefore, the hydrological impacts of deforestation are still frequently debated in the hydrological community (Oudin et al., 2008; Zhou et al., 2015; Wang et al., 2016). Clearly, the effects on hydrological functioning are acknowledged, but it remains unclear how certain parts of the system are affected on different temporal and spatial scales and how these changes act together.

1.1 Limitations of Forest Hydrological Research

"Qualitatively, to understand the behaviour of a complex system, we must understand not only the behaviour of the parts but also how they act together to form the behaviour of the whole" (Sivakumar, 2017).

Hydrological processes take place at a variety of scales both in time and in space (Figure 1.2; Blöschl and Sivapalan, 1995; Sivapalan, 2003; Skøien et al., 2003; Western et al., 2004; Blöschl et al., 2013). The spatial and temporal dynamics of hydrological processes are mostly governed by the interactions between the atmosphere (climate conditions) and the land surface, which is directly affected by vegetation and thus by deforestation. The removal of vegetation in a catchment can cause the hydrological system to shift from a stationary system, where variables fluctuate within a certain "envelope of variability" to a system with nonstationarity, where the system changes its flow characteristics, resulting in a change of mean and extreme states and fluxes (Clarke, 2007; Bayazit, 2015). A crucial question remains whether nonstationary changes can be predicted accurately with the current status of process understanding and the developed models (Semenova and Beven, 2015; Nijzink et al., 2016; Pathiraja et al., 2016; Savenije and Hrachowitz, 2017).

To provide a better understanding of the research needed in forest hydrological research, I would like to highlight four key limitations in forest hydrological research.

1. *Deforestation studies have mainly focused on discharge.*

A large database with paired and single catchment studies has been created in previous decades (Andréassian, 2004; Oudin et al., 2008; Brown et al., 2013). Well-known examples of such paired catchments studies were performed in Fernow (Patric and Reinhart, 1971), Marcell Experimental Forest (Sebestyen and Verry, 2011), Hubbard Brook (Hornbeck et al., 1970), Leading Ridge (Hornbeck et al., 1993), and Coweeta (Webster et al., 1992). Although highly relevant, a limitation of these paired catchment studies is that most of them only considered precipitation and discharge time series, and did not provide information on changes in subsurface storage and actual evapotranspiration. At the same time, available studies on the effects of deforestation

on actual evapotranspiration typically do not consider the entire water balance (Calder, 1990; Montes-Helu et al., 2009; Teuling et al., 2013), and quantifications of changes in actual evapotranspiration are limited (Hirano et al., 2017).

2. *Deforestation studies mostly do not provide sufficient details on changes in soil hydrological processes.*

Soil hydrological processes are typically observed at a small scale (plot/hillslope) and with a short time interval (minute – daily). They are of crucial importance to understand water exchange between the atmosphere (e.g Teuling et al., 2006; Teuling, 2007) and the land surface (e.g. high and low flow conditions; Weill et al., 2011; Ghasemizade and Schirmer, 2013; Pan et al., 2015). Land use is considered as one of the dominant factors determining the movement of water in the vadose zone. Interesting examples of studies that focus on the effects of vegetation on subsurface states and fluxes are provided by van Schaik (2009), Ivanov et al. (2010), Alaoui et al. (2011) and Acharya et al. (2017). Despite previous research, our knowledge on the effect of vegetation on soil hydrological processes, such as interflow (subsurface stormflow), (deep) percolation, preferential (macropore) flow, and groundwater flow remains limited.

3. *Datasets in deforestation studies typically have a low temporal resolution.*

Generally, classical paired catchment studies mainly focused on short term (< 20 years; Figure 1.2) annual changes in discharge for relatively small catchments (< 1 km^2; Figure 1.2) (Hewlett and Pienaar, 1973; Bosch and Hewlett, 1982; Brown et al., 2005; Oudin et al., 2008). The impact of land use change was shown to be unstable over time (Hornbeck et al., 1993; Andréassian, 2004), which complicates the generalization of such studies. Changes in intra-annual discharge (monthly/ daily) have been evaluated less frequently (Wahl et al., 2005; Jackson et al., 2008; Green and Alila, 2012; Brown et al., 2013). Here, the results with respect to the expected impact of land use change on the frequency of low and high flow conditions are controversial (Ahn and Merwade, 2017; Rogger et al., 2017).

4. *Deforestation studies lack high resolution datasets for model validation.*

Modelling studies aiming to represent hydrological changes due to land use change have evolved from purely predictive studies (Bultot et al., 1990) to

more sophisticated approaches in which uncertainties in measurements (Eckhardt et al., 2003; Huisman et al., 2004), model structure (Breuer et al., 2009; Jung et al., 2011; Cornelissen et al., 2013; Morán-Tejeda et al., 2015), and model parameters (Hundecha and Bárdossy, 2004; Brath et al., 2006; Breuer et al., 2006; Jung et al., 2011) have been considered. Despite this progress, many of such modelling studies are still limited by the lack of extensive validation of spatially distributed model predictions before and, more importantly, after land use and management change (DeFries and Eshleman, 2004; Jackson et al., 2008; Huisman et al., 2009; Beven, 2012). Clearly, there is a need for more comprehensive datasets that capture how land use change affects the spatiotemporal dynamics of hydrological states and fluxes within catchments in order to increase the predictability of hydrological responses to land use and management change. However, only a limited amount of highly instrumented catchments are currently available to provide such detailed information (Guo and Lin, 2016).

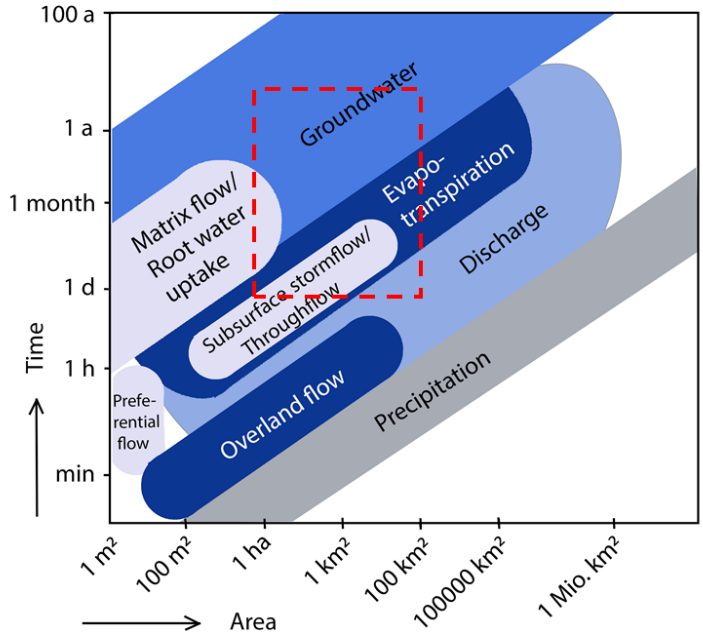

FIGURE 1.2: Hydrological processes in time and space and characteristic scales for forest hydrological research (in red). Figure is based on Blöschl and Sivapalan (1995) and Van Loon (2015).

There are several reasons for the imbalance in information at different spatial and temporal scales (e.g. discharge vs. evapotranspiration; annual fluxes vs. high and low flow conditions). First of all, the setup of many observation networks is mainly focused on a single subsystem (e.g. vadose zone, atmosphere layers, etc. Bogena et al., 2017). Second, more complex measurement infrastructures come with scaling problems, data storage issues, high instrumentation costs, and high labor requirements. Third, there is still no consensus on how to combine the variety of hydrological processes that take place at different spatial and temporal scales for hydrological forecasting. Currently, there are, for example, still no clear concepts on how to upscale small-scale subsurface processes (e.g. preferential flow) to the catchment scale.

1.2 Thesis Objectives and Structure

In the previous section, I have argued that deforestation studies mostly lack detailed spatiotemporal observations that are essential to provide better insights in changes in hydrological processes. Innovative measurement setups and high-resolution observations are crucial for improved forecasting in a world that is changing rapidly. Within this context, the overall objective of this thesis is to use innovative observations combined with distributed hydrological modelling to provide new insight in spatiotemporal changes in hydrological processes that are caused by deforestation measures. In order to address this general objective, four sub-objectives have been formulated:

1. To quantify hydrological changes in spatiotemporal fluxes related to partial deforestation measures with a focus on discharge, actual evapotranspiration, and soil moisture.

2. To determine the spatial and temporal characteristics of water movement in the vadose zone (piston flow, preferential flow) and to identify factors that control these processes.

3. To determine changes in spatial and temporal characteristics of water movement in the vadose zone related to partial deforestation.

4. To simulate the effects of partial deforestation with a distributed hydrological model (ParFlow-CLM) and test the predictive ability of the model by comparing the simulated results with observed changes.

To reach these aims, this thesis relies on data from the TERENO test site Wüstebach. This monitoring site provides a unique high-resolution spatiotemporal dataset before and after deforestation. The dataset includes measurements of states and fluxes for multiple zones in the hydrological system (Bogena et al., 2015), including a wireless soil moisture sensor network, eddy covariance towers to determine actual evapotranspiration, precipitation, and discharge stations.

The remainder of this thesis is organized as follows. Chapter 2 provides a more detailed overview of the state-of-the-art in deforestation/vegetation manipulation studies. The measurement setup in the Wüstebach catchment and the details of the deforestation experiment are described in Chapter 3. Chapter 4 focusses on the spatiotemporal analysis of different water budget components before and after deforestation (sub-aim 1). The analysed dataset includes five years of measured soil moisture data, evapotranspiration data, discharge data and precipitation data with 3 years before and 2 years after the partial deforestation. Chapter 5 and 6 are focused on water movement in the unsaturated (vadose) zone of the Wüstebach catchment before and after deforestation, respectively. Chapter 5 describes how high-resolution soil moisture measurements can be used to detect preferential flow occurrence in time and space (sub-aim 2). In particular, soil moisture sensor response times (Lin and Zhou, 2008; Graham and Lin, 2011; Hardie et al., 2013; Liu and Lin, 2015) are used to determine the dominant controls on preferential flow in space and time. In a second step, Chapter 6 uses the analysis workflow developed in Chapter 5 to analyse how soil moisture sensor response times and preferential and sequential flow occurrence are affected by deforestation (sub-aim 3). Chapter 7 evaluates the capability of the integrated hydrological framework TerrSysMP to predict spatiotemporal changes associated with deforestation (sub-aim 4). This chapter combines the key monitoring results from the partial deforestation experiment (Chapter 4) with modelling results from the TerrSysMP framework. Finally, Chapter 8 synthesizes the results of this thesis and provides an outlook with future research perspectives.

Chapter 2

State-of-the-Art in Hydrological Land Use Change Studies in the Temperate Forest Biome

"By its nature, science is forward looking but there is no sounder basis for future development than critical recognition of the legacy of the past" (McCulloch, 2007).

The impact of afforestation, deforestation and other land use changes on hydrological processes is a topic that has already been studied since the beginning of the antiquity. One of the first descriptions of the potentially disastrous consequences of deforestation on hydrology was already reported by Pliny the Elder in the first century AD (Andréassian, 2004). Many centuries later in 1902, one of the first paired catchment experiments was carried out in the Emmental region (Switzerland) to understand the effects of deforestation on sediment transport and flood flows in mountainous areas (Swank et al., 1994). In 1909, the first paired catchment experiments were carried out in the United States of America (Southeast Colorado, USA) with the aim to evaluate the effects of deforestation on streamflow, erosion and sediment transport (Andréassian, 2004; Bosch and Hewlett, 1982; Zégre, 2008).

Since these first catchment-scale experiments, more and more research has focused on understanding the effects of vegetation change on catchment hydrology. A large variety of review studies have evaluated the effects of land use change on the hydrology, focusing either on experimental studies (e.g. Hibbert, 1967; Bosch and Hewlett, 1982; Bruijnzeel, 1990; Hornbeck et al., 1993; Sahin and Hall, 1996; Best et al., 2003; Andréassian, 2004; Brown et al., 2005; Farley et al., 2005; D'Almeida et al., 2007; Filoso et al., 2017; Rogger et al., 2017), or modelling studies (e.g. Dwarakish and Ganasri, 2015; Krysanova and Arnold, 2008; Chen et al., 2015; Ma et al., 2016). Although

these reviews cover a wide range of scales, measurement techniques, and modelling approaches, they also show clear tendencies for preferred measurement and modelling approaches and preferred scales. Most experimental studies have a focus on the short-term effects of vegetation change (often deforestation) on streamflow (e.g. first five years; Hibbert, 1967; Bosch and Hewlett, 1982). Existing reviews therefore mostly focus on paired catchment studies that evaluate discharge changes, while leaving most other hydrological fluxes out. At the same time, almost none of the existing reviews compare and combine the existing knowledge from experimental and modelling studies to look at contradictions and agreements in obtained knowledge. Currently, there is only one state-of-the-art review paper that combines experimental and modelling studies to provide an overview for ecohydrological research (Asbjornsen et al., 2011). This review, however, focusses on identifying general cross cutting themes and remaining challenges that exist within the field, and does not have a focus on deforestation or land use change. A mixed review with a focus on hydrological modelling and experimental land use change studies is not yet available. Such a combined assessment may, however provide additional insights on similarities and differences between observed and modelled changes in hydrological fluxes, missing links between the work of hydrological modelers and experimentalists, and thus suggest possible ways forward.

This chapter summarizes progress in experimental and modelling studies dealing with the hydrological impact of land use change in the temperate forest biome with a focus on deforestation and afforestation. This review focusses on forest hydrological research in the temperate zone for two reasons. First and foremost, work in this thesis is carried out in the Wüstebach catchment, which is a forested catchment located in the temperate climate zone (see Chapter 3 for more details). Second, most catchment hydrology and deforestation studies have been performed in the temperate region. From the experimental point of view, this review will provide an overview of the variety of methods that have been used to investigate the hydrological effects of land use change at different scales in the different compartments of the hydrological system (atmosphere, surface, subsurface). In the case of modelling studies, this review summarizes knowledge gained from hydrological simulation studies and its subsequent evaluation methods. Specific attention is given to the data sources used for model evaluation.

2.1 The Temperate Forest Biome

The temperate region is a climate zone characterized by substantial precipitation and moderate temperature. According to Köppen (1884), the temperate climate zone (class C) is represented by regions that have moderate monthly average temperatures (10 to 20 °C) for at least four months, and high monthly average temperatures (>20 °C) for not more than four months. In this type of climate, sufficient water is available in most months. In addition, the potential evapotranspiration does not exceed actual evapotranspiration, which implies that solar radiation often is the limiting factor for evapotranspiration.

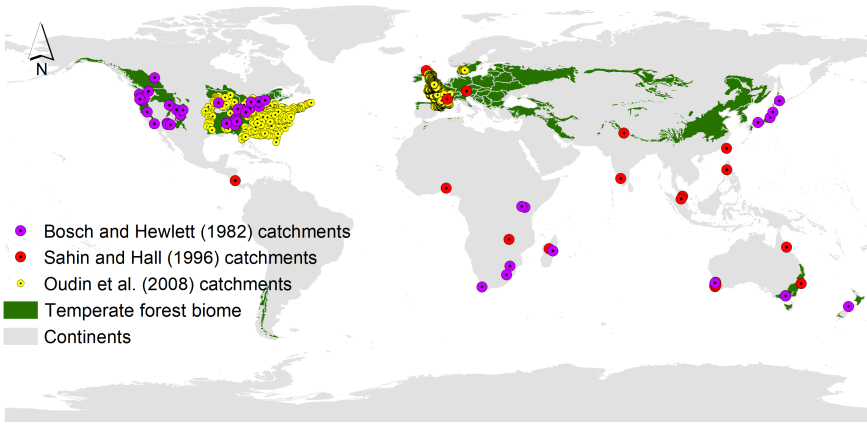

FIGURE 2.1: Distribution of experimental catchments used in the reviews by Bosch and Hewlett (1982), Sahin and Hall (1996, only the 51 additional studies that were not reported by Bosch and Hewlett are marked in red) and Oudin et al. (2008), and the distribution of the temperate forest biome, which is based on The Nature Conservancy (2009), WWF's ecoregions (Olson et al., 2001), Bailey (1994) and Wiken (1986).

Figure 2.1 shows the global distribution of the temperate forest biome and the location of the catchment data used in several paired catchment review studies (Hibbert, 1967; Bosch and Hewlett, 1982; Sahin and Hall, 1996; Oudin et al., 2008). Clearly, most of the catchments from some of the most prominent reviews are located within this biome. Most of the studies are located within the USA, Canada and Europe. Only some of the catchments from Bosch and Hewlett (1982) and some of the 51 additional catchments studied by Sahin and Hall (1996) are located outside of the temperate forest biome. Most of

these locations belong to the tropical forest biome and have been reviewed by Bruijnzeel (1990).

2.2 Water Balance Components

The establishment of a water balance is an important component of catchment studies. The water balance describes the partitioning of the incoming precipitation into discharge, storage and evapotranspiration:

$$P = Q + ET_a + \Delta S \tag{2.1}$$

where P [mm] is incoming precipitation, which is partitioned into discharge (Q) [mm], actual evapotranspiration (ET_a) [mm], and ΔS [mm] accounts for changes in storage within the system. ET_a can be further divided into evaporation of intercepted water (E_i) [mm], transpiration (T) [mm] and ground evaporation (E_g) [mm]:

$$ET_a = E_i + T + E_g \tag{2.2}$$

Although these water balance equations are rather simple and straightforward, the calculation of a water budget through time and space can be challenging, as it is difficult to quantify all components of the water balance independently (P, Q, ΔS, ET_a). In most cases, the balance is calculated on an annual scale, where ΔS is assumed to be close to zero. This allows to estimate ET_a indirectly from measurements of Q and P. This is, however, not generally applicable, since deep percolation to ground water may also be relevant. Furthermore, information on Q and P alone is not sufficient and additional information on ΔS and ET_a is required when hydrological impacts of land use change are investigated at a higher temporal resolution.

Vegetation is known to have a clear effect on ET_a (E_i, T and E_g) Q and ΔS. Plant transpiration influences the transport of water from the soil (ΔS) into the atmosphere and interception storage controls the amount of water available for evaporation directly from the leaves. Changes in ET_a and ΔS in turn affect the discharge regime. At the same time, the climate also plays an important role in the partitioning of the incoming precipitation into discharge, evapotranspiration and storage. In water limiting systems, most of the precipitation is converted into ET_a. In energy limited systems, on the other hand,

a lower percentage of the incoming precipitation is converted into ET_a.

In the next sections, the effect of vegetation change on the components of the water balance is described in three separate sections, each focussing on one individual flux (Q, ΔS, ET_a). For each individual flux, the following two questions will be addressed:

1. What are the most commonly investigated scales in time and space to study the hydrological impacts of deforestation?
2. What significant advances have been made at those different scales regarding the hydrological impacts of deforestation?

2.3 Discharge: Measurement Setup and Data Analysis Approaches

2.3.1 Annual Discharge Analysis

The impact of forest cover on the mean annual streamflow is one of the most studied topics in catchment hydrology and has been reviewed throughout different hydrological research eras. For such studies, the paired catchment approach is one of the most common methods (Figure 2.2). The paired catchment approach belongs to the BACI (Before-After-Control-Impact) designs, where the goal is to detect changes in a natural environment that also is affected by natural variability (Smith, 2002). The main focus of this approach is to describe relative differences in discharge behaviour between two catchments.

Paired catchment studies provide a controlled approach in which two (or sometimes more) catchments with similar characteristics are compared in a first reference period (Andréassian, 2004). In the second phase of a paired catchment study, land use or management is changed in one of the catchments and the observed differences between the control and treated catchment are attributed to the change in land use or management. Typically, paired catchment studies have been limited to a comparison of monthly or annual differences in incoming precipitation and outgoing discharge for relatively short monitoring periods (ca. 5 years). However, in some specific

cases, shorter term effects (section 2.3.2) or longer monitoring periods (section 2.3.3) have been investigated.

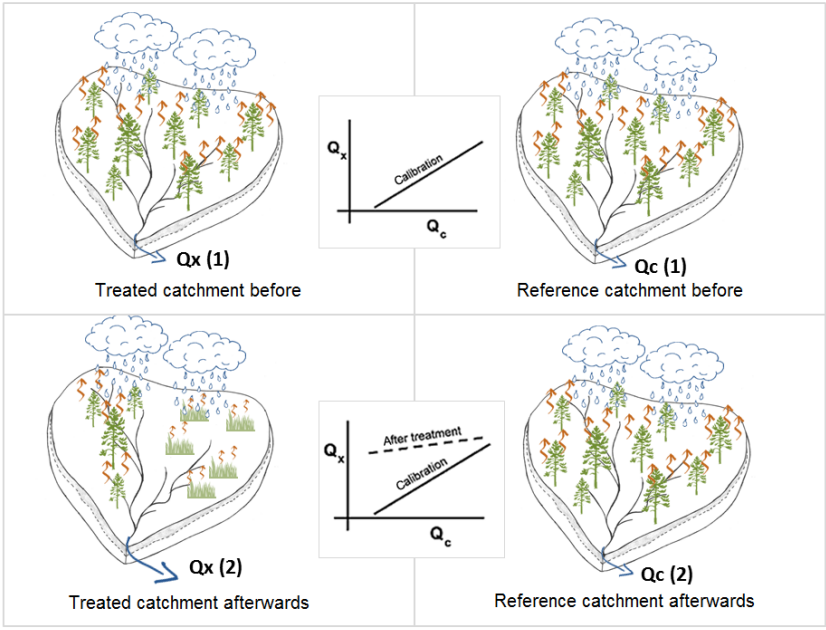

FIGURE 2.2: Schematic representation of a paired catchment experiment. In the calibration period, both catchments have the same vegetation (top row). In the treatment period (bottom row), catchment x undergoes a treatment (e.g. forested area is converted into grassland).

An alternative approach to study the hydrological impact of land cover change is a time series analysis of data from a single catchment experiment that has undergone a certain type of vegetation conversion (Zhang et al., 2011). To analyse the data, the response factor of interest (e.g. Q, ET_a) is plotted as a function of time or other independent variables (Hewlett and Pienaar, 1973). A big disadvantage of such an analysis is the lack of a control catchment to account for climatic variability. Therefore, the results of single catchment studies can be rather problematic to interpret (Bosch and Hewlett, 1982; Andréassian, 2004; Zhang et al., 2011).

Paired catchment studies have provided important insights on the effects of deforestation on annual discharge. On the short term, deforestation is

generally believed to increase the annual discharge. Due to the lack of vegetation, less water is transpired to the atmosphere, leaving more water at the land surface. This obvious expectation was already postulated in the first reviews discussing the effects of land use change at the annual scale by Hibbert (1967), Douglass and Swank (1975), McMinn and Hewlett (1975), and Bosch and Hewlett (1982). These reviews presented meta-analyses of a large number of paired catchment studies, and found that a decrease in forest coverage can increase the annual water yield if at least 20% of the area is affected. Additionally, the absolute change in discharge was found to be related to the mean annual precipitation and the vegetation type. It was found that the expected change in discharge in response to a given forest cover change is larger for higher mean annual precipitation. The change in vegetation (species before vs. species afterwards) also played an important role in determining the amount of change in annual discharge. After the deforestation of coniferous forest, larger changes in discharge were observed compared to the deforestation of deciduous forest.

In the 90's, reviews by Sahin and Hall (1996) and Stednick (1996) provided more detailed insights into the effects of deforestation on discharge. Sahin and Hall (1996) analysed a dataset comprising 145 catchment studies (mainly paired catchment studies; Figure 2.1). This study provided the first estimates of generalized annual discharge changes using a large (worldwide) dataset for different forest types (e.g. coniferous forest, eucalyptus, etc.). At the same time, Stednick (1996) focussed on the variability in detection limits of land use change effects (e.g. the fraction of deforestation required to obtain a detectable increase in discharge). He used a data set that comprised 95 catchments located in different parts of the USA (mainly temperate climate zone). Based on this regional data set, Stednick(1996) proposed that the effective minimum size of affected area required to obtain measurable changes in annual discharge is not constant (e.g. 20% as suggested by Bosch and Hewlett, 1982), and could be as low as 15% (Rocky Mountains, USA), or much higher in the case of the Central Plains, USA (50%).

One of the main aims in more recent work has been to provide more accurate predictions of annual discharge changes in response to a land cover change. Using a dataset of 166 catchments, Brown et al. (2005) showed that the empirical relationships between land cover and mean annual ET_a proposed by Zhang et al. (2001) provide a reasonable prediction for streamflow

changes in response to land cover change:

$$\frac{ET_a}{P} = \frac{1 + w * \frac{ET_0}{P}}{1 + w * \frac{ET_0}{P} + (\frac{ET_0}{P})^{-1}} \tag{2.3}$$

where ET_0 [mm] is the potential evapotranspiration and w [-] is the plant available water coefficient, which represents differences in water use by plants (e.g. rooting depth). This equation is a first step towards a more quantitative assessment of the effect of vegetation on water partitioning. Adams and Fowler (2006) investigated the scatter in the relationship between annual discharge and vegetation cover change to identify ways to improve the strength and accuracy of this relationship. They identified three causes for this scatter: (1) joint use of both deforestation and afforestation experiments in a single relationship, (2) differences in the format of the reported change (e.g. maximum or mean change in discharge), and (3) inter-annual variability in precipitation. In addition, they concluded that homogenisation of streamflow data is required to improve the accuracy of such empirical relationships.

Farley et al. (2005) also investigated whether the effects of afforestation and deforestation were similar. Since most previously analysed databases were dominated by deforestation studies, they focussed on afforestation studies only. They analysed 26 catchment datasets for the effect of afforestation on annual discharge and low flow conditions. Their findings were consistent with earlier meta-analyses, and showed that annual discharge decreased after afforestation. However, they also mentioned that the absolute change in discharge depended on forest type and age.

The abovementioned review studies have played an important role in generalizing the results from individual catchments in order to obtain a more global synthesis of the hydrological impacts of land use change. Nevertheless, there are several drawbacks that remain in these studies. One of the main drawbacks of both single and paired catchment studies has always been the limited spatial and temporal extent. The size of most catchments is limited to several hectares and most results are based on relatively short term monitoring results (typically less than 5 years). This relatively short temporal extent of most time series does not provide a lot of flexibility in analysis. Best (2003) additionally emphasized that the empirical relationships based on short-term monitoring results are not always consistent with results from

permanent land use change experiments, which have shown that it might take longer to observe a maximum change. Another complication of these studies is the variation in experimental conditions and setup descriptions between individual studies, which makes synthesis less straightforward. In addition, one may wonder whether simple linear regression analysis of discharge data is sufficient to describe the effects of land use change, since many processes in hydrology are non-linear. In this context, Andréassian (2004) already emphasized that it is impossible to make a stationary relationship between discharge and precipitation, as vegetation change impacts are not constant over time.

2.3.2 Intra-Annual Discharge Analysis

The effects of forest conversion on hydrological processes may differ considerably between observation scales. For example, soil moisture fluctuations hardly affect annual streamflow, but they can affect the water balance and runoff generation processes on shorter time intervals (Brown et al., 2005). Therefore, it is vital to also investigate the effects of land use change on the intra-annual variability in discharge. Notable reviews and opinion papers about discharge changes on the intra-annual time scale have been presented by Johnson (1998), Best (2003), Andréassian (2004), Brown et al. (2005), Brown et al.(2013) and Rogger et al. (2017).

Although deforestation can have clear effects on discharge peaks, it can be difficult to generalize observed changes in timing and volume. Hydrograph analysis can help to detect differences in response to land use change using characteristic summary parameters, such as peak discharge (height of rise), mean peak flow, time to peak, recession time and quick flow duration. Figure 2.3 illustrates possible differences in response with two examples of possible deforestation effects on the storm hydrograph. Troendle and King (1985) reported that deforestation in the Fool Creek Watershed (40% of catchment) caused the flood to start earlier with an increased total water volume (red curve, Figure 2.3). Although Burton (1997) also reported an increase in total water volume after deforestation (25% of catchment), he found that time to peak flow increased after deforestation (blue curve, Figure 2.3).

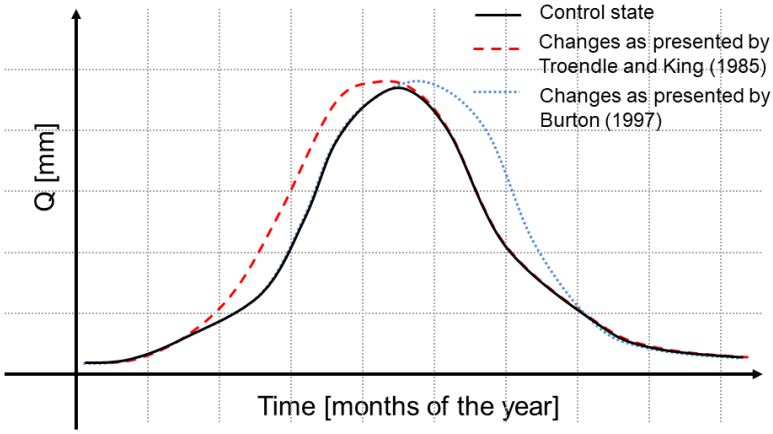

FIGURE 2.3: Schematic representation of changes in hydrograph shape related to forest management. The examples are inspired by observed changes reported in Troendle and King (1985) and Burton (1997).

Overall, there is no consensus in the magnitude and direction of change in the storm hydrograph in response to forest cover change. Multiple studies have reported that deforestation causes an increase in peak discharge (Harper, 1969; Van Haveren, 1988; Troendle and King, 1985; Jones and Grant, 1996; Burton, 1997), but there are also multiple studies that report otherwise (Thomas and Megahan, 1998; Thomas and Megahan, 2001; Alila et al., 2009; Rogger et al., 2017). Thomas and Megahan (1998; 2001) criticized the work of Jones and Grant (1996; 2001), and stated that a significant increase in peak flow can only be observed for the smallest events. They furthermore stated that the effects of deforestation on discharge peaks for large catchments are inconclusive. From a technical perspective, Alila et al. (2009) criticized that both frequency pairing and a sufficiently long peak flow record are needed to evaluate the effects of deforestation on floods. Rogger et al. (2017) stated that it is generally hard to evaluate the effect of forest cutting on storm hydrographs due to the non-linearity of runoff generation processes and the non-stationarity nature of deforestation activities.

Another tool to investigate the effects of deforestation on discharge peaks (e.g. timing and volume) are flow duration curves (FDCs). An FDC provides

statistical information on streamflow variability (magnitude, frequency, duration, timing and rate) for a certain location and can be used to analyse annual, monthly or daily flows. The shape of an FDC depends on the size, precipitation patterns and the geomorphological characteristics of a catchment. FDCs have also been used to analyse the hydrological effects of deforestation. Figure 2.4 exemplarily shows three distinct changes in the FDC that have been observed after land use change according to Brown et al. (Brown et al., 2013):

- A change in the number of no flow days, e.g. an increase after afforestation (yellow curve)
- A large increase in absolute discharge during low flow conditions after deforestation (red curve)
- An overall increase in flow after deforestation (green curve)

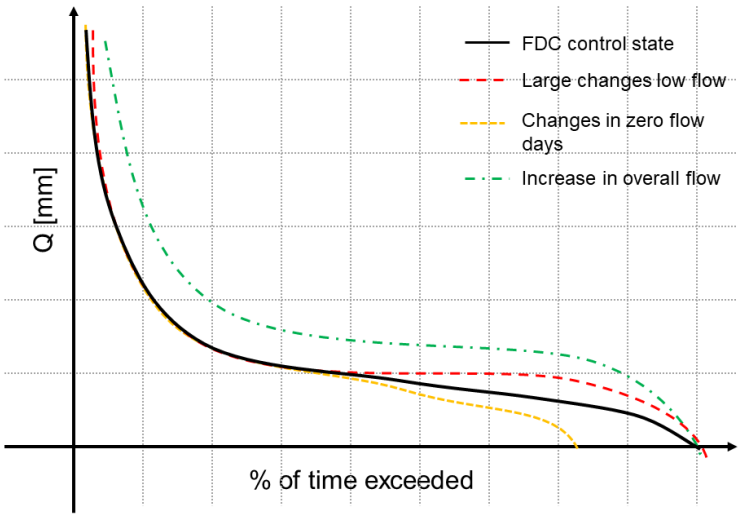

FIGURE 2.4: Schematic flow duration curves presenting three types of change related to land use change according to Brown et al. (2013).

.

This example illustrates that FDC's allow comparing differences in flow regimes between catchments, and can thus help to identify changes in flow regimes before and after deforestation.

Several studies have used FDCs to analyse changes in flow regime after forest cover change. Brown et al. (2013) argued that most of the differences in catchment response to land use change can be related to climatic conditions. Catchments with a low annual precipitation showed a quicker response to afforestation than catchments with high precipitation amounts. Not only the speed of response was different in different climates, but also the shape of the FDCs was altered in different ways (e.g. alteration of amount of no-flow days and high flow). Hornbeck et al. (1997) used FDCs to interpret changes in seasonal variability of streamflow after deforestation. Their work showed that deforestation activities in the Hubbard Brook catchment caused a more frequent occurrence of low flow conditions during the growing season, but only marginally increased the occurrence of high flow conditions. Lane et al. (2005) interpreted the effects of planation age on streamflow using climate-adjusted FDCs. Their results suggested that plantation age can either increase the number of zero flow days, or increase the overall flow.

In summary, these studies indicate that changes in low flow and high flow conditions in response to forest cover change can be quite variable, even for similar vegetation treatments. In addition, Brown et al. (2013) showed that the required time for catchments to reach a new equilibrium after vegetation change can be quite variable (between 8 - 25 years). Clearly, there are still a lot of unknowns in the understanding of land use change impacts on high and low flow conditions. Johnson (1998) pointed out that this is partly related to the small amount of studies focussed on intra-annual changes in low flow conditions. Furthermore, the impact of land use change on seasonal or monthly flow has not often been reported in a quantitative manner (Best et al., 2003). It can be concluded that available information on intra-annual flow changes is still too limited to reach a more general understanding.

2.3.3 Long-Term Discharge Analysis

There is a need to better understand the long-term effects of land use change on hydrological states and fluxes, since there are important implications for worldwide issues, such as water shortage and climate change. Observed increases in discharge after forest cover removal diminishes with time, but can persist for more than a decade (Swift and Swank, 1981; Troendle and King, 1985; Hornbeck et al., 1993; Brown et al., 2005; Brown et al., 2013). In many cases, the reduced increase in discharge depends substantially on the amount

and type of regrowth (e.g. controlled regrowth, permanent change in vegetation, or natural regrowth). Still, the long-term effects of land use change on hydrology are not well understood, which is also related to the costs and workload associated with long-term monitoring site.

A quantitative or even qualitative assessment of the long-term hydrological response to deforestation can be challenging, due to many factors that can affect the outcome, such as changes in species composition and regrowth stages (Hornbeck et al., 1993; Swank et al., 2001). Results from currently available studies show a high variability in response. Swift and Swank (1981) showed that although the initial response to a first clear-cut was very similar to that of a second clear-cut, the longer term effects were different. They attributed this difference to the variation in regrowth regime, stem density and forest composition. Although Brown et al.(2005) showed that disturbed systems were generally able to return to pre-treatment levels after a recovery period, they also observed several long-term changes in systems that underwent permanent changes from forest to agricultural land. The work by Farley et al. (2005) suggests that the largest change in discharge in response to afforestation is reached relatively rapidly, but that it may take one or multiple decades to reach a new equilibrium state. On the other hand, Hawtree et al. (2015) found no significant long-term reduction in annual discharge after afforestation.

Insights about long-term changes in intra-annual flow variability are even more difficult to obtain. One of the few datasets available was published by Troendle and King (1985), who presented long-term peakflow and mean annual discharge trends for a deforestation experiment in the Fool Creek watershed (Rocky Mountains, USA). They observed that changes in peak flow over time were much more variable than mean annual discharge (Figure 2.5). This result is likely related to climate variability, since short-term changes in peak flow are heavily influenced by inter-annual variability. It clearly demonstrates the current limitations of studying the hydrological impacts of clear-cut activities on floods.

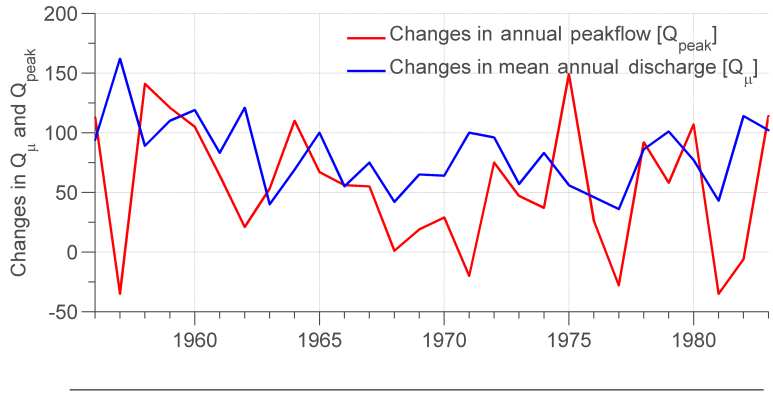

FIGURE 2.5: Changes in mean annual discharge and peak discharge in the Fool Water Creek watershed after a clear-cut in 1957. Data from Troendle and King (1985), after Andréassian (Andréassian, 2004).

Altogether, the results of these studies suggest that in many cases the initial increase or decrease in discharge might not be representative for the long-term behaviour. The full effects of deforestation might take longer to appear, and seem to depend on management practices (e.g. regrowth or permanent change). Generalizations about the hydrological impact of forest cover change remain challenging because changes in discharge are very dependent on catchment characteristics, vegetation composition, and regrowth regime. Generalizations about the impact on intra-annual flow are even more difficult, as little information is available and intra-annual changes in climatic conditions are often large.

2.3.4 Spatial Extent of Experimental Discharge Studies

It is important to consider the spatial extent of the catchments used to investigate changes in discharge related to vegetation manipulation experiments for generalization and transferability purposes. Generally, experimental catchments in hydrology are relatively small (headwater) catchments, as they are easier to control and manage (Siriwardena et al., 2006; Pilgrim et al., 1982) Obviously, controlled vegetation manipulation experiments become more and more challenging when the size of the catchment increases.

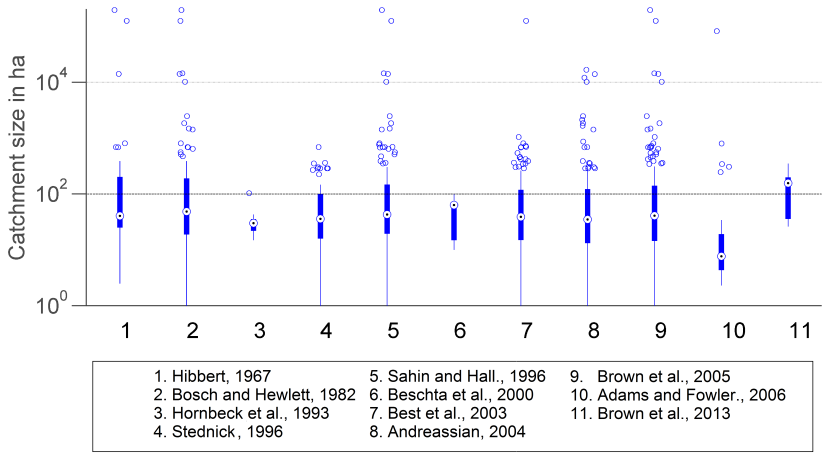

FIGURE 2.6: Distribution of catchment sizes of studies from eleven different review studies. Table 2.1 provides mean and median catchment sizes and % of catchment studies > 100 ha.

Figure 2.6 shows the distribution of catchment sizes used in eleven review studies on the hydrological impact of land use change. The selection of these studies was based on the availability of areal information and a required minimum number of investigated catchments (>10). Table 2.1 additionally provides the mean and median catchment size and the percentage of studies with a catchment size smaller than 100 ha. The median catchment size of the eleven review studies is relatively small and similar (average of median catchment size: 49.2 ha), but the mean catchment size and the percentage of catchment studies below 100 ha (1 km^2) are highly variable. Whereas Hornbeck et al. (1993), Beschta et al. (2000) and Adams and Fowler (2006) mainly considered catchments below 100 ha (>85%), Brown et al. (Brown et al., 2013) reviewed a considerable amount of paired catchment studies (four deforestation experiments; twelve afforestation experiments) above 100 ha. Still, Figure 2.6 and Table 2.1 clearly show a bias in the spatial extent of vegetation manipulation studies towards relatively small catchments.

TABLE 2.1: Mean and median catchment sizes and % of catchment studies < 100 ha from 11 different review studies.

Reference	**Medium Size [ha]**	**Mean Size [ha]**	**% of Catchment Studies < 100 ha**
Hibbert, 1967	40.5	8813.3	61.5
Bosch and Hewlett, 1982	48.5	4052.9	62.8
Hornbeck et al., 1993	30	34.5	90.9
Stednick, 1996	36	82.8	66.3
Sahin and Hall, 1996	43	2835.7	61.4
Beschta et al., 2000	63.5	55.2	90.0
Best et al., 2003	39	986	69.8
Andréassian, 2004	35	558.5	69.6
Brown et al., 2005	41.1	2370.1	67.5
Adams and Fowler, 2006	7.7	2428.4	85.7
Brown et al., 2013	157	147.4	40.4
Average	49.2	2033.2	69.6

One may wonder if small scale manipulation experiments are representative enough to generalize the effects of land use change to large scales. Such fundamental questions on the transferability of small catchment hydrology to large scales have already been raised in the 1980's (e.g. Pilgrim et al., 1982). Pilgrim et al. (1982) studied the effects of catchment size on runoff relationships, and also discussed impacts of land use change. They highlighted that results from experiments on smaller catchments have rarely been reproduced in larger catchments. In principle, discharge effects of manipulation experiments in larger basins can be assessed by extrapolating results from smaller basins using hydrological models or by using pre-manipulation periods as a reference (e.g. Wilk et al., 2001; Siriwardena et al., 2006). However, there are little to no controlled large catchment experiments that could provide a good comparison to small-scale studies. Moreover, large-scale catchment require a large amount of data (e.g. to accurately represent spatial variability of precipitation).

2.4 Evapotranspiration: Measurement Setup and Data Analysis Approaches

Evapotranspiration, the sum of plant transpiration, soil evaporation and interception evaporation, is a vital process that generates a direct feedback between the hydrological cycle and the energy cycle. As land use change can alter not only the available water, but also the available energy and photosynthesis, it is of crucial importance to understand differences in evapotranspiration related to land use. Currently, the topic of water use by plants is still very relevant and widely considered as a "cross-cutting theme" in ecohydrology (Asbjornsen et al., 2011). Although the number of publications within the field of forest evapotranspiration is substantial (> 1100 on forest evapotranspiration by 2011 Baldocchi and Ryu, 2011), there is still too little quantitative information on evapotranspiration changes after deforestation or other types of land use change (Hirano et al., 2017).

2.4.1 Spatial and Temporal Coverage of Evapotranspiration Measurements

The main source of information on evapotranspiration fluxes related to land use change in hydrology is based on water budget studies, which provided indirect information on yearly sums (Hewlett, 1961; Bosch and Hewlett, 1982). The advantage of this approach is that yearly evapotranspiration sums can be obtained for large and complex terrain (catchments) without additional equipment. At the same time, this method does not provide information on shorter (intra-annual) timescales or on the partitioning of evapotranspiration into its components.

In the past decades, many alternative techniques have been developed within the field of micrometeorology, hydrology and plant science that can provide transpiration, soil evaporation, interception evaporation or evapotranspiration data at different temporal and spatial scales. The best known methods include weighing lysimeters (Edwards, 1986; Calder, 1990), sap flow measurements (Smith and Allen, 1996), plant chambers (Dekker, 2000), isotope tracers (Calder, 1991), soil moisture monitoring (Calder, 1990), plant physiology and tree cutting (Jarvis and Stewart, 1979), gamma ray attenuation (Calder, 1990), microwave transmission (Bouten et al., 1991), the flux

gradient method (Droppo and Hamilton, 1973) and the eddy covariance method (Baldocchi et al., 1988; Dyer, 1961). Most studies dealing with evaporation, transpiration and evapotranspiration measurements rely on lysimeters, eddy covariance measurements, soil water budgeting, sap flow measurements and catchment water budgets. The typical spatial and temporal resolution for these measurements is summarized in Table 2.2. Most of the measurement methods show a clear trade-off between temporal resolution and spatial extent. The eddy covariance method is the only measurement technique that provides ET_a at a high temporal resolution for a relatively large area.

TABLE 2.2: Comparison of spatial scale and temporal resolution for different state-of-the-art evapotranspiration measurement methods, adapted from Wilson et al. (2001).

Method	**Measurement components**	**Spatial scale [m]**	**Temporal resolution**
Weighing lysimeters	Evapotranspiration	10^2	half-hourly
Soil water budgeting	Transpiration & soil evaporation	1	daily
Sap flow	Transpiration	10^2	half-hourly
Eddy covariance (above canopy)	Evapotranspiration	10^4	half-hourly
Eddy covariance (below canopy)	Soil evaporation	10^2	half-hourly
Catchment water budgetting	Evapotranspiration	10^6	yearly

Information on regional and global evapotranspiration patterns is mainly provided by (1) satellite data in combination with energy balance models, (2) airplane-based eddy covariance measurements, (3) global eddy covariance tower-based data- sets such as FLUXNET (Figure 2.7) and (4) simulation results from global land surface models. Global eddy covariance datasets provide the most accurate evapotranspiration data, but do not cover all relevant regions on the globe (Figure 2.7).

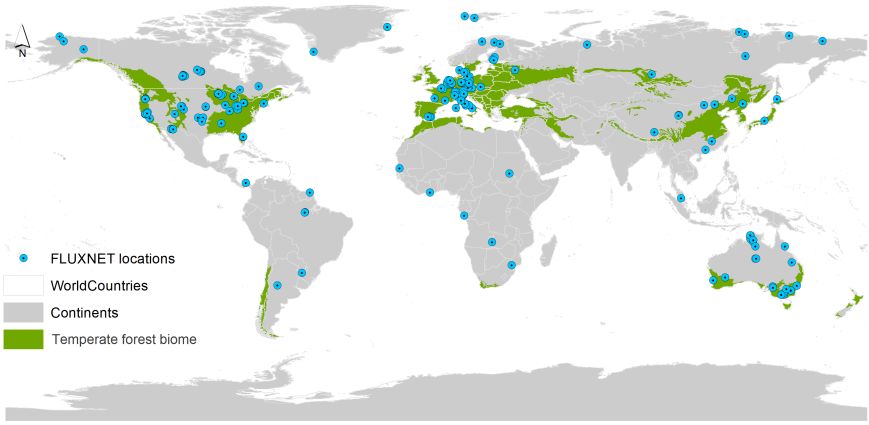

FIGURE 2.7: Global distribution of FLUXNET 2015 locations (Source: https://fluxnet.fluxdata.org/sites/site-list-and-pages/) and the distribution of the temperate forest biome, which is based on The Nature Conservancy (2009), WWF's ecoregions (Olson et al., 2001), Bailey (1994) and Wiken (1986).

Regional measurements that cover larger areas, but have low temporal resolution, can be provided by airborne eddy covariance measurements. For example, Gioli et al. (2004) reported a good match between airborne and tower-based eddy covariance observations in the case of relatively homogeneous surfaces. For regional to global scales, indirect evapotranspiration estimates have been obtained using satellite data and land surface models. According to Long et al. (2014) and Wang et al. (2015a), the lowest uncertainty in evapotranspiration estimates are provided by land surface models at these scales. Moderate uncertainties exist for the satellite-based MODIS ET product, but this alternative offers a set of high resolution surface parameters while requiring only little atmospheric forcing data (Wang et al., 2015a). Overall, more eddy covariance datasets are required to better constrain MODIS ET and land surface model products.

2.4.2 Regional to Global Evapotranspiration Analysis

At the regional and global scale, vegetation plays a vital role in determining evapotranspiration fluxes. Globally, terrestrial evapotranspiration amounts to ca. 59 – 67% of the total precipitation (Oki and Kanae, 2006; Trenberth et al., 2007; Wang and Dickinson, 2012). Although there seems to be a general increase in global evapotranspiration in the last three decades, more recent declines in global evapotranspiration have also been reported. According to

Zhang et al. (2016), global greening as expressed by an increase of LAI and plant productivity in the last 30 years has caused a global increase in evapotranspiration through increased transpiration and interception evaporation. On the other hand, Jung et al. (2010) reported a more recent decline in global terrestrial evapotranspiration since 2008 due to a limited amount of available stored soil moisture. Sterling et al. (2012) predicted that future land use change will result in a decline of terrestrial evapotranspiration by ca. 5% due to potential disturbance of areas with high evapotranspiration.

Although the importance of evapotranspiration in the global hydrological cycle is acknowledged, there is still no full understanding of core principles that globally govern the severity of land use related changes in evapotranspiration (Moore et al., 2011). Moore and Heilman (2011) proposed a set of principles that could be used to predict land use related changes in transpiration. They stated that changes in transpiration will be noticeable if:

- the available energy and the Bowen ratio (ratio of latent heat to sensible heat flux) is affected;
- the rooting depth changes and the soil water availability is affected;
- the system's water usage over a longer period is affected significantly.

Williams et al. (2012) also studied global evapotranspiration controls using FLUX- NET data in combination with the Budyko framework, which uses simple parameterized models (e.g Zhang et al., 2001, Equation 2.3) to predict changes in evapotranspiration for different vegetation types. They found that net radiation and precipitation are the two limiting drivers globally for evapotranspiration, but that the climate type and vegetation type also played an important role in explaining the global variability in evapotranspiration.

At the regional scale, different vegetation-specific landscapes also have their own characteristic evapotranspiration. Data from a 46 km long flight transects in the USA (flux tower data and fair weather data) showed that the partitioning of net radiation into evapotranspiration (latent heat) and sensible heat depended mainly on the type of vegetation and soil moisture regime. High latent heat fluxes and low sensible heat fluxes were found in green vegetation patches, whereas low latent heat fluxes and high sensible heat fluxes were found for sparse and dormant vegetation areas (LeMone et al., 2007). Vellinga et al. (2010) also showed that seasonal and spatial variability in

evapotranspiration fluxes are related to the underlying landscapes, which can be useful to predict regional-scale energy fluxes. Stoy et al. (2006) used a linear perturbation algorithm on eddy covariance measurements to show that ecosystems in the southwest USA have different sensitivity to climatic variability.

Although the datasets available at the regional and global scale have provided important insights on the drivers of evapotranspiration, there are still many open questions that have not been adequately addressed yet. More high-quality regional estimates (based on eddy covariance datasets or the like) are needed to validate global evapotranspiration satellite products and to provide an improved understanding of evapotranspiration and its spatial distribution at the regional scale. Only when a larger amount of regional datasets will be made available, an improved understanding of driving factors and interrelationships between landscapes and the atmosphere can be obtained.

2.4.3 Small Scale Evapotranspiration Analysis

Most information on the effect of vegetation on evapotranspiration originates from local scale measurements. At the small scale (plot – catchment scale), a variety of eddy-covariance and sap flow measurement studies have shown that vegetation change can have a large effect on evapotranspiration fluxes. For example, Rannik et al. (2002) showed that forest evapotranspiration was higher for a 38-year old forest compared to a 5-year old cleared site due to the additional transpiration at the forest site. Montes-Helu et al. (2009) showed that evapotranspiration from a previously burned grassland site was much lower compared to evapotranspiration from a ponderosa pine (*Pinus Ponderosa*) forest site. Dore et al. (2012) also found that forest fires at several *Ponderosa* pine stands reduced evapotranspiration by 12 – 30% and Liu et al. (2005) reported a decrease of 33% in evapotranspiration between a post-burned grassland site and a 80 year old broadleaf forest. Williams et al. (2014) also observed an annual decrease in evapotranspiration of 30% after the deforestation of 8 ha of forest and a subsequent increase in evapotranspiration in the recovery years. These examples show good agreement with results from paired catchment studies.

Although there are multiple studies that report clear changes in evapotranspiration after land use change, quantified generalizations of change in ET remain difficult. There are currently only few reports that provide a quantitative description of changes in energy balance and evapotranspiration due to deforestation (Hirano et al., 2017). The direction and amount of change in evapotranspiration due to vegetation change and even the recovery time of the system remain ambiguous due to the broad range of factors that potentially influence evapotranspiration (Figure 2.8), including vegetation stand characteristics (e.g. density, age composition, species composition, understory composition), atmospheric conditions (e.g. vapour pressure deficit), and land surface conditions (e.g. soil water content profile). In the following, these factors will be discussed in more detail.

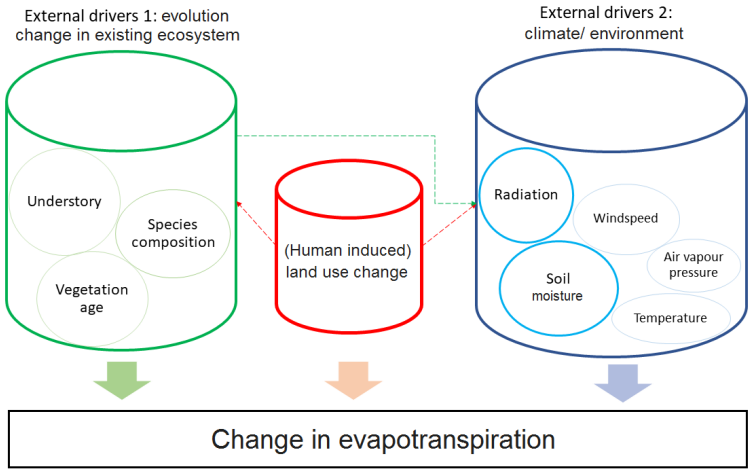

FIGURE 2.8: Visualization of external drivers that can affect evapotranspiration. Potential interactions amongst drivers are shown using dotted lines. Please note that the balloons point out important examples of drivers (which are also mentioned in this section), but do not represent all possible examples.

Changes in species composition affect evapotranspiration via the specific water retention capacity, interception properties, root distribution and canopy characteristics (Armbruster et al., 2004). A clear example of the effect of stand composition was presented by Amiro et al. (2006), who showed that the trajectory of successional species can affect energy balance partitioning. An increase in the area of deciduous trees resulted in a higher summer albedo, higher evapotranspiration, and lower Bowen ratios. Clenciala

et al. (1998) compared water use estimated from sap flow measurements in two contrasting forest stands and found that spruce was more sensitive to droughts than pine, probably due to its shallow root architecture. Effects of different root architecture were also observed by Schume et al. (2004) using Time Domain Reflectometry (TDR) soil moisture sensors. They also observed large differences in water abstraction rates in the upper 60 cm of soil between a mixed and a pure spruce stand during periods of high evaporative demand.

Two other factors that can significantly alter the evapotranspiration are the age of the forest and the understory within the forest. Anthoni et al. (2002) found that during water stress periods, a young pine system (15 years old) was having much lower evapotranspiration rates compared to an old forest (>50 years old). Young trees invest more in developing foliage than in the stem, and are therefore more vulnerable to drier conditions. Mature trees generate deeper roots, and thus have access to more water during droughts (Anthoni et al., 2002). Especially during summer, the understory can contribute significantly to evapotranspiration. Heijmans et al. (2004b; 2004a) showed that moss evaporation (*Sphagnum* and *Hylocomium*) in summer contributed up to 15-45 % of total evapotranspiration in a boreal black spruce forest. Vincke et al. (2005a; 2005b) found that transpiration from the forest floor was larger than transpiration from the oak trees, which only contributed 21-38% of the total stand transpiration. In both cases, the role of understory evapotranspiration was closely linked to the openness (Heijmans et al., 2004b) and the structure of the canopy (Vincke et al., 2005a).

The effect of stand density on evapotranspiration, on the other hand, seems to be ambiguous. Vincke et al. (2005a; 2005b) found clear differences in annual and maximum evapotranspiration in the first two years after thinning activities. However, Dore et al. (2012) found a decrease of only 4% in evapotranspiration for the first three years after thinning. In the fourth year, they were not able to observe any differences in evapotranspiration between the thinned and the reference forest anymore. Vesala et al. (2005) also did not find a significant decrease in evapotranspiration after 25-30% reduction in basal area, which was probably caused by changes in wind speed, winter albedo and light penetration, which in turn compensated for the reduction in foliage.

External drivers, including climate and soil related conditions can also

strongly affect evapotranspiration. According to Teuling et al. (2009), the two most important limiting drivers in evapotranspiration are soil moisture (e.g. Moore et al., 2011; Rodriguez-Iturbe, 2000; Teuling et al., 2010) and global radiation as they provide the most important requirements for evapotranspiration to occur: a sufficient amount of water and available energy. Other external drivers that affect evapotranspiration include temperature, wind speed and water vapour pressure. In some cases, changes in one of these external conditions have reduced direct changes associated with a change in vegetation. Examples of such cases were provided by Biederman et al. (2014; 2015), who found no clear changes in evapotranspiration after tree mortality due to Bark beetle attacks. It was argued that the decrease in transpiration was offset by a proportional increase in evaporation, which was attributed to a reduction in canopy shading of shortwave radiation (Biederman et al., 2014). Hirano et al. (2017) also found that two systems with very different biomass showed very similar evapotranspiration, which was steered by external conditions (clear difference in net radiation to global radiation ratio). Therefore, Teuling et al. (2010) advocated that trends in evapotranspiration can only be understood by appropriate consideration of the limiting drivers.

Large temporal variability in external drivers can also lead to strong contrasts between vegetation types. Rannik et al. (2002) observed the largest differences in evapotranspiration between a forested site and a grassland site (forest ET > grassland ET) when monthly precipitation was only 13 mm. Williams et al. (2014) showed that post-clear-cut recovery of evapotranspiration was highly variable for different seasons. Summer and autumn evapotranspiration were highly increased during the first three recovery years, where gross ecosystem productivity (GEP) was the largest, whereas winter and spring evapotranspiration changed only moderately. In some cases, external factors can cause unexpected contrasts between vegetation types. During a heat wave, Teuling et al. (2010) found larger evapotranspiration rates for a grassland site as compared to a forested site. Similar observations were made by Ponton et al. (2006). One possible cause for this behaviour is a mitigation strategy of trees to be more conservative with water in periods with water stress.

Altogether, this section shows that the dynamic properties of plant-controlled systems are complex, and water-plant relationships can be highly heterogeneous in time and space due to stand properties and external drivers (e.g.

climate and soil conditions) that influence the system. At the same time, this section also highlights that systems that undergo vegetation change due to anthropogenic measures, such as deforestation, are still not fully understood and need to be further studied in the act of "ecohydrological triggers of non-linear relationships, thresholds and stable states" (section cross cutting themes in hydroecology; Asbjornsen et al., 2011).

2.5 Soil Moisture: Measurement Setups and Data Analysis Approaches

Soil moisture is not only a key driver for many hydrological processes, it also influences the energy and carbon cycle and plays an important role in agricultural science, biogeochemistry and ecology (Lawrence et al., 2007). Although the change in soil moisture storage in the annual water balance typically is rather small, soil moisture does play a vital role within the hydrological cycle. At shorter time scales, soil moisture directly interacts with the vegetation, the surface, and the atmosphere, and therewith is a key driver for multiple hydrological processes, such as evapotranspiration, discharge, and subsurface stormflow. The spatial variability of soil moisture also plays a crucial role for groundwater recharge and solute transport in the subsurface.

Vegetation plays an important role for soil moisture trends at multiple scales. It can, for example, regulate changes in global soil moisture trends caused by climate change (Feng, 2016). Still, the interaction between vegetation and soil moisture is highly complex and not fully understood (D'Odorico et al., 2007). Although soil moisture provides a direct link between spatiotemporal climate and vegetation dynamics, there is no universal rule-set that can explain the interplay between vegetation, climate and soil moisture. Climate-soil-vegetation dynamics can show fundamental differences for different vegetation types, which shows the need to link ecology, hydrology and micrometeorology (Rodriguez-Iturbe, 2000).

There is a large number of reviews available that summarize soil moisture and subsurface water movement related topics (Vereecken et al., 2008; Seneviratne et al., 2010; Vereecken et al., 2015; Binley et al., 2015; Jarvis et al., 2016), including specific soil-vegetation related reviews (Rodriguez-Iturbe, 2000; Vereecken et al., 2010; Neumann and Cardon, 2012). However, the latter reviews were mainly focussed on the formation of vegetation patterns

and root zone-soil interactions, and also strongly emphasized modelling approaches. Here, the focus is mainly on interactions between land use change and soil moisture from the profile to the catchment scale and the connection with hydrological processes.

2.5.1 Spatial and Temporal Extent of Soil Moisture Measurements

Monitoring soil moisture dynamics is crucial to answer hydrological questions related to land use change and to improve our understanding of land surface-atmos- phere feedbacks. Plant growth and transpiration are regulated by soil moisture and vegetation affects the available moisture in the soil. At the same time, it is hard to obtain data on subsurface hydrological processes at an appropriate scale. High-resolution spatiotemporal soil moisture data is needed to understand the links between land use and climate interactions, which is, however, rather difficult to obtain with many of the currently available measurement techniques. Most soil moisture measurement techniques provide data with either a high temporal or a high spatial resolution. There are several reviews available that provide a good overview on the wide range of measurement methods available to directly and indirectly measure soil moisture and subsurface hydrological processes (Vereecken et al., 2008; Bittelli, 2011; Binley et al., 2015; Susha Lekshmi et al., 2014; Srivastava, 2017). These reviews also give a good description of the applications, limitations and advantages of different soil moisture measurement methods. This section therefore only provides a compact overview of the available methods and related spatiotemporal resolutions.

The most commonly used soil moisture method groups are: soil moisture probes, remote sensing methods and geophysical methods. Table 2.3 provides an overview on the spatial and temporal coverage and resolution of the most common methods within each group. Presented in the first group are in-situ soil moisture probes, which can provide high temporal coverage, but only provides point information (i.e. a few cm^3). The combination of wireless network technology with low-cost soil moisture sensors is promising, as this provides soil moisture data at high spatiotemporal resolution with catchment-wide coverage (Bogena et al., 2010). The second group of soil moisture methods covers remote sensing methods, which provide the

largest spatial coverage, but often lack spatial resolution, have a low temporal resolution (> 3 days) and only measure the top few centimetres of the soil.

TABLE 2.3: Comparison of spatial extent and temporal resolution for different state-of-the-art soil moisture measurement methods.

Research Field	**Method**	**Spatial Coverage/ Resolution**	**Temporal Resolution**	**Depth Information**
Soil moisture probes	Wireless sensor networks	Intermediate/ high	High	Discrete depths
	Time Domain Reflectometry (TDR)	Low/low	High	Discrete depths
	Cosmic-ray neutron probe (CRNP)	Intermediate/ low	High	< 0.5 m
Remote Sensing	Passive Microwafe Radiometers	High/ low	Low	< 0.01m
	Synthetic Aperture Radars	High/high	Low	< 0.05m
	Scatterometers	High/ low	Low	< 0.05 m
	Thermal Methods	High/ low	Low	< 0.05 m
Geophysics	Ground Penetrating Radar (GPR)	Intermediate/ high	Low*	2D profile(s)
	Electrical Resistivity Tomography (ERT)	Intermediate/ high	Low*	2D profile(s)
	Electromagnetic Induction (EMI)	Intermediate/ high	Low*	profile

*The temporal resolution of geophysical measurements is campaign-based.

Electrical Resistivity Tomography (ERT), Ground Penetrating Radar (GPR) and Electro-Magnetic Induction (EMI) are presented in the third measurement group with geophysical methods and provide a non-invasive approach to indirectly estimate soil moisture from the dielectric properties of the soil.

These methods provide an emerging approach to monitor subsurface hydrological processes (Binley et al., 2015), including root water uptake (e.g Garré et al., 2011). Amongst these methods, EMI is a promising and relatively simple method to map soil moisture for areas up to the small catchment scale (Robinson et al., 2012; Hebel et al., 2014; Altdorff et al., 2017; Martini et al., 2017).

2.5.2 Profile-Based Soil Moisture Observations

Temporally highly resolved soil moisture profile data can already provide a lot of information on the interactions between soil moisture and vegetation (e.g. root water uptake). Clearly, soil moisture variability can be affected by the vegetation, i.e. by the root distribution and the water stress characteristics of the plants (e.g Rabbel et al., 2018). Patric (1973) showed that temporal soil moisture fluctuations were much larger in a forested soil profile compared to a bare soil profile. James et al. (2003), on the other hand, observed the temporal variation in soil moisture during the growing season was higher at a grassland site, as compared to a forested site. At the beginning of the growing season, the grassland had the highest soil moisture content, but at the end of the season, the grassland site was the driest, which can be related to the different water stress characteristics of the grassland and the forest. Again another study by Wang et al. (2012) showed that during dry periods, shrub-grassland patches had higher soil moisture content compared to forest-shrub patches (Loess Plateau, China). Even though shrub-grassland patches had larger post-rainfall soil moisture losses, their soil moisture remained higher due to their retention characteristics. These examples illustrate that moisture fluctuations might be highly variable during the different stages of natural regeneration after deforestation and can highly depend on the sequence of ecolgical succession.

In some cases, initial soil moisture conditions do also determine the soil-vegeta- tion interplay. Jost et al. (2004) and Schume et al. (2004) used TDR to monitor soil moisture, and found that during strong rainfall events after a dry period, infiltration patterns were governed by the dry clay topsoil that caused irregular infiltration patterns between 30 to 60 cm depth. Similar rainfall events for intermediate soil moisture conditions caused infiltration patterns dominated by vegetation characteristics as infiltration was higher

around the beech trees compared to the spruce trees due to interception differences. Geris et al. (2015), on the other hand, showed that soil moisture differences were rather governed by vegetation (grass vs. forest) during dry soil moisture conditions.

Spatiotemporal soil moisture information, provided by e.g. ERT measurements can provided additional insights in the interactions between vegetation, soil moisture and groundwater. ERT is a geoelectrical method that uses the changes in electrical properties of the soil to visualize 2-dimensional changes in soil moisture dynamics. ERT has extensively been used to investigate soil moisture dynamics in the root zone. Jayawickreme et al. (2008; 2010) used ERT to monitor soil moisture variation at the interface between a forested and a grassland area. They found large differences in vertical moisture abstraction due to differences in rooting depth. Overall, the forest generated less recharge as the soil moisture deficit was much larger and extended to deeper layers in the forested region. With the help of ERT, Nijland et al. (2010) showed that vegetation was able to extract water from the weathered bedrock below the soil, which was located between 3 – 6 m depth. Acharya et al. (2017) showed that ERT can detect the effects of vegetation on temporal soil moisture patterns. In their study, a vegetation change from Juniper to grassland caused a reduction in deep recharge. It was concluded that Juniper trees facilitated deep water infiltration via their root structure, thus generating higher soil moisture deeper in the soil. Alltogether, these results demonstrate that ERT is a promising method to look at soil moisture and groundwater abstraction for different types of vegetation.

2.5.3 Spatiotemporal Soil Moisture Patterns: 3D - 4D Analyses

Nowadays, methods are available to measure soil moisture in three or four dimensions (e.g. via wireless soil moisture networks). This provides opportunities for new data analysis approaches that could be (or are already) applied to analyse the effects of land use change on soil moisture fluctuations. Three concepts that provide innovate ways to look at high resolution spatiotemporal soil moisture data are an analysis of the relationship between mean soil moisture and variance or standard deviation, a temporal stability analysis, and a spatial correlation analysis. These methods can be useful tools

to look at the effects of vegetation on three-dimensional or four-dimensional soil moisture variations.

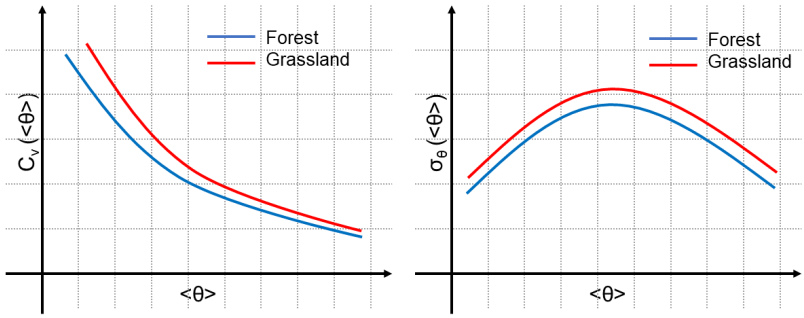

FIGURE 2.9: Schematic representation of the relationship between (a) the mean soil moisture content and the coefficient of variation (b) the mean soil moisture content and the standard deviation for a forested and a grassland site (simplified version of the results by Zucco et al. 2014.

The relationship between mean soil moisture (<θ>) and the coefficient of variation ($C_{v\theta}$) or the standard deviation (σ_θ) has been widely used to investigate spatiotemporal variability of soil moisture (Figure 2.9). A common shape for this σ_θ(<θ>) relationship is convex with a maximum in the intermediate soil moisture range (Vereecken et al., 2007; Korres et al., 2015). Commonly, $C_{v\theta}$(<θ>) relationships peak at low moisture content and decrease with increasing mean soil moisture (Korres et al., 2015). A range of studies has shown that these relationships are affected by climate (e.g. Teuling, 2007; Lawrence et al., 2007), soil hydraulic properties (e.g. Lawrence et al., 2007; Vereecken et al., 2007; Qu et al., 2015; Wang et al., 2015a), scale (e.g Korres et al., 2015) and topography (e.g Vivoni et al., 2010). Unfortunately, there are only few studies available that actively studied the effect of vegetation change on the shape of the σ_θ(<θ>) and the $C_{v\theta}$(<θ>) relationship. Moreover, results from the existing studies show a large variety in possible effects of vegetation change, and are partially based on model simulations only. Figure 2.9 shows simplified σ_θ(<θ>) and the $C_{v\theta}$(<θ>) relationships based on the results by Zucco et al. (2014). This study showed that two contrasting vegetation types (forest and grassland) had very similar σ_θ(<θ>) and $C_{v\theta}$(<θ>) relationships, which might suggest that these relationships are dominated by soil properties instead of vegetation. On the other hand, Wang et al. (2015b) showed that the σ_θ(<θ>) relationship was different for a bare soil compared

to a vegetated surface using a mixture of model simulations and field measurements. A modeling study by Ivanov et al. (2010) also showed that the $C_{v\theta}(<\theta>)$ relationship was different between a fully vegetated surface and a bare soil. A virtual experiment by Teuling and Troch (2005) showed that the observed soil moisture variability can be largely generated by vegetation anomalies.

A temporal stability analysis of soil moisture can help finding measurement locations within the catchment that represents the mean soil moisture and the variability of the catchment best. Different measures such as the Mean Relative Difference (MRD), Index of Time Stability (IST), Root Mean Square Error (RMSE) and the Standard Deviation of the Relative Difference (SDRD) have been used to identify such representative measurement locations (Wei et al., 2017). There are only a few studies that have evaluated the effect of vegetation on the temporal stability of the soil moisture. Wei et al. (2017) analysed the temporal stability for a catchment with 293 sampling points and six different vegetation types (evergreen needleleaf, deciduous broadleaf, mixed forest, woodland, wooded grassland, cropland), and found that vegetation and topography were key factors determining temporal stability. In particular, cropland and grassland showed negative mean MRD values indicating low representativeness for the entire catchment, whereas the forested sites were more representative because their mean MRD values were close to zero. Yang et al. (2016) investigated the spatiotemporal development of relative differences of the matrix potential ($\Psi_{m'}$) over a transition zone between cropland and grassland. In the upper layers (especially -10 and -30 cm), the cropland showed larger fluctuations in$\Psi_{m'}$ than the grassland, suggesting a lower temporal stability compared to the grassland site. Higher temporal stability of Ψ_m was found in the deeper soil (-110 cm) along the entire transect, suggesting limited influence of time-variant boundary conditions.

A third interesting approach to study spatiotemporal soil moisture patterns is to analyse the temporal evolution of the soil moisture's spatial correlation. Western et al. (2004) have already shown that there is a strong link between the spatial correlation of soil moisture and the dominant hydrological processes. One of the few existing studies was presented by Korres et

al. (2015), who showed that the spatial correlation of soil moisture was affected by (1) mean soil wetness (<θ>), (2) measurement scale and (3) vegetation. Similar to an earlier geostatistical study by Western et al. (1998), Korres et al. (2015) found shorter correlation lengths during wet days compared to dry days. They also found that the variograms of a forested area had in general higher sills and lower effective ranges compared to a cropped catchment, which could however also be related to the different data products used in this study (remote sensing for cropland versus soil moisture sensor network for forest). These existing studies show that spatial correlation evolution could be a promising method to better understand the effects of vegetation on spatiotemporal soil moisture evolution.

2.5.4 Subsurface Water Movement and Soil Properties

Water movement in the soil, including infiltration (e.g. piston flow, preferential flow) and subsurface stormflow play an important role in discharge generation (e.g Lin, 2006). Vegetation can directly and indirectly alter subsurface water movement through (1) root water uptake, (2) the generation of root structures, (3) alteration of soil properties, and (4) a direct impact on the hydrological fluxes (e.g. evapotranspiration, interception etc.).

Although often not considered in land use change studies, vegetation can affect soil moisture patterns and subsurface water movement indirectly by affecting the soil properties. Forest soils typically have high root density and large root diameters, low bulk density, more soil fauna and more organic matter enhancement from litter, which can increase the macroporosity and infiltration capacity of soil (Beven and Germann, 1982; Chandler and Chappell, 2008; Price et al., 2010; Ghestem et al., 2011; Archer et al., 2013). In the temperate climate zone, there are only a few studies that have directly investigated the effect of vegetation on soil properties (Archer et al., 2013). Several studies suggested that there is a link between vegetation and infiltration-related soil properties. Chandler and Chappell (2008), Archer et al. (2013) and Price et al. (2010) all found a higher saturated hydraulic conductivity for forested areas as compared to grassland areas. Price et al. (2010) also found that forested sites had lower bulk density and higher moisture storage as compared to lawns and pasture areas. Other studies, however, suggested that this link might not always be present. Although Thompson et al. (2010) found a clear increase in infiltration capacity with increased aboveground

biomass in water-limited ecosystems, the biomass did not seem to affect the infiltration capacity in wetter ecosystems. Geris et al. (2015) also showed that the temporal variability in soil moisture storage was determined by soil properties and not so much by vegetation type. They suggested that the soil properties masked the effect of the above-growing vegetation, and blurred the direct link with the spatial variability in soil moisture.

It is well-established that vegetation can enhance preferential water flow in soil, causing water to bypass a large fraction of the soil matrix (e.g. Beven and Germann, 1982). Preferential flow can be induced by roots, which may even be a strategy to provide the root zone with additional nutrients (Johnson and Lehmann, 2006). Dye tracer studies have shown a large difference in preferential flow occurrence for different vegetation cover and have illustrated the role of trees in subsurface infiltration (Bachmair et al., 2009; Schaik, 2009; Schaik, 2010; Alaoui et al., 2011; Benegas et al., 2014; Bargués Tobella et al., 2014). However, only a small part of these studies are representative for the temperate climate zone (Bachmair et al., 2009; Alaoui et al., 2011). Furthermore, the use of dye tracers provides only a single snapshot in time. Therefore, two recent studies by Demand et al. (2019) and Jin et al. (2018) have used soil moisture response time analysis to characterize difference in flow behaviour related to vegetation. Both studies showed that both the occurrence of preferential flow and the infiltration capacity can be significantly larger in forests as compared to grassland sites.

Overall, these studies showed that the effect of vegetation on soil properties and soil hydrological processes can be ambiguous and that the detection of direct effects of vegetation on soil properties can be rather complex. Unfortunately, the amount of studies that focus on this topic remains limited. A complication within this field is that changes in soil properties by vegetation can be quite slow. Additionally, the distribution of soil hydraulic properties can also be governed by a combination of factors (e.g. geomorphology and landscape-related soil formation; as explained by Lin, 2010), which makes it difficult to assess the direct impact of deforestation.

2.6 Modelling Concepts to Analyse Land Use Change

Hydrological models and their simulation results are an important resource within the field of hydrology, providing (1) an alternative source of information (we cannot measure everywhere), (2) a framework to test existing hypotheses regarding our current understanding of hydrological processes and (3) a platform for forecasting purposes (including uncertainty). Hydrological models can thus also be helpful to analyse hydrological impacts of land use change, for example to test our current understanding of plant-water related processes and to forecast the effects of land use change. Many hydrological models have been developed in a stationary context (Ehret et al., 2014), which implies that future conditions (e.g. discharge or soil moisture) are "statistically indistinguishable from the past" (Matalas, 1998). Therefore, modelling non-stationary conditions, such as those occurring after a land use change, generates a manifold of challenges that hydrologists have been trying to overcome. In the last decades, modelling the effects of vegetation change on hydrological processes has evolved from studies that provided unverified predictions only (e.g. Bultot et al., 1990) to studies where model calibration, time-dynamic parameterizations (e.g Nijzink et al., 2016), validation, and uncertainty in measurements, model structure and parameters played a more important role.

There is a large amount of literature available that reviews the progress in hydrological modelling (Todini, 2007; Beven, 2012; Guswa et al., 2014; Semenova and Beven, 2015; Fatichi et al., 2016), the types of models available (Devi et al., 2015) and their performance (Maxwell et al., 2014; Kollet et al., 2017). Besides these more general topics, there are several reviews available that cover topics directly related to this thesis, including hydrological modelling studies under change (Peel and Blöschl, 2011; Schaefli et al., 2011; Ebel and Mirus, 2014; Ehret et al., 2014; Chen et al., 2015), the modelling of plant-water interactions (Ma et al., 2016; Fatichi et al., 2016), and land use change specific modelling studies (Bronstert et al., 2002; Dwarakish and Ganasri, 2015). Dwarakish and Ganasri (2015) already provided an overview on recent land use related studies within the field of hydrological modelling, which covers a variety of topics (model comparison, scenario-based analysis, validation). Their study, however, does not cover many studies in the

temperate zone and does not provide a detailed comparison of the used approaches (type of model, calibration, validation, etc.).

Here, a set of 53 modelling studies dealing with hydrological impacts of land use change in the temperate zone is compared based on differences in the applied approaches (e.g. area modelled, model used, aim, calibration method, validation method, etc.) in order to illustrate the diversity of existing studies and the development within the field over the past decades. To further limit the scope, only studies that apply hillslope or catchment models have been considered. Most of the considered studies have been conducted in the 21st century, but some older studies have also been included.

2.6.1 Study Area Characteristics and Case Description

As an introduction to the 53 modelling studies, the study site location, the size, and the Mean Annual Precipitation (MAP) of each study is given in Table 2.4. The studies are mainly based in Europe (58.5%) and in the USA and Canada (32%). Several studies use existing data from well-known paired catchment study areas, including Fernow Experimental Forest (Hillman and Verschuren, 1988), H.J. Andrews Experimental forest (Tague and Band, 2001; Waichler et al., 2005; Nijzink et al., 2016), Coweeta (Kokkonen and Jakeman, 2002) and Hubbard Brook (Nijzink et al., 2016), whereas other studies forecast land use related discharge changes in areas that are much larger (e.g. Thames, Rhine and Oder river basin).

Only three studies did not focus on reproducing the hydrological behaviour of an actual catchment. The studies by Eckhardt et al. (2003) and Huisman et al. (2004) used a virtual V-shaped catchment to study effects of land use change on hydrology. Hillman and Verschuren (1988) modelled hillslopes with a finite element model to check the validity of their developed model with different vegetation scenarios (from a full vegetation cover to a bare soil). On average, the investigated catchments have 1100 mm of precipitation per year, an average size of 124900 km^2, and a median size of 311 km^2. Compared to the average size of the experimental catchments (Figure 2.6; Table 2.1), the average size of the modelled catchments is much larger, showing already one big discrepancy between modelling and experimental studies.

TABLE 2.4: Summary of the 53 modelling studies on the effects of land use change on the hydrology in the temperate zone: Information about the study site (location, size and Mean Annual Precipitation (MAP*)). The "S" behind the ID number stands for "Single" model used and the "M" represent the studies with "Multiple" models used.

ID	Reference	Study area	Size [km^2]	MAP* [mm]
1S	Bathurst et al., 2004	Slapton Wood catchment (United Kingdom)	0.94	1500 - 1750*
2S	Brath et al., 2006	Samoggia River basin (Italy)	178	938
3S	Breuer et al., 2006	Upper Aar catchment (Germany)	60	± 800 - 850
4S	Bronstert et al., 2002	Lein catchment (Gernany)	115	770
5S	Bultot et al., 1990	Houille River basin (Belgium)	113.7	± 1000 - 1100
6S	Crooks and Davies, 2001	Thames (England)	± 10000	1480
7S	De Roo et al., 2001	Meuse River basin and upper Oder catchment (EU)	32457; 59162	950; 800
8S	Dunn and Mackay, 1995	Tyne catchment (England)	2000	600 - 1500
9S	Eckhardt et al., 2003	Artificial catchment (V-shape)	2	880
10S	Elfert and Bormann, 2010	Hunte catchment (Germany)	2141	780
11S	Farjad et al., 2017	Elbow River basin (Canada)	1235	1100
12S	Fenicia et al., 2009	Meuse River basin (EU)	± 33000	950
13S	Gilfedder et al., 2012	Tarcutta Creek catchment (Australia)	1700	580 - 1200
14S	Hillman and Verschuren, 1988	Fernow Experimental Forest (USA)	56 m slope	± 1470

TABLE 2.4: Summary of the 53 modelling studies on the effects of land use change on the hydrology in the temperate zone: Information about the study site (location, size and Mean Annual Precipitation (MAP*)). The "S" behind the ID number stands for "Single" model used and the "M" represent the studies with "Multiple" models used.

ID	Reference	Study area	Size [km^2]	MAP* [mm]
15S	Huisman et al., 2004	Artificial catchment (V-shape)	2	880
16S	Hundecha and Bárdossy, 2004	Subarea River Rhine basin (EU)	110000	± 500 - 900
17S	Hurkmans et al., 2009	The Rhine River basin (upstream of Lobitz)	185000	± 500 - 700
18S	Isik et al., 2013	10 sub-catchments Middle Chattahoochee watershed (Georgia, USA)	3.6 - 6.6	± 1270 - 1370
19S	Jackson et al., 2008	Monitoring area Pontbren catchment (United Kingdom)	12.5	1200
20S	Jung et al., 2011	Fanno and Johnson creek catchments (USA)	80.5; 68.3	1300; 1000 - 1530
21S	Kokkonen and Jakeman, 2002	All Coweeta catchments (USA), Yass catchment (Australia)	0.09 - 0.61; 388	1870 - 2500; 630
22S	Krause et al., 2007	Lower Havel River basin (Germany)	198	540
23S	Lahmer et al., 2001	Stepenitz basin and Upper Stör basin (Germany)	575; 1158	650; 890
24S	Lavigne et al., 2004	Famine River watershed (Canada)	728	1170 (923 - 1528)
25S	Nandakumar and Mein, 1997	Stewarts creek, Parwan, Reefton, Black spur, Coranderrk (Australia)	0.016 - 5.20	600 - 1600
26S	Niehoff et al., 2002	Three catchments in the Rhine River basin (EU)	100 – 500	± 500 - 900

TABLE 2.4: Summary of the 53 modelling studies on the effects of land use change on the hydrology in the temperate zone: Information about the study site (location, size and Mean Annual Precipitation (MAP*)). The "S" behind the ID number stands for "Single" model used and the "M" represent the studies with "Multiple" models used.

ID	Reference	Study area	Size [km^2]	MAP* [mm]
27S	Ott and Uhlenbrook, 2004	Dreisam basin (Germany)	258	1500
28S	Ranzi et al., 2002	Mella River basin (Italy)	311.08	$\pm$ 1250
29S	Qi et al., 2009	Trent River basin (USA)	377	1300
30S	Quilbé et al., 2008	Chaudière River watershed (Canada)	6682	1200
31S	Schilling et al., 2014	Racoon River watershed (USA)	$\pm$ 9400	850
32S	Schnorbus and Alila, 2004	Redfish Creek (Canada)	26	1100 - 1600
33S	Sun et al., 1998	Gator National Forest and Bradford Forest (USA)	0.42; 1.40	1329 (839 - 1995)
34S	Sun et al., 2008	Chequamegon-Nicolet National Forest (USA)	6194.31	600 - 900
35S	Sun et al., 2015	Conterminous United States	8080464.3	1200 - 2500
36S	Tague and Band, 2001	Watershed 3, HJ Andrews Experimental Forest (USA)	1.01	>2000
37S	Roosmalen et al., 2009	Western part of Jutland (Denmark), Skjern River basin	1038	1100
38S	Waichler et al., 2005	Watershed 1,2 and 3, HJ Andrews Experimental Forest (USA)	0.96; 0.60; 1.01	2300
39S	Wang et al., 2014	Wolf Bay watershed (USA)	126	1713
40S	Ward et al., 2008	Meuse River basin (EU)	33000	950

TABLE 2.4: Summary of the 53 modelling studies on the effects of land use change on the hydrology in the temperate zone: Information about the study site (location, size and Mean Annual Precipitation (MAP*)). The "S" behind the ID number stands for "Single" model used and the "M" represent the studies with "Multiple" models used.

ID	Reference	Study area	Size [km^2]	MAP* [mm]
41S	Wattenbach et al., 2007	Federal State of Brandenburg (Germany)	29,479	540
42S	Wijesekara et al., 2012	Elbow River watershed (Canada)	1,238	600 - 700
43S	Yu et al., 2015	Lysina Critical Zone Observatory (Czech)	0.293	834.5
44M	Bormann et al., 2007	Dill Catchment (Germany)	693	700-1100
45M	Bormann et al., 2009	Dill Catchment (Germany)	693	700-1100
46M	Breuer et al., 2009	Dill Catchment (Germany)	693	700-1100
47M	Huisman et al., 2009	Dill Catchment (Germany)	693	700-1100
48M	Li et al., 2012	Crawford River catchment, Darlot Creek catchment, Tinana Creek catchment (Australia)	698; 760; 1174	1091; 700; 1038
49M	Morán-Tejeda et al., 2015	Upper Aragin catchment (northern Spain)	1500	750 - 1600
50M	Nijzink et al., 2016	WS1 and WS2 HJ Andrews Experimental Forest, USA; WS2, WS3 and WS5, Hubbard Brook Experimental Forest (USA)	0.96; 0.60; 0.156 ;0.424; 0.219	2300; 1200 - 1500
51M	Richter and Schultz, 1987	Kirchhöder Bach, Leitherbach, Gotenbach (Germany)	6.2; 4.2; 4.4	$\pm$ 800 - 850

TABLE 2.4: Summary of the 53 modelling studies on the effects of land use change on the hydrology in the temperate zone: Information about the study site (location, size and Mean Annual Precipitation (MAP*)). The "S" behind the ID number stands for "Single" model used and the "M" represent the studies with "Multiple" models used.

ID	Reference	Study area	Size [km^2]	MAP* [mm]
52M	Viney et al., 2009	Dill Catchment (Germany)	693	700-1100
53M	VanShaar et al., 2002	Mores Creek, Entiat River, Swan River, Mica Creek (Columbia River basin, USA)	1033, 527, 179, 26.9	850; 1177; 1344; 1190

Table 2.5 provides information on the type of study (land use change scenario or actual land use change) and the specific set-up. The majority of the studies are based on scenarios (64%) or a mixture of a real case and scenarios (13%). A range of studies with multiple scenarios focus on the effects of deforestation and afforestation (Hillman and Verschuren, 1988; Sun et al., 1998; Lavigne et al., 2004; Schnorbus and Alila, 2004; Jackson et al., 2008; Morán-Tejeda et al., 2015; Yu et al., 2015) and urbanization (or % impervious surface) (Richter and Schultz, 1987; Tague and Band, 2001; Bronstert et al., 2002; Ranzi et al., 2002; Hundecha and Bárdossy, 2004; Isik et al., 2013; Wang et al., 2014). Other scenarios are based on land use change models (Niehoff et al., 2002; Ott and Uhlenbrook, 2004; Wattenbach et al., 2007; Huisman et al., 2009; Hurkmans et al., 2009; Viney et al., 2009; Jung et al., 2011; Wijesekara et al., 2012), or specifically focus on a change in spatial arrangement of land use (Dunn and Mackay, 1995; Eckhardt et al., 2003; Breuer et al., 2006; Bormann et al., 2009). Although the majority of the studies has a strict focus on simulating the hydrological effects of land use change, ten studies include the simultaneous effects of climate and land use change (Sun et al., 1998; Lahmer et al., 2001; Waichler et al., 2005; Quilbé et al., 2008; Ward et al., 2008; Roosmalen et al., 2009; Elfert and Bormann, 2010; Jung et al., 2011; Wang et al., 2014; Farjad et al., 2017).

TABLE 2.5: Information about the specific case study/ scenarios used in the 53 modelling studies (on the effects of land use change on the hydrology in the temperate zone).

ID	Reference	Scenario/ Real case	Simulated case(s)
1S	Bathurst et al., 2004	Real case	Hydrology at Slapton Woods (1989 - 1991).
2S	Brath et al., 2006	Real case	Flood simulation for reference years 1955, 1980, 1992.
3S	Breuer et al., 2006	Scenarios	Introduction of outwintering suckler cow management (>0,25 and 50% land rent increase).
4S	Bronstert et al., 2002	Scenarios	The effects of urbanization (increase of 10 and 50%) and the importance of incorporating preferential flow in a modelling framework.
5S	Bultot et al., 1990	Scenarios	(1) Simulation of the same catchment under different land use conditions and (2) increase of impervious surface area within the catchment.
6S	Crooks and Davies, 2001	Real case	Land use change in the Thames river basin.
7S	De Roo et al., 2001	Real case	Simulation of land use change using classified land use maps (1975; 1992).
8S	Dunn and Mackay, 1995	Scenarios	Application of different land use types to an upland and a lowland sub-catchment of the Tyne Basin.
9S	Eckhardt et al., 2003	Scenarios	(1) Uniform land use - arable land, pasture, deciduous forest, coniferous forest, (2) land cover change in only parts of the catchment (different start vegetation and different vegetation changes).
10S	Elfert and Bormann, 2010	Scenarios and real case	Real observed land use change between 1990 - 2000. Agricultural land use change scenarios based on the Special Report on Emissions Scenarios (SRES) of the IPCC.
11S	Farjad et al., 2017	Scenarios	Mixture of land use change and climate change scenarios.

TABLE 2.5: Information about the specific case study/ scenarios used in the 53 modelling studies (on the effects of land use change on the hydrology in the temperate zone).

ID	Reference	Scenario/ Real case	Simulated case(s)
12S	Fenicia et al., 2009	Real case	Ninety years of discharge data from the Meuse River basin.
13S	Gilfedder et al., 2012	Scenarios	Plantation expansion scenarios (increase in stem volume).
14S	Hillman and Verschuren, 1988	Real case and scenarios	1D Vertical infiltration, 2D Forest slope simulation, Reynold creek experimental catchment case study.
15S	Huisman et al., 2004	Scenarios	Land use change: stepwise transition from cropland to pasture, including five sensitivity scenarios with changes in soil hydraulic properties.
16S	Hundecha and Bárdossy, 2004	Scenarios	(1) Doubling of urbanization (uniform in space); (2) changing the land use of the whole catchment into forest.
17S	Hurkmans et al., 2009	Scenarios	Four land use scenarios from the EURURALIS project (www.EURURALIS.EU).
18S	Isik et al., 2013	10 Scenarios and real case	Ten land use change scenarios, generated by changing the percentage in forested, pasture and urban area (5 cases) within the two reference catchments.
19S	Jackson et al., 2008	Scenarios	Placement of a (1) horizontal or (2) vertical tree belt (80 * 15 m) within a 100 * 100 m hillslope area.
20S	Jung et al., 2011	Scenarios	Two land use change scenarios based on the Pacific Northwest Ecosystem Research Consortium: (1) ecosystem protection and restoration (2) development - greater expansion of urban growth boundaries. Additionally, two climate scenarios based on coupled atmosphere-ocean general circulation model simulations (medium and low emission scenarios).

TABLE 2.5: Information about the specific case study/ scenarios used in the 53 modelling studies (on the effects of land use change on the hydrology in the temperate zone).

ID	Reference	Scenario/ Real case	Simulated case(s)
21S	Kokkonen and Jakeman, 2002	Real case	Simulating discharge in Coweeta catchments for the entire monitoring period. Evaluating the effect of irrigation dams in the Yass catchment.
22S	Krause et al., 2007	Scenarios	Four land use scenarios: (1) 'best nature conservation', (2) 'actual trend', (3) 'best water quality' and (4) 'best management practice' and one drainage network change scenario, (5) drainage density reduction scenario.
23S	Lahmer et al., 2001	Scenarios	A reference scenario (data 1951 -1990), two climate scenarios (1.5 K and 3.0K increase between 1996 and 2050) and land use change scenarios: conversion of arable land into (1) pasture, (2) meadow, (3) forest, and (4) set aside.
24S	Lavigne et al., 2004	Scenarios	Basic scenario (actual land use) and a deforestation scenario (change of deciduous and coniferous forests into bare soil areas - 71% of the area was altered).
25S	Nandakumar and Mein, 1997	Real case and scenarios	Error/uncertainty implications for detectable change (significance level of 90%) in discharge.
26S	Niehoff et al., 2002	Scenarios	Land use change scenarios using the LUCK (Land Use Scenario Kit) modelling tool: (1) urbanization; (2) altered agricultural management.
27S	Ott and Uhlenbrook, 2004	Scenarios	Land use change: (1) urbanization (Land Use Scenario Kit model; 100% increase); (2) natural conditions. Rainfall scenarios: 4 different storm durations, reoccurrence intervals & intensity distribution.

TABLE 2.5: Information about the specific case study/ scenarios used in the 53 modelling studies (on the effects of land use change on the hydrology in the temperate zone).

ID	Reference	Scenario/ Real case	Simulated case(s)
28S	Ranzi et al., 2002	Real case	Land use cases for the year 1954 and 1994 based on areal photographs, showing an increase in forest in the upper part of the basin and an increase of urbanization in the valley bottom.
29S	Qi et al., 2009	Scenarios	One baseline case and 7 alternative scenarios with a variety in % forest, % crop/grass, % urban, and% water.
30S	Quilbé et al., 2008	Scenarios	Meteorological scenario 1970 - 1999 and 2010 - 2039. Land use scenarios: (a) increase in agricultural land use increase and (b) afforestation ,which include future climate change (scenario 2010 -2039).
31S	Schilling et al., 2014	Scenarios	One baseline scenario and 4 land use change scenarios: (SG) cropland conversion to switchgrass; (SW50) 50% - upper part of cropland area replaced by switchgrass; (SGSouth) Switchgrass plantation in the South Racoon catchment; (CSCAAA) Cropland replaced by Corn/ soybean/ alfalfa rotation.
32S	Schnorbus and Alila, 2004	Scenarios	11 Scenarios: one current forest condition, 7 scenarios with 1/3 and 2/3 - proportion of sub catchment deforestation, 3 with total deforestation of part of the subcatchments (including one with complete deforestation).
33S	Sun et al., 1998	Scenarios & real case	Three forest harvesting methods + three climatic conditions. Long term effects of deforestation: Bradford forest data.

TABLE 2.5: Information about the specific case study/ scenarios used in the 53 modelling studies (on the effects of land use change on the hydrology in the temperate zone).

ID	Reference	Scenario/ Real case	Simulated case(s)
34S	Sun et al., 2008	Real case	Evapotranspiration at five different sites in the Chequamegon-Nicolet National Forest, USA over two growing cycles.
35S	Sun et al., 2015	Scenarios	18 Scenarios, including a baseline scenario, several LAI change scenarios, several precipitation and temperature scenarios, other climate change scenarios (based on general circulation models), and a mixture of climate and LAI change scenarios.
36S	Tague and Band, 2001	Real case and scenarios	Scenarios with different road cut depths and road-stream connectivity.
37S	Roosmalen et al., 2009	Scenarios	Climate change scenarios: special report on emission scenarios A2 and B2, including a sea level rise of 0.5 and 1 m respectively. Land use change: increase in agricultural demand; doubling forest area (originally grass and agriculture).; changes in crop development dates; reduction in transpiration (climate case).
38S	Waichler et al., 2005	Real cases	Reproducing the basic conditions in the H.J. Andrews catchments, simulating the effects of actual land use change, assessing the additional impact of different climate conditions. Plus a scenario based approach: simulate two different land use trajectories in the same catchment.
39S	Wang et al., 2014	Scenarios	4 main scenarios: (1) a baseline scenario, (2) a set of climate 252 change scenarios (2) a set of 3 land use change scenarios - urbanization scenarios (4) a set of 756 mixed climate change-land use change scenarios.

TABLE 2.5: Information about the specific case study/ scenarios used in the 53 modelling studies (on the effects of land use change on the hydrology in the temperate zone).

ID	Reference	Scenario/ Real case	Simulated case(s)
40S	Ward et al., 2008	Scenarios	Discharge simulations for two time-slices (scenarios) including land use and climate specific information: 4000 - 3000 BP (land use: fully forested) and 1000 - 2000 AD (land use: anthropogenic influence, reconstruction from historic sources).
41S	Wattenbach et al., 2007	Scenarios	A baseline condition and two scenarios: (1) partial liberalisation (9.4% of the total state area - agricultural land - converted to forest) and (2) forest management (stepwise 100% conversion of coniferous forest to deciduous forest - 29.2% of the total state area)
42S	Wijesekara et al., 2012	Scenarios	Different land use change scenarios based on a cellular automata algorithm. Scenarios include one initial condition, and conditions for the years 2011, 2016, 2021, 2026, and 2031.
43S	Yu et al., 2015	Scenarios	Selective cutting scenarios: rotation of patch age based on a catchment with 10 different types of patches. These past scenarios are based on the real history of the area.
44M	Bormann et al., 2007	Scenarios	1 baseline and 3 alternative scenarios: (0.5 ha) - increase in forest and pasture, (1.5 ha) - a decrease in forest and pasture and an increase in crops, (5.0 ha) - decrease in forest and increase in crops.

TABLE 2.5: Information about the specific case study/ scenarios used in the 53 modelling studies (on the effects of land use change on the hydrology in the temperate zone).

ID	Reference	Scenario/ Real case	Simulated case(s)
45M	Bormann et al., 2009	Scenarios	Resolution scenarios: the use of datasets, aggregated datasets (25 m) to grid sizes of 50 m, 75 m, 100 m, 150 m, 200 m, 300 m, 500 m, 1 km, and 2 km. Land use scenarios: (1) random distribution, and (2) height based scenarios (different land use is placed at different elevations)
46M	Breuer et al., 2009	Scenarios	(1) Present-day simulations, compared to real discharge observations in the Dill catchment. (2)Assessing the effect of two model input data sets on the outcome (heterogeneous vs. homogeneous).
47M	Huisman et al., 2009	Scenarios	Land use change scenarios generated by the ProLand model. The different land use change scenarios were based on different "average field sizes" (0.5, 1.5 and 5 ha). Generally: a shift from a more forested environment to more agriculture and pasture landscape for an increasing average field size is given.
48M	Li et al., 2012	Real case	Calibration for one of the periods (forested/deforested) and predicting the discharge of the other period under similar conditions.
49M	Morán-Tejeda et al., 2015	Scenarios	Three climate scenarios (from three different regional climate model projections: highest, medium and lowest temperature increase). Land use scenarios include: (1) the current land use (2) afforestation of altitudinal forest (replacement of pastures/shrubs), (3) wildfire scenario.

TABLE 2.5: Information about the specific case study/ scenarios used in the 53 modelling studies (on the effects of land use change on the hydrology in the temperate zone).

ID	Reference	Scenario/ Real case	Simulated case(s)
50M	Nijzink et al., 2016	Real case	Investigation of temporal changes in root zone capacities for three different catchments at HJ Andrews that were deforested (and had a regrowth phase afterwards).
51M	Richter and Schultz, 1987	Real case	61 Storm events of 3 "test catchments" with different percentages of impervious surface areas.
52M	Viney et al., 2009	Scenarios	Current land use simulations with different model ensembles.
53M	VanShaar et al., 2002	Scenario and real case	Simulation of four different catchments in the Columbia River basin with 2 vegetation scenarios (1990 and 1900), using "current" (1990) and historical "vegetation images".

2.6.2 Hydrological Models

A wide range of models has been used to study the effect of land use change on hydrology (Table 2.6). Each of these models represents its own hypothesis on how vegetation influences the hydrological cycle, including specific equations used to describe the involved hydrological processes with parameters and different input data requirements. To compare the different approaches used in the set of modelling studies, two important model functionality and complexity criteria have been used: the level of process description and the spatial discretization. The level of process description evaluates the conversion of hydrological processes into mathematical formulations and is divided into three categories: physically based, conceptual and empirical. Empirical models are based on regression analysis of experimental datasets, and include parameters that do not have a specific physical meaning. Conceptual models often use heuristic equations that represent processes in a hydrological system in a simplified manner. Physically-based models typically use partial differential equations to express the movement of water through space (subsurface, surface and atmosphere). The spatial discretization of

hydrological models can be roughly divided into three groups: distributed, semi-distributed and lumped. Whereas lumped models represent the catchment as one main unit (often with multiple "vertical" compartments in it to represent the different storages), distributed models divide the catchment into many user-defined sub-units (mostly both in horizontal and vertical direction). Semi-distributed models are in between both approaches and provide the option to divide the catchment into a user-defined amount of subcatchments or Hydrological Response Units (HRU). In catchment hydrology, lumped and semi-distributed models are typically of a conceptual nature, whereas physically-based models are typically distributed.

The value of distributed physically based (bottom-up) versus lumped/ semi-distributed conceptual modelling strategies (top-down) is a topic of continuing controversy in catchment hydrology (e.g. Savenije and Hrachowitz, 2017; Beven et al., 2015; Fatichi et al., 2016). In general, both approaches have their benefits and disadvantages when it comes to modelling abrupt system changes, such as deforestation. Distributed physically-based models can account for spatially complex changes in land use (Beven, 2012) and use a more realistic representation of the physics of the hydrological processes, but are often more challenging to calibrate due to the large amount of parameters that can be tuned. In the end, the model choice often depends on the variables of interest and the related question to be answered.

In the evaluated modelling studies, mainly conceptual and physically based models have been applied. Only Isik et al. (2013) used an empirical modelling approach to study the hydrological effects of land use change. They used an artificial neural network (ANN) mixed with the Soil Conservation Service curve number approach to predict discharge in catchments with different land use. Frequently used models in the 53 modelling studies considered here include different versions of the physically-based fully distributed models MIKE-SHE (versions: SHETRAN, MIKE-SHE, MIKE 11), WaSiM (versions: WaSiM, WaSiM-ETH), and the more conceptual semi-distributed model SWAT (versions: SWAT, SWAT-G). In combination with seven other hydrological models of varying complexity and spatial discretization (DHSVM, HBV, IHACRES, LASCAM, PRMS, SLURP, TOPLATS), these three models were used in four inter-comparison studies (Bormann et al., 2009; Breuer and Huisman, 2009; Breuer et al., 2009; Huisman et al., 2009; Viney

et al., 2009). Other models that occur more frequently include the conceptual semi-distributed models HBV (versions: HBV-IMS, HBV), VIC, FLEX and PRMS and the fully-distributed physically based models DHSVM and RHESSys.

Evaluation of the applied models in the 53 assessed deforestation studies mainly emphasized the large arsenal of different models that already have been applied to carry out deforestation or land use change related studied, which has both its pros and cons. A positive aspect of the available range of models is that hydrological land use change forecast can be individualized based on the available data and study objective. A negative aspect of this variety of models, combined with the different research aims, is that this limits the opportunity to directly compare studies. The existing model variety requires detailed knowledge on differences in process description of all individual models. This directly signalizes the importance of model intercomparison studies, such as the LUCHEM project ("assessing the impact of Land Use Change on Hydrology by Ensemble Modelling"; Breuer et al., 2009; Huisman et al., 2009; Viney et al., 2009; Bormann et al., 2009), where differences and similarities in current system simulations and future predictions can be assessed in detail.

TABLE 2.6: Information about models applied in the 53 modelling studies (on the effects of land use change on the hydrology in the temperate zone), ID: S = single model studies, M = multiple models studies. Certain models contain a mixture of physically based and conceptual approaches. Here, the main tendency of the model is given.

ID	Reference	Hydrological Model(s)	Process description	Spatial discretization
1S	Bathurst et al., 2004	SHETRAN	Physically based	Distributed
2S	Brath et al., 2006	Spatially distributed continuous simulation approach	Physically based	Distributed
3S	Breuer et al., 2006	SWAT-G	Conceptual	Semi-distributed

TABLE 2.6: Information about models applied in the 53 modelling studies (on the effects of land use change on the hydrology in the temperate zone), ID: S = single model studies, M = multiple models studies. Certain models contain a mixture of physically based and conceptual approaches. Here, the main tendency of the model is given.

ID	Reference	Hydrological Model(s)	Process description	Spatial discretization
4S	Bronstert et al., 2002	WaSiM-ETH	Physically based	Distributed
5S	Bultot et al., 1990	IRMB	Conceptual	Lumped
6S	Crooks and Davies, 2001	CLASSIC	Conceptual	Semi-distributed
7S	De Roo et al., 2001	LISFLOOD	Physically based	Distributed
8S	Dunn and Mackay, 1995	SHETRAN	Physically based	Distributed
9S	Eckhardt et al., 2003	SWAT-G	Conceptual	Semi-distributed
10S	Elfert and Bormann, 2010	WaSiM-ETH	Physically based	Distributed
11S	Farjad et al., 2017	MIKE-SHE/ MIKE 11	Physically based	Distributed
12S	Fenicia et al., 2009	FLEX model	Conceptual	Lumped
13S	Gilfedder et al., 2012	Gwlag + PERFECT	Conceptual	Lumped
14S	Hillman and Verschuren, 1988	SUBFEM	Physically based	Distributed
15S	Huisman et al., 2004	SWAT-G	Conceptual	Semi-distributed
16S	Hundecha and Bárdossy, 2004	HBV-IWS	Conceptual	Semi-distributed
17S	Hurkmans et al., 2009	VIC	Conceptual	Semi-distributed
18S	Isik et al., 2013	Hybrid ANN model (Artificial Neural Network)	Empirical	Lumped

TABLE 2.6: Information about models applied in the 53 modelling studies (on the effects of land use change on the hydrology in the temperate zone), ID: S = single model studies, M = multiple models studies. Certain models contain a mixture of physically based and conceptual approaches. Here, the main tendency of the model is given.

ID	Reference	Hydrological Model(s)	Process description	Spatial discretization
19S	Jackson et al., 2008	SPW	Physically based	Distributed
20S	Jung et al., 2011	PRMS	Physically based	Distributed
21S	Kokkonen and Jakeman, 2002	IHACRES	Conceptual	Lumped
22S	Krause et al., 2007	IWAN (WaSiM-ETH and MODFLOW)	Physically based	Distributed
23S	Lahmer et al., 2001	ArcEGMO	Physically based	Distributed
24S	Lavigne et al., 2004	HYDROTEL	Physically based	Semi-distributed
25S	Nandakumar and Mein, 1997	Monash model (HYDROLOG)	Conceptual	Semi-distributed
26S	Niehoff et al., 2002	WaSiM-ETH (incl. Macropore module)	Physically based	Distributed
27S	Ott and Uhlenbrook, 2004	TACd	Conceptual	Distributed
28S	Ranzi et al., 2002	Hydrological flood model	Conceptual	Distributed
29S	Qi et al., 2009	PRMS	Physically based	Distributed
30S	Quilbé et al., 2008	HYDROTEL	Physically based	Semi-distributed
31S	Schilling et al., 2014	SWAT	Conceptual	Semi-distributed
32S	Schnorbus and Alila, 2004	DHSVM	Physically based	Distributed

TABLE 2.6: Information about models applied in the 53 modelling studies (on the effects of land use change on the hydrology in the temperate zone), ID: S = single model studies, M = multiple models studies. Certain models contain a mixture of physically based and conceptual approaches. Here, the main tendency of the model is given.

ID	Reference	Hydrological Model(s)	Process description	Spatial discretization
33S	Sun et al., 1998	FLATWOODS	Physically based	Distributed
34S	Sun et al., 2008	MIKE-SHE	Physically based	Distributed
35S	Sun et al., 2015	WaSSI	Conceptual	Semi-distributed
36S	Tague and Band, 2001	RHESSys	Physical based	Distributed
37S	Roosmalen et al., 2009	DK Model (version MIKE-SHE)	Physically based	Distributed
38S	Waichler et al., 2005	DHSVM	Physically based	Distributed
39S	Wang et al., 2014	SWAT	Conceptual	Semi-distributed
40S	Ward et al., 2008	STREAM	Conceptual	Distributed
41S	Wattenbach et al., 2007	SWIM + Forest Growth (Wattenbach et al., 2005)	Conceptual	Semi-distributed
42S	Wijesekara et al., 2012	MIKE-SHE/MIKE-11	Physically based	Distributed
43S	Yu et al., 2015	PIHM	Physically based	Distributed
44M	Bormann et al., 2007	SWAT, TOPLATS, WASIM	Conceptual, physically based, physically based	Semi-distributed, distributed, distributed

TABLE 2.6: Information about models applied in the 53 modelling studies (on the effects of land use change on the hydrology in the temperate zone), ID: S = single model studies, M = multiple models studies. Certain models contain a mixture of physically based and conceptual approaches. Here, the main tendency of the model is given.

ID	Reference	Hydrological Model(s)	Process description	Spatial discretization
45M	Bormann et al., 2009	SWAT, TOPLATS, WASIM	Conceptual, physically based, physically based	Semi-distributed, distributed, distributed
46M	Breuer et al., 2009	DHSVM, HBV, IHACRES, LASCAM, MIKE-SHE, PRMS, SLURP, SWAT, TOPLATS, WASIM	p, c, c, c, p, p, c, c, p, p*	d, s, l, s, d, s, s, s, d, d**
47M	Huisman et al., 2009	DHSVM, HBV, IHACRES, LASCAM, MIKE-SHE, PRMS, SLURP, SWAT, TOPLATS, WASIM	p, c, c, c, p, p, c, c, p, p*	d, s, l, s, d, s, s, s, d, d**
48M	Li et al., 2012	Xinanjiang and SIMHYD	Conceptual, conceptual	Semi-distributed, lumped
49M	Morán-Tejeda et al., 2015	RHESSis and SWAT	Physically based, conceptual	Distributed, semi-distributed

TABLE 2.6: Information about models applied in the 53 modelling studies (on the effects of land use change on the hydrology in the temperate zone), ID: S = single model studies, M = multiple models studies. Certain models contain a mixture of physically based and conceptual approaches. Here, the main tendency of the model is given.

ID	Reference	Hydrological Model(s)	Process description	Spatial discretization
50M	Nijzink et al., 2016	FLEX, TUW, HYMOD, HYPE	All conceptual	Lumped, semi-distributed, lumped, semi-distributed
51M	Richter and Schultz, 1987	Idealized unit hydrograph model, HYREUN model, parallel cascade model	Conceptual, conceptual, empirical	Lumped, semi-distributed, lumped
52M	Viney et al., 2009	DHSVM, HBV, IHACRES, LASCAM, MIKE-SHE, PRMS, SLURP, SWAT, TOPLATS, WASIM	p, c, c, c, p, p, c, c, p, p*	d, s, l, s, d, s, s, s, d, d**
53M	VanShaar et al., 2002	DHSVM, VIC	Physically based, conceptual	Distributed, semi-distributed

* p = physically based, c = conceptual, ** d = distributed, s = semi-distributed, l = lumped.

2.6.3 Calibration and Validation

To assess the value of a given model in predicting the hydrological effects of land use change, the modelling results need to be put into context. For this purpose, the assessment of model performance in the calibration and validation phase is a crucial first step. Table 2.7 and Table 2.8 provide information

on the calibration and validation used in the different studies, including information on the type of calibration (if any), the type of measurements used for evaluation, and the measure of fit used in the evaluation. Overall, the majority of the studies have used calibration (80%). A similar percentage of all studies (75%) have considered a validation period, although not all of these studies also included a calibration period (blind validation). Generally, model calibration and validation does only assure that streamflow response (or other assigned calibration variables) are reproduced. It does not ensure that the behaviour of the catchment is accurately represented. Therefore, calibration of predicted changes to measured effects can be rather problematic for further predictions, which is why Ewen and Parkin (1996) proposed a blind validation strategy, where the modeller is not allowed to see the output data of the catchment and can thus not calibrate. A good example of the use of blind validation is the study by Bathurst et al. (2004), who applied this concept for the SHETRAN model and showed that the water balance and important event-based features could be represented. Although this method proposes a very objective way to look at models, it is probably the harshest test available.

TABLE 2.7: Information about the calibration of the 53 modelling studies (on the effects of land use change on hydrology in the temperate zone), including the calibrated variable(s) (Q = discharge, ET = evapotranspiration, GW = groundwater, Ssnow = snow storage, ψ_m = matrix potential), and the evaluation criteria (Emb = mass balance errors, Ev = volume errors, Ewb = water balance errors, KGE = Kling-Gupta Efficiency, MAE = mean absolute error, MSE = mean square error, Pearson R = Pearson correlation coefficient, R = correlation coefficient, R^2 = coefficient of determination, RMSE = root mean square error, SSWR = squared sum of weighted residuals). The ID indicates whether it was a single (S) or a multi-model study (M).

ID	Reference	Calibration	Type (manual/ automatic)	Calibration data	Measure(s) of fit
1S	Bathurst et al., 2004	No	-	No calibration	No calibration
2S	Brath et al., 2006	Yes	Manual	Q (storm event)	Visual inspection
3S	Breuer et al., 2006	No	-	No calibration	No calibration

TABLE 2.7: Information about the calibration of the 53 modelling studies on the effects of land use change on hydrology in the temperate zone, including the calibrated variable(s) (Q = discharge, ET = evapotranspiration, GW = groundwater, Ssnow = snow storage, ψ_m = matrix potential), and the evaluation criteria (Emb = mass balance errors, Ev = volume errors, Ewb = water balance errors, KGE = Kling-Gupta Efficiency, MAE = mean absolute error, MSE = mean square error, Pearson R = Pearson correlation coefficient, R = correlation coefficient, R^2 = coefficient of determination, RMSE = root mean square error, SSWR = squared sum of weighted residuals). The ID indicates whether it was a single (S) or a multi-model study (M).

ID	Reference	Calibration	Type (manual/ automatic)	Calibration data	Measure(s) of fit
4S	Bronstert et al., 2002	No	-	No calibration	No calibration
5S	Bultot et al., 1990	Yes	(No information)	(No information)	(No information)
6S	Crooks and Davies, 2001	Yes	(No information)	Q (daily)	NSE
7S	De Roo et al., 2001	No	-	No calibration	No calibration
8S	Dunn and Mackay, 1995	No	-	No calibration	No calibration
9S	Eckhardt et al., 2003	Yes	(No information)	Q (outlet)	Long term means, NSE
10S	Elfert and Bormann, 2010	Yes	(No information)	Q (different gauges)	Ewb, R^2 and NSE
11S	Farjad et al., 2017	Yes	(No information)	Ssnow,Q, GW	MAE, Pearson R

TABLE 2.7: Information about the calibration of the 53 modelling studies on the effects of land use change on hydrology in the temperate zone, including the calibrated variable(s) (Q = discharge, ET = evapotranspiration, GW = groundwater, Ssnow = snow storage, ψ_m = matrix potential), and the evaluation criteria (Emb = mass balance errors, Ev = volume errors, Ewb = water balance errors, KGE = Kling-Gupta Efficiency, MAE = mean absolute error, MSE = mean square error, Pearson R = Pearson correlation coefficient, R = correlation coefficient, R^2 = coefficient of determination, RMSE = root mean square error, SSWR = squared sum of weighted residuals). The ID indicates whether it was a single (S) or a multi-model study (M).

ID	Reference	Calibration	Type (manual/ automatic)	Calibration data	Measure(s) of fit
12S	Fenicia et al., 2009	Yes***	Automatic, GLUE	Q	NSE (4 year window, 20% best scores)
13S	Gilfedder et al., 2012	Yes	Automatic, PEST	Q (daily)	SSWR, NSE
14S	Hillman and Verschuren, 1988	No	-	No calibration	No calibration
15S	Huisman et al., 2004	Yes	(No information)	Q (outlet)	Long term means, NSE
16S	Hundecha and Bárdossy, 2004	Yes	Automatic, numerical optimization algorithm	Q	R^2(Q weighted)
17S	Hurkmans et al., 2009	Yes	Build-in optimization algorithm	Q	R,NSE
18S	Isik et al., 2013	Yes	Training algorithm (ANN)	Q (baseflow, stormflow)	R^2, NSE, bias ratio

TABLE 2.7: Information about the calibration of the 53 modelling studies on the effects of land use change on hydrology in the temperate zone, including the calibrated variable(s) (Q = discharge, ET = evapotranspiration, GW = groundwater, Ssnow = snow storage, ψ_m = matrix potential), and the evaluation criteria (Emb = mass balance errors, Ev = volume errors, Ewb = water balance errors, KGE = Kling-Gupta Efficiency, MAE = mean absolute error, MSE = mean square error, Pearson R = Pearson correlation coefficient, R = correlation coefficient, R^2 = coefficient of determination, RMSE = root mean square error, SSWR = squared sum of weighted residuals). The ID indicates whether it was a single (S) or a multi-model study (M).

ID	Reference	Calibration	Type (manual/ automatic)	Calibration data	Measure(s) of fit
19S	Jackson et al., 2008	Yes	Automatic, Monte Carlo	Drain flow, overland flow and ψ_m	Visual inspection
20S	Jung et al., 2011	Yes	Automatic optimization	Q	(No information)
21S	Kokkonen and Jakeman, 2002	Yes	Automatic optimization	Q	Ewb (relative), NSE
22S	Krause et al., 2007	Yes	(No information)	GW (spatiotemporal)	MSE
23S	Lahmer et al., 2001	No	-	No calibration	No calibration
24S	Lavigne et al., 2004	Yes	(No information)	Q	NSE
25S	Nandakumar and Mein, 1997	Yes	Automatic	Q	R^2, NSE
26S	Niehoff et al., 2002	No	-	No calibration	No calibration

TABLE 2.7: Information about the calibration of the 53 modelling studies on the effects of land use change on hydrology in the temperate zone, including the calibrated variable(s) (Q = discharge, ET = evapotranspiration, GW = groundwater, Ssnow = snow storage, ψ_m = matrix potential), and the evaluation criteria (Emb = mass balance errors, Ev = volume errors, Ewb = water balance errors, KGE = Kling-Gupta Efficiency, MAE = mean absolute error, MSE = mean square error, Pearson R = Pearson correlation coefficient, R = correlation coefficient, R^2 = coefficient of determination, RMSE = root mean square error, SSWR = squared sum of weighted residuals). The ID indicates whether it was a single (S) or a multi-model study (M).

ID	Reference	Calibration	Type (manual/ automatic)	Calibration data	Measure(s) of fit
27S	Ott and Uhlenbrook, 2004	Yes	Manual	Q (subbasins)	NSE, log (NSE), Ev, R^2
28S	Ranzi et al., 2002	No	-	No calibration	No calibration
29S	Qi et al., 2009	Yes	(No information)	Q (of 22 HRU)	NSE, relative Ev (day, month)
30	Quilbé et al., 2008	Yes	(No information)	Q(outlet)	NSE
31S	Schilling et al., 2014	Yes	(No information)	Q (monthly)	NSE, R^2
32S	Schnorbus and Alila, 2004	Yes	Manual	Q (forested +clearcut)	NSE, R^2, Ev (relative)
33S	Sun et al., 1998	Yes	(No information)	Q and GW (wet + dry)	Pearson R
34S	Sun et al., 2008	No	-	No calibration	No calibration
35S	Sun et al., 2015	No	-	No calibration	No calibration

TABLE 2.7: Information about the calibration of the 53 modelling studies on the effects of land use change on hydrology in the temperate zone, including the calibrated variable(s) (Q = discharge, ET = evapotranspiration, GW = groundwater, Ssnow = snow storage, ψ_m = matrix potential), and the evaluation criteria (Emb = mass balance errors, Ev = volume errors, Ewb = water balance errors, KGE = Kling-Gupta Efficiency, MAE = mean absolute error, MSE = mean square error, Pearson R = Pearson correlation coefficient, R = correlation coefficient, R^2 = coefficient of determination, RMSE = root mean square error, SSWR = squared sum of weighted residuals). The ID indicates whether it was a single (S) or a multi-model study (M).

ID	Reference	Calibration	Type (manual/ automatic)	Calibration data	Measure(s) of fit
36S	Tague and Band, 2001	Yes	Automatic, Simplex	Q (daily, unharvested WS 2 (H.J. Andrews)	NSE
37S	Roosmalen et al., 2009	Yes	Automatic, UCODE in steady state	ΔGW (annual +month), Q	RMSE and NSE
38S	Waichler et al., 2005	Yes	Trial-and-error process: Q (annual, month, day)	ET (annual, month, day)	MAE (Q), NSE
39S	Wang et al., 2014	Yes	(No information)	Q (Magnolia River watershed)	Emb, R^2, and NSE
40S	Ward et al., 2008	Yes	(No information)	Q (month, year - wet period, hydrograph	Modelled/ measured, NSE, R^2

TABLE 2.7: Information about the calibration of the 53 modelling studies on the effects of land use change on hydrology in the temperate zone, including the calibrated variable(s) (Q = discharge, ET = evapotranspiration, GW = groundwater, Ssnow = snow storage, ψ_m = matrix potential), and the evaluation criteria (Emb = mass balance errors, Ev = volume errors, Ewb = water balance errors, KGE = Kling-Gupta Efficiency, MAE = mean absolute error, MSE = mean square error, Pearson R = Pearson correlation coefficient, R = correlation coefficient, R^2 = coefficient of determination, RMSE = root mean square error, SSWR = squared sum of weighted residuals). The ID indicates whether it was a single (S) or a multi-model study (M).

ID	Reference	Calibration	Type (manual/ automatic)	Calibration data	Measure(s) of fit
41S	Wattenbach et al., 2007	Yes	(No information)	Q(monthly, multiple catchments)	NSE, Q-difference in %
42S	Wijesekara et al., 2012	Yes	(No information)	Q (three stations)	NSE (monthly)
43S	Yu et al., 2015	Yes	Automatic, Evolutionary algorithm	GW (spatial) and Q (outlet)	relative error (E), Pearson R, NSE
44M	Bormann et al., 2007	Yes	WASIM TOPLATS: manually, SWAT: automatically	Q	Water balance efficiency, NSE
45M	Bormann et al., 2009	Yes	WASIM TOPLATS: manually, SWAT: automatically	Q	NSE, bias
46M	Breuer et al., 2009	Yes**	Manual: DHSVM, MIKE-SHE, TOPLATS, WASIM, SLURP. automatic: SWAT, PRMS, HBV, LASCAM. manual and automatic: IHACRES.	Q (outlet)	NSE, R^2, bias, sum of absolute difference Q

TABLE 2.7: Information about the calibration of the 53 modelling studies on the effects of land use change on hydrology in the temperate zone, including the calibrated variable(s) (Q = discharge, ET = evapotranspiration, GW = groundwater, Ssnow = snow storage, ψ_m = matrix potential), and the evaluation criteria (Emb = mass balance errors, Ev = volume errors, Ewb = water balance errors, KGE = Kling-Gupta Efficiency, MAE = mean absolute error, MSE = mean square error, Pearson R = Pearson correlation coefficient, R = correlation coefficient, R^2 = coefficient of determination, RMSE = root mean square error, SSWR = squared sum of weighted residuals). The ID indicates whether it was a single (S) or a multi-model study (M).

ID	Reference	Calibration	Type (manual/ automatic)	Calibration data	Measure(s) of fit
47M	Huisman et al., 2009	Yes**	manual: DHSVM, MIKE-SHE, TOPLATS, WASIM, SLURP. automatic: SWAT, PRMS, HBV, LASCAM. manual and automatic: IHACRES.	Q (outlet)	NSE, R^2, bias, sum of absolute difference Q
48M	Li et al., 2012	Yes	Generalized pattern search algorithm with linear inequality constraint (MATLAB)	Q (before and after deforestation)	NSE, WBE
49M	Morán-Tejeda et al., 2015	Yes	(1) Manual for vegetation parameters, (2) automatic: Monte Carlo for RHESSis and AMALGAM (Multi-Algorithm optimization) for SWAT.	Q (10 years)	NSE and percentage of bias

TABLE 2.7: Information about the calibration of the 53 modelling studies on the effects of land use change on hydrology in the temperate zone, including the calibrated variable(s) (Q = discharge, ET = evapotranspiration, GW = groundwater, Ssnow = snow storage, ψ_m = matrix potential), and the evaluation criteria (Emb = mass balance errors, Ev = volume errors, Ewb = water balance errors, KGE = Kling-Gupta Efficiency, MAE = mean absolute error, MSE = mean square error, Pearson R = Pearson correlation coefficient, R = correlation coefficient, R^2 = coefficient of determination, RMSE = root mean square error, SSWR = squared sum of weighted residuals). The ID indicates whether it was a single (S) or a multi-model study (M).

ID	Reference	Calibration	Type (manual/ automatic)	Calibration data	Measure(s) of fit
50M	Nijzink et al., 2016	Yes	Automatic: Monte Carlo approach	Q	KGE and log (KGE) and Euclidian distance of the objective functions.
51M	Richter and Schultz, 1987	Yes	(No information provided)	Hydrograph (Q)	Normalized (measured - simulated)
52M	Viney et al., 2009	Yes **	Manual: DHSVM, MIKE-SHE, TOPLATS, WASIM, SLURP. automatic: SWAT, PRMS, HBV, LASCAM. manual and automatic: IHACRES.	Q (outlet)	NSE, R^2, bias, sum of absolute difference (simulated - observed)
53M	VanShaar et al., 2002	Yes	Manual: trial and error	Q (4 years)	Visual inspection

* The model was calibrated twice, one time for a more heterogeneous input dataset (P, LAI and Temp), and a second time for a more homogeneous

input dataset. **Visual inspection is used: only graphs of measured and modelled data have been used to assess model performance (no quantitative evaluation criteria). *** Temporally variable calibration was used in this study.

In total, 62% of all studies have both a calibration and a validation phase, whereas only three studies did not use calibration or validation. In Table 2.7, additional information about the type of calibration (manual or automatic) is also provided. Automatic optimization relies on search algorithms iteratively moving through the parameter space to find one or multiple suitable sets of parameters based on one or multiple measures of fit. Generally, automatic optimization is more objective, but requires more computational effort (also depending on the amount of parameters to be calibrated). Manual calibration, on the other hand, is more subjective, but is fast and simple and might be the only alternative to calibrate computationally intensive physically based distributed hydrological models. About 40% of all modelling studies that used calibration provided no detailed information about the type of calibration that was used. In 34% of the modelling studies, automatic optimization was used to calibrate both physically-based and conceptual models. In most of the ensemble modelling studies, physically-based models were typically calibrated manually, whereas conceptual models relied on automatic calibration (Bormann et al., 2007; Bormann et al., 2009; Breuer et al., 2009; Huisman et al., 2009; Nijzink et al., 2016). Most studies only used discharge data (Q) for calibration and validation (64% and 49% of all studies respectively), often measured at a single station at the catchment outlet. Only a small amount of studies (13% during the calibration period and 23% for the validation period) used other variables, such as groundwater levels (e.g Sun et al., 1998), snow storage (e.g. Farjad et al., 2017), or actual evapotranspiration (e.g. Sun et al., 2008). Some studies also used multiple discharge stations (calibration and validation: 4 studies) and other spatial data for calibration and validation (calibration and validation: 2 studies). Often, only one or two measures of fit were chosen for model evaluation. The most widely used measures of fit were the Nash Sufflex Efficiency (NSE) and the coefficient of determination (R^2).

The evaluation of the presented studies clearly shows some important deficits of current state-of-the-art procedures. One important shortcoming of the presented studies is that none of them has used pre- and post-deforestation data to thoroughly validate. Most of the existing studies that incorporated a

validation procedure used data from the catchment in its current state, and did not evaluate the validity of forecasted scenarios (often future-based). Additionally, the large variety of evaluation criteria makes it harder to compare the results between different studies. The current analysis, however, also provides an overview of performance measures that are more frequently used (e.g. NSE) and therefore offer more chances for model study intercomparison. Finally, the calibration and validation was mostly carried out on one discharge time series only, which is a common problem in hydrological modelling studies and points out the need for datasets with more spatial validation datasets (e.g. Doppler et al., 2014).

TABLE 2.8: Information about the validation of the 53 modelling studies (on the effects of land use change on hydrology in the temperate zone), including the validated variable(s) (Q = discharge, ET = evapotranspiration, GW = groundwater, Ssnow = snow storage, ψ_m = matrix potential), and the evaluation criteria (Emb = mass balance errors, Ev = volume errors, Ewb = water balance errors, KGE = Kling-Gupta Efficiency, MAE = mean absolute error, MSE = mean square error, Pearson R = Pearson correlation coefficient, R = correlation coefficient, R^2 = coefficient of determination, RMSE = root mean square error, SSWR = squared sum of weighted residuals). The ID indicates whether it was a single (S) or a multi-model study (M).

ID	Reference	Validation	Validation data	Measure(s) of fit
1S	Bathurst et al., 2004	Yes	GW, Q, ψ_m	80% of the measurements within the predictive bounds
2S	Brath et al., 2006	Yes	Q	NSE
3S	Breuer et al., 2006	No	No validation	No validation
4S	Bronstert et al., 2002	No	No validation	No validation
5S	Bultot et al., 1990	No	No validation	No validation
6S	Crooks and Davies, 2001	Yes	Q (daily)	NSE
7S	De Roo et al., 2001	Yes (Oder)	Q, ET_0	R^2 with correlation plot

TABLE 2.8: Information about the validation of the 53 modelling studies on the effects of land use change on hydrology in the temperate zone, including the validated variable(s) (Q = discharge, ET = evapotranspiration, GW = groundwater, Ssnow = snow storage, ψ_m = matrix potential), and the evaluation criteria (Emb = mass balance errors, Ev = volume errors, Ewb = water balance errors, KGE = Kling-Gupta Efficiency, MAE = mean absolute error, MSE = mean square error, Pearson R = Pearson correlation coefficient, R = correlation coefficient, R^2 = coefficient of determination, RMSE = root mean square error, SSWR = squared sum of weighted residuals).

ID	Reference	Validation	Validation data	Measure(s) of fit
8S	Dunn and Mackay, 1995	No	No validation	No validation
9S	Eckhardt et al., 2003	No	No validation	No validation
10S	Elfert and Bormann, 2010	Yes	Q (spatial)	Ewb, R^2 and NSE
11S	Farjad et al., 2017	Yes	Ssnow,Q, GW	MAE, Pearson R
12S	Fenicia et al., 2009	No	No validation	No validation
13S	Gilfedder et al., 2012	Yes	Q (daily)	NSE
14S	Hillman and Verschuren, 1988	Yes, partly	Outflow	Only process observation
15S	Huisman et al., 2004	No	No validation	No validation
16S	Hundecha and Bárdossy, 2004	Yes	Q	R^2(Q weighted)
17S	Hurkmans et al., 2009	Yes	Q	R,NSE
18S	Isik et al., 2013	Yes	Q (baseflow, stormflow)	R^2, NSE, bias ratio
19S	Jackson et al., 2008	No	No validation	No validation

TABLE 2.8: Information about the validation of the 53 modelling studies on the effects of land use change on hydrology in the temperate zone, including the validated variable(s) (Q = discharge, ET = evapotranspiration, GW = groundwater, Ssnow = snow storage, ψ_m = matrix potential), and the evaluation criteria (Emb = mass balance errors, Ev = volume errors, Ewb = water balance errors, KGE = Kling-Gupta Efficiency, MAE = mean absolute error, MSE = mean square error, Pearson R = Pearson correlation coefficient, R = correlation coefficient, R^2 = coefficient of determination, RMSE = root mean square error, SSWR = squared sum of weighted residuals).

ID	Reference	Validation	Validation data	Measure(s) of fit
20S	Jung et al., 2011	No	No validation	No validation
21S	Kokkonen and Jakeman, 2002	Yes	Q (17 Coweeta catchments)	Ewb (relative), NSE
22S	Krause et al., 2007	Yes	GW (spatiotemporal)	MSE
23S	Lahmer et al., 2001	Yes	Q (outlet)	Not described
24S	Lavigne et al., 2004	Yes	Q	NSE
25S	Nandakumar and Mein, 1997	No	No validation	No validation
26S	Niehoff et al., 2002	Yes	Urbanisation rate	Correlation of more than 50% between the modelled and the present conditions
27S	Ott and Uhlenbrook, 2004	Yes	Q (subbasins)	NSE, log (NSE), Ev, R^2
28S	Ranzi et al., 2002	Yes	Hydrographs, Q-peaks, Q-volume	Visual inspection and error analysis
29S	Qi et al., 2009	Yes	Q (of 22 HRU)	NSE, relative Ev (day, month)
30	Quilbé et al., 2008	Yes	Q(outlet)	NSE

TABLE 2.8: Information about the validation of the 53 modelling studies on the effects of land use change on hydrology in the temperate zone, including the validated variable(s) (Q = discharge, ET = evapotranspiration, GW = groundwater, Ssnow = snow storage, ψ_m = matrix potential), and the evaluation criteria (Emb = mass balance errors, Ev = volume errors, Ewb = water balance errors, KGE = Kling-Gupta Efficiency, MAE = mean absolute error, MSE = mean square error, Pearson R = Pearson correlation coefficient, R = correlation coefficient, R^2 = coefficient of determination, RMSE = root mean square error, SSWR = squared sum of weighted residuals).

ID	Reference	Validation	Validation data	Measure(s) of fit
31S	Schilling et al., 2014	Yes	Q (monthly)	NSE, R^2
32S	Schnorbus and Alila, 2004	Yes	ΔSsnow, Q	Visual comparison, total flow comparison
33S	Sun et al., 1998	Yes	Q and GW (wet + dry)	Pearson R
34S	Sun et al., 2008	Yes	ET (Eddy Covariance)	Visual comparison, 1:1 line of ET (monthly mean)
35S	Sun et al., 2015	Yes	ET (MODIS) and Q	ET-ET plot and R^2
36S	Tague and Band, 2001	No	No validation	No validation
37S	Roosmalen et al., 2009	Yes	ΔGW (annual +month), Q	RMSE and NSE
38S	Waichler et al., 2005	Yes	Q-relationships (catchments)	Q - regression
39S	Wang et al., 2014	Yes	Q (Magnolia River watershed)	Emb, R^2, and NSE
40S	Ward et al., 2008	Yes	Q (month, year - wet period, hydrograph	Modelled/ measured, NSE, R^2

TABLE 2.8: Information about the validation of the 53 modelling studies on the effects of land use change on hydrology in the temperate zone, including the validated variable(s) (Q = discharge, ET = evapotranspiration, GW = groundwater, Ssnow = snow storage, ψ_m = matrix potential), and the evaluation criteria (Emb = mass balance errors, Ev = volume errors, Ewb = water balance errors, KGE = Kling-Gupta Efficiency, MAE = mean absolute error, MSE = mean square error, Pearson R = Pearson correlation coefficient, R = correlation coefficient, R^2 = coefficient of determination, RMSE = root mean square error, SSWR = squared sum of weighted residuals).

ID	Reference	Validation	Validation data	Measure(s) of fit
41S	Wattenbach et al., 2007	Yes	Q (monthly, spatial)	NSE, Q-difference in %
42S	Wijesekara et al., 2012	Yes	Q (3 stations)	NSE (monthly)
43S	Yu et al., 2015	Yes	GW (spatial) and Q (outlet)	Relative error (E), Pearson R, NSE
44M	Bormann et al., 2007	Yes	Q	bias, NSE and R^2
45M	Bormann et al., 2009	Yes	Q	NSE, bias
46M	Breuer et al., 2009	Yes**	Q (outlet)	NSE, R^2, bias, sum of absolute difference Q
47M	Huisman et al., 2009	Yes **	Q (outlet)	NSE, R^2, bias, sum of absolute difference Q
48M	Li et al., 2012	Yes	Q (before and after deforestation)	NSE, WBE
49M	Morán-Tejeda et al., 2015	Yes	Q (10 years)	NSE and percentage of bias
50M	Nijzink et al., 2016	No	No validation	No validation
51M	Richter and Schultz, 1987	No	No validation	No validation
52M	Viney et al., 2009	Yes**	Q (outlet)	NSE, R^2, bias, sum of absolute difference (simulated - observed)

TABLE 2.8: Information about the validation of the 53 modelling studies on the effects of land use change on hydrology in the temperate zone, including the validated variable(s) (Q = discharge, ET = evapotranspiration, GW = groundwater, Ssnow = snow storage, ψ_m = matrix potential), and the evaluation criteria (Emb = mass balance errors, Ev = volume errors, Ewb = water balance errors, KGE = Kling-Gupta Efficiency, MAE = mean absolute error, MSE = mean square error, Pearson R = Pearson correlation coefficient, R = correlation coefficient, R^2 = coefficient of determination, RMSE = root mean square error, SSWR = squared sum of weighted residuals).

ID	Reference	Validation	Validation data	Measure(s) of fit
53M	VanShaar et al., 2002	Yes	Q (4 years)	Visual inspection

**Visual inspection is used: only graphs of measured and modelled data have been used to assess model performance (no quantitative evaluation criteria).

2.6.4 Predictive Uncertainty (Single Model Studies)

To assess the significance of the predicted hydrological impacts of land use change, an uncertainty propagation analysis should ideally be performed. In such an analysis, different sources of uncertainty should be considered: input uncertainty, parameter uncertainty, and model structural uncertainty. Table 2.9 summarizes eleven single model studies (25.6% of all single model studies considered here) that have quantified the propagation of at least part of the uncertainty to the predicted hydrological impacts. In most cases, only model parameter uncertainty has been analysed. For example, Breuer et al. (2006), Eckhardt et al. (2003), and Huisman et al. (2004) assessed the importance of uncertainty in plant parameters for hydrological predictions based on different land use change scenarios. The propagation of input data uncertainty has also been considered in some studies, for example to account for uncertainty in future climate change predictions (Jung et al., 2011; Wang et al., 2014) or in economic growth predictions (Farjad et al., 2017). It is difficult to assess model structural uncertainty in single model studies. Multi-model studies are best suited for this, as discussed separately in the next section.

TABLE 2.9: Information about the incorporation of uncertainty propagation (result) for the 11/ 43 single model studies on the effects of land use change on the hydrology in the temperate zone that use this approach.

ID	Reference	Type of uncertainty considered	Aim
1S	Bathurst et al., 2004	Parameter uncertainty, instrument and timing uncertainty	Is model within bounds of measurement output + uncertainty?
2S	Brath et al., 2006	Model error (uncertainty)	Asses the uncertainty of the model simulation.
3S	Breuer et al., 2006	Parameter uncertainty (plant)	Is there a significant difference in outcome between 2 vegetation types, considering plant parameter uncertainty?
9S	Eckhardt et al., 2003	Parameter uncertainty (land cover related)	Asses the effect of land-use related parameter uncertainty on output to determine minimum area for which significant changes can be observed.
10S	Elfert and Bormann, 2010	Model uncertainty (water balance error)	To compare the significance of scenario changes to model uncertainty.
11S	Farjad et al., 2017	Predictive uncertainty	Consider uncertainty in long term predictions (economic growth).
12S	Fenicia et al., 2009	Parameter uncertainty	Assess the temporal trend of model parameters (including uncertainty).
15S	Huisman et al., 2004	Parameter uncertainty (plant)	Comparing model sensitivity to model uncertainty - significance of simulations.

TABLE 2.9: Information about the incorporation of uncertainty propagation (result) for the 11/ 43 single model studies on the effects of land use change on the hydrology in the temperate zone that use this approach.

ID	Reference	Type of uncertainty considered	Aim
20S	Jung et al., 2011	Parameter uncertainty and input uncertainty, future land use uncertainty, future emissions uncertainty, natural variability (climate)	Investigate what the main sources of uncertainties are (that affect flood frequency changes).
25S	Nandakumar and Mein, 1997	Parameter uncertainty, input uncertainty	Assess the effect of parameter and input uncertainty - significance of simulations.
39S	Wang et al., 2014	Input uncertainty (climate and rainfall conditions)	Analysing uncertainties from model input (ensemble projections of climate change, land use change and combinations).

2.6.5 Ensemble Modelling and Model Inter-Comparison

Multi-model studies can fulfil multiple purposes. They can provide information on the model structural uncertainty (i.e. uncertainty in the description of the hydrological processes) by simultaneously analysing all simulations as an ensemble. Alternatively, they can be used to compare the predictive quality of individual models, which might help to choose the most suitable model. Table 2.10 summarizes the aim of the ten multi-model studies that were selected here.

TABLE 2.10: Information about the aim of the multi-model studies focussed on the effects of land use change on hydrology in the temperate zone.

ID	Reference	Aim of study
44M	Bormann et al., 2007	Compare the models' sensitivity to land use change with and without the incorporation of changes in soil hydraulic properties.
45M	Bormann et al., 2009	Comparing the models' sensitivity to model resolution (data aggregation - e.g. soil, vegetation and digital elevation model) and to spatial redistribution of land use.
46M	Breuer et al., 2009	Model inter-comparison, using current land use data (present day simulations).
47M	Huisman et al., 2009	Compare the model results for different land use change scenarios and asses the reason for the difference in scenario results among models.
48M	Li et al., 2012	Investigating the increase/decrease in plantations and climate variability on the hydrological cycle.
49M	Morán-Tejeda et al., 2015	Assessing the models' sensitivity to land use and climate change.
50M	Nijzink et al., 2016	To show the importance of incorporating temporally variable root zone capacity in several conceptual hydrological models to simulate vegetation dynamics (in this case: land use change).
51M	Richter and Schultz, 1987	Compare 3 runoff models in their capability to reproduce the hydrological output of real catchments with different impervious surface areas.
52M	Viney et al., 2009	Compare single model - ensemble model output for the Dill river dataset to assess the approach that is best to simulate land use change.
53M	VanShaar et al., 2002	Comparison of the DHSVM and VIC model in simulating the effects of land use change on the hydrology for 4 different catchments in the Columbia River basin.

The oldest study within this group is the study by Richter and Schulz (1987), who performed a model inter-comparison for discharge predictions

for three catchments with different percentages of impervious surface to assess the difference in model performance. Other multi-model studies are documented by VanShaar et al. (2002), Li et al. (2012), Moran-Tejeda et al. (2015), Nijzink et al. (2016). Moran-Tejeda et al. (2015) predicted the hydrological effects of land use and climate change and focussed on model sensitivity and model intercomparison. They reported that SWAT predicted larger changes in hydrological fluxes for climate related scenarios, whereas RHESSys was more sensitive to land use change. Li et al. (2012) simulated the effects of an increase or decrease in plantations with the Xinanjiang and SIMHYD models, and showed that both models had a very similar performance (calibration and validation) and predicted similar hydrological changes. VanShaar et al. (2002) also compared the simulated effects of land use change for the VIC and DHSVM model, showing larger discharge changes being simulated by DHSVM. Nijzink et al. (2016) used an ensemble of four lumped models to simulate root zone storage capacity evolution that were related to land use change. Simulation results showed that root-zone storage capacities were significantly different after deforestation.

A set of five more recent studies by Bormann et al. (2007; 2009), Breuer et al. (2009), Huisman et al. (2009), and Viney et al. (2009) have been conducted within the framework of the LUCHEM project. In this project, ten hydrological models (DHSVM, MIKE-SHE, TOPLATS, WASIM-ETH, SWAT, PRMS, SLURP, HBV, LASCAM and IHACRES) were used to simulate current hydrological catchment behaviour and a set of future scenarios using the same set of input data (Breuer and Huisman, 2009). In these studies, the main interest was (1) a model inter-comparison, (2) a comparative model sensitivity analysis, and (3) analysis of the ensemble model output. Generally, the lumped and semi-distributed models had a better performance during the simulation of the current land use, because they could be automatically calibrated (Breuer et al., 2009). Main differences in long-term water balances between the models could be attributed to their mathematical representation of evapotranspiration. On top of that, model ensembles provided superior predictions compared to single model outcomes (Viney et al., 2009) and increased the reliability of the model predictions (Huisman et al., 2009).

Clearly, the presented studies show that the use of a multi-model framework provides a variety of added values as compared to single modelling

studies. Some of the most important benefits that these studies have demonstrated are that:

- the quality and reliability of model predictions can be increased;
- difference in model performance can be assessed;
- more information about the uncertainty in forecast scenarios can be provided;
- differences in model sensitivity towards scenarios can be evaluated.

2.6.6 Model Outcome Comparison

As clearly demonstrated in the past sections, the selected studies had different aims, used different models, might have used very different study area set-ups and used a large variety of scenarios. Although this made it difficult to directly compare all the results of these studies, the following section aims to summarize the outcome of the different studies. Here, the focus is rather on highlight coherences and controversies in the results of the 53 selected studies, to point out the main strengths of these existing studies, and to follow up with current and future research opportunities that arise from this review.

Markedly, the selected modelling studies that focussed on deforestation showed clear similarities with experimental studies. Most of the modelling studies did not only predict an increase in discharge after deforestation, but also reported additional information on expected changes in the hydrological system. Modelling results by Lavigne et al. (2004) suggested that deforestation increased the soil saturation level and the summer runoff, and generated larger spring peak flows and larger Q/P-ratios. Sun et al. (2008) predicted clear reductions in evapotranspiration in the growing season after forest fire. Sun et al. (1998) did not only simulated a reduced evapotranspiration and an increased discharge, but also predicted increased groundwater levels after deforestation.

Modelling studies that included afforestation scenarios mainly suggested a decrease in discharge, which is also in line with observations from experimental studies. Hundecha and Bárdossy (2004), for example, predicted a clear decrease in discharge and peak flow after afforestation measures.

Quilbe et al. (2008) also predicted a decrease in discharge due to afforestation activities. Jackson et al. (2008) simulated afforestation on a hillslope, suggesting a reduction in peak flow. Simulation results by Isik et al. (2013) suggested that the hydrology in forested system was overall less flashy and that average flow conditions were lower. Van Roosmalen et al. (2009) also predicted a clear increase in evapotranspiration and groundwater recharge after afforestation. Conversely, simulations by Wattenbach et al. (2007) only suggest a slight increase in the total evapotranspiration after an increase in forested area.

In most cases, the urban modelling studies predicted flashier system responses due to an increase in urban area. Simulations by Farjad et al. (2017) suggested that rapid urbanization can cause substantial changes in discharge and increased peak flow. Isik et al. (2013) not only predicted an increase in high flows, but also predicted an overall flashier system after urbanization. Modelling results by Hundecha and Bárdossy (2004), on the other hand, suggested that urbanization mainly affects summer peak flow, but does not significantly affect the winter peak flows. Wijesekara et al. (2012) predicted that that an increase in urbanisation and agricultural fields reduced the water retention in the watershed and can decrease the baseflow, resulting in higher surface runoff, less infiltration and less groundwater recharge. Very different simulation results were reported by Ott and Uhlenbrook (2004), who predicted only minor changes in seasonal and event based discharge after urbanization, which might be related to the relatively small increase in urban area from 2.5 to 5%.

Similar to the measurement studies, the predicted effect of land use change on discharge can also be unambiguous. This can be demonstrated by a subset of the modelling studies that focussed on the effect of the location of the treatment on the predicted impact. Sun et al. (2015), for example, reported that the simulated effect of forest thinning activities on discharge was the strongest in the wetter forest regions. Similarly, Dunn and Mackay (1995) showed that land use change had a significant effect on streamflow in a lowland sub-catchment, but was insignificant for an upland sub-catchment. Jackson et al. (2008) reported that discharge reductions were larger when trees were planted perpendicular to the slope instead of parallel. In contrast, Bormann et al. (2009) reported that a set of three models only showed a limited sensitivity to the spatial redistribution of land use.

The presented modelling studies do not only inform about potential hydrological changes related to land use change scenarios, they also reveal the potentials of the current state-of-the-art in hydrological land use change modelling. This chapter showed that the presented modelling strategies also informed about existing model uncertainty, best calibration and validation practices, model choice and other model strategies that can be applied to model the hydrological effects of land use change. The LUCHEM project demonstrated that model inter-comparison approaches can help to understand differences in underlying mechanisms between models, which could simplify the model choice. For example, Breuer et al. (2009) reported large differences in performance between the 10 LUCHEM models. Generally, the less complex (less parameter) semi-distributed and lumped models performed better for the current land use than the distributed models. Differences in performance are related to differences in input data, model conceptualization (discharge and evapotranspiration), but were mostly related to the intensity of model calibration. The complex models were mainly manually calibrated, whereas the semi-distributed and lumped models could be automatically calibrated, which increased their performance. The LUCHEM modelling studies also demonstrated the predictive power of ensemble modelling studies. Viney et al. (2009) reported that ensemble model predictions performed better for streamflow predictions of the current land use in the Dill catchment, compared to any of the ten individual LUCHEM models. They mentioned that even weaker models were able to contribute to "their" ensemble and that the ensembles that performed best did not necessarily contain the best individual models. Combining the different strengths of individual models could lead to better overall predictions of land use change on hydrological states and fluxes.

An important strength of hydrological modelling studies is that they can inform about the effect of different land use strategies. Experimental studies mostly only provide information about one land use change scenario. Modelling studies, on the other hand, can evaluate multiple scenarios, providing the opportunity to compare different strategies, which is extremely valuable for policy makers. One of these examples is given by Qi et al. (2009), who's simulation results suggested that the conversion from forest to grassland generated smaller changes in discharge compared to a conversion from

forest to urban area. Another example by Schnorbus and Alila (2004) suggested that the location of the treatment is important and that change in discharge depends on the specific elevation of the deforestation measures.

The strength of a multiple-scenario analysis is also shown for studies that both address climate and land use change in their analysis. This clearly show that changing climate conditions can enhance or reduce the effect of land use change. Lahmer et al. (2001) and Niehoff et al. (2002) found that the severity of the effect of land use change was governed by rainfall and antecedent moisture, which could be highly affected by climate change conditions. Bronstert et al. (2002) and Niehoff et al. (2002) also reported that the influence of land use change on storm flow is more severe for convective storms (high precipitation intensity), which are only of minor relevance for larger European River basins. Sun et al. (2015), Lahmer et al. (2001), Quilbe et al. (2008), Van Roosmalen et al. (2009) and Wang et al. (2014) reported more significant changes in discharge for a combination of land use and climate change scenarios. These results show that land use change can cause larger changes in discharge, if the climate is altered at the same time.

At the same time, the current review also demonstrated some clear limitations in the existing modelling studies. The most important caveats are summarized below:

- modelling studies are discharge focused
- there is a large discrepancy in size between measured and modelled catchments
- the simulated effects of land use change are almost never validated with experimental datasets
- distributed hydrological modelling results often lack spatial validation

To overcome these limitations, the next generation of modelling studies need to incorporate more validation data, using either existing datasets from paired catchment experiments or new datasets that include more spatiotemporal information (e.g. evapotranspiration, storage, etc.).

2.7 General Conclusion

This review has looked at a large range of experimental studies and compared the available data and experimental approach for discharge, evapotranspiration and soil moisture storages. Currently, there are no clear examples of studies that integrate all three water balance components to study deforestation or other types of land use change. Most experimental studies focus on short term annual and monthly discharge data, which already revealed that discharge is generally increased after deforestation. However, the currently available information is insufficient to make quantitative generalization on the impact of deforestation, because questions on "How much will the discharge change?" and "Why?" can still not fully be answered. There are many factors that affect the amount of change: the precipitation regime, the initial vegetation, the final vegetation, the rooting depths of the vegetation, the age of the vegetation, and the size of the treatment area. Another important variable that determines the effect of land use change is the time scale. This review has shown that the intra-annual, short term, long term and long term intra-annual effects of deforestation on the hydrology are highly variable. Unfortunately, there is only few data available to describe and quantify the intra-annual, long term, and long term intra-annual effects of land use change on discharge.

The typically used measurement setups and the distribution and type of measurements are not sufficient to generalize the effects of land use change on hydrology. There are too few studies that directly measure land-use related changes in evapotranspiration and soil moisture. Similar to discharge, there are a lot of external factors that can influence the severity of observed change in evapotranspiration, such as the species composition, the age of the forest, the type of understory, climate conditions, soil conditions. As climate and soil conditions can be highly variable in time, the effects of land use change on evapotranspiration can also be affected by this temporal variability. Available studies on vegetation related soil moisture changes clearly demonstrate that moisture conditions can be highly altered in space and time. Indirectly, soil moisture can also be changed when vegetation changes the existing soil properties. As soil moisture is a driver of many hydrological processes, the changes in soil moisture related to deforestation and the coupling with processes is crucial for a more complete understanding of vegetation change effects on hydrological processes.

To understand the current status of land use change studies in the field of hydrological modelling studies, 53 existing studies were evaluated and compared. Comparisons were based on the study site, type of model, calibration and validation methods. Furthermore, the implementation of an uncertainty analysis and the evaluation of the fitness of different models and ensembles was evaluated. Most of the study sites were location in Europe, the USA and Canada. The mean annual precipitation of the studies ranged from 800 to 1500 mm. Most models were either physically based or conceptual. The more conceptual models could be better calibrated for the current land use, the fully distributed and physically based models on the other hand are better at reproducing more complex heterogeneous landscapes. Most studies used a scenario-based approach, where effects of potential future land use change scenarios were evaluated. The majority of the modelling had a calibration phase, and in many cases the model results were also validated. In some specific cases, a blind validation was used. In most modelling studies, only discharge data was used to validate or calibrate the model, and one or two measures of fit were used to decide the quality of the output (majority: NSE and R^2). Only a few studies used spatial information or additional snow storage, groundwater and evapotranspiration data. Overall, the current state of the art is not sufficient to fully understand the effects of land use change. Although the conceptual models can be calibrated and evaluated with the current discharge data, the question remains if changes in hydrological processes are accurately represented when simulating land use change scenarios. Distributed models, on the other hand, require a variety of measurements and different measures of fit to better evaluate their performance.

After reviewing a range of modelling and experimental studies, clear differences, similarities and connections between these studies can be made. Clearly, a lot of modelling studies have focussed on catchments that are much larger in size than the experimental catchments. An intercomparison between these studies could help to understand if the results of the smaller experimental catchment studies can be scaled to larger basins. The focus of most modelling and measurement studies is on discharge. This focus might be a consequence of the lower availability of experimental studies that use evapotranspiration and soil moisture data. Too little datasets are currently available to evaluate the predictive quality of models for other states and fluxes under current conditions, and more importantly after land use change.

Therefore, it is of great interest to analyse spatiotemporal datasets that represent multiple states and fluxes in the hydrological system and to test complex distributed models against these data to better understand the hydrological impact of land use change. This will be pursued in the remainder of this thesis.

Chapter 3

The TERENO Test Site Wüstebach

The review of the state-of-the-art in Chapter 2 clearly demonstrated the need for integrated observation networks that provide observations from fluxes and state variables of the hydrological system (atmosphere, surface, vadose zone, groundwater zone) at multiple temporal and spatial scales. Such observation networks could not only improve our knowledge on land use change related issues, but might also be able to answer relevant questions beyond this scope, for example, how different ecosystems can cope with or adapt to climate change. Examples of existing networks include HOBE (the Danish hydrological observatory; http://www.hobe.dk/), CAOS (Catchments As Organized Systems; http://www.caos-project.de), LTER (Long-Term Ecosystem Research; https://lternet.edu), CZOs (Critical Zone Observatories; http://criticalzone.org) and TERENO (TERrestrial ENvironmental Observatories, http://www.tereno.net). The work in this thesis is directly linked to TERENO (http://www.tereno.net), which is a measurement network within Germany (multiple catchments) that provides multi-compart-ment and multi-scale long-term observations specifically designed to answer research questions related to climate and land use change (Zacharias et al., 2011; Bogena et al., 2012; Bogena et al., 2017). For this thesis, data from the Wüstebach catchment, a small headwater catchment located in the Eifel National Park, Germany (Figure 3.1), was used. The catchment is part of the TERENO-Rur hydrological observatory in Germany (Zacharias et al., 2011; Bogena et al., 2018).

3.1 Site Characterization

The Wüstebach catchment covers an area of 38.5 ha (Graf et al., 2014b). The catchment has a mean annual precipitation of ca. 1200 mm and a mean temperature of 7 degrees Celcius. Altitudes range from 595 to 630 m (Bogena

et al., 2010; Bogena et al., 2015), the mean slope in the catchment is 3.6% and the maximum slope is 10.4% (Bogena et al., 2015). The soil types in the Wüstebach catchment vary from Cambisols and Planosols in the groundwater distant areas to Gleysols and Histosols in the riparian zone (Figure 3.1 and 3.2). The soil texture is silty clay loam with a medium to high fraction of coarse material (>2 mm up to several centimeters). The underlying bedrock consists of fractured Devonian shale (lightly silty, strongly schistose) with occasional fine- to medium-grained sandstone inclusions (Rosenbaum et al., 2012; Graf et al., 2014b).

Up to August 2013 the vegetation in the catchment consisted solely of Norway spruce (*Picea abis L.*) and Sitka spruce (*Picea sitchensis*) that were planted at the end of the 1940's (Etmann, 2009). The average tree density was 370 trees/ha (Etmann, 2009; Baatz et al., 2015) and the average tree height was 25 m. Due to the homogeneous planting date, 94% of the trees are between 20 m and 30 m high (based on Etmann, 2009).

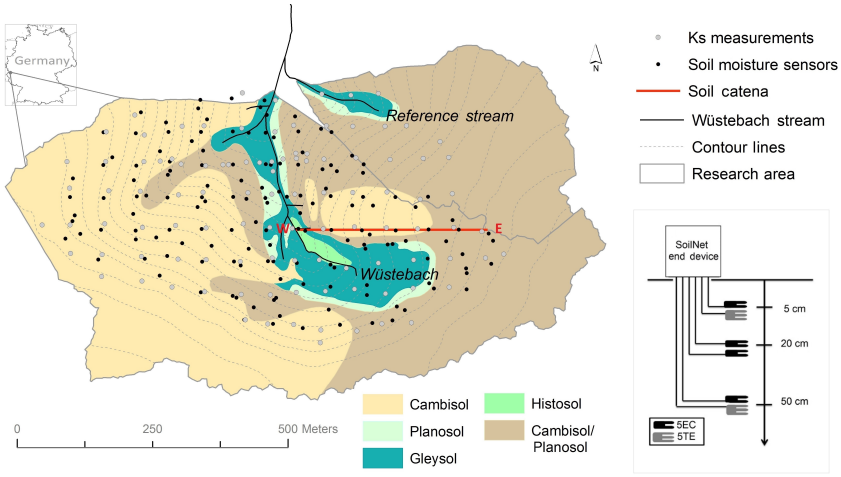

FIGURE 3.1: The Wüstebach catchment in Germany, including the location of SoilNet sensor units and saturated hydraulic conductivity (K_s) measurements. The spatial distribution of soil types according to the FAO classification is also shown (recording scale 1:2500; source: (Richter, 2008)). The position of the soil catena presented in Figure 3.2 is indicated by a red line.

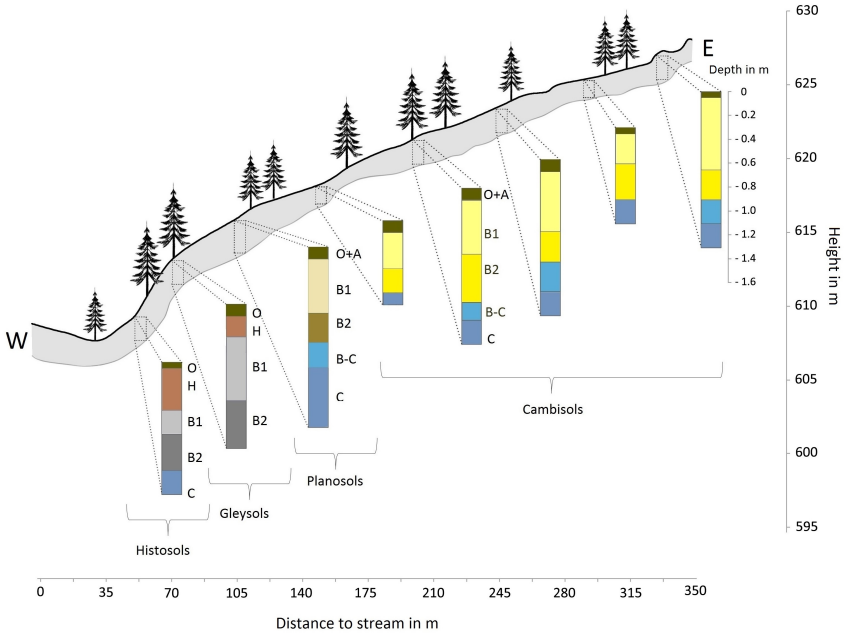

FIGURE 3.2: Characteristic east–west soil catena for the Wüstebach catchment (location shown in Fig. 3.1). Sequence of soil types as found along a transect of 8 SoilNet locations. Individual soil layers are indicated with different colors (related to actual colors) based on soil profile descriptions from in situ measurements by Richter (2008). Letters indicate horizon names based on FAO classification guidelines. The light gray areas along the hillslope indicate soil thickness based on Richter(2008). Note the two different scales for the hillslope and the soil profile depth.

A reference catchment of 11 ha (Figure 3.1) is situated directly northeast of the Wüstebach catchment. The reference catchment has similar soil, geology and vegetation conditions and drains into the Wüstebach several meters after the outlet of the Wüstebach headwater catchment (Figure 3.1). In August and September 2013, 8.6 ha of the Wüstebach catchment was deforested (22.3%, see Figure 3.3). The deforested region is located in the wettest part of the catchment and was conducted to allow for natural regeneration of beech forest. A cut-to-length logging method was applied, where only tree stumps and litter remained, leaving only 3% of the original biomass on-site (Baatz et al., 2015; Bogena et al., 2015). The logging activities mainly affected the Gleysols and Histosols in the riparian zone, but also took place in the eastern upslope section of the Cambisol region.

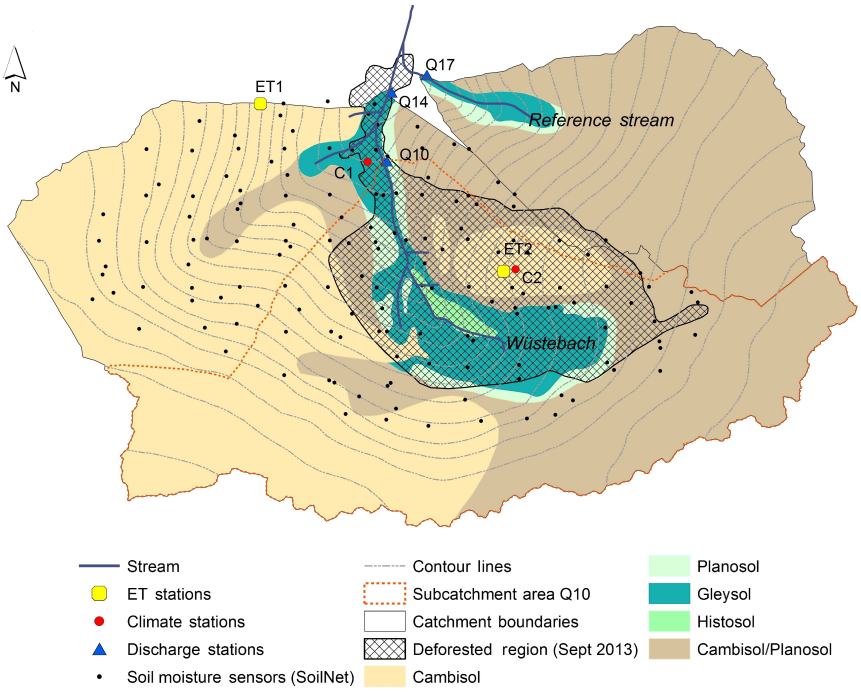

FIGURE 3.3: Wüstebach catchment with hydrological measurement setup, including SoilNet, three discharge stations (Q10, Q14, Q17), two eddy covariance towers (*ET1*, *ET2*), and a climate station (*C1*). The hatched area indicates the extent of the deforestation.

3.2 Measurement Setup

Between 2007 and 2010, the Wüstebach site has been instrumented with a large variety of measurement equipment to obtain information about hydrological, chemical, and meteorological states and fluxes (Bogena et al., 2015). In this section, the measurement setup that was used for this thesis is described. A list with an overview of all measurement equipment is given in Table 3.1.

TABLE 3.1: Measurement setup in the Wüstebach catchment, including information on the type of measurement, number of locations and measurement interval. Q = discharge, ΔGW = change in groundwater, P = precipitation, ET_a = actual evapotranspiration, ΔS = change in storage.

Environmental Variable(s)	**Measurement Setup**	**Measurement Station(s)**	**Measurement Interval**
Q	V-notch weir, Parshall flume	3 (2 Wüstebach, 1 reference stream)	10 Minutes
ΔGW	Piezometers	8 Locations (groundwater-near region)	10 Minutes
Water temperature	Multi-probes (2 locations) + grab samples (WTW, Xylem Inc., USA)	16 Stream locations, 8 groundwater sites	15 Minutes (automatic), weekly (sampling)
pH (water)	Multi-probes (2 locations) + grab samples (WTW, Xylem Inc., USA)	16 Stream locations, 8 groundwater sites	15 Minutes (automatic), weekly (sampling)
Electrical conductivity (water)	Multi-probes (2 locations) + grab samples (WTW, Xylem Inc., USA)	16 Stream locations, 8 groundwater sites	15 Minutes (automatic), weekly (sampling)
Redox potential	Grab samples (WTW, Xylem Inc., USA)	16 Stream locations, 8 groundwater sites	Weekly
Cl^-, NO_3^-, SO_4^-, NH_4^+, PO_4^{2-}, Na^+	Grab samples (IC)	16 Stream locations, 8 groundwater sites	Weekly

TABLE 3.1: Measurement setup in the Wüstebach catchment, including information on the type of measurement, number of locations and measurement interval. Q = discharge, ΔGW = change in groundwater, P = precipitation, ET_a = actual evapotranspiration, ΔS = change in storage.

Environmental Variable(s)	**Measurement Setup**	**Measurement Station(s)**	**Measurement Interval**
Al^{3+}, K^{+}, Fe_{tot}, Ca^{2+}, Mg^{2+}	Grab samples (ICP-OES)	16 Stream locations, 8 groundwater sites	Weekly
SAK_{254}	Grab samples (spectrophotometer - Varian)	16 Stream locations, 8 groundwater sites	Weekly
DOC	Grab samples (Shimadzu TOC-VCPN)	16 Stream locations, 8 groundwater sites	Weekly
Precipitation (on site - since Nov 2013)	Pluvio2, OTT Hydromet, Kempten, Germany	1 Location (deforested area)	10 Minute
Precipitation (off site)	Official meteorological station Kalterherberg (DWD, German Weather Service)	1 Location	10 Minute
Windspeed	Campbell Scientific CSAT3 sonic anemometer	2 Locations (deforested, forested)	20 Hz
Wind direction	Campbell Scientific CSAT3 sonic anemometer	2 Locations (deforested, forested)	20 Hz
Air humidity	Li-7500 open-path infrared gas analyzer (Li-Cor, Lincoln, NE, USA)	2 Locations (deforested, forested)	20 Hz

TABLE 3.1: Measurement setup in the Wüstebach catchment, including information on the type of measurement, number of locations and measurement interval. Q = discharge, ΔGW = change in groundwater, P = precipitation, ET_a = actual evapotranspiration, ΔS = change in storage.

Environmental Variable(s)	**Measurement Setup**	**Measurement Station(s)**	**Measurement Interval**
CO_2 concentration	Li-7500 open-path infrared gas analyzer (Li-Cor, Lincoln, NE, USA)	2 Locations (deforested, forested)	20 Hz
Air temperature	Vaisala weather transmitter (WXT510, Vaisala, Helsinki, Finland)	2 Locations (deforested, forested)	20 Hz
Up- and downwelling shortwave and longwave radiation	Hukseflux NR01 net radiometer and Skye SKP215 PAR sensor	2 Locations (deforested, forested)	10 Minute averages
Photosynthetically active radiation	Hukseflux NR01 net radiometer and Skye SKP215 PAR sensor	2 Locations (deforested, forested)	10 minute averages
Stem and surface temperature	One horizontally-looking and two downward-looking infrared thermometers, Campbell IR120	2 Locations (deforested, forested)	10 Minute averages
Soil heat flux	Hukseflux HFP1 heat-flux plates	2 Locations (deforested, forested)	10 minute averages
Soil temperature and soil moisture (EC towers)	Campbell thermistors and CS616 water content reflectometers	2 Locations (deforested, forested) at 2, 5, 10, 20, 50, and 100 cm	10 Minute averages
Soil respiration	Closed dynamic chamber system (LI-8100-101, Licor Biosciences Ltd)	35 Locations + 49 locations	Weekly

TABLE 3.1: Measurement setup in the Wüstebach catchment, including information on the type of measurement, number of locations and measurement interval. Q = discharge, ΔGW = change in groundwater, P = precipitation, ET_a = actual evapotranspiration, ΔS = change in storage.

Environmental Variable(s)	**Measurement Setup**	**Measurement Station(s)**	**Measurement Interval**
Precipitation, ET_a, ΔS	Lysimeters (surface area: 1.0 m2; depth: 1.5 m), matric potential sensors, tensiometers, temperature sensors, heat flux plates, soil moisture content, and CO2-sensors (depth: 10, 30, 50 and 140 cm)	6 Locations (circle)	1 Minute
Soil moisture (SoilNet)	per site: 4 ECH2O EC-5 and 2 ECH2O 5TE sensors	150 Locations (2 at 5, 20 and 50 cm depth)	15 Minutes
On site soil moisture (CRP)	Cosmic Ray Rrobe (CRP)	1 Location (partly variable location in time)	Hourly
Sapflow	Granier sensors w. 4 needles (Ecomatik SF-L sensors; Ecomatik, 2005)	2 Sites (near river, hillslope)	Each 3 trees 30 Minutes
Precipitation isotopes (δ18O, δ2H)	grab samples (Isotope-Ratio Mass Spectrometry + high T-pyrolisis)	1 Site (off site)	Weekly
Discharge isotopes (δ18O, δ2H)	grab samples (Isotope-Ratio Mass Spectrometry + high T-pyrolisis)	16 Stream locations, 8 groundwater sites	Weekly

TABLE 3.1: Measurement setup in the Wüstebach catchment, including information on the type of measurement, number of locations and measurement interval. Q = discharge, ΔGW = change in groundwater, P = precipitation, ET_a = actual evapotranspiration, ΔS = change in storage.

Environmental Variable(s)	**Measurement Setup**	**Measurement Station(s)**	**Measurement Interval**
Water content, Bulk density, Total C, Total N, pH, $P_{(1)}$, $P_{(2)}$, K, Mn, Fe, Na, S, Ca, NO_3-N, $SO4^{2-}$	Detailed explanation of chemical analysis provided by Gottselig et al., 2017	Campaign 2013: 155 locations, 4 layers (mainly L/Of, Oh A and B), later campaigns: selection (2/3)	Campaign 2013, 2014 and 2018
Na, Mg, Mn, Fe, Cu, Zn, Mo, Al, Se, Rb, Ba, Cr, Co, Ni, Ga, As, Ag, Cd, Sb, Hg, Tl, Pb, U, Sc, Y, La, Ce, Pr, Nd, Sm, Eu, Gd, Tb, Dy, Ho, Er, Tm, Yb, Lu	ICP-MS and ICP-MS analysis for more information, see Wu et al., 2017	Campaign 2013: 155 locations, 4 layers (mainly L/Of, Oh A and B), later campaigns: selection (2/3)	Campaign 2013, 2014 and 2018

3.2.1 Discharge

Discharge was measured in 10-minute intervals at three stations. Two stations are located within the Wüstebach catchment (Q10 and Q14, Figure 3.3), and the third station is located within the reference stream adjacent to the Wüstebach catchment (Q17). The discharge stations Q10 and Q14 are equipped with a V-notch weir and a Parshall flume.

The V-notch weir measurements were used for low flow conditions (water level below 5 cm) and the Parshall flume measurements were used for high flow conditions (water level above 10 cm). During intermediate flow

conditions (water level between 5 and 10 cm), a weighted average of the V-notch weir and the Parshall flume measurements was used. Discharge in the reference stream was measured using a V-notch weir only as the catchment size was smaller.

3.2.2 Precipitation

Before deforestation, 10-minute precipitation data was obtained from the nearest official meteorological station at Kalterherberg (DWD, German Weather Service), which is located 8 km to the west of the catchment at 595 m a.s.l (Graf et al., 2014b). In January 2014, a new climatological station was deployed in the deforested area of the catchment (C2, Figure 3.3). Here, precipitation was additionally monitored on site every 10 minutes using a pluviometer (Pluvio2, OTT Hydromet, Kempten, Germany). The daily precipitation sums measured at Kalterherberg and on-site showed a good agreement (R^2 = 0.96, slope = 0.98). This confirms that the precipitation measurements at Kalterherberg are representative for the Wüstebach catchment. For consistency, precipitation data from the Kalterherberg station was only used here.

3.2.3 Potential Evapotranspiration

Potential grass reference evapotranspiration (ET_0) was calculated according to Allen et al (1998):

$$\lambda \cdot ET_0 = \frac{\Delta(R_n - G) + \rho_{atm} c_p \frac{e_s - e}{r_a}}{\Delta + \gamma(1 + \frac{r_s}{r_a})} \tag{3.1}$$

where $\Delta$is the saturation vapor pressure divided by temperature [Pa/K], Rn - G is the difference between the net radiation (Rn) and the ground heat flux (G) [W/m^2], ρ_{atm} is the air density [kg/m^3], c_p is the heat capacity of air at a constant pressure [$1.013 \cdot 10^3$ J/K/kg], e_s - e is the vapor pressure deficit [Pa], γ the psychrometric constant [Pa/K], r_a and r_s are the aerodynamic and the stomatal resistance of a reference grass surface [s/m], and $\lambda$is the latent heat vaporization [$2.45 \cdot 10^6$ J/kg]. For each hourly time step, r_a, r_s, ρ_{atm}, γ, Δ, and e_s were calculated following the approach by Graf et al. (2014b). The required climate data to calculate ET_0 was obtained from the meteorological station at Schöneseiffen, which is located 3.5 km east of the Wüstebach catchment

at 610 m a.s.l. In case of missing data, a simple linear regression between the climate data measured at Schöneseiffen and the on-site climate station (or with the meteorological station at Selhausen, which is 40 km north of the catchment) was used for gap-filling. Climate data included wind speed, air pressure, air temperature, and air humidity, which were obtained with a Vaisala weather transmitter (WXT510, Vaisala, Helsinki, Finland). Shortwave global radiation was measured using a CMP3 sensor (Kipp and Zonen, Delft, Netherlands). Determination of net radiation from shortwave radiation and ground heat flux followed the guidelines in Allen et al. (1998) as described in more detail in Graf et al. (2014b).

3.2.4 Actual Evapotranspiration

Data from an eddy covariance (EC) station installed on top of a 38 m high tower (ET1, Figure 3.3) located in the northwestern part of the catchment was used to determine ET_a above the forest. After the deforestation, an additional eddy covariance station was installed in the deforested area (ET2, Figure 3.3) at a height of 2.5 m above the surface to compare the ET_a of the forested and the deforested area. The EC measurement setup of both stations is identical and includes a CSAT3 ultrasonic anemometer (Campbell Scientific, Logan, UT, USA) for wind speed measurements and a Li-7500 open-path infrared gas analyser (Li-Cor, Lincoln, NE, USA) at a 0.15 m distance from the ultrasonic anemometer to determine air humidity. ET_a was obtained as 30-min averages from both EC stations following the procedures described in detail in Drüe et al. (2012) and Graf et al. (2014b). In brief, the EC method assumes that evapotranspiration fluxes can be approximated by summing up the multiplied differences in high frequency measurements of vertical wind fluxes and specific humidity divided by the amount of measurements (N-1) taken within a 30-minute time window:

$$ET_a = \rho \sum_{i=1}^{n} \frac{(wv, i - \bar{wv})(q_{atm,i} - \bar{q_{atm}})}{N-1} \tag{3.2}$$

where wv is the vertical wind component [m/s], and q_{atm} is the specific air humidity [kg vapor/kg air]. The details of data processing including corrections and quality control followed the procedures described in Mauder et al. (2013). Until the end of April 2013, the software implementation for EC station ET1 (ET_a of forested area) was based on ECpack (Van Dijk et al., 2004) with an additional quality control extensions after Drüe et al. (2012). After this period, data processing of both EC stations (ET1 and ET2) was based on

the TK3 software (Mauder and Foken, 2011).

The difference in measurement height between the two stations ET1 and ET2 is required to maximize the comparability of the measurements above the forested and deforested area in spite of the different surface roughness and the limited size of the deforested area. To avoid problems associated with measuring in the roughness sublayer (Moore, 1986; Foken, 2008; Rebmann et al., 2018), and to avoid a severe underestimation of the EC fluxes, EC measurements should ideally be performed at a minimum height above the displacement height d of the vegetation canopy (generally 2/3 of the canopy height). This satisfies the conditions that the height should be about 10 times the sensor separation between anemometer and gas analyser (avoiding high-frequency flux losses), as well as being ca.10 times the roughness length z_0. These rules-of-thumb suggest a minimum measurement height of 36 m to 42 m above ground for the forest and a height of 2 m to 3 m for the deforested area, depending on the parametrization of d and z_0 as a function of canopy height (Graf et al., 2014a) and the varying grass canopy height in the deforested area. On the other hand, it is important to keep the majority of the footprint (area of influence, e.g. Schmid, 1997) of the measurement within the target land use type, which requires a low measurement height in case of small ecosystems such as the deforested area. Therefore, both ET1 (forest) and ET2 (deforested area) were installed near their respective minimum possible heights.

In Graf et al. (2014b), it was shown that 50% of the cumulative footprint of ET1 stems from a region that extends to a direction-dependent distance of at most 240 m in southwestern direction, and completely avoids the now deforested area during any wind direction. The 90% footprint includes most of the catchment, but also the surrounding forest of the same species and age with a maximum extension of 900 m. Due to the fact that the forest is even-aged and strongly dominated by a single species of a well-confined height and density, and because ET1 together with precipitation and catchment runoff was able to tightly close the annual water budget before the deforestation (Graf et al., 2014b), it was concluded that forest ET_a is well represented by ET1. The 50% and 90% footprint areas of ET2 have a corresponding maximum extension of 30 m and 180 m, respectively. The latter extension corresponds roughly

with the limits of the deforested area. Since the variety of soils in the deforested area might cause some spatial heterogeneity in ET that cannot be represented by the EC measurements, manual sample measurements of fluxes were also performed with a 1.7 m^2 chamber system as described in Graf et al. (2013) on five different points both within the Cambisol and the Gleysol area. While there was considerable scatter in the comparison between chamber and eddy-covariance ET measurements (RMSE = 0.067 mm/hr), the mean difference was low (0.009 mm/hr, which corresponds to 6% of the mean ET of all chamber measurements; Valler and Graf, 2015).

The EC measurements needed to be gap-filled to obtain a continuous dataset. In total, almost 44% of the hourly ET_a data for ET1 were missing or discarded by the processing software (ECpack or TK3). However, the majority of discarded data was found during nighttime (61%) and other periods with low ET_a. The distribution of gaps in the data for the forested area was rather heterogeneous. There were five large gaps, mainly found in the winter seasons (Figure 3.4), where ET_a values were relatively low. The EC measurements with ET2 had a larger overall percentage of missing data (56%), but the gaps were more homogeneously spread in time. Most of the gaps were found during nighttime (73%), where the ET_a is mostly negligible. Gap-filling was performed using a zero-intercept linear regression between ET_a and ET_0 with a flexible time window following Graf et al. (2014a). In a first step, the RMSE and the regression coefficient were calculated for the minimum time window length of 24 hours. Next, the window was increased by one hour increments and the RMSE and the regression coefficient were calculated again. If the RMSE of the larger time window decreased, the time window was increased again. This procedure was repeated until the RMSE increased with increasing time window. Finally, the regression coefficient (slope of the relationship between ET_a and ET_0) for the selected time window was used to fill the data gap under evaluation. This procedure was repeated for all data gaps.

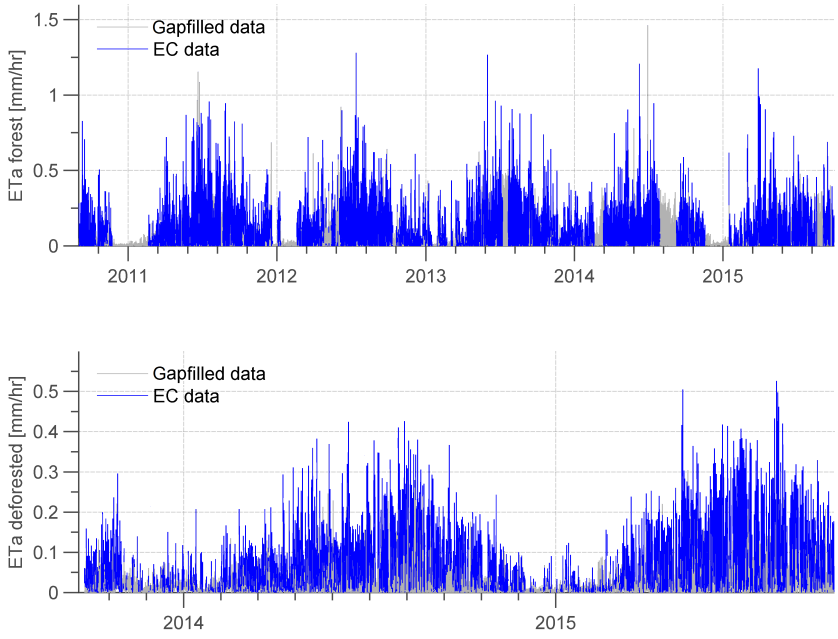

FIGURE 3.4: Hourly actual evapotranspiration obtained from eddy covariance stations in the (a) forested and (b) deforested area. Time periods where reliable measurement data were available are in blue and periods with gap-filling are in grey.

3.2.5 Soil Moisture

Volumetric soil moisture content was measured using the wireless sensor network SoilNet (Figure 3.1 and Figure 3.3). Soil moisture has been monitored since August 2009 with a temporal resolution of 15 minutes. SoilNet provides measurements of soil moisture content at 150 locations every 15 minutes with two replicates at three depths (0.05 m, 0.20 m, and 0.50 m). The soil moisture at 0.05 and 0.50 m depth was monitored with one ECHO-EC5 sensor and one ECHO-5TE sensor (Decagon, Devices Inc., Pullman, USA). Additionally, two ECHO-EC5 sensors monitored the soil moisture content at 0.20 m. Both sensor types have the same measurement principle (see Bogena et al., 2007), but the 5TE sensor has a digital output and additionally allows to measure temperature and soil bulk electrical conductivity. According to Blonquist et al. (2005), the sampling volume of both types of ECHO sensors can be as small as 2 cm^3 in unfavorable wet soil conditions, although the sampling volume is expected to be larger in dry soil conditions.

The sensor response was converted into volumetric soil moisture content based on a two-step calibration procedure as described in Rosenbaum et al. (2012). All measurements were checked for sufficient quality as outlined below. To avoid that data inconsistency affected the analysis, sensors with large data gaps were removed. Additionally, sensors with a low signal to noise ratio as characterized by unrealistically large oscillations (> 5 vol. %) over longer time intervals were visually detected and removed. Next, soil moisture values outside of the 1 – 90 vol. % range and local spikes were automatically detected and removed. Local spikes were described as unrealistic changes in soil moisture within subsequent measurements. The spike detection method is similar to the method described by Dorigo et al. (2013). A threshold of -1 vol. % was used to identify potential downward spikes and a threshold of +5 vol. % was used to identify potential upward spikes. The higher positive threshold was used to avoid that actual abrupt increases in soil moisture were misclassified as spurious spikes. For all potential spikes, it was evaluated whether the difference in soil moisture before and after the spike was below 1 vol. %. If this was the case, the measurement was classified as a spike and removed from the dataset.

3.3 Brief Overview of Previous Work in the Wüstebach Catchment

Due to the complex instrumentation and the large amount of research activities, there is a large variety of relevant papers published about the Wüstebach catchment. In the remainder of this chapter, a brief overview of relevant publications involving the Wüstebach catchment is provided. The more general papers on the observatory include the work of Zacharias et al. (2011), Bogena et al. (2015), Lehmkuhl et al. (2010) and Richter et al. (2008). Zacharias et al. (2011) explained the TERENO framework and the role of the Wüstebach catchment within this framework. Bogena et al. (2015) provided an overview of the ongoing measurement activities within the Wüstebach catchment. Geomorphological maps of the catchment were presented by Lehmkuhl et al. (2010) and soil maps were presented by Richter et al. (2008).

A considerable part of the research in the Wüstebach catchment is related

to spatiotemporal soil moisture characterization. Bogena et al. (2010) provided a first description of the soil moisture network SoilNet in the Wüstebach catchment. Rosenbaum et al. (2012) analysed these soil moisture data to characterize spatial, temporal and spatiotemporal patterns of soil moisture variability in the Wüstebach catchment. Qu et al. (2015) and Korres et al. (2015) used soil moisture data from Wüstebach and other monitoring locations to analyse spatiotemporal soil moisture patterns and soil moisture variability (σ_θ(<θ>) - relationship). Altdorff et al. (2017) compared SoilNet data with time-lapse ElectroMagnetic Induction (EMI) data to study the relationship between soil moisture content and apparent electrical conductivity (EC_a). More general hydrological research in the Wüstebach catchment was presented by Borchardt (2012) and Graf et al. (2014b). Graf et al. (2014b) provided a detailed overview of the water budget in Wüstebach and spatiotemporal relations between the different water budget components. Borchardt (2012) studied the influence of the Pleistocene cover bed structure in the Wüstebach catchment on the hydrological behavior of the catchment. Besides the SoilNet data, soil moisture information in Wüstebach is also provided by a Cosmic-Ray Neutron Probe (CRNP), which is documented by Bogena et al. (2013), Baatz et al. (2015), Iwema et al. (2015) and Andreasen et al. (2016).

Water chemistry and isotopy within the Wüstebach catchment has also been extensively investigated (Stockinger et al., 2014; Gottselig et al., 2014; Stockinger et al., 2015; Bol et al., 2015; Stockinger et al., 2016; Weigand et al., 2017). Due to the adopted sampling strategy with 16 locations that are sampled on a weekly basis, all these studies have a spatiotemporal character. Stockinger et al. (2014; 2015; 2016) used water isotopy to improve understanding of the hydrological functioning in the Wüstebach catchment. In particular, Stockinger et al. (2014) investigated the spatial variability in water isotopy and median transit time distributions in the catchment. Gottselig et al. (2014) studied the spatial variability in occurrence of phosphorus-containing colloids and nanoparticles in the Wüstebach catchment. Bol et al. (2015) investigated the spatiotemporal variability in Dissolved Organic Carbon (DOC), and Weigand et al. (2017) continued this research and looked at the spatiotemporal patterns of DOC and nitrate in the Wüstebach catchment using wavelet analysis.

The soil chemical properties and the influence of the partial deforestation

on these properties have also been analysed. The dataset papers by Gottselig et al. (2017) and Wu et al. (2017) present a detailed three-dimensional characterization of the soil chemical properties in the Wüstebach catchment. Liu et al. (2016) studied the spatial distribution of hydroxylamine content in Wüstebach soils and its relationship to the spatial distribution of N_2O formation. Missong et al. (2016) investigated the presence of fine colloids in the Wüstebach soils and their relationship to the presence of organic and inorganic phosphorous. The spatial distribution of soil CO_2 efflux in the Wüstebach catchment was investigated by Dwersteg (2012).

Finally, several tree ecology studies were performed in the Wüstebach catchment (Etmann, 2009; Rabbel et al., 2016; Rabbel et al., 2018; Thomas et al., 2018). Etmann et al. (2009) provided a dendrological characterization of the trees within the Wüstebach catchment, giving estimates of the carbon stock of dendrological biomass in the catchment. Rabbel et al. (2016) provided detailed sapflow characterization and analysis for the trees within the Wüstebach catchment. Rabbel et al. (2018) and Thomas et al. (2018) investigated the effect of moisture on the growth and isotopic signal of the Norway spruce (*Picea abies*) in the catchment.

The wealth of data makes the Wüstebach catchment interesting for hydrological model studies (Cornelissen et al., 2013; Cornelissen et al., 2014; Fang et al., 2015; Koch et al., 2016). Cornelissen et al. (2013; 2014) used the HydroGeoSphere model to simulate 3D states and fluxes in the Wüstebach catchment and analysed the relevance of model resolution (Cornelissen et al., 2013) and selected boundary conditions (Cornelissen et al., 2014). Fang et al. (2015) used Parflow-CLM to simulate 3D states and fluxes in the Wüstebach catchment, and investigated different approaches to verify the complex model outcomes with the extensive hydrological data that are available. Fang et al. (2016) developed scale-dependent parameterization methods for Parflow-CLM applications in the Wüstebach catchment. As an overarching study, Koch et al. (2016) compared model simulations of HydroGeoSphere, Parflow-CLM and Mike-SHE for the Wüstebach catchment using innovative validation methods.

Chapter 4

Measured Changes in Spatio-temporal Patterns of Hydrological Response after Partial Deforestation[1]

4.1 Introduction

In Chapter 2, it was argued that the current state in paired catchment studies does not provide the means to fully understand the impact of deforestation on water fluxes at the catchment scale. In Chapter 3, the Wüstebach catchment was introduced where extensive and novel monitoring approaches are being used to better understand the changes in spatiotemporal dynamics of hydrological states and fluxes related to partial deforestation measures. In this chapter, data from the Wüstebach catchment is analysed to answer the following questions:

1. How is the annual water balance affected by a partial deforestation measure?
2. What is the difference in ET_a between the forested and the deforested area, and how does it change over time?
3. How are the spatiotemporal soil moisture patterns affected by the partial deforestation, and how do they relate to the hydrological processes that are active within the catchment?

[1]This chapter is adapted from a journal article published as: I. Wiekenkamp, J.A. Huisman, H.R. Bogena, A. Graf, H.S. Lin, C. Drüe, H. Vereecken,2016. Changes in measured spatiotemporal patterns of hydrological response after partial deforestation in a headwater catchment. Journal of Hydrology, 542, pp 648–661.

For this, five years of measured hydrological data will be analysed, including all relevant water budget components for 3 years before and 2 years after a partial deforestation. A data-driven analysis was used to understand changes and related feedback mechanisms in spatiotemporal hydrological response patterns.

4.2 Materials and Methods

4.2.1 The Selected Dataset

In this chapter, discharge (Q), precipitation (P), actual evapotranspiration (ET_a), potential evapotranspiration (ET_0) and soil moisture data were analysed to look at spatiotemporal hydrological changes related to the deforestation in the catchment. For details about the measurement setup and the data processing, the reader is referred to Chapter 3. The water balance terms Q and ET_a were used to evaluate differences in water partitioning prior to and after the deforestation. For the period before deforestation, gap-filled evapotranspiration of the forested area (ET_{af}) was used to evaluate water balance closure. For the period after deforestation, a weighted average of the evapotranspiration of the reference area (ET_{af}) and the treated area (ET_{ad}) was used (ET_{am}) for this evaluation, where the weights were based on the relative size of the forested and deforested area (0.78 vs. 0.22, respectively). In this chapter, the results of the overall water balance for five hydrological years are presented first (HY 2011 - HY2015). Each hydrological year starts at the 1st of September of the previous year and ends at the 31st of August in the following (assigned) year. Afterwards, the evapotranspiration and discharge data are presented for different timescales. In the end, the soil moisture data from 108 sensor locations was used to look at changes in spatiotemporal patterns. The selected locations are based on the earlier selection by Rosenbaum et al. (2012), minus the sensors that did not perform well during the deforestation period (for information on the quality control, see Chapter 3).

4.2.2 The Budyko Framework

The link between energy and water consumption in the catchment was evaluated for the five-year monitoring period using the Budyko framework. The general Budyko framework assumes a relationship between the evaporative index and the dryness index (ET_0/P). Recently, the Budyko framework has

been applied in a variety of studies to separate effects of land cover and climate change (Renner et al., 2014; Velde et al., 2014) on the evaporative index as a function of the dryness index, to analyse the resilience of different vegetation and climate systems to global warming (Creed et al., 2014; Greve et al., 2014), and to predict water availability in ungauged basins (Blöschl et al., 2013). In the following, the Budyko framework is used to further examine the interaction between vegetation and water yield, and the system resilience after deforestation. For this purpose, simple parameterized models (e.g Zhang et al., 2001) can be used to predict changes in evapotranspiration under different vegetation as a function of precipitation (Brown et al., 2005). Here, Choudhury's formulation (Choudhury, 1999) was used to express this relationship:

$$\frac{ET_a}{P} = \frac{1}{(1 + (\frac{P}{ET_0})^{n_c})^{\frac{1}{n_c}}} \tag{4.1}$$

where n_c defines the curvature of the function. Here, n_c = 1.49 was used. This is a global average value derived from EC measurements in a large variety of vegetation types and climate zones (Williams et al., 2012). Zhang et al. (2001) used a slightly altered two-parameter model to describe the same relationship using an additional empirical parameter (w) to account for differences in vegetation properties (see Chapter 2; Equation 2.3). Here w was set to 2 for forested systems and w was set to 0.5 for grasslands.

4.2.3 Analysis of Intra-Annual Variability in Evapotranspiration and Discharge

A two-year dataset of ET_{af} and ET_{ad} was used to analyse the effects of deforestation on monthly, daily and hourly evapotranspiration. Daily ET_{af} and ET_{ad} data were compared to look at general differences in ET_a. Monthly evaporative indices (ET_a /P) were calculated to investigate monthly water use characteristics in the catchment and to identify differences between the forested and the deforested area within the catchment. Hourly ET_{af} and ET_{ad} data were used to look at periods with contrasting ET_{af} - ET_{ad} behavior.

Similar to previous paired catchment studies, daily discharge data from the Wüstebach catchment (Q10 and Q14) and the reference stream (Q17) was used to identify the relationship between the control and treated catchment before and after deforestation (Andréassian, 2004). In this case, a double

mass plot was created (Biederman et al., 2015) and linear regression analysis and monthly discharge characteristics (minimum, mean, max Q, and Q/P ratios) were used to quantify these differences. In this analysis, it was assumed that the cumulative precipitation and actual evapotranspiration of the Wüstebach catchment is representative for the reference catchment, and thus it was expected that the cumulative discharge (in mm/day) was similar. This was, however, not the case, which was attributed to the misevaluation of the drainage area of gauging station Q17. Therefore, a constant correction factor of 1.45 was obtained from the relationship between the discharge of Q17 and Q10 before deforestation. After application of this correction factor to the discharge measured at Q17, the water balance of the reference catchment was reasonably closed (considering the ET_a and P conditions from the Wüstebach catchment; see Section 4.3.1).

4.2.4 Spatiotemporal Soil Moisture Characteristics

Changes in spatiotemporal soil moisture characteristics were assessed using

1. the relationship between the mean soil moisture (<θ>) and the associated standard deviation (σ_θ) and

2. interpolated spatial soil moisture distributions as a function of time obtained using ordinary kriging.

For this, hourly soil moisture data of 108 sensor locations and three different depths (5, 20 and 50 cm) were used to generate σ_θ(<θ>) relationships of the treated and reference area (Figure 3.1) before and after partial deforestation. Daily mean gap-filled soil moisture data were then used to perform ordinary kriging following the approach described by Rosenbaum et al. (2012). First, the spatial autocorrelation was assessed by calculating the omnidirectional experimental semivariance:

$$\gamma_s(h) = \frac{1}{2N(h)} \sum_{i=1}^{N(h)} (\theta_i - \theta_{i+h})^2 \tag{4.2}$$

where *N(h)* is the number of pairs within a given distance class, θ_i is the soil moisture at a given location, and θ_{i+h} is the soil moisture within distance class *h* away from location θ_i. Here, we used eight distance classes with a width of 40 m each. Additionally, the semivariance (γ_s) for a separation of 0.05 m was calculated from the replicate soil sensors that were installed at the same depth at each location to assess short-distance variability. An exponential

variogram model was automatically fitted to the experimental variograms using the MATLAB curve fitting package (MathWorks, Natick, MA). Finally, these exponential variogram models were used to interpolate the data from all 108 sensor locations using ordinary kriging (Goovaerts, 1998).

4.3 Results and Discussion

4.3.1 Changes in the Annual Water Balance

Graf et al. (2014b) already showed that the water balance of the Wüstebach catchment could be practically closed prior to the deforestation without considering deep percolation to the ground water. Figure 4.1 shows the cumulative time series of the water balance components of the Wüstebach catchment for the five-year period that covers three years before and two years after deforestation. Table 4.1 provides the annual sums of all water budget components and yearly runoff coefficients. Additionally, the cumulative ET_a of the forested and deforested areas (ET_{af} and ET_{ad}) is provided for the period after the clear-cut. Mean annual precipitation ranged from 1192 to 1304 mm/yr. For all five years, the measured water balance was reasonably closed with a maximum deviation of 8% (Table 4.1).

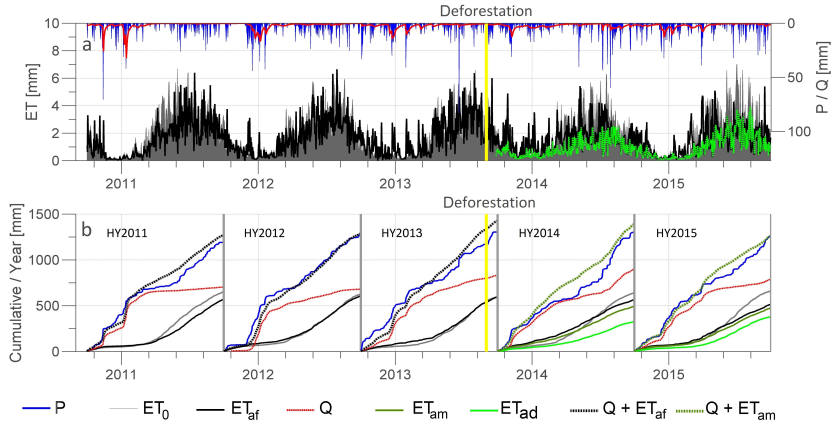

FIGURE 4.1: Yearly cumulative water balance for the five-year monitoring period: three years before and two years after the deforestation. The evapotranspiration of the forested area (ET_{af}), the deforested area (ET_{ad}), and the area-averaged evapotranspiration (ET_{am}) are plotted separately. Annual sums of all water balance components and runoff coefficients are given in Table 4.1

Before the deforestation, the annual ET_{af} was always relatively close to the annual grass reference ET_0, and made up between 40-50 % of the annual precipitation. In HY2014 and HY2015 after deforestation, the annual ET_{af} was slightly lower, which could be related to uncertainties in the EC measurements. In HY2011 and HY2012, less than 60% of all the precipitation was converted into discharge. For HY2013, the annual runoff coefficient was higher (0.64; Table 4.1), which might be related to the deforestation that took place between August and September 2013. However, the difference in runoff coefficients was only moderate and could still lie within the natural variability of the catchment ($\pm$ 5%).

TABLE 4.1: Water balance components for the three hydrological years before and two hydrological years after the partial deforestation (September 2013) in mm. The table includes yearly precipitation sums (P), discharge (Q), potential grass reference evapotranspiration (ET_0), actual evapotranspiration (ET_a), runoff coefficients (Q/P), and the difference between the measured precipitation and the cumulative discharge and evapotranspiration (Res). For the two years after the partial deforestation, the evapotranspiration is divided into forested (ET_{af}), deforested evapotranspiration (ET_{ad}). Additionally, the area-averaged evapotranspiration (ET_{am}) sums are given. Cumulative discharge sums were calculated for discharge station 14. Footnotes relate to the yearly Budyko ratios for different ET_a as shown in Figure 4.2.

Period	**P**	**Q**	**ET_0**	**ET_{af}**	**ET_{ad}**	**ET_{am}**	**ET_{af}-ET_{ad}**	**Q - ET_{am}**	**RES**	**Q/P**
HY2011	1192	703	656	569[a]	-	569	-	1272	-6.7%	0.59
HY2012	1279	680	626	608[b]	-	608	-	1288	-0.7%	0.53
HY2013	1304	830	601	578[c]	-	578	-	1408	-8.0%	0.64
HY2014	1304	898	641	566[d]	312[f]	510[h]	254	1408	-8.0%	0.69
HY2015	1250	789	663	515[e]	369[g]	483[i]	146	1272	-1.8%	0.63

The yearly runoff coefficients after the deforestation ranged from 0.63 to 0.69. The difference between the runoff coefficients before and after the partial deforestation was only small, although a profound difference in actual evapotranspiration (146 – 254 mm) was observed for the forested and deforested area (Table 4.1). In the first year after the deforestation (HY2014), the runoff coefficient was somewhat higher (ca. 10%) in comparison to the earlier years. The runoff coefficient in the second year after the deforestation (HY2015) was, however, similar to the period before the deforestation. This might be related to the natural regrowth of grass that already started in the second year after the deforestation, which is supported by the much smaller

difference in actual evapotranspiration between the forested and deforested area (ET_{af} - ET_{ad} = 146 mm).

In summary, these measurements show an increase in annual discharge after the deforestation, especially in the first year. This is not unexpected, as this has been reported in many previous studies (e.g Hibbert, 1967; Hornbeck et al., 1970; Webster et al., 1992). Although these changes are detectable, they are relatively small on a yearly time scale (an increase of ca. 100 mm), which is clearly related to the size of the deforested area. Although the differences in ET_{af} and ET_{ad} are clear, the limited size of the deforested area reduces the effect on ET_{am}. Again, this is in agreement with earlier work, which has also reported that clear-cutting in a relatively small areal fraction of the catchment (< 20% of the total area) only has minor effects on mean annual discharge (Brown et al., 2005; Bosch and Hewlett, 1982; Andréassian, 2004).

4.3.2 Analysing Annual Changes Using the Budyko Framework

Figure 4.2 shows a Budyko diagram where the measured and predicted annual evaporative index (ET_a/P) is presented as a function of the dryness index (ET_0/P) for the Wüstebach catchment. In addition, the relationship between the evaporative index and the dryness index is presented separately for the treated and reference area after deforestation (assuming that ET_0 is identical for both areas). The grey triangles represent the catchment before the deforestation (additionally marked with A, B and C in Figure 4.2). These years are characterized by measured ratios between the evaporative index and the dryness index close to the Budyko limits. These measured ratios fall above the relationship reported by Williams et al. (2012), and are close to the curve of Zhang et al. (2001) for forested systems ($w = 2$) in Equation 2.3.

The measured ratio of the evaporative index and the dryness index of the untreated area after deforestation (D and E in Figure 4.2) show comparable dryness indices, but somewhat lower evaporative indices. These measured ratios are located closer to the curve of Williams et al. (2012) and the curve of Zhang et al. (2001) for grassland systems ($w = 0.5$). The deviations between ET_{af} values and the evaporative index before and after the deforestation are attributed to intra-annual variability of water partitioning as well as measurement uncertainties. It was analysed in detail whether this observed

reduction of ET_{af} is related to the presence of the clear-cut area near the ET1 station (see Figure 4.3). Half-hourly average ET_{af} decreased 15 – 20 W/m^2 per 30 minutes for wind directions between 210 and 330 degrees. The larger differences in ET_{af} for westerly winds suggested that the measured decrease in ET_{af} is not related to the deforestation measures in the treated area, which is located in the east. The measured ratio between the evaporative index and the dryness index for the entire catchment after the deforestation (F and G in Figure 4.2) falls very close to those of the forested area because the deforested area is relatively small. The measured ratios between the evaporative index and the dryness index for the deforested area fall below most of the previously reported relationships. The evaporative index of the first year after the deforestation (H) is much lower than the evaporative index of the second year (I).

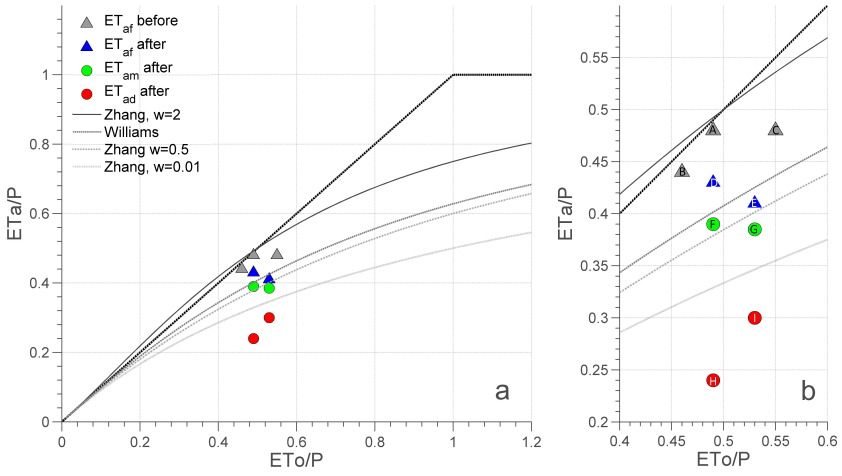

FIGURE 4.2: a) Budyko diagram with b) close-up showing the yearly share of actual and potential evapotranspiration in the water balance in relation to different Zhang and Budyko curves (dataset: Williams et al., 2012). Letters and colors relate to the different actual evapotranspiration measurements used (data in Table 4.1), while the potential grass reference evapotranspiration (ET0) and precipitation were kept constant for a given hydrological year.

The analysis with the Budyko framework shows that energy-limited conditions prevail in the Wüstebach catchment, particularly in the first three years of observations. The evaporative indices were close to the upper limit

proposed within the Budyko framework. This indicates that almost all potentially available energy was consumed to reach the highest possible ET_a of the system. The evaporative indices decreased especially in the treated area after the deforestation. Although changes in the dryness index could also be expected, it is reasonable to assume that these changes are relatively small compared to changes in the evaporative index (Renner et al., 2014). The loss of vegetation resulted in a loss of energy consumed for water vapor transport into the atmosphere, and a direct increase in discharge. These results fit within the framework of Zhang et al. (2001), and are confirmed by traditional paired catchment setups (Bosch and Hewlett, 1982). The decrease in the measured ratio between the evaporative index and the dryness index for the deforested area clearly indicate a change in water partitioning and a disturbance of the equilibrium, where changes in storage are to be expected (Donohue et al., 2007).

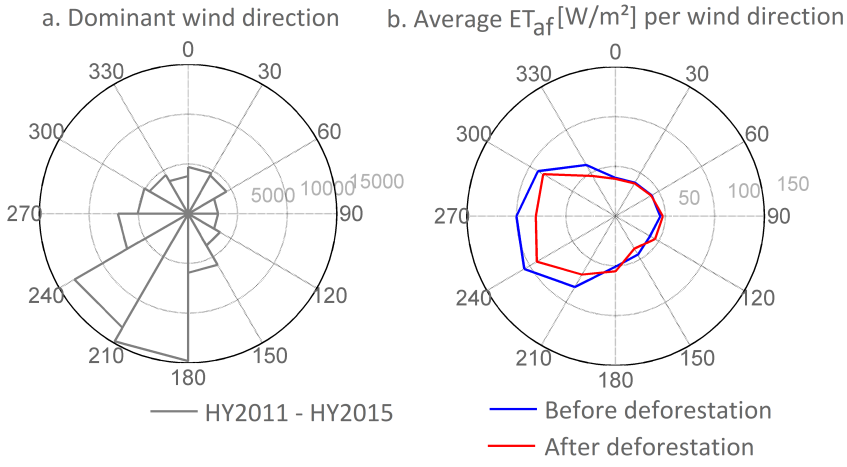

FIGURE 4.3: The dominant wind direction in the catchment given by (a) the number of observations per wind direction, and (b) the average evapotranspiration in the reference area (ET_{af} in W/m^2) per wind direction before and after deforestation in the treated area.

4.3.3 Changes at the Intra-Annual Time Scale

4.3.3.1 Evapotranspiration

To investigate the effects of deforestation beyond the annual time scale, which was already investigated extensively in paired-catchment studies before, intra-annual variations in ET_a of the forested and the deforested area were compared (Figure 4.4).

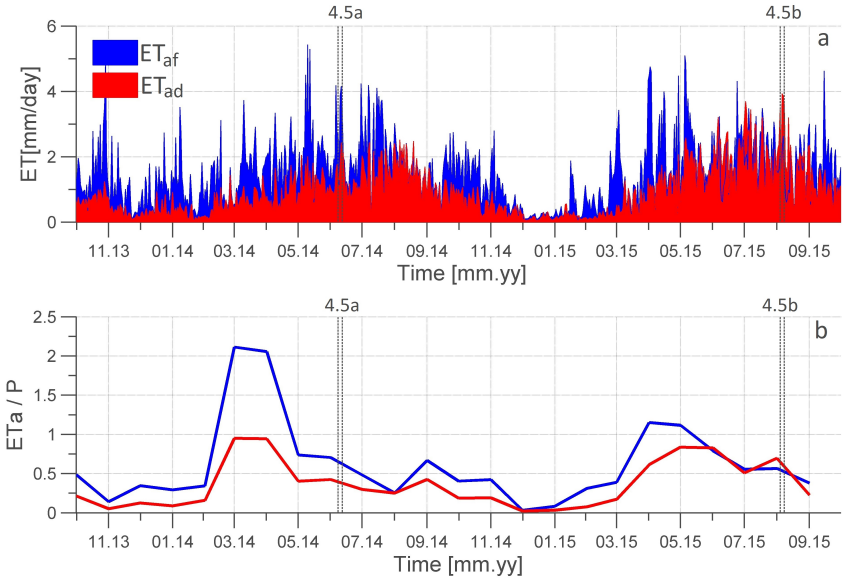

FIGURE 4.4: Daily ET_a in mm (a) from the Eddy Covariance stations in the forested and deforested region of the Wüstebach catchment and (b) monthly evaporative indices for both stations. The vertical striped lines indicate the timeframe used in Figure 4.5a and 4.5b. The locations of the eddy covariance towers are shown on Figure 3.3.

For most of the observation period, the evapotranspiration of the forested area (ET_{af}) was higher than the evapotranspiration of the deforested area (ET_{ad}). Figure 4.4b provides the corresponding values of ET_a/P, which show a clear seasonality with low ET_a/P values in the winter months and high ET_a/P values in summer. Generally, ET_a/P values in both areas were below 1, indicating that monthly evapotranspiration typically was lower than monthly precipitation. Striking differences in ET_a/P were observed in March and April 2014, where ET_{af} was almost twice the incoming precipitation and twice the ET_{ad}. Such high ET_a/P values (around 2) indicate that the trees

have used previously stored water during these months. With the absence of vegetation in the deforested area, water transport to the atmosphere is limited, explaining the large difference. In August 2015, ET_a/P of the deforested area was slightly larger than that of the remaining forest, which is likely related to the reestablishment of a vegetation cover (mainly grass) in the deforested area and differences in water storage between both areas.

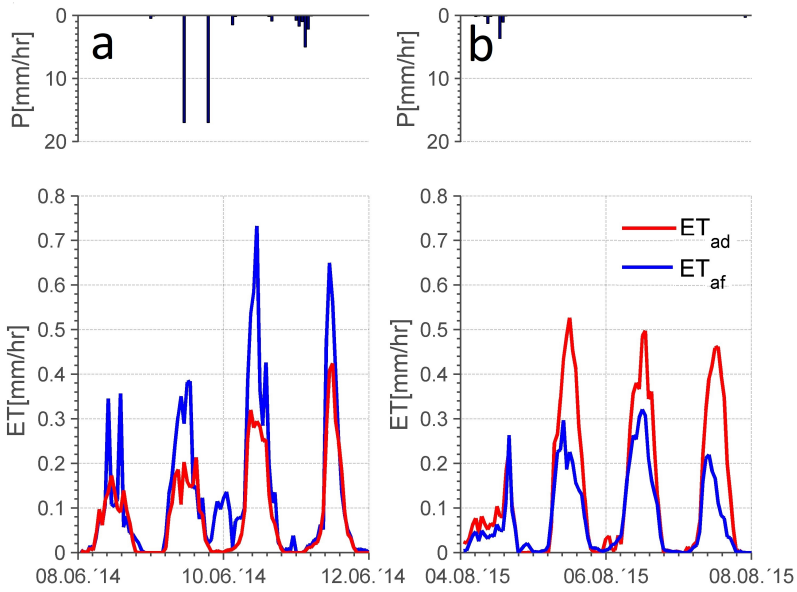

FIGURE 4.5: Hourly actual evapotranspiration (ET_{af} and ET_{ad}) for two contrasting situations: (a) $ET_{af} > ET_{ad}$; (b) $ET_{af} < ET_{ad}$.

Figure 4.5a and 4.5b exemplary highlight two contrasting situations within the post-deforestation monitoring period. In the first case (Figure 4.5a), ET_{af} is higher than ET_{ad}, which is in agreement with expected effects after deforestation (i.e. reduced transpiration). At this intra-annual time scale, there were also time periods where ET_{af} was lower than ET_{ad}, particularly after the establishment of the grass cover in the deforested area. Although higher ET_{ad} values are generally not expected in energy-limited regions, the measurements indicate that water limitation occurred in short time-periods. This (the reversed ET_a conditions) was attributed to differences in water storage,

which will be further discussed in Section 4.3.3.3.

The results of this study are generally in good agreement with the work of Calder (1990) amongst others. They showed that evapotranspiration in a Scottish catchment with pine forest was much larger than evapotranspiration in a similar grassland catchment. At the same time, Calder (1990) showed that the sources of high losses from temperate forests are largely attributed to interception, which was twice as high as the transpiration. This may explain why the regrowth of grassland did not fully compensate the difference in evapotranspiration.

Overall, these findings demonstrate that the ET_a response to deforestation can be ambiguous and highly variable at the intra-annual time scale. Especially during the second year after the establishment of grass cover, differences in ET_a between both areas became smaller. The establishment of grass is a resilience mechanism of the forest ecosystem leading to an increase in ET_a, which is also indicated by the relative high ET_{ad} values in August 2015. These findings need to be considered against the background of the well-known energy balance closure problem associated with EC measurements. It has been found that the sum of the measured sensible and latent heat (ET_a) is on average 10% to 30% smaller than the available energy estimated from net radiation and ground heat flux (e.g Wilson et al., 2002). Although heat storage in the vegetation and photosynthetic energy conversion were not accounted for, an energy balance closure between 81% and 85% was obtained for ET2 in the deforested area depending on the evaluation method (EBR and RMA, Wilson et al., 2002). A similar energy balance closure was earlier determined for ET1 in the forested area (Graf et al., 2014b). It is unknown and subject to debate if and to which degree the energy balance closure gap indicates a systematic underestimation of ET_a (e.g Foken et al., 2011). The fact that the water budget in this study area was closed to within 8% supports the notion that the sensible heat flux is mainly responsible for the closure gap, as also hypothesized by Ingwersen et al. (2011). Alternatively, a hypothetical systematic underestimation of ET_a could have been compensated by uncertainties in the determination of precipitation and discharge. Notwithstanding such uncertainties, the relative comparison of ET_{ad} and ET_{af} as presented here is expected to be relatively insensitive to energy closure problems because the closure is similar for ET1 and ET2.

4.3.3.2 Discharge

In general, discharge is expected to increase in response to deforestation, but the magnitude of this increase is generally less certain when only a small fraction of a catchment is deforested (Bosch and Hewlett, 1982). For example, a recent study by Biederman et al. (2015) has shown that tree die off due to a bark beetle epidemic only had a limited effect on streamflow. In their study, two out of five catchments did not show a significant change in streamflow, whereas a decrease by 11-29% was observed in the other catchments (Biederman et al., 2015).

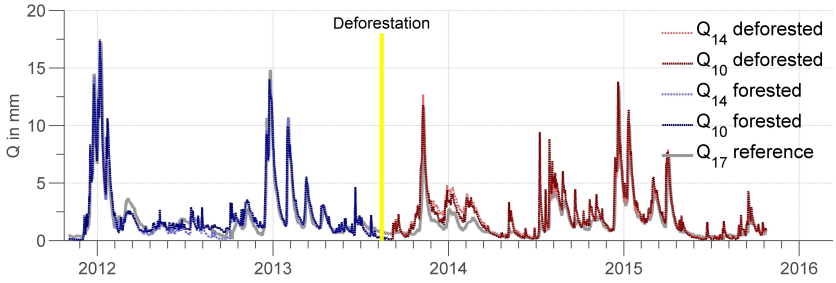

FIGURE 4.6: Daily discharge data for the three different measurement stations (Q10 and Q14 within the Wüstebach catchment, Q17 in the reference stream). The yellow line indicates the time of deforestation.

Figure 4.6 provides daily discharge time series for two points in the Wüstebach catchment (Q10, Q14) and the corrected discharge time series of the reference catchment (Q17) before and after deforestation. Before deforestation, the temporal discharge characteristics of the Wüstebach and the reference catchment were quite similar. Shortly after the deforestation, temporal differences in discharge characteristics between the partly deforested Wüstebach and the reference catchment were clearly visible (January – May 2014). However, these differences are much less prominent afterwards. Next, a double mass-plot was created for a two-year pre-deforestation and a two-year post-deforestation period (Biederman et al., 2015) to compare the slope of the relationship between cumulative annual discharge of the reference and the altered catchment (Figure 4.7a). This figure clearly shows an increase in cumulative discharge of $\tilde{2}00$ mm associated with deforestation. Figure 4.7b shows a scatter plot of the daily discharge of the Wüstebach and reference

catchment before and after deforestation. A linear regression with Confidence Intervals (C.I., α= 95%) was calculated for these data. The slope of the regression line changed from 0.99 $\pm$ 0.02 before deforestation to 1.16 $\pm$ 0.03 after deforestation. According to the performed ANCOVA analysis, the change in slope was, however, not statistically significant (F=1.03, p=0.303). Still, more scatter in the relationship between Q14 and Q17 was observed after deforestation, which indicates a flashier runoff response of the Wüstebach catchment after deforestation.

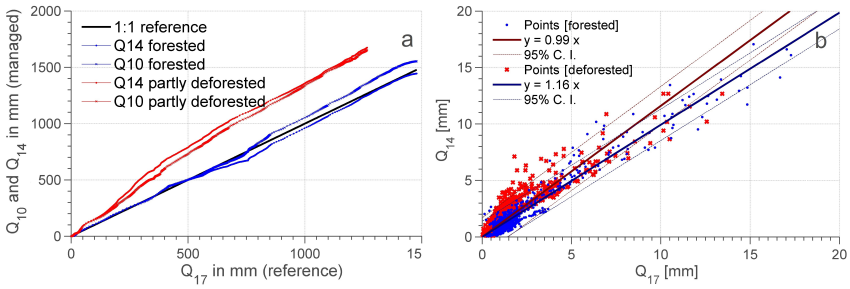

FIGURE 4.7: (a) Double mass plot for a two-year period before and after the deforestation and (b) linear regression between the reference stream (Q17) and Q14 before and after deforestation, including Confidence Intervals (C.I.) of prediction (α= 95%). The locations of the discharge stations are shown in Figure 3.3.

To further analyse the deforestation effects on runoff characteristics, Figure 4.8 shows the monthly maximum, minimum, and mean runoff values, as well as runoff ratios for the Wüstebach and the reference catchment. Before deforestation, these four runoff characteristics were similar, with minor exceptions for the minimum runoff. After deforestation, the values of all discharge characteristics started to differ considerably. This period of strongly deviating runoff characteristics extends from January to May 2014. For the remaining period, the discharge characteristics were more similar. This further confirms that deforestation not only led to an increase in total discharge amount, but also induced a flashier rainfall-runoff response. This was attributed to the fact that the deforestation took mainly place in the riparian zone, which increased the probability of subsurface stormflow and saturation excess overland flow to the stream. Removing vegetation in the riparian zone generally seems to have a larger effect on annual discharge, as compared to management activities in other zones of the catchment (Scott and Lesch, 1996; Salemi et al., 2012). To investigate the effects of deforestation in

the riparian zone in more detail, the response of Q10 and Q14 were compared because the deforested region at discharge station Q14 incorporates a larger part of the riparian zone (39% for Q10, 51% for Q14). However, the difference in response is very small due to the small relative difference in deforested riparian zone (+12%).

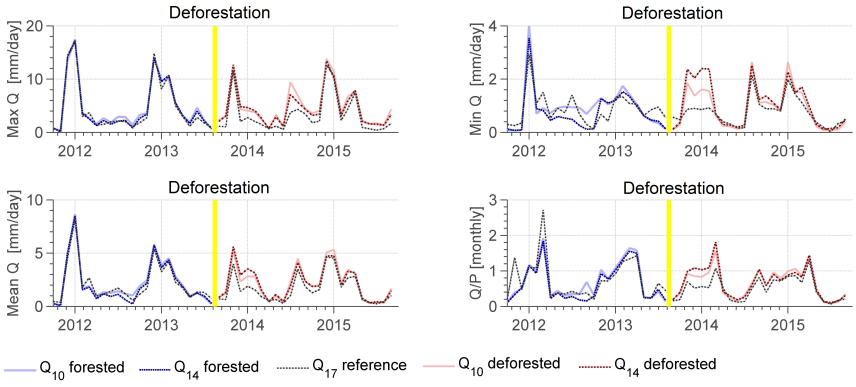

FIGURE 4.8: Monthly discharge characteristics for the three different measurement stations (Q10 and Q14 within the Wüstebach catchment, Q17 in the reference stream). The yellow line indicates the time of deforestation.

Overall, it was found that differences in discharge are especially clear directly after the deforestation. In this period, the largest differences in actual evapotranspiration were observed, which is obviously also reflected in the discharge. In addition, the decrease in difference in ET_a between the deforested and forested area coincides with reduced differences in discharge, which again illustrates the resilience of the forest ecosystem.

4.3.3.3 Soil Water Storage

In a next step, it was investigated whether deforestation affected soil water storage in the catchment. To this end, data from the soil moisture network were compared for the treated and the untreated area before and after partial deforestation. Figure 4.9 shows the temporal development of the mean soil moisture for the treated and the reference area at 5 cm depth (Figure 4.9a), and for the entire profile (Figure4.9b). Figure4.9c and 4.9d show scatter plots of the soil water content in the treated and reference area before and after deforestation. Generally, the treated area was wetter than the reference area, as

it includes the riparian zone and therewith the lowest and wettest region of the catchment. The difference in wetness was more profound for 5 cm depth as compared to the entire profile.

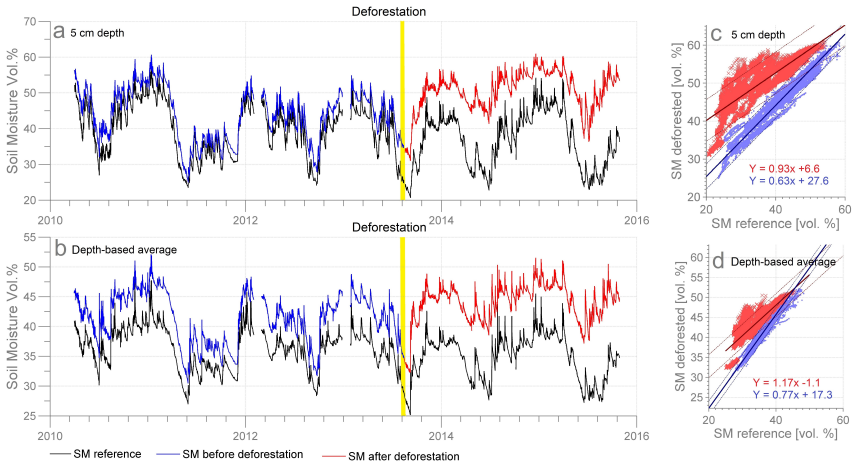

FIGURE 4.9: Time series of mean soil moisture at 5 cm depth (a) and for the entire soil profile (b). Figure 9c and 9d show the relationship between the mean soil moisture before (blue) and after deforestation (red) for the forested and the deforested area, including confidence intervals.

The seasonal soil moisture dynamics for the reference area remained similar for the entire monitoring period. Although the treated area also showed seasonal fluctuations before and after deforestation, the seasonal dynamics clearly decreased after the deforestation. This was most pronounced at 5 cm depth (Figure 4.9a-c versus 4.9b-d), where the minimum soil moisture increased by 3.4 vol. % and the mean soil moisture increased by 3.7 vol. %. The stronger differences at 5 cm depth are attributed to the stronger influence of ET_a at this depth as compared with the entire soil profile. Generally, the difference in average soil moisture between the untreated and the deforested area was largest during the summer period, where the absolute differences in ET_{ad} and ET_{af} were most pronounced (Figure 4.4). Compared to the control period,the soil moisture increased with ca. 15 – 20 vol. % during dry conditions, and the difference with pre-deforestation conditions decreased with increasing wetness (Figure 4.9c-d). At 5 cm depth, there was still a clear effect of the deforestation on the average soil moisture, whereas this was less

pronounced for the entire profile.

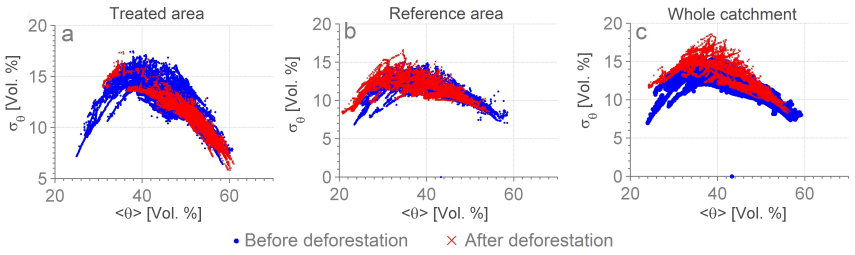

FIGURE 4.10: Mean soil moisture (<θ>) versus standard deviation (σ_θ) of soil moisture at 5 cm depth before and after the deforestation for the treated area (a), reference area (b), and the combined (mixed) area (c).

Figure 4.10 shows the relationship between mean soil moisture (<θ>) and the spatial variability of soil moisture (σ_θ) for the treated area, the reference area, and the entire catchment at 5 cm depth. Here, it is of particular interest to identify effects of vegetation dynamics on the spatial variability of soil moisture. Overall, these results show that the general pattern of the σ_θ(<θ>) relationship in the treated area was not affected by deforestation. Mean soil moisture in the deforested area was higher after the deforestation, and rarely dropped below 40 vol. % (Figure 4.10a). The spatial variability of soil moisture during dry conditions increased after the deforestation when the entire catchment was considered (Figure 4.10c). This is attributed to the increased wetness of the deforested area, which led to a stronger contrast between the drier hillslope and the wetter riparian zone.

Figure 4.11 shows interpolated maps of mean soil moisture content for a two-year period before (Figure 4.11a) and after deforestation (Figure 4.11b). Although the spatial smoothing due to ordinary kriging reduced the spatial variability, these maps clearly show an increased contrast between the forested and deforested area. At the same time, the semivariance increased after deforestation. When focusing on the summer months only, differences in spatial soil moisture patterns are even clearer. Figure 4.12 shows interpolated maps of mean soil moisture content in summer 2011 before deforestation (Figure 4.12a) and summer 2014 after deforestation (Figure 4.12b). Besides an increased contrast between the forested and the wetter deforested area, a clear difference in the shape of the semivariogram (higher variance

and correlation length) can be observed.

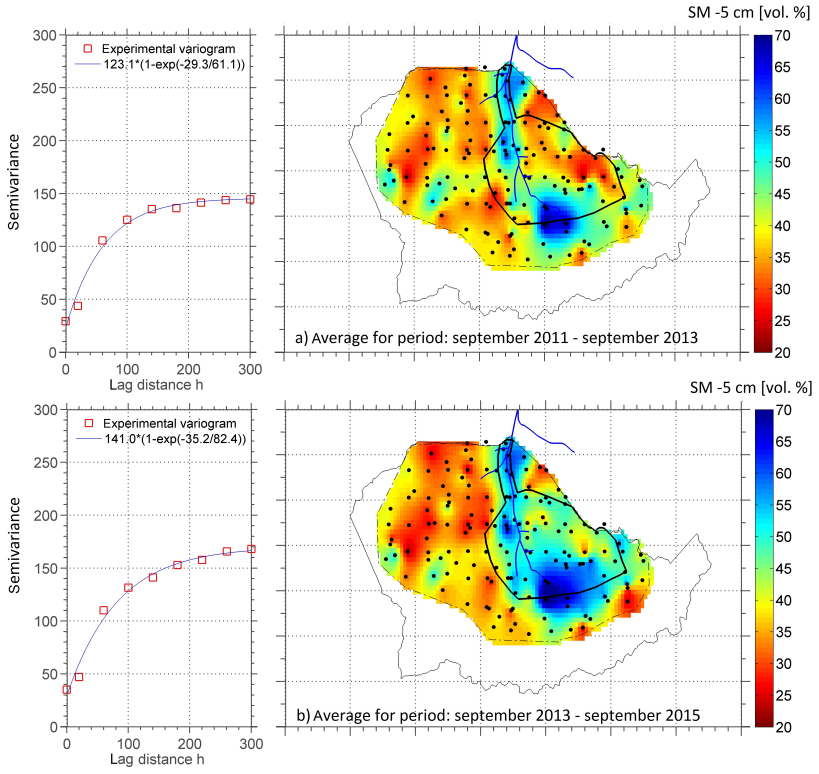

FIGURE 4.11: Experimental variograms and interpolated maps (ordinary kriging) of the mean soil moisture for (a) two years prior to the deforestation and (b) two years after deforestation (b). As a reference, the deforested area within the catchment is marked on both maps.

Overall, these results clearly show that soil moisture storage increased and inter-annual variability decreased due to deforestation, which was also found by Patric (1973). From a yearly water balance perspective (Section 4.3.1), these changes in storage are marginal. However, they can strongly affect surface-atmosphere interactions and the division between latent and sensible heat flux (Teuling et al., 2010).

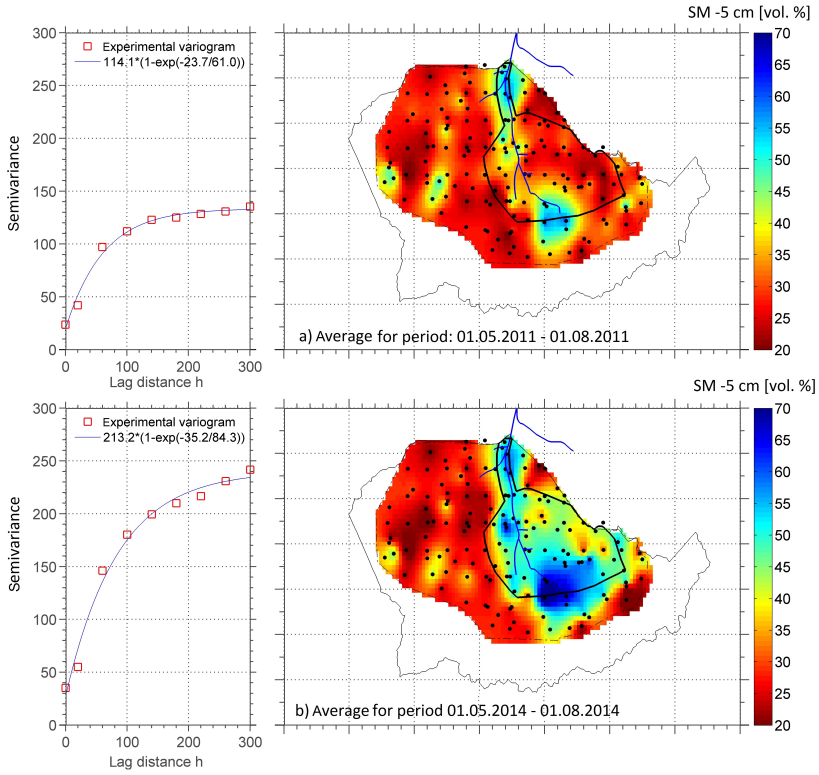

FIGURE 4.12: Experimental variograms and interpolated maps (ordinary kriging) of mean soil moisture content in (a) summer 2011 prior to the deforestation and (b) summer 2014 after the deforestation. As a reference, the deforested area within the catchment is marked on both maps.

The spatiotemporal changes in soil moisture are related to changes in ET_a driven by the large contrast in vegetation type. The higher soil moisture in turn can explain the flashier discharge response as observed in Figure 4.7b, because wetter conditions facilitate subsurface stormflow or saturated overland flow in this catchment (Stockinger et al., 2014). The wetter soil conditions can also lead to occasionally higher ET_a rates in the deforested area after grass establishment, which could explain the higher ET_{ad} rates in the second year after the deforestation (Figure 4.5). Similar contrasting responses have been reported by Teuling et al. (2010) during hot summer conditions. Although Calder (1990) generally agreed that extreme differences in soil moisture can cause such response, his study on a Spruce forest lysimeter during an extremely dry summer found no evidence to support that soil moisture

restricted ET_a.

Previous research has shown clear links between soil physical properties and the $\sigma_\theta(<\theta>)$ relationship (Qu et al., 2015; Wang et al., 2015; Poltoradnev, Ingwersen and Streck, 2016). Wang et al. (2015) investigated the joint effects of variation in vegetation, soil physical properties, and climate on the $\sigma_\theta(<\theta>)$ relationship. Their synthetic modelling study suggested that $\sigma_\theta(<\theta>)$ relationships were different for bare soil and vegetated conditions. The data presented here does not confirm this, because the $\sigma_\theta(<\theta>)$ relationship of the deforested area is relatively similar after vegetation removal. This suggests that variation in soil physical properties generally dominates the $\sigma_\theta(<\theta>)$ relationship of an area, and that knowledge of variation in soil physical properties may be sufficient to predict soil moisture spatial variability, as also suggested by (Qu et al., 2015). At the same time, the increase in mean soil moisture in the deforested area caused a moderate increase in σ_θ for the entire catchment during dry conditions. This suggests that large contrasts in vegetation within a catchment may affect the $\sigma_\theta(<\theta>)$ relationship to some extent.

4.4 Conclusions

In this chapter, spatiotemporal changes in measured hydrological states and fluxes related to partial deforestation were investigated. The results revealed an effect on all components of the water balance. On the annual time scale, water partitioning was affected marginally, resulting in a slight increase in discharge and a corresponding decrease in ET_a. On the intra-annual time scale, increases in monthly discharge were also connected to decreases in monthly ET_a (beginning of 2014). This decrease in evapotranspiration in the deforested area led to an increase in soil moisture storage. This increased soil moisture storage, on its turn, produced a more flashy discharge response associated with increased subsurface stormflow and/or saturated overland flow. The resilience of the catchment was revealed by an increase in ET_a during the second year after the deforestation, which was linked to the establishment of a grass cover. The regrowth of vegetation combined with the increased soil moisture storage facilitated higher ET_a rates during the warm summer conditions.

It was concluded that full-scale monitoring of all relevant hydrological variables as presented here is valuable in elucidating the coupling between different hydrological processes and is highly recommended in future deforestation studies. Additionally, a longer time series of spatiotemporal data can reveal more information on the eco-hydrological resilience of the catchment. This chapter clearly showed that a combination of local EC measurements and soil moisture measurements may reveal interesting surface-atmosphere interactions.

Chapter 5

Spatial and Temporal Occurrence of Preferential Flow in a Forested Headwater Catchment[1]

5.1 Introduction

Despite the large amount of research related to preferential flow occurrence, no general set of rules exists that clearly explains the spatial and temporal patterns of preferential flow at the landscape scale. The lack of understanding concerning factors that promote preferential flow at the landscape scale is at least partly related to the fact that monitoring the occurrence of preferential flow through time and in space remains a challenging task (Allaire et al., 2009; Beven and Germann, 2013; Lin and Zhou, 2008). Although there is an arsenal of available methods to study preferential flow, methods for landscape-wide quantification across space and time remain lacking (Allaire et al., 2009). For example, dye tracers have been used to visualize water movement in the subsurface. However, the destructive nature of this method prohibits the investigation of the temporal dynamics of preferential flow at a specific site. For this purpose, geophysical measurement methods such as ground penetrating radar and electrical resistivity tomography offer non-destructive alternatives to characterize preferential flow (Greve et al., 2012; Guo et al., 2014; Kim et al., 2010; Moysey and Liu, 2012). However, such geophysical methods often lack sufficient spatial extent to cover large catchment areas.

[1]This chapter is adapted from a journal article published as: I. Wiekenkamp, J.A. Huisman, H.R. Bogena, H.S. Lin, H. Vereecken, 2016. Spatial and temporal occurrence of preferential flow in a forested headwater catchment. Journal of Hydrology, 534, pp 139-149.

A promising alternative method to study spatial and temporal variability of preferential flow at the catchment scale is the use of soil moisture sensor response times (Lin and Zhou, 2008; Graham and Lin, 2011; Hardie et al., 2013; Liu and Lin, 2015). After determining the sequence of soil moisture sensor response times at different depths, the spatial occurrence of preferential flow and other flow regimes can be identified for individual precipitation events. Lin and Zhou (2008) identified lateral and vertical preferential flow by applying this method at seven monitoring sites in the Shale Hills catchment. Graham and Lin (2011) extended this study by evaluating soil moisture response at the hillslope scale for 175 events and found that the frequency of preferential flow occurrence ranged from 17 to 54% of all the precipitation events. Liu and Lin (2015) extended the spatial extent of this approach to the catchment scale and revealed a subsurface flow network in the catchment and some degree of topographic control. Although such work in the Shale Hills catchment is promising, similar investigations of preferential flow occurrence in different soils and climate conditions are clearly needed.

In this chapter, the dominant controls on preferential flow in the Wüstebach catchment prior to deforestation are investigated using the dense wireless soil moisture sensor network. The data set comprises three-year long soil moisture time series measured at three depths at 101 locations. A conceptual model that represents the initial understanding of preferential flow occurrence within the catchment was proposed for hypothesis testing. To test the conceptual model and to better understand the factors and processes that cause spatial and temporal variability in preferential flow, results of the sensor response time analysis were related to site (soil and topographic features) and event characteristics (total precipitation, precipitation intensity, antecedent wetness conditions).

5.2 Materials and Methods

5.2.1 Conceptual Model

For hypothesis testing, a conceptual model of preferential flow occurrence (Figure 5.1) is proposed that integrates site-specific knowledge and concepts taken from the literature. It is expected that preferential flow occurs mainly in the riparian zone during lower intensity storm events (area C), because

water accumulates here due to its topographic position. This creates wetter conditions that facilitate preferential flow. For storms with moderate intensity or during wetter initial moisture conditions, it was expected that the slopes of the Wüstebach catchment become increasingly wet, thus activating preferential flow paths particularly in the more susceptible Planosols on the lower hillslopes (area B). The remaining part of the catchment (area A) was expected to react only during high intensity storm events. This area mainly consists of Cambisols, which are expected to be the least susceptible to preferential flow. Nonetheless, earlier research proves that even less susceptible soils can show a preferential response during high intensity rainfall events (e.g. Graham and Lin, 2011).

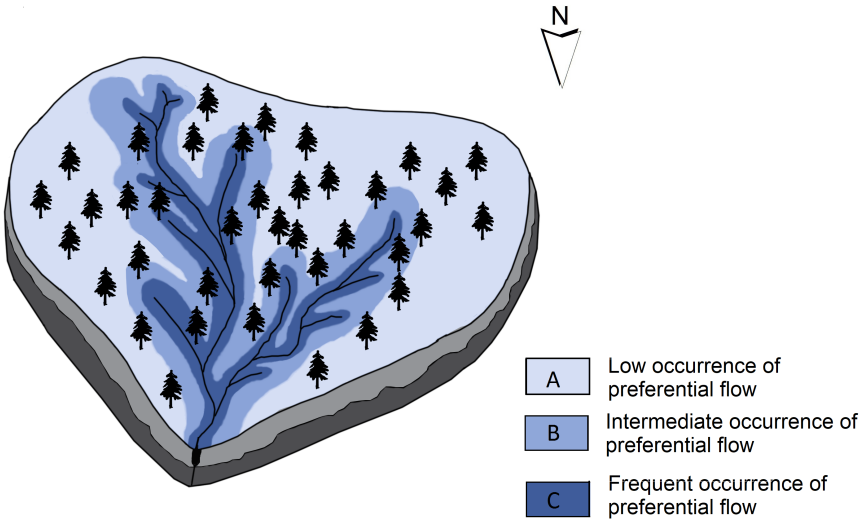

FIGURE 5.1: Proposed initial conceptual model with the spatial and temporal component of preferential flow based on site-specific knowledge and concepts taken from the literature.

5.2.2 Soil Moisture Measurements

This study relies on soil moisture data from SoilNet (Wüstebach). Information about the measurement setup can be found in Chapter 3. For the preferential flow analysis before deforestation presented here, I have focused on a three-year dataset that started in April 2010 and ended in April 2013. To avoid effects of data inconsistency on the analysis, the entire data set was screened for data quality. Sensor locations where more than 25% of all events

could not be classified (see Section 5.2.5) were not considered. In total, 49 out of 150 sensor locations did not pass this qualitative check and were not considered in the following analysis. In a second step, a quantitative plausibility check (See Chapter 3) was performed for the remaining 101 locations.

For the preferential flow analysis, the soil moisture data were further processed to obtain soil moisture time series with identical temporal resolution. Although the temporal sampling interval of each node of the sensor network is approximately 15 minutes, this additional step is required because the sensor units do not contain an internal clock. As this hindered the exact synchronization between the nodes of the sensor network, all sensor data were linearly interpolated to a common time axis with a 15 minute interval. To avoid filling data gaps with insufficient data coverage, a time window of $\pm$ 30 minutes was used around each target time. If no measurements were present in this window, a missing value was assigned to the target time. When at least one soil moisture measurement was available within this moving window, soil water content at the target time was interpolated using available soil water content data without consideration of the moving window.

5.2.3 Precipitation and Event Delineation

Hourly precipitation data from the meteorological station Kaltenherberg (DWD, German Weather Service) was used, which is located 8 km west of the Wüstebach catchment (Bogena et al., 2015). For the preferential flow analysis, the continuous precipitation time series was separated into precipitation events. A heuristic event separation method was used which relied on two thresholds: the minimum period without rain (T_p) and the minimum precipitation amount (T_a). A new precipitation event starts when T_p is exceeded and ends when T_p has passed. All events with a precipitation amount below T_a were removed from the analysis. In addition, events where more than 20% of all available sensors did not provide sufficient data and events where SoilNet indicated frozen soil conditions were left out of the analysis.

5.2.4 Event and Soil Characteristics

The temporal component of the conceptual model was evaluated using several precipitation characteristics, including precipitation intensity, total precipitation, and duration. In addition, antecedent catchment wetness three

hours before the start of an event was considered. The antecedent wetness was obtained by first calculating the depth-weighted average soil moisture for each individual location using the EC-5 sensors at 5, 20 and 50 cm, where weights of 0.1, 0.2 and 0.7 were assigned based on the depth range that each sensor represents (0 – 0.1 m; 0.1 – 0.3 m; 0.3 – 1 m). Afterwards, the depth-weighted values were averaged over the entire catchment for each individual event to obtain the antecedent catchment wetness.

TABLE 5.1: Chemical and physical soil characteristics for the different soil types (mean and standard deviation). Please note that there was only one location with sufficient measurement quality in the Histosol region. θ= soil moisture, [A] and [B] represent the soil horizons.

	Cambisols	**Cambi- & Planosols**	**Gleysols**	**Planosols**	**Histosols**
Locations	45	37	9	9	1
Bulk density [A]	0.64 ± 0.20	0.64 ± 0.19	0.56 ± 0.18	0.56 ± 0.13	0.55
Bulk density [B]	1.05 ± 0.22	0.99 ± 0.19	1.10 ± 0.43	0.62 ± 0.38	2.09
Porosity [A]	0.75 ± 0.08	0.75 ± 0.07	0.78 ± 0.07	0.78 ± 0.38	0.81
Porosity [B]	0.60 ± 0.11	0.60 ± 0.07	0.59 ± 0.16	0.61 ± 0.14	0.2
Mean initial θ	34 ± 4.6	38.5 ± 5.5	48.6 ± 6.4	48.4 ±9.0	51.7
Total C [A]	8.8 ± 3.7	10.6± 4.8	11.6 ± 4.1	13.8 ± 6.8	21.2
Total C [B]	1.9 ± 0.7	2.1± 0.8	1.8 ± 1.3	2.9 ± 0.8	1.98

To evaluate the spatial component of the conceptual model, the mean and standard deviation of the antecedent wetness for a given location (integrated over time), the bulk density of the A (ca. 5 – 10 cm thick) and B horizon (ca. 20 cm thick), the carbon content of the A and B horizons, and the total porosity as potential explanatory soil variables were considered. The bulk density and carbon content were determined from soil samples taken near (< 2 m distance) SoilNet locations between the 24th and the 28th of June 2013 (Figure 3.1). The bulk density was determined from the dry weight of a known volume of soil after 24 hours of drying at 105 °C. The carbon content was measured after dry combustion according to ISO 10694 (1995). The total porosity

was calculated from the dry bulk density according to Danielson and Sutherland (1986) with an additional particle density of 1.5 g/cm^3 for the organic part of the soil. More information regarding the soil sampling campaign can be found in Bogena et al. (2015). Table 5.1 shows the mean and standard deviation of characteristic physical and chemical soil properties per soil type. Generally, the Cambisols and Cambisols/ Planosols regions have soils with higher bulk density, higher initial soil moisture, lower porosity, and lower carbon content.

Topographic attributes were obtained from a digital elevation model with 1 meter resolution (Land Surveying Office of North Rhine-Westphalia). Altitude, local slope, curvature, and wetness index (calculated in ArcGIS version 9.3.1, ESRI, Redlands, CA, USA) were considered. In addition, throughfall was measured weekly at all SoilNet locations with a direct-reading rain gauge located in close proximity to the sensor network locations (<1 m). For this study, the total throughfall between the 6^{th} of April 2011 and the 23^{rd} of December 2011 was divided by the total precipitation over the same period, resulting in the average throughfall expressed as percentage of rainfall. This information was used to investigate whether local differences in interception and throughfall affected soil moisture response times and the subsequent flow classification.

5.2.5 Characterizing Soil Moisture Response

For all the delineated precipitation events, the soil moisture time series were analysed to determine soil moisture response times. The soil moisture response time was based on the first appearance of an increase in soil moisture content. The response time for a particular sensor was only determined if the soil moisture increased by more than 1 vol. % within the delineated event. The response time was defined as the time when the soil moisture starts to increase beyond the instrumental noise (Graham and Lin, 2011). Based on the noise level for the EC-5 and 5TE sensors (Rosenbaum et al., 2010), this threshold was set to 0.4 vol. %.

After the response times were determined for each sensor, the sequence of response times at a particular location was used to classify the flow behaviour. Graham and Lin (2011) described preferential flow as a non-sequential response to precipitation input, indicated by a quicker response of deeper

soil moisture sensors compared to shallower sensors. In addition, preferential flow can also lead to a sequential response with very small differences in arrival time due to high flow velocities (Germann and Hensel, 2006; Hardie et al., 2013; Oberdörster et al., 2010). In this study, both definitions were incorporated into the automatic flow classification that was implemented in MATLAB (MathWorks, Natick, MA) using the following set of rules:

1. Non-sequential preferential flow was identified by a non-sequential order of response times for the three sensor depths. When at least one of the six sensors showed an out-of-sequence response (e.g. sensor at 50 cm depth increased first), flow for that particular location was classified as preferential flow.

2. Velocity-based preferential flow was assigned to events with a sequential order of sensor response times, but with excessively high wetting front velocities. Wetting front velocities were calculated from the distance between two sensors and the difference in response time between two sensors (Germann and Hensel, 2006). To assign a meaningful threshold for the wetting front velocity, measurements of the saturated soil hydraulic conductivity (K_s) made with double-ring infiltrometers at the soil surface in the Wüstebach catchment by Borchardt (2012) were considered (Figure 5.2). As the high K_s values measured with the double-ring infiltrometer are most likely influenced by preferential flow in macropores, the velocity threshold was set to 100 mm/h based on this K_s distribution.

3. Sequential flow was assigned to response time sequences with the expected sequence with depth and wetting front velocities below 100 mm/h.

4. No response was assigned to soil moisture sequences where none of the sensors exceeded the 1 vol. % threshold. Events where at least one of the sensors at a particular sensor location had more than 70 % missing values were not classified.

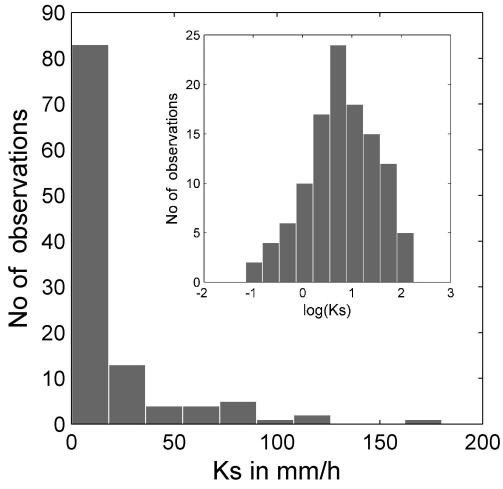

FIGURE 5.2: Distribution of soil saturated hydraulic conductivity (K_s) measured with a double ring infiltrometer at the soil surface: a non-transformed and log-transformed dataset (inset figure). The measurement locations are shown in Figure 3.1 and data were obtained from Borchardt (2012).

The flow classification based on sensor response times is illustrated in Figure 5.3 for a single event that started on the 4th of August 2010, 12:00 CET. During this event, all four types of flow regimes occurred at different locations in the catchment. Location 139 showed sequential behaviour (Figure 5.3a) , while locations 135 and 136 showed two different kinds of preferential flow response (Figure 5.3b and 5.3c). Location 135 was classified as non-sequential preferential flow (later response of the top sensors), whereas location 136 was classified as velocity-based preferential flow (high wetting front velocity). At location 27 (Figure 5.3d), no sensor response to the precipitation event was observed. These results show that similar precipitation input can cause different responses in space, reflecting heterogeneity and local controls on flow regime.

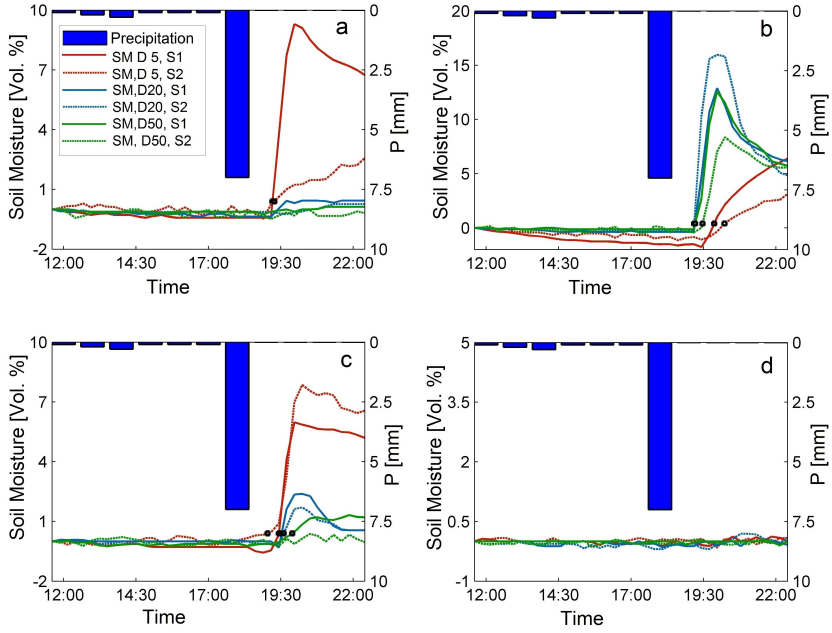

FIGURE 5.3: Examples of four flow types classified in this study: (a) sequential flow, (b) non-sequential preferential flow, (c) velocity-based preferential flow, and (d) no flow. In the legend, the D stands for the depth of soil moisture sensor in cm and the S represents the sensor number (1 or 2). The black dots represent the position of initial rise in soil moisture beyond sensor noise. Note that the y-axes have varying ranges.

5.3 Results and Discussion

5.3.1 Event Delineation

Precipitation in the Wüstebach catchment is characterized by short events with small precipitation sums (< 20 mm). Figure 5.4 shows the event characteristics (event duration, mean total precipitation, and number of events) as a function of different thresholds for the period without rain (T_p) and the minimum amount of precipitation (T_a). By increasing T_p, the number of events decreases, whereas the mean total precipitation and the event duration increase. By not considering small events (e.g., T_a = 1 mm), consecutive short events can still be separated, which is important for the preferential flow analysis. As a compromise between the number of events and event duration, event delineation was based on a rainless period of 3 hours. In addition,

events with a total precipitation of less than 1 mm were not further considered in the analysis.

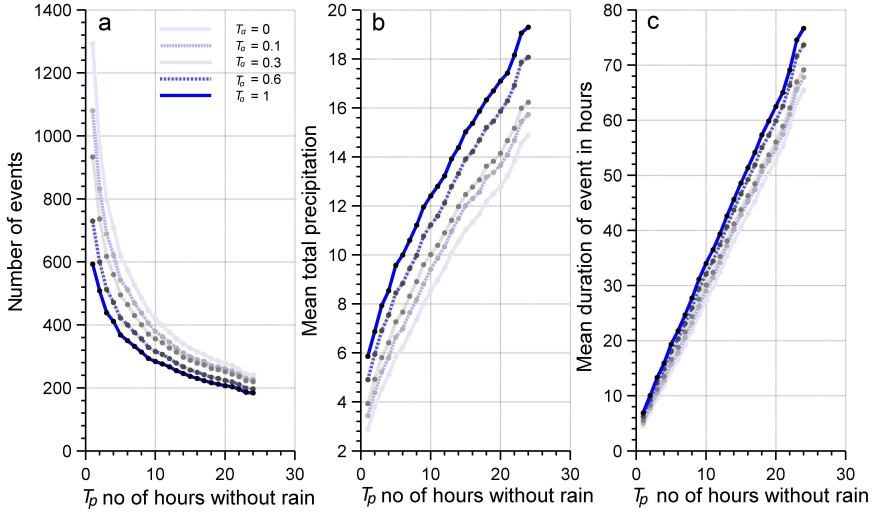

FIGURE 5.4: Precipitation event characteristics: (a) number of events, (b) mean total precipitation, (c) mean duration of events in hours for different threshold settings for the minimum period without rain (x-axes, T_p) and the minimum precipitation amount (T_a in mm).

This approach resulted in a total of 367 events that were used to characterize preferential flow processes at 101 locations within the Wüstebach catchment. Although the distribution of precipitation over the year is non-uniform, the amount of events in different seasons was relatively similar with the lowest amount of events in the winter of 2012 - 2013 (3.5%) and the highest amount of events (13.9%) in summer (Figure 5.5). The lower number of events during the winter period is mainly related to the occurrence of soil frost.

5.3.2 Flow Classification for Single Events

Figure 5.6 presents results for the flow classification for six events with increasing precipitation amounts and variable antecedent catchment wetness conditions (Table 5.2). The occurrence of non-sequential preferential flow increased with increasing precipitation. At the same time, this increase was

also associated with a decrease in catchment-wide mean antecedent catchment wetness. During events with relatively small (1.9 mm) or large precipitation amounts (16.2 and 30.8 mm), the catchment seems to react as one unit, resulting in a similar response within the entire catchment. For events with intermediate precipitation amounts (b: 3.9 mm; c: 5.5 mm; d: 11.7 mm), there is a spatially more heterogeneous flow response. To further investigate this, the response at all individual sensor locations can be integrated over time (section 5.3.3). To investigate the event-based responses, the response at each individual event can be integrated in space (section 5.3.4).

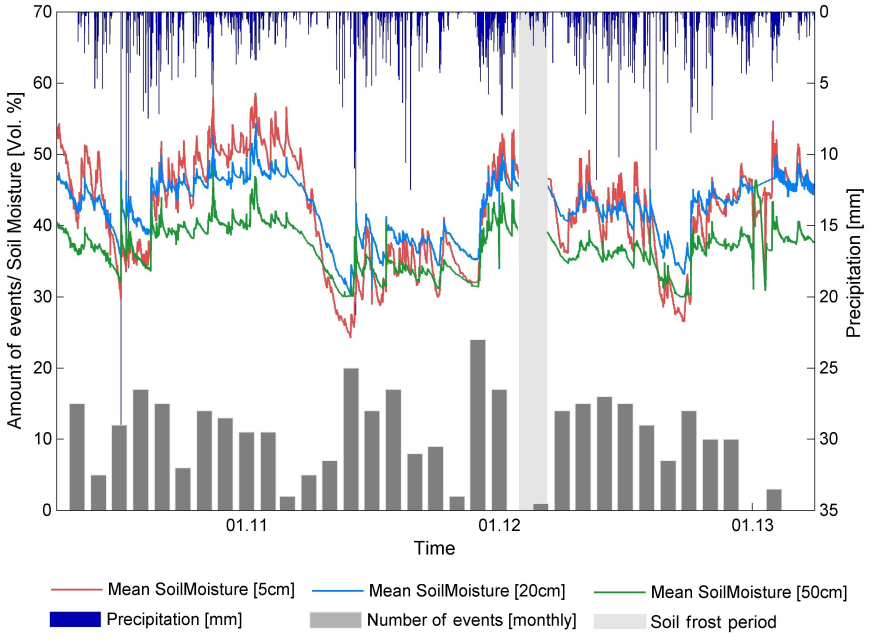

FIGURE 5.5: Overview of the dataset used in this study, with temporal distribution of precipitation, monthly event number, and average soil moisture content at 5, 20, and 50 cm depths. A soil frost period (early February to mid-March in 2012) has been excluded from the analysis.

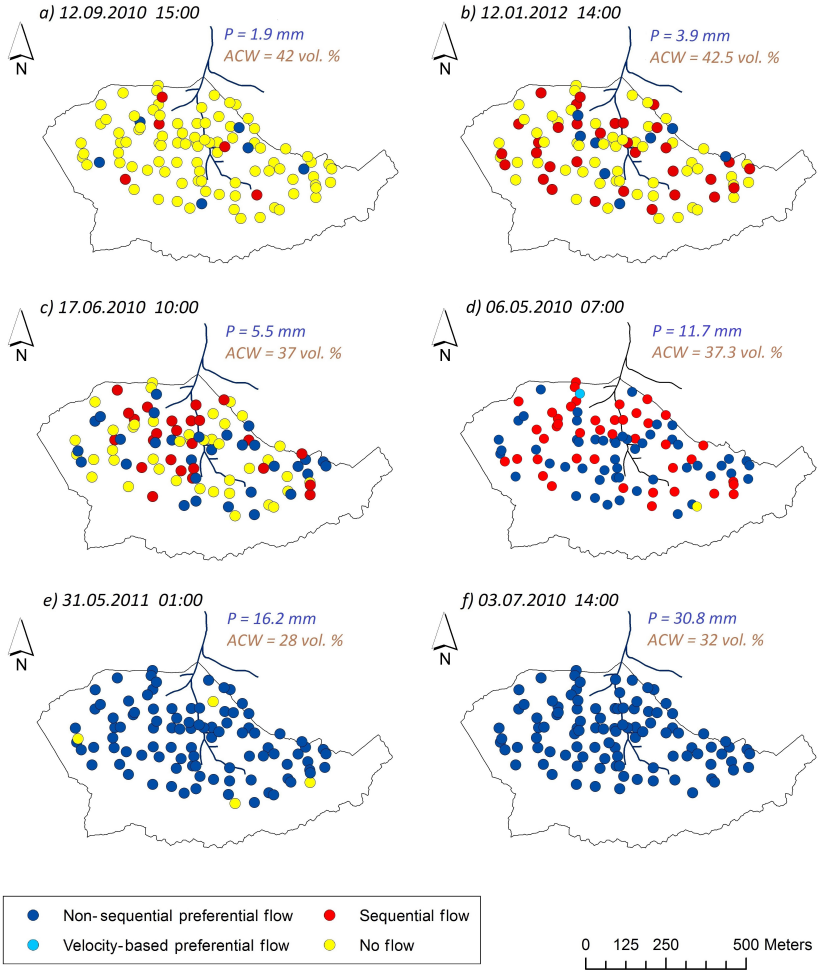

FIGURE 5.6: Effect of precipitation amount on preferential flow generation, showing the spatial response for six individual events with different precipitation sums (P) (from 1.9 to 30.8 mm) and antecedent catchment wetness (ACW) (between 28% and 42.5% by volume). Specific features of the six events are given in Table 5.2.

TABLE 5.2: Characteristics for the six events that are shown in Figure 5.6, including different precipitation (P) features and the averaged Antecedent Catchment Wetness (ACW).

Event	Total P [mm]	Max. P intensity [mm/hr.]	Mean P intensity [mm/hr.]	Event duration [hr.]	ACW [Vol.%]
A	1.9	1.5	0.32	5	42.31
B	3.9	1.5	0.43	8	42.49
C	5.5	2.3	0.55	9	37.01
D	11.7	1.1	0.33	35	37.30
E	16.2	3.2	0.60	26	27.67
F	30.8	30.3	5.13	5	3.15

5.3.3 Spatial Frequency of Preferential Flow Occurrence

The overall frequency of preferential flow occurrence during the 3-year monitoring period varied considerably in space with values ranging from 7% to 51% (Figure 5.7a). Similar to Graham and Lin (2011), nearby sensors can show striking differences in the frequency of preferential flow occurrence, suggesting a high variability of preferential flow at the small scale. Figure 5.7b and 5.7c show the corresponding patterns of non-sequential preferential flow and velocity-based preferential flow occurrence separately. Generally, non-sequential preferential flow is much more common than velocity-based preferential flow and their spatial occurrence patterns differ considerably. Additionally, the results suggest that preferential flow is present throughout the catchment, which agrees with the findings of van Schaik (2009) and Liu and Lin (2015).

The correlation between the total occurrence of preferential flow over the 3-year period and fourteen spatial attributes is shown in Table 5.3. Generally, the correlation is rather low with Pearson correlation coefficients (R) of less than 0.2 and a Spearman correlation coefficient (R) of less than 0.4. There was also no relationship between throughfall and the occurrence of preferential flow, suggesting that throughfall variability is not determining the pattern of preferential flow occurrence in this spruce forest.

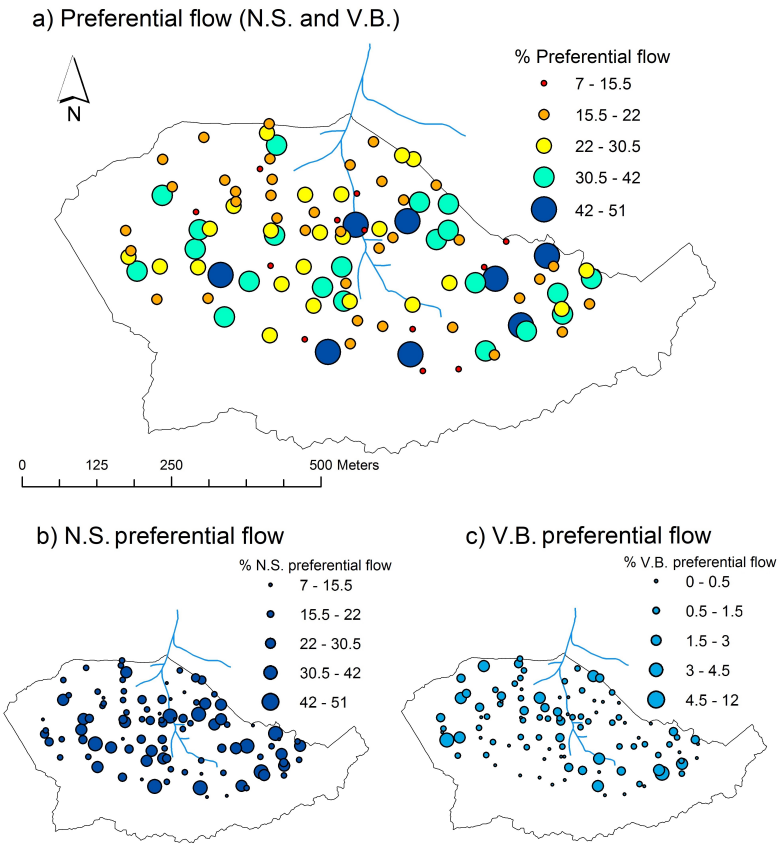

FIGURE 5.7: Spatial distribution of the frequency of preferential flow occurrence (a) combined, (b) non-sequential (N.S.) and (c) velocity-Based (V.B.) at 101 SoilNet locations within the Wüstebach catchment. Results are based on 367 precipitation events during a 3-year monitoring period (April 2010 to April 2013). Classes are based on natural breaks.

In contradiction to the findings of the catchment-wide studies of Liu and Lin (2015) and van Schaik (2009), the distribution of preferential flow in space could not be explained by the selected attributes. This result disagrees with the initial conceptual model that relates spatial variability in preferential flow occurrence to soil type and landscape position. However, these results are consistent with the results of the hillslope study by Graham and Lin (2011), which showed that the frequency of preferential flow was insensitive to topographic position at a single hillslope in the Shale Hills catchment.

Overall, it has to be stressed here that sensor response time analysis provides only one piece of evidence for preferential flow occurrence. The current measurement setup (two sensors at each depth) clearly has it limits with respect to spatial representation, and thus cannot identify all preferential pathways. However, this is currently one of the only methods that can be used to investigate preferential flow occurrence with a high spatial and temporal resolution for relatively large areas up to the catchment scale.

TABLE 5.3: Linear and non-linear correlation between the overall occurrence of preferential flow at a given location and its topographic attributes, soil physical and chemical properties (R = correlation coefficient).

Parameter	**Spearman R**	**Pearson R**
Height	0.12	0.15
Aspect	-0.11	-0.03
Wetness	-0.02	0.04
Curvature	-0.11	-0.07
Slope	0.11	0.05
Throughfall	-0.05	-0.05
Bulk density [A]	-0.12	-0.16
Bulk density [B]	0.12	0.05
Porosity [A]	0.12	0.16
Porosity [B]	-0.13	-0.04
Carbon content [A]	0.02	0.1
Carbon content [B]	-0.08	-0.05
Initial soil moisture content (σ)	0.13	0.10
Initial soil moisture content (μ)	0.39^{***}	0.19^{*}

significance: * = 0.1, ** = 0.05, ***= 0.005

5.3.4 Event-Based Analysis of Preferential Flow Occurrence

To investigate whether precipitation characteristics can explain the observed catchment-wide response, the relationship between total precipitation and the amount of sensors that reacted preferentially, sequentially, or showed a no-flow response was investigated for all 367 precipitation events (Figure 5.8). Figure 5.6 already suggested the existence of a precipitation threshold on preferential flow occurrence in this catchment. Figure 5.8a confirms this

finding and shows that there is an overall positive relationship between the total amount of precipitation within an event and the amount of sensor locations with non-sequential preferential flow. The relationship between precipitation amount and velocity-based preferential flow occurrence is similar, albeit with a less clear trend (Figure 5.8b). As expected, the number of sensors that showed no response quickly decreased with increasing precipitation amount (Figure 5.8d). The occurrence of a sequential response initially increased with increasing precipitation (Figure 5.8c) and decreased for precipitation events of more than 20 mm. Similar trends were found for the relation between the occurrence of these four flow types and precipitation intensity.

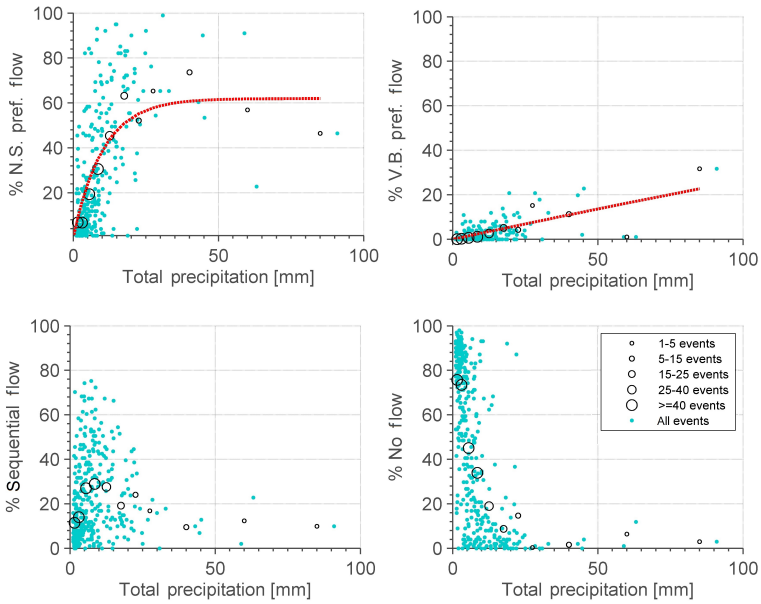

FIGURE 5.8: Effect of total precipitation on preferential flow generation. The turquoise dots show the relationship between precipitation amount and various types of flow for all 367 individual events: (a) non-sequential preferential flow, (b) velocity-based preferential flow, (c) sequential flow, (d) no flow. The black circles indicate the average flow occurrence for a given precipitation class. The size of the black circles indicates the number of events within the given class and the red line presents the fitted regression function through these circles.

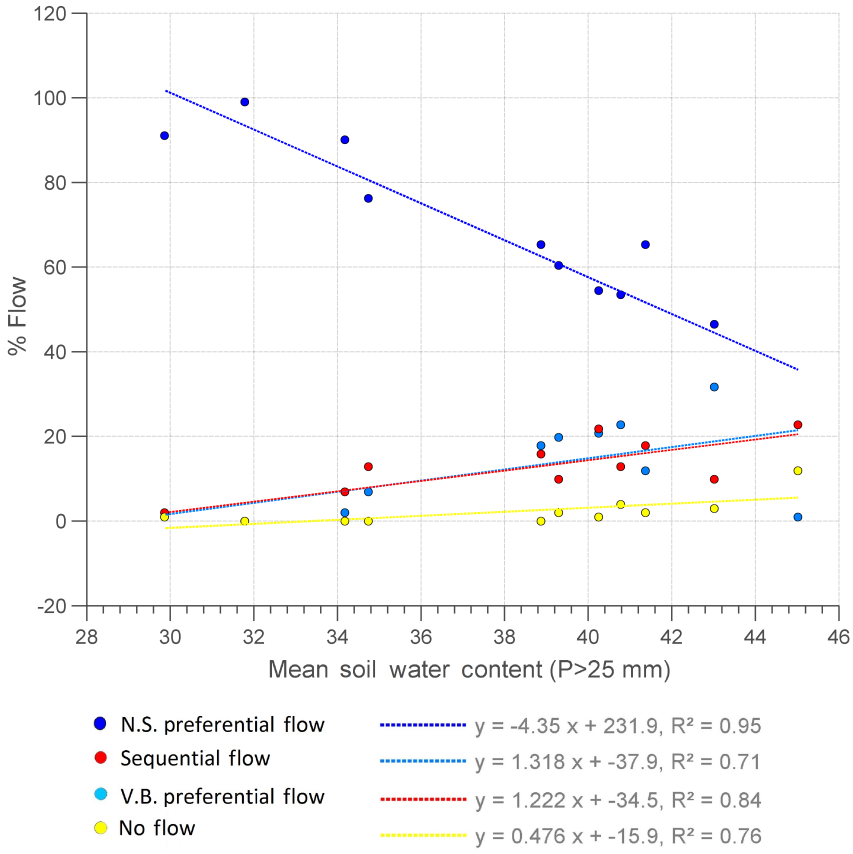

FIGURE 5.9: Effect of antecedent catchment wetness on the generation of non-sequential preferential flow for events with more than 25 mm of precipitation, displaying velocity-based preferential flow, sequential flow, and no flow occurrence frequency.

The relationship between antecedent catchment wetness and the number of locations that showed non-sequential preferential flow was also analysed. No clear relationship between the antecedent catchment wetness and non-sequential preferential flow occurrence was observed. As the variability in the occurrence of non-sequential preferential flow may be caused by different precipitation amounts for the same antecedent moisture, the relationship between mean soil moisture content and preferential flow occurrence was studied for different classes of precipitation amount. A strong negative relationship between antecedent catchment wetness and non-sequential preferential flow occurrence was found when events with more than 25 mm

of precipitation were considered only (Figure 5.9, R^2 = 0.95). At the same time, the occurrence of sequential and velocity-based preferential flow increased, whereas the amount of sensors that did not show any response did not change significantly. This is also illustrated in Figure 5.10, where the flow classification is shown spatially for representative large precipitation events (>25 mm) as a function of antecedent catchment wetness. With an increase in antecedent catchment wetness, more sensors show velocity-based preferential flow and sequential flow behaviour.

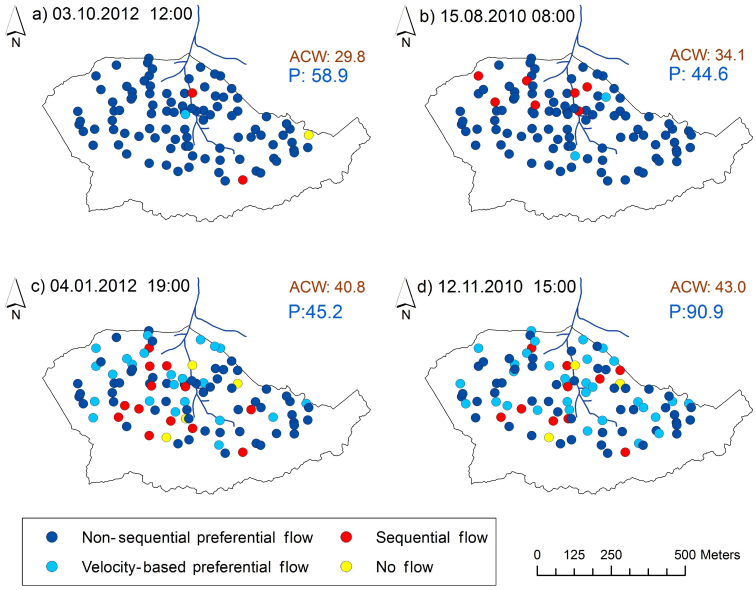

FIGURE 5.10: Difference in flow response for four events with the largest sums of precipitation, but with varying antecedent catchment wetness (ACW: 30 – 43 Vol. %).

The relationship between the occurrence of preferential flow and precipitation amount suggests that an increase in precipitation will increase the occurrence of preferential flow. This is in agreement with the conceptual model, where an increased rainfall input causes preferential flow occurrence over a larger region. This finding is also in agreement with other studies (Graham and Lin, 2011; Hardie, 2011; Hardie et al., 2013; Koestel and Jorda, 2014). For instance, McGrath et al. (2010) found that pesticide transport through preferential pathways was strongly associated with larger storms. As a logical

consequence, the large amount of rainfall that enters the soil in a relatively short time activates preferential flow paths. Comparable to infiltration excess overland flow, the soil quickly develops a mechanism that releases the large amount of water via various kinds of macropores or other types of preferential flow. Unfortunately, there is only a small amount of high rainfall events available within the 3-year timeframe, which is related to the larger return period of such events. Due to this limited number of events, the observed relationship between preferential flow occurrence and precipitation amount has to be taken with care.

When analysing all precipitation events, the antecedent catchment wetness seems to have no clear relationship to the occurrence of preferential flow. This result was not in agreement with the conceptual model, where a clear increase in preferential flow occurrence with higher antecedent moisture conditions was expected. Nevertheless, several other field studies have also shown that antecedent wetness does not necessarily govern preferential flow occurrence for specific soils (Flury et al., 1994) or in particular horizons (Hardie, 2011). This is also consistent with the non-equilibrium flow theory as discussed by Jarvis (2007), which indirectly implies that water flow through macropores occurs independently of antecedent wetness conditions (Beven and Germann, 2013).

When analysing larger storms only (> 25 mm), a clear negative correlation with the antecedent catchment wetness was obtained. Part of the decrease in non-sequenatial preferential flow is compensated by an increase in velocity-based preferential flow. The remaining negative trend could be related to the stronger effect of soil hydrophobicity during dry conditions, which has also been observed by Graham and Lin (2011) and Hardie et al. (2011; 2013). During dry soil conditions, forest soils are more water-repellent and prone to preferential flow. During wet conditions, the water repellency becomes less severe, cancelling out part of the preferential pathways and creating improved conditions for matrix flow. This is in agreement with the increase in sequential flow under wet catchment conditions. In addition, very local infiltration-excess overland flow might enhance water movement through macropores for dry and water-repellent soils. For high antecedent catchment wetness conditions, however, the strong interaction between the active matrix and macropores causes an increased occurrence of velocity-based preferential flow and sequential flow.

The observed negative relationship between preferential flow occurrence and antecedent wetness for strong precipitation events needs to be interpreted with care. It is possible that this result is affected by the limited amount of events with high sums of precipitation in the catchment. The negative relationship may also reflect the inability of the soil moisture sensors and the analysis approach to capture water movement close to saturation. Once a sensor is close to saturation, the changes in soil moisture are difficult to observe, even if water is still moving through the profile. This is, however, most probably not the case, as Figure 5.8 and 5.9 show no strong increase in sensor locations with a "no flow" classification. Rather, there is an increase in sequential flow and velocity-based preferential flow, which would rather favor explanations associated with hydrophobicity.

5.3.5 Combining Spatial and Temporal Components of Preferential Flow Occurrence

Figure 5.11 attempts to integrate the results of the spatial and temporal analysis. Figure 5.11a visualizes the mean precipitation for each sensor location for events that showed a preferential flow response (both velocity-based and non-sequential). The pattern of the mean precipitation that causes preferential flow occurrence is very heterogeneous and is inversely related to the occurrence of preferential flow, i.e. the mean precipitation is larger at locations where preferential flow occurs less often. This is also illustrated in Figure 5.11b, which indirectly highlights spatial differences in importance of rainfall input for the occurrence of preferential flow. Figure 5.11 suggests a spatially variable threshold for preferential flow initiation that varies considerably in terms of mean precipitation, which may have contributed to the difficulty in identifying relationships between temporal and spatial controls on preferential flow.

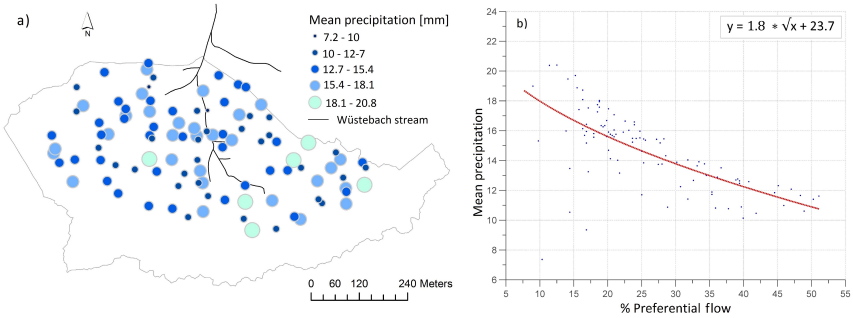

FIGURE 5.11: Spatial distribution of average event precipitation for all events that resulted in preferential flow at a given sensor location during the three-year monitoring period, showing: (a) the spatial distribution of the average preferential flow induced precipitation event across the catchment (natural breaks), (b) the relationship between the overall catchment-wide occurrence of preferential flow (in %, Fig. 5.7a) and the average event precipitation in mm for the events that caused preferential flow.

5.4 Conclusions

Results of the sensor response time analysis for 101 locations and 367 events were used to understand the spatial and temporal occurrence of preferential flow in the Wüstebach catchment. Results confirmed that preferential flow is triggered by the amount and intensity of precipitation. During events with relatively low and high amounts of precipitation, the catchment behaved as a unit, with no response during the dryer and an almost entirely non-sequential preferential response during events with high precipitation sums. For large events (> 25 mm), the occurrence of preferential flow was negatively correlated to antecedent wetness conditions. Relatively dry initial soil moisture conditions provided more suitable conditions for preferential flow, allowing catchment-wide occurrence of preferential flow. Results of the spatial analysis showed that the overall heterogeneous occurrence of preferential flow could not be explained by catchment-wide topographic or soil-specific controls. This suggests that the occurrence of preferential flow in this catchment is governed by unresolved small-scale structures and processes. When combining the results of the spatial and temporal analysis, a spatiotemporal image of the occurrence of preferential flow in the Wüstebach catchment appeared. During relatively dry and extreme wet events, there is a catchment wide-response governed by a temporal threshold in precipitation. During

intermediate events, locations that are more prone to preferential flow may already be active, whereas other locations still show no response or sequential flow behaviour. These local differences are most likely governed by local soil structures, biological features, and small-scale flow processes.

This chapter highlights that the use of sensor response time series in combination with temporal and spatial data analysis provides a powerful tool to increase understanding of the occurrence of preferential flow in space and time. However, this method does not provide information on the fate of water, although this would be interesting to better understand the impact of catchment-wide preferential response on runoff processes. No landscape-unit based controls for preferential flow were found, which is likely related to the relatively homogenous soil types and geology in the Wüstebach catchment.

Chapter 6

Spatiotemporal Changes in Sequential and Preferential Flow Occurrence after Partial Deforestation [1]

6.1 Introduction

In the previous chapter, a soil moisture sensor response time analysis (Lin and Zhou, 2008; Graham and Lin, 2011; Hardie et al., 2013; Liu and Lin, 2015) was introduced, which provides an innovative approach to study the occurrence of preferential flow. This chapter uses the same analysis strategy to detect changes in subsurface flow behaviour related to the partial deforestation in the Wüstebach catchment. One of the first studies that used a soil moisture sensor response time analysis to identify differences in flow behaviour associated with different vegetation types (grassland and forested sites) was provided by Jin et al. (2018). Their results indicated that vegetation combined with topographic characteristics and rainfall event characteristics determined the soil moisture response for a given event. This study was, however, limited to four sites (each site equipped with five sensors), represented only one growing season, and did not contain a reference period. Demand et al. (2019) also used a response time analysis and found clear differences in preferential flow occurrence related to vegetation (grassland or forest) and precipitation intensity.

[1] This chapter is adapted from a journal article published as: I. Wiekenkamp, J.A. Huisman, H.R. Bogena, H. Vereecken, 2019. Effects of Deforestation on Water Flow in the Vadose Zone. Water, 12(1):35.

In this study, the SoilNet Wüstebach dataset is used in a paired catchment approach with a control period and a reference area (instead of a reference catchment). This dataset is used to analyse whether deforestation had a significant effect on the infiltration patterns (type of flow, wetting depth, and antecedent moisture). In this chapter, the following questions will be addressed: (1) How does partial deforestation affect the occurrence of preferential and sequential (piston) flow? (2) Are spatial differences in unsaturated flow behavior observed after deforestation? (3) What are potential mechanisms for the observed changes in flow behavior (if any)?

6.2 Methodology

6.2.1 Measurement Setup

Partial deforestation in the Wüstebach catchment took place in August 2013. All trees in the riparian zone and its close vicinity were removed (Figure 6.1). More information about the catchment and the partial deforestation can be found in Chapter 3. Two different time periods were selected for comparison. A control period where no treatment took place (April 2010 – May 2013; analysed in detail in Chapter 5), and a treatment period after the partial deforestation (September 2013 – November 2015). Although part of the deforested area has different soils than the remainder of the catchment, it was already concluded from the results presented in Chapter 5 that there was no clear difference in preferential and sequential flow occurrence related to soil types.

In the analysis presented here, it was important to only use SoilNet sensor locations that had high-quality soil moisture information and little missing data for all six sensors installed at three depths for the entire five-year period. In total, 51 sensor locations out of 150 locations fulfilled this requirement, including 19 locations where deforestation took place after August 2013 and 32 locations that remained under forest throughout the entire monitoring period (Figure 6.1). Although the majority of sensors (>60%) provide sufficient quality to analyse hourly soil moisture fluctuations, only these 51 locations had high-resolution 15-minute data for all six sensors with sufficient quality. Overall, the distribution of the sensors in space was not entirely equal. No sensor location in the southern part of the catchment was considered, which

is mainly related to the high moisture conditions in this area. This resulted in a high amount of sensors that either stopped recording within the monitoring period or that produced unrealistic data. For the soil moisture response analysis, all SoilNet data were processed as described in Chapter 3 and Chapter 5. Most importantly, extremely high and low soil moisture values and spikes were removed and data were linearly interpolated to a common time axis with a 15 minute interval.

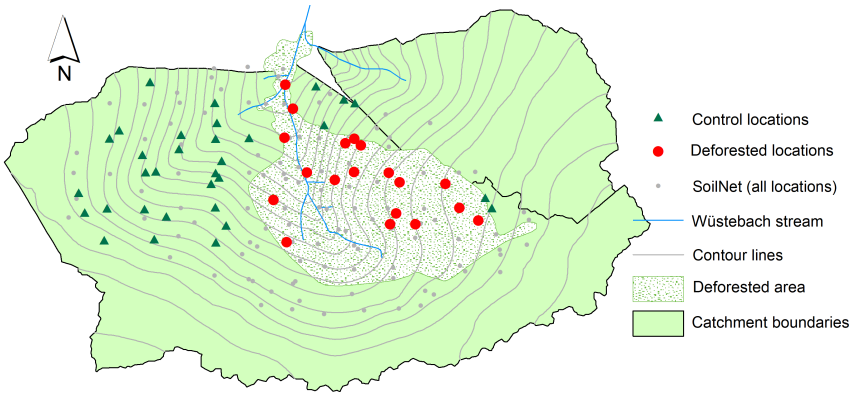

FIGURE 6.1: Positions of the 51 selected SoilNet locations in the reference area (32 locations) and the treatment area (19 locations).

6.2.2 Event Delineation and Soil Moisture Response

Hourly precipitation data from the meteorological station Kalterherberg (DWD, German Weather Service) located 8 km west of the Wüstebach catchment was used for the event delineation and to determine event characteristics. Although precipitation data from the deforested region in the Wüstebach catchment were available after deforestation (Figure 6.1), data from the Kalterherberg station were used for the entire time period for consistency. However, the on-site measurements showed a good agreement with the data from the Kalterherberg station (Chapter 3 and 4). Similar to Chapter 5, the precipitation time series was separated into events using a heuristic event separation with a minimum period without rain (T_p) of 3 hours and a minimum precipitation amount (T_a) of 1 mm. Events where more than 20% of all available sensors did not provide sufficient data were removed. This resulted in the 367 events that were already analysed in Chapter 5 and an additional

350 events after the deforestation.

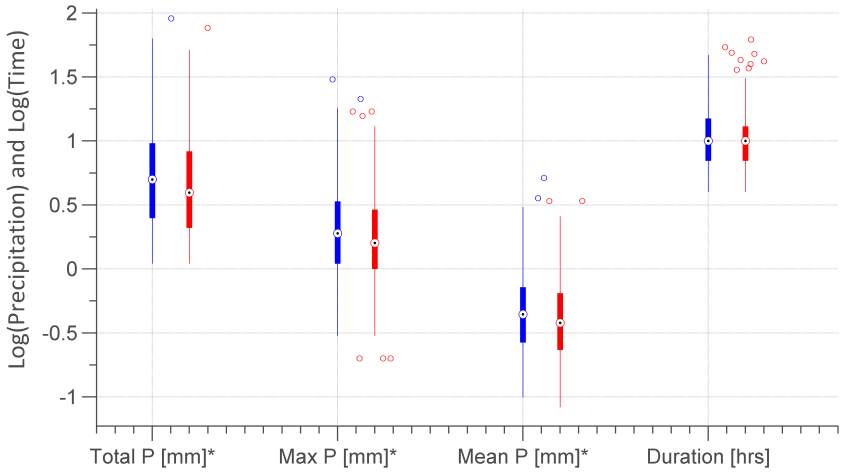

FIGURE 6.2: Comparison of precipitation event characteristics before (blue) and after (red) partial deforestation using a normal y-axis (right) and a log-scaled y-axis (left). Characteristics marked with an asterisk were significantly different (5% significance level; t-test in MATLAB 7.12). Data identified as outliers are indicated with a red '+' symbol.

Figure 6.2 shows a comparison of the events before and after partial deforestation (i.e. the control and the treatment period). Because of the skewed nature of the precipitation data, the event information was log-transformed. The number of events before and after deforestation was very similar (350 vs. 367 events). To test the similarity between the two sets of events, a two-sided t-test was performed (MATLAB 7.12). It was found that the total, maximum and mean precipitation were significantly different (5% significance level) for the control and the treatment period (Figure 6.2). In particular, the total precipitation, maximum precipitation, and mean precipitation of an event were significantly lower for the events that belong to the treatment period. Even if the events characteristics are significantly different for both periods, the BACI (Before- After Control Impact) approach where a reference area is used for the entire period (i.e. the control and treatment period) allows to compare the results of the sensor response time analysis before and after deforestation. The soil moisture response of the first 367 events was already analysed in detail and described in Chapter 5. For the precipitation events after the deforestation that are in focus in this chapter, the soil moisture time

series were also analysed according to the soil moisture response time analysis described in Chapter 5.

6.3 Results and Discussion

6.3.1 Time Series of Precipitation and Soil Moisture

Figure 6.3 shows time series of precipitation and average soil moisture at different depths for the entire time period (control and treatment period) for both monitoring areas (reference and deforested area). Additionally, the monthly number of delineated events is provided. There are fewer events per month during the control period than after partial deforestation. This is related to the fact that 72 events were omitted during the control period, whereas only one event was not considered for the treatment period. Clearly, the soil moisture in the treatment area deviated more from the soil moisture in the reference area after the partial deforestation. The differences in soil moisture dynamics were larger in the dryer period. Especially during summer, the deforested area remained wetter after deforestation, whereas this area dried up during the control period. Clearly, this will affect initial moisture conditions for individual precipitation events and therewith water flow in the vadose zone. Overall, the differences between the treatment and reference area are largest for the uppermost sensors (5 cm depth) and smallest for the deepest sensors (50 cm depth). More details about the general changes in soil moisture characteristics can be found in Chapter 4.

It is important to consider that our current analysis assumed that the precipitation was representative for the control and the treated area in the Wüstebach catchment. On this small scale (38.5 hectares), we do not expect large differences in precipitation between the forested and the deforested area. It is also important to mention that events with frozen soil conditions were removed, but that snow events were not excluded from the analysis. Some of the precipitation events during the winter months might have included snow or snow melt conditions, potentially resulting in no or a delayed soil moisture response. This should, however, not largely affect the outcome of this study, as the focus here is on finding differences in flow response between the control and treatment area.

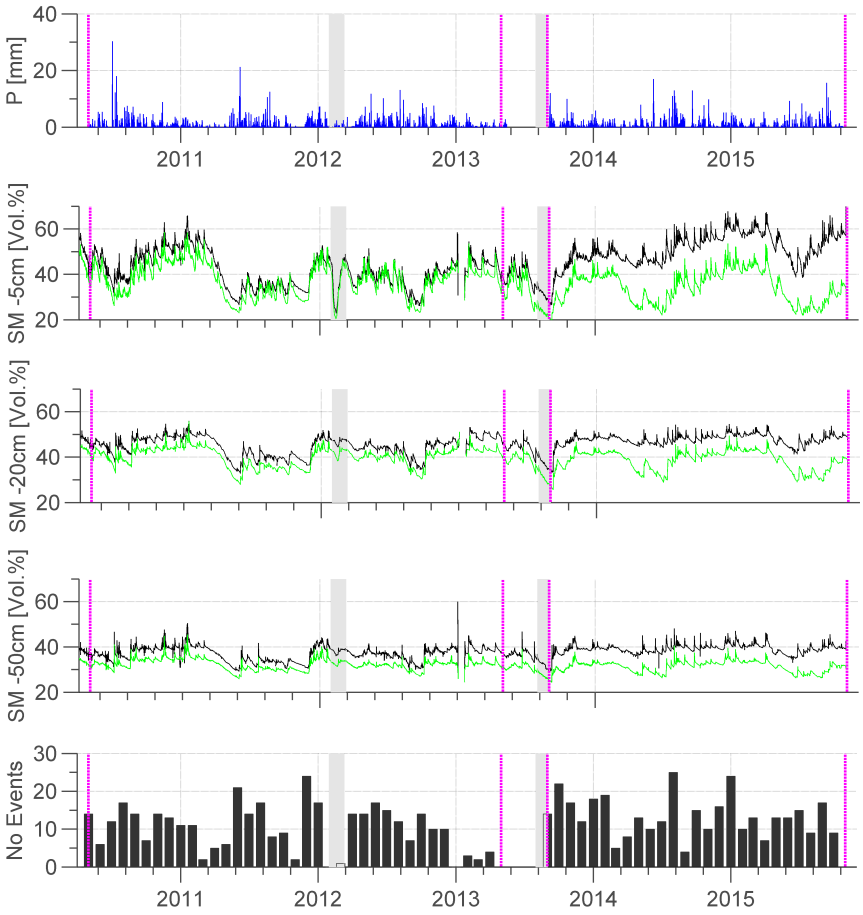

FIGURE 6.3: Precipitation(a), soil moisture at 5, 20 and 50 cm depth (b-d), respectively, and the number of events per month for the control and treatment period (e). The black lines in panels b-d show the average moisture content in the treatment area (before and after the deforestation). The green lines in panels b-d show the average moisture content of the 32 locations that remained untreated throughout the entire monitoring period. The vertical magenta lines indicate the start and end of the control period and treatment period. The first time period marked in grey indicates a soil freezing period that was left out of the analysis, and the second period marked with grey indicates the period in which the deforestation took place.

6.3.2 Analysis of Differences in Sensor Response due to Deforestation

To investigate whether deforestation affected flow behavior in the subsurface, changes in preferential, sequential, and no-flow occurrence were analysed by comparing the location-averaged percentage of flow (sequential, preferential, no-flow) for the control and treatment group before and after partial deforestation. Figure 6.4 shows the distribution of the temporally–averaged flow characteristics of the 19 treated SoilNet locations and the 32 non-treated SoilNet locations for both periods. Two-sample t-tests (Snedecor and Cochran, 1989) between the two analysis periods were performed (MATLAB 7.12) to determine the significance of the observed changes in flow behaviour.

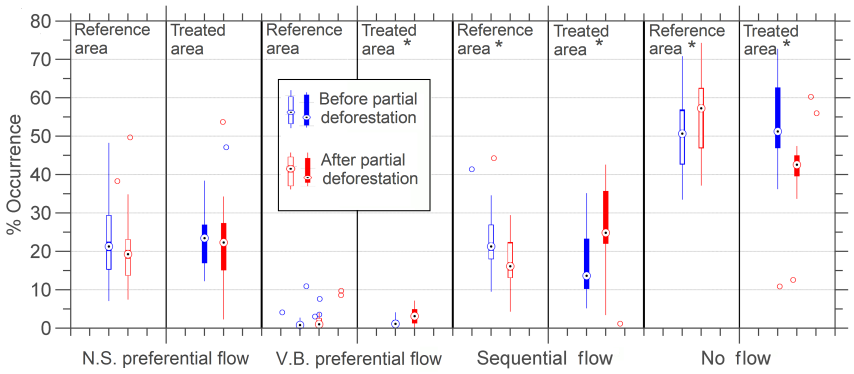

FIGURE 6.4: Comparison of temporally-averaged flow occurrence for the untreated and treated area before and after partial deforestation. Blue boxplots (filled and empty) show the results for the control period, whereas red boxplots (filled and empty) show the results for the period after deforestation. The asterisk (*) indicates a significant difference (5% significance level) between the two monitoring periods. Data identified as outliers are indicated with a red '+' symbol.

The average non-sequential preferential flow occurrence slightly decreased between the control and treatment period for both sensor location groups (reference and treatment area). In both cases, the difference was not significant. The occurrence of velocity-based preferential flow, on the other hand, increased slightly after partial deforestation for both sensor groups. However, the increase in the occurrence of velocity-based preferential flow was only significant for the treated area. A different impact of deforestation was observed for the occurrence of sequential flow (piston flow) and no flow. IIn

both cases, the sensors in the control group showed the opposite response as the sensors in the treatment area. For the reference area, the occurrence of sequential flow generally decreased significantly and the no-flow response increased significantly. These changes are related to the precipitation characteristics of the events after the deforestation (Figure 6.2) with lower total amounts and lower maximum intensities. In the treatment area, on the other hand, sequential flow occurred more frequently and events with a no-flow response were reduced (both also significant). Due to the difference in response between the reference and the treatment area, the observed differences are likely directly linked to deforestation.

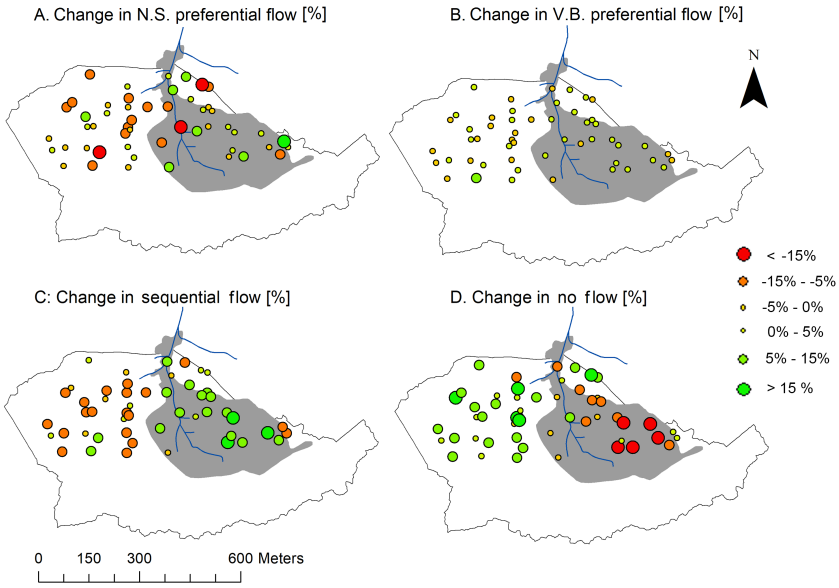

FIGURE 6.5: Spatial change in frequency of flow occurrence between the control and the treatment period for the reference and treatment area (shown in grey) in the Wüstebach catchment.

After analysing the overall change in flow behavior, it is also interesting to investigate the change in response for individual sensors. This helps to identify whether the general direction of change discussed above was observed for all locations, or if this general trend emerged from spatially highly variable changes for individual locations. For this, changes in flow behavior

before and after partial deforestation are visualized in Figure 6.5 for individual sensor locations. Although no clear and consistent pattern in change could be observed for non-sequential preferential flow (Figure 6.5a), there were more locations with a strong decrease in non-sequential preferential flow in the reference area. The change in velocity-based preferential flow was generally small at all sensor locations, and no clear differences between the treatment and reference area could be identified (Figure 6.5b). However, a clear and consistent pattern in the change of sequential flow (Figure 6.5c) and no flow (Figure 6.5d) was observed for the sensor locations in the control and the treatment area. Whereas the occurrence of sequential flow decreased for almost all sensors in the reference area, sequential flow increased for most locations in the treatment area. An opposite trend was observed for the occurrence of a no-flow response. Here, the frequency of no flow decreased at almost all locations in the treatment area and increased at most of the locations in the reference area.

Overall, clear changes in sequential and no flow occurrence were observed, which could directly be linked to the partial deforestation in the Wüstebach catchment. The observed differences are likely related to wetter conditions in the deforested part of the catchment (Figure 6.3) and the larger amount of direct rainfall (no interception). Whereas the results presented here showed clear differences in sequential flow occurrence, several earlier studies have reported clear differences in preferential flow occurrence that were related to different vegetation types (Alaoui et al., 2011; Zhao et al., 2012; Jin et al., 2018; Demand et al., 2019). Alaoui et al (2011) found preferential flow both in forest and in grassland soil, but dye patterns suggest higher interactions between the macropores and the matrix of the forest soils. The macropores in the grassland soils, on the other hand, showed little interaction with the surrounding. Jin et al. (2018) and Demand et al. (2019) found clear differences in preferential flow occurrence between grassland and forested sites. Zhao et al. (2012) also observed more preferential flow occurrence for a forest site as compared to a grassland site.

There are several possible explanations for this discrepancy in results. First of all, differences in preferential flow occurrence were only significant for certain landscapes and precipitation conditions (Demand et al., 2019) or for certain landscape positions (Jin et al., 2018) in part of these studies. The results of Zhao et al. (2012) can potentially also be explained by differences

in soil type between the grassland and forest site. Most importantly, all these studies compared two steady-state landscapes (mostly forest and grassland). In this study, the deforested area is in a transient stage. Generally, deforestation measures can also indirectly affect water infiltration and soil moisture fluctuations via (1) soil compaction, (2) changes in soil structure, and (3) the leftover material from tree felling. In this study, we however assume that the soil system has maintained many of the characteristics of the original soil and that the soil properties were only slightly affected by the tracks of the harvester (Wohlleben, 2014). At the same time, part of the hydrological states and fluxes were heavily affected by the deforestation, including the antecedent moisture conditions. These differences in the states and fluxes will however not remain. When the deforested area reaches a new steady state, the soil system may have a stronger imprint of the new vegetation, and the hydrological states and fluxes will have adapted to the new vegetation and changed subsurface flow processes.

6.3.3 Event Conditions: Antecedent Moisture and Precipitation

In the previous section, the lack of interception and the increase in soil moisture were proposed to explain the increase in sequential flow behavior and the corresponding decrease in no flow occurrence. To investigate this in more detail, Figure 6.6 and 6.7 show the antecedent soil moisture conditions (i.e. soil moisture at the start of an event) for the reference and the treatment area for both monitoring periods. Generally, the distribution of the antecedent soil moisture was widest for the uppermost layer. For the reference area (Figure 6.6), no clear difference in the distribution of initial soil moisture for the two monitoring periods was observed. For the treated area (Figure 6.7), a clear difference in the initial moisture conditions before and after deforestation was observed. Soils in the treated area were generally wetter after the deforestation. In the deeper layers, the distributions were narrower after the deforestation. This indicates that the variability in initial moisture conditions in the deeper soil layers (20 and 50 cm depth soil moisture data) was smaller after the treatment.

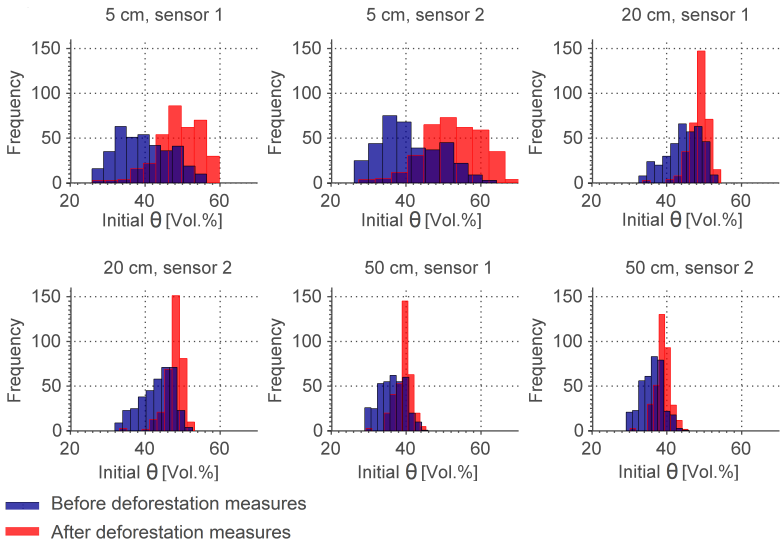

FIGURE 6.7: Distribution of initial soil moisture conditions (antecedent catchment wetness) for the two monitoring periods at all treatment locations (deforested area).

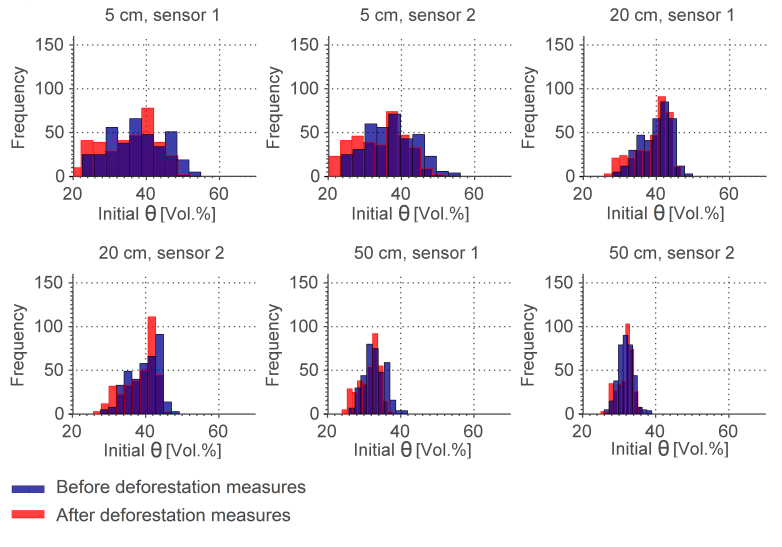

FIGURE 6.6: Distribution of initial soil moisture conditions for the two monitoring periods (Figure 6.3) at all reference locations. Please note that no deforestation took place in the reference area.

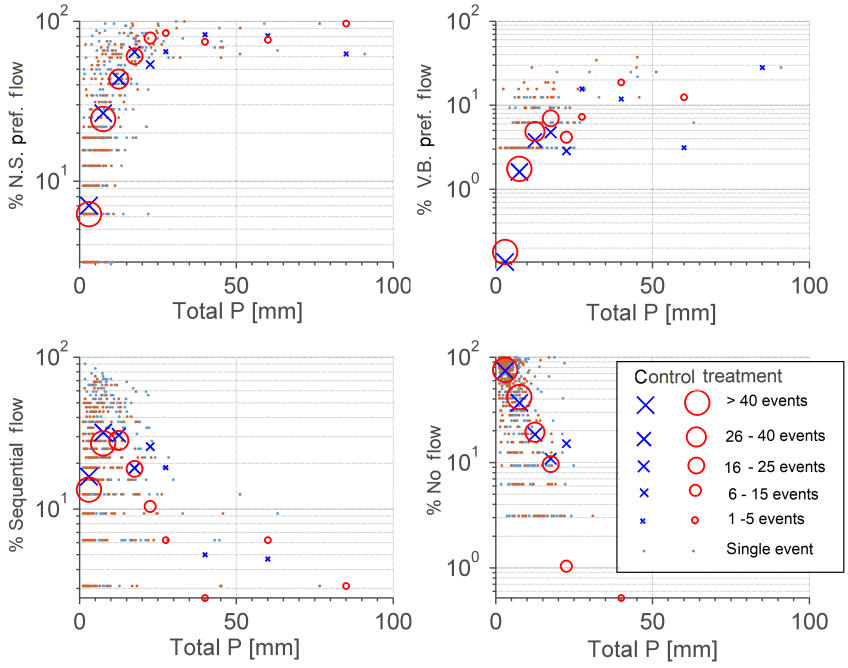

FIGURE 6.8: Effect of total precipitation on preferential flow generation for all 367 individual events before treatment (blue) and 350 events after the treatment (red) in the reference area. The larger circles and crosses indicate the average flow occurrence for a given precipitation class (see legend). The size of the crosses and circles indicates the number of events within the given class. N.S. = Non-Sequential and V.B. = Velocity-Based.

Previous studies have already shown that precipitation characteristics can explain part of the temporal variation in preferential flow dynamics (Hardie et al., 2013; Wiekenkamp et al., 2016; McGrath et al., 2010; Jarvis et al., 2016). In this study, possible changes in these observed patterns were also analysed. Figure 6.8 and Figure 6.9 show the relationship between the percentage of sensors that were classified in a given response group and precipitation amount for the reference and deforested area, respectively. Similar to Figure 5.8 (Chapter 5), an increase in preferential flow occurrence with increasing precipitation amount was observed. For the reference area (Figure 6.8), the observed trends are very similar for both monitoring periods. For the treated area (Figure 6.9), the general patterns were similar, but clear differences in trends were observed between the control and treatment period. For the same amount of rainfall, more sensor locations showed a sequential or preferential response after deforestation and less sensor locations showed

no response. Even though no clear changes in the temporally-averaged occurrence of preferential flow were observed (Figure 6.4), more preferential flow was observed in the deforested area for events with similar precipitation characteristics (Figure 6.8 and Figure 6.9). The increase in preferential flow is probably mainly caused by the lack of interception in the deforested area. Likely, this increase cannot be observed in the temporally-averaged boxplots (Figure 6.4), since the rainfall events after the deforestation were generally less intensive (less total, maximum and mean precipitation). Clearer differences in temporally-averaged preferential flow occurrence between the reference and treatment area (Figure 6.4) might have potentially occurred if the precipitation events would have been more similar.

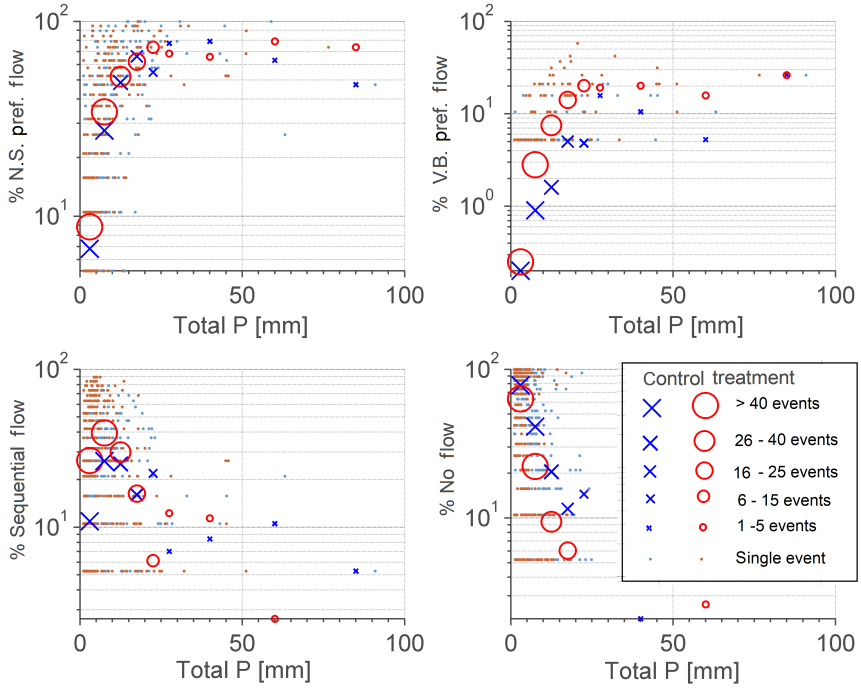

FIGURE 6.9: Effect of total precipitation on preferential flow generation for all 367 individual events before (blue) and 350 events after the treatment (red) in the treated (deforested) area. The larger circles and crosses indicate the average flow occurrence for a given precipitation class (see legend). The size of the crosses and circles indicates the number of events within the given class. N.S. = Non-Sequential and V.B. = Velocity-Based.

Altogether, the soils were wetter in the treated area after the deforestation

and the response to rainfall was stronger (less no flow conditions; more sequential flow and preferential flow, probably related to a higher hydraulic conductivity). Previous studies have already indicated that higher initial moisture content can increase the occurrence of preferential flow (e.g Hardie et al., 2013). Liu and Lin (2015) also reported more preferential flow during wetter soil conditions in the downslope region of the Shale Hills catchment. This might be one explanation for the observed increase in preferential flow response for similar rainfall events after the deforestation. However, the increase in preferential response might also be related to a lack of interception. In this study, the occurrence of sequential flow especially increased for the wetter soil conditions after the deforestation. Here, the question remains whether the wetter antecedent moisture conditions and the lack of interception steered the increase in sequential flow, or if a higher frequency in sequential flow would also be observed for the bare soil during dryer soil conditions.

6.3.4 Implications of the Presented Results

The current study clearly demonstrates the short-term effects of deforestation on water flow in the vadose zone, which has a variety of implications. An increase in surface runoff is generally expected after deforestation. However, in the current study, an increase in infiltration (via piston flow and preferential flow) was observed after deforestation in the treated area, which is expected to reduce surface runoff. This is most likely related to the deforestation practices, and it is likely that the use of skid rails made from branches and logs have indeed caused a minimum impact on the soil structure and maintained the preferential flow paths of the forested soil.

A change in preferential and sequential water flow in the soil can also affect water quality and transport of nutrients in the subsurface. It is well-known that preferential flow can either enhance or reduce the filter capacity of the soil (Jarvis, 2007) and that preferential flow can reduce the time that is needed to transport solutes and export nutrients from the surface to the groundwater (Flury et al., 1994; Julich et al., 2017). We anticipate that the increase of piston flow will cause an increase in nutrients in the upper layers, which might assist the natural regrowth of plants in the catchment. The observed increase in preferential flow after deforestation (for similar precipitation events), on the other hand, will likely enhance the transport and export of nutrients, such as Phosphorus (e.g Grant et al., 2019) to deeper soil layers

and the groundwater.

The increase in water infiltration into the subsurface via preferential and piston flow can also affect soil carbon allocation. Carbon stored in soil and plant residues is receiving considerable interest, because they present a long-term carbon sink that can be affected by climate and land use change (Lal, 2008). This, on its turn can affect the transport of dissolved organic carbon (DOC) through the vadose zone (e.g. Weigand et al., 2017). Clearly, the transport of DOC is closely linked to its transit time as it reflects the potential of soils to buffer DOC (Manzoni et al., 2009; Stockinger et al., 2019). The results of this study suggest that DOC export at the catchment scale will also be influenced by the direct effect of deforestation on preferential flow processes. We anticipate that the observed increase in preferential flow occurrence after deforestation 8during similar precipitation conditions) may cause increased DOC export especially during intensive precipitation events.

6.4 Conclusions

This chapter focussed on the effects of the partial deforestation on flow conditions in the vadose zone of the Wüstebach catchments. A total amount of 717 precipitation events were analysed for 51 locations, including 367 pre-deforestation events (Chapter 5) and 350 additional post-deforestation events. It was shown that partial deforestation increased the occurrence of sequential flow and decreased the occurrence of no flow in the treated area. Similar precipitation events caused a spatially more extensive sequential and preferential response in the deforested area, which can be explained by the higher antecedent moisture conditions in the area and the lack of interception. The conditions in the reference area served as a control and showed that the observed changes in the deforested area are not caused by differences in climate conditions. This study highlights that the use of sensor response time analysis in combination with vegetation change measures can be a powerful tool to increase understanding of the occurrence of preferential and sequential flow related to land use change.

Chapter 7

Distributed Hydrological Modelling of Partial Deforestation in a Small Headwater Catchment

7.1 Introduction

The three previous chapters of this thesis focussed on the analysis of different types of hydrological data to investigate the effects of partial deforestation in the Wüstebach catchment. This chapter, on the other hand, focusses rather on the conceptualization, parameterization and evaluation of a distributed physically-based hydrological model with a focus on predicting the effects of partial deforestation. Distributed physically-based hydrological models can account for spatially complex land surface characteristics (e.g. topography, spatial distribution of soil properties, climate distributions; Dwarakish and Ganasri, 2015), and are therefore suitable to predict the effect of spatial changes in land use in a catchment (Beven, 2012; Fatichi et al., 2016). As already discussed in Chapter 1 and 2, the prediction of spatiotemporal (surface and subsurface) states and fluxes with such models remains challenging (Gebler et al., 2017). There are only few datasets available to test the predictive capability of distributed hydrological models under (non-linear) change conditions.

In this chapter, the parallel variably saturated subsurface model ParFlow (Kollet and Maxwell, 2006; Maxwell, 2013) will be used in combination with the land-surface model CLM (Community Land Model-CLM Version 3.5; Oleson et al., 2008). Both model components are contained within the Terrestrial System Modelling Platform (TerrSysMP; Shrestha et al., 2014; Gasper et al., 2014). The predictive capability of ParFlow-CLM under unchanged and changed land use conditions will be evaluated for the Wüstebach catchment,

which dataset provides the unique opportunity to perform multi-criteria evaluation as it includes complete water balance information with distributed soil moisture data (see Chapter 3 and 4). Three main questions will be addressed in this chapter:

1. What are the capabilities of ParFlow-CLM to predict the hydrological effects of partial deforestation?
2. What are the limitations of ParFlow-CLM in predicting the hydrological effects of partial deforestation?
3. What could be improved to obtain better predictions?

7.2 Methodology

7.2.1 TerrSysMP

In the past years, a series of novel, two-way coupled atmospheric-hydrological modelling systems have been created to improve the representation of hydrometeorological processes and to provide improved hydrological forecasts related to land use and climate change (e.g. Senatore et al., 2015). One of these modelling systems is the Terrestrial System Modelling Platform (TerrSys MP; Shrestha et al., 2014; Gasper et al., 2014), which simulates water and energy cycles from the deeper subsurface into the atmosphere using a scale consistent coupling of three environmental models. The modular platform currently contains ParFlow (Parallel Flow version 3.1; Ashby and Falgout, 1996; Jones and Grant, 2001; Kollet and Maxwell, 2006; Maxwell, 2013), CLM (Community Land Model-CLM Version 3.5; Oleson et al., 2008) and COSMO (Consortium for Small-Scale Modelling; Baldauf et al., 2011; Steppeler et al., 2003), which can be configured using any combination of the available models via the OASIS (Ocean Atmosphere Sea Ice Soil, version 3.0) coupler (Valcke, 2013).

Examples of studies that have used the ParFlow-CLM configuration within TerrSysMP are Rahman et al. (2014), Shrestha et al. (2015), Kurtz et al. (2016), Gebler et al. (2017), Shrestha et al. (2018) and Zhang et al. (2018). Other applications where CLM was combined with ParFlow outside of TerrSysMP have been presented by Jefferson and Maxwell (2015), Condon and Maxwell (2015), Maxwell et al. (2015), Maxwell and Condon (2016), Jefferson (2016), Jefferson et al. (2017), and Condon and Maxwell (2017). These studies clearly

showed that ParFlow-CLM can provide acceptable mass and energy fluxes even without calibration (e.g Rahman et al., 2014). When a suitable hydraulic parameterization of the subsurface is used, ParFlow-CLM can also reproduce the spatial variability of soil moisture (Gebler et al., 2017). Examples of different TerrSysMP applications using the COSMO-ParFlow-CLM configuration are provided by Keune et al. (2016), Keune et al. (2018), Rahman (2015), Sulis et al. (2017), and Sulis et al. (2018). With the incorporation of an atmospheric prediction model, fully distributed predictions of hydrology-weather feedbacks become feasible, and potentially enable to investigate the effect of deforestation on precipitation at larger scales (e.g. Amazon basin). As the current study is at a very small scale, feedbacks to weather are not relevant. Therefore, this study is restricted to the ParFlow-CLM configuration of TerrSysMP (from now on referred to as ParFlow-CLM).

In ParFlow-CLM, the water balance (mass balance) in the subsurface is calculated by ParFlow, and the water and energy balance at the surface are calculated by CLM 3.5 (Figure 7.1). A description of the most important hydrological processes that are simulated by ParFlow and CLM 3.5, the corresponding equations, and the coupling mechanisms are given below. More details about these model components and the entire TerrSysMP framework can be found in Shrestha et al. (2014).

7.2.1.1 ParFlow Model

ParFlow is a variably saturated subsurface flow model that also simulates overland flow. To simulate saturated and unsaturated water flow in the subsurface, the 3-D transient Richards' equation in the mixed form is solved (Kollet and Maxwell, 2006):

$$S_s \cdot S_w(\psi_p) = \frac{\delta \psi_p}{\delta t} \cdot \phi \cdot \frac{\delta S_w(\psi_p)}{\delta t} = \bigtriangledown \cdot q + q_s + \frac{q_e}{m'} \tag{7.1}$$

with

$$q = -K_s(x) \cdot K_r(\psi_p) \cdot \bigtriangledown(\psi_p - z) \tag{7.2}$$

In these equations, S_s [m^{-1}] represents the specific storage coefficient, S_w [-] is the relative saturation, ψ_p [m] is the pressure head, $\delta\psi_p / \delta t$ [m/s] represents the pressure head gradient in time, $(\delta S_w(\psi_p))/\delta t$ [s^{-1}] is the change in relative saturation (under a specific pressure) in time, ϕ [-] is the porosity, q [m^3/s] is the volume specific Darcy flux, q_s [m^3/s] is a source/sink term (which is

negligible in this study), q_e/m' is the exchange rate with the surface [m/s] divided by the surface-subsurface interface thickness, $K_s(x)$ is the saturated hydraulic conductivity [m/s], k_r [-] the relative permeability, and z [m] the vertical downward position (Kollet and Maxwell, 2006). ParFlow discretizes these functions in space by using a cell-centred finite difference method. Discretization in time is done via an implicit backward Euler scheme.

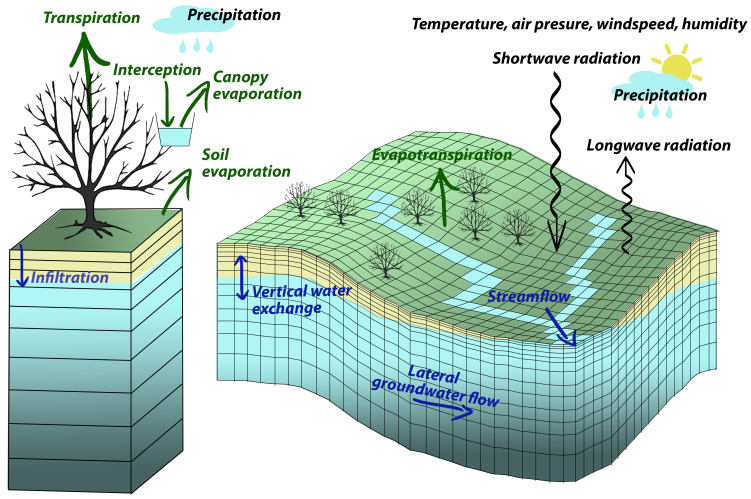

FIGURE 7.1: Visualization of the required input information and the resulting water and energy fluxes in the ParFlow-CLM 3.5 configuration of TerrSysMP. The black arrows indicate the required climatic input data for both models, the green arrows indicate the fluxes calculated by CLM 3.5, and the blue arrows indicate the fluxes calculated by ParFlow.

Overland flow is considered in ParFlow in the form of an upper boundary condition using a kinetic wave approximation by assuming that there is no vertical change in momentum in ponded water columns and that there is a continuity of pressure and flux at the surface:

$$-K_s(\psi) \cdot \bigtriangledown \psi \cdot n_m = \frac{\delta \, \| \psi, 0 \|}{\delta t} - \bigtriangledown \cdot (\vec{v} \, \| \psi, 0 \|) - q_{\mathrm{r}}(x) \tag{7.3}$$

where $q_r(x)$ is the precipitation or evapotranspiration rate [m/s] and n_m [(s/m)$^{-1/3}$] is the Manning's coefficient, which represents the surface roughness and therewith affects the speed at which water can move over the surface. The vector $- \bigtriangledown \cdot (\vec{v} \, \| \psi, 0 \|)$ represents the lateral flow and is set to 0 if ψ<0, or set to ψ if ψ>0. ParFlow discretizes this function in space with a finite

control volume approach. Again, discretization in time is done via an implicit backward Euler scheme. To solve equations 7.1 – 7.3, a Newton-Krylov method with multigrid preconditioning (multigrid preconditioned conjugate gradient (MGCG) algorithm) is used (Ashby and Falgout, 1996; Kollet and Maxwell, 2008).

7.2.1.2 CLM 3.5 Model

The CLM 3.5 model was developed to simulate land surface processes in global climate simulations. In the TerrSysMP framework, this model is coupled to ParFlow to simulate water and energy fluxes at the land surface. For this, each pixel in CLM is assigned a certain percentage of five different main classes of land cover (vegetation, glacier, lake, wetland and urban). The land cover class "vegetation" is further divided into 17 so-called Plant Functional Types (PFT). All PFT and land cover classes are connected to sets of equations and parameters that are used to simulate the water and energy cycle.

In the coupled version of ParFlow-CLM, CLM is used to simulate interception and evapotranspiration. In particular, interception is determined from the incoming precipitation (P_{rain}+P_{sno}) [mm/s], a scaling factor α_{sc} [set to 0.25, -], the exposed Leaf Area Index *LAI* [-] and the Stem Area Index *SAI* [-]:

$$I = \alpha_{sc}(P_{rain} + P_{sno}) \cdot [1 - exp(-0.5 \cdot (LAI + SAI))] \tag{7.4}$$

The actual evapotranspiration (ET_a) [mm/s] of non-vegetated surfaces is determined by the evaporation at the surface (soil evaporation, E_g):

$$E_g = -\rho_{atm} \frac{q_{atm} - q_g}{r_a + r_{soil}} \tag{7.5}$$

where the water vapour flux is determined by air density, ρ_{atm} [kg/m^3], the difference in specific humidity between the atmosphere (q_{atm}) [kg/kg] and the surface (q_g) [kg/kg], and the aerodynamic and soil resistance (r_a + r_{soil}) [s/m]. The soil resistance, r_{soil}, was added to CLM 3.5 to avoid excessive soil evaporation commonly found in previous CLM versions. It is calculated as:

$$r_{soil} = (1 - f_{sno}) \cdot exp(8.206 - 4.255 \cdot s_1) \tag{7.6}$$

where f_{sno} [-] is the fraction of snow-covered soil and s_1 a soil moisture term, which depends on the volumetric water content of the ice fraction $\theta_{ice,1}$ [vol.

%], the water fraction $\theta_{liq,1}$ [vol. %] and the saturated water content $\theta_{sat,1}$ [vol. %]:

$$s_1 = (\theta_{ice,1} + \theta_{liq,1)}/\theta_{sat,1} \leq 1 \tag{7.7}$$

The actual evapotranspiration (ET_a) of vegetated surfaces is defined as the sum of the evaporation of intercepted water from the canopy (stem and leaves, E_i) [m/s], the soil evaporation (E_g) [m/s] and the transpiration of the vegetation (dry leaves surfaces, $T_)$, which was already described in equation 2.2. The evaporation of interception (E_i) depends on the difference between the saturated specific humidity at the given vegetation temperature ($q_{sat,T}$) [kg/kg] and the specific humidity within the canopy (q_s) [kg/kg]:

$$E_i = -\rho_{atm} \cdot f_w(LAI + SAI)\frac{q_c - q_{csat,T}}{r_b} \tag{7.8}$$

where f_w [-] is the fraction of wet leaves and stems and r_b [s/m] is the leaf boundary layer resistance, which is calculation according to Equation 7.10:

$$r_b = \frac{1}{C_v}(U_{av}/d_{leaf})^{-1/2} \tag{7.9}$$

where C_v is the turbulent transfer coefficient (between the canopy surface and the canopy air) [0.01 m/s $^{-1/2}$], d_{leaf} [m] is the leaf dimension (wind flow direction), and U_{av} [m/s] the (leaf) friction velocity. The actual transpiration of the vegetation, T, depends on the soil wetness index, β_t [-], the potential transpiration, T_{pot} [m/s], and a calculated actual T_{pot}-fraction (r_d'') [-] using:

$$T = T_{pot} \cdot r_d'' \quad for;\ T_{pot} > 0 \ \ and \ \ \beta_t > 1 \cdot 10^{-10} \tag{7.10}$$

$$T = 0 \qquad for \ \ T_{pot} \leq 0, \ \ or \ \ \beta_t \leq 1 \cdot 10^{-10} \tag{7.11}$$

The soil wetness index b_t [unitless; 0 - 1] is defined as:

$$\beta_t = \sum_i w_i r_i \tag{7.12}$$

where r_i [-] is the fraction of roots in a given layer i and w_i [-] is the plant wilting factor, which is calculated as follows:

$$w_i = \left\{ \left(\frac{\theta_{sat,1} - \theta_{ice,1}}{\theta_{sat,1}} \right) \left(\frac{\psi_m - \psi_{close}}{\psi_{open} - \psi_{close}} \right) \right\} \tag{7.13}$$

Here, ψ_i, ψ_{open} and ψ_{close} [mm] are the actual soil water matric potential of a given soil layer (i = 1:10), the matric potential at which the plant stomata

are fully open, and the matric potential at which the stomata close (wilting point), respectively. The potential transpiration depends again on air density, ρ_{atm}, the gradient in the specific humidity, $q_c - q_{csat,T}$ [kg/kg], and the leaf boundary layer resistance to transpiration (r_b):

$$T_{pot} = -\frac{\rho_{atm}(q_c - q_{csat,T})}{r_b} \tag{7.14}$$

The actual fraction of the potential transpiration, r_d'' [-], is determined by the fraction of dry leaves f_d [-], the LAI of the shaded and sunlit leaves (LAI_{sun} and LAI_{sha}) [-], r_b, the stomatal resistance of the shaded and sunlit leaves ($r_{s,sun}$ and $r_{s,sha}$) [s/m]:

$$r_d'' = \frac{f_d \cdot r_b}{LAI}\left(\frac{LAI_{sun}}{r_b + r_{s,sun}} + \frac{LAI_{sha}}{r_b + r_{s,sha}}\right) \tag{7.15}$$

The stomatal resistance of the sunlit and shaded leaves (r_s) [s/m] is calculated using the Ball-Berry equation:

$$1/r_s = m_p \cdot \frac{A}{c_s} \cdot \frac{e_{ls}}{e_{li}} \cdot P_{atm} + b_p \tag{7.16}$$

where m_p is an empirical parameter that depends on the vegetation type, P_{atm} [Pa] is the atmospheric pressure, c_s [Pa] is the leaf surface's CO_2 concentration, b_p is the minimal stomatal conductance, which is set to 2000 [$\mu molCO_2$ $m^{-2}s^{-1}$] (hardcoded in CLM 3.5), A is the leaf photosynthesis [$\mu molCO_2 m^{-2}s^{-1}$], e_{ls} [Pa] is the actual vapour pressure at the leaf surface and e_{li} is the saturated vapour pressure at a given leaf temperature.

7.2.1.3 Model Coupling

The OASIS3 coupler is used to exchange information between ParFlow and CLM in a sequential manner. As visualized in Figure 7.1, CLM and ParFlow both account for the calculation of parts of the fluxes in the hydrological cycle. To enable both models to calculate their assigned fluxes, the following information exchange procedure was used. For each time step, ParFlow provides information about the relative soil saturation and pressure of the top 10 soil layers. Then, CLM provides information about interception of the incoming precipitation (P) and is used to calculate abstracted water via evapotranspiration (ET_a). This information is afterwards used to update the soil saturation and pressure in ParFlow.

7.2.2 Model Setup of ParFlow-CLM for the Wüstebach Catchment

7.2.2.1 General Setup

A ParFlow-CLM model was set-up for the Wüstebach catchment using hourly input information for meteorological data and a 10 m by 10 m grid cell size with a terrain-following grid. A flow direction grid of the area was obtained from a digital elevation model of the Wüstebach area with a 10 m resolution using build-in tools (slope and sink-fill tools). The total modelling domain was 1180 m by 740 m, which includes the entire Wüstebach catchment, the reference catchment and some surrounding area. The DEM pre-processing and the generated slope files were tested using a so-called parking lot test, which is explained in detail in section 7.2.3.2. The Wüstebach model is vertically discretised in 4 soil layers and 13 model layers, with thinner model layers near the surface and thicker model layers with increasing depth where less vertical resolution is required (Table 7.1). The 10 upper layers of the ParFlow model (1 m of mineral soil + litter layer) were used to link ParFlow and CLM, which is sufficient to represent the root zone of the spruce forest (Figure 7.2).

To solve the Richards' equation, ParFlow uses soil hydraulic properties based on the Mualem-van Genuchten parameterization (Kollet and Maxwell, 2006; Maxwell, 2013). In this study, the parameterization of these hydraulic properties was based on a HYDRUS-1D calibration by Bogena et al. (2013), who used inverse modelling to estimate soil hydraulic parameters from soil moisture measurements at 5, 20 and 50 cm depth in the Wüstebach catchment. This approach was selected because it is computationally inexpensive, and was already successfully implemented in Mike-SHE, HydroGeoSphere, and an earlier (stand-alone) version of ParFlow-CLM (Cornelissen et al., 2013). However, due to convergence issues within ParFlow using the current setup, the n_{mvg} parameter (n parameter in the Mualem - van Genuchten equation) needed to be increased to 2.0 for all layers (Table 7.2; Figure 7.2).

TABLE 7.1: Layering (vertical discretization) of the ParFlow-CLM model, including information on the common sequence of soil horizons (based on: Gottselig et al., 2017), the assigned thickness and depth of the individual layers, and the corresponding model(s). Figure 7.2 provides a 2D image of the model setup.

Layer No.	**Soil layer**	**Soil horizon***	**Thickness [cm]**	**Starting depth[cm]**	**Final depth[cm]**	**Model(s)**
1	Litter layer	L+ O_f + O_h	2.5	5	2.5	ParFlow + CLM
2	Litter layer	L+ O_f + O_h	2.5	2.5	0	ParFlow + CLM
3	Mineral soil layer 1	A	5	0	-5	ParFlow + CLM
4	Mineral soil layer 1	A	5	-5	-10	ParFlow + CLM
5	Mineral soil layer 2	B	10	-10	-20	ParFlow + CLM
6	Mineral soil layer 2	B	10	-20	-30	ParFlow + CLM
7	Mineral soil layer 2	B	10	-30	-40	ParFlow + CLM
8	Mineral soil layer 3	B-C	20	-40	-60	ParFlow + CLM
9	Mineral soil layer 3	B-C	20	-60	-80	ParFlow + CLM
10	Mineral soil layer 3	B-C	20	-80	-100	ParFlow + CLM
11	Mineral soil layer 3	B-C	20	-100	-120	ParFlow
12	Mineral soil layer 3	B-C	20	-120	-140	ParFlow
13	Mineral soil layer 3	B-C	20	-140	-160	ParFlow

TABLE 7.2: Mualem-van Genuchten soil hydraulic properties used in the ParFlow-CLM model of the Wüstebach catchment for the four different soil layers. Images of the porosity are shown in Figure 7.3.

	α**[1/cm]**	n_{mvg} **[-]**	K_s **[m/s]**	**Porosity**	**Res. saturation**	**Anisotropy factor**
Litter layer	0.0264	2	$2.31 \cdot 10^{-5}$	Fig 7.3	0	1
Layer 1	0.01	2	$9.39 \cdot 10^{-5}$	Fig 7.3	0.12	1
Layer 2	0.01	2	$1.73 \cdot 10^{-4}$	Fig 7.3	0.15	1
Layer 3	0.01	2	$1.14 \cdot 10^{-5}$	Fig 7.3	0.12	20

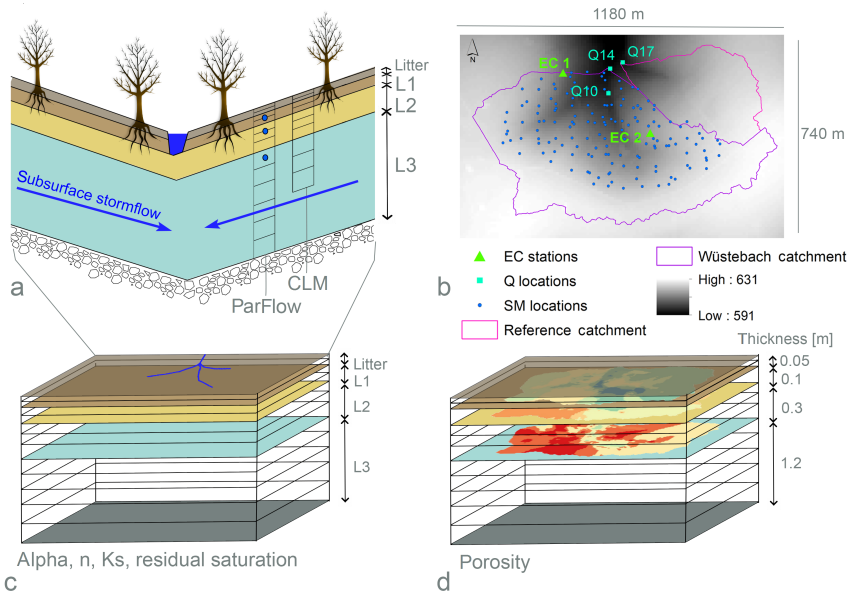

FIGURE 7.2: Schematic representation of the ParFlow-CLM model for the Wüstebach catchment, showing (a) a cross-section with the vertical discretization for the ParFlow and CLM model and the assignment of the different soil layers in the model, (b) the extent of the ParFlow-CLM model for the Wüstebach catchment and the discharge (Q10,Q14 and Q17), ET (EC1 and EC2), and soil moisture (SM) measurement locations, (c) the spatial parametrization of the α, n_{mvg}, K_s and residual saturation (see Table 7.2) and (d) the spatial parameterization of the porosity (more detail shown in Figure 7.3).

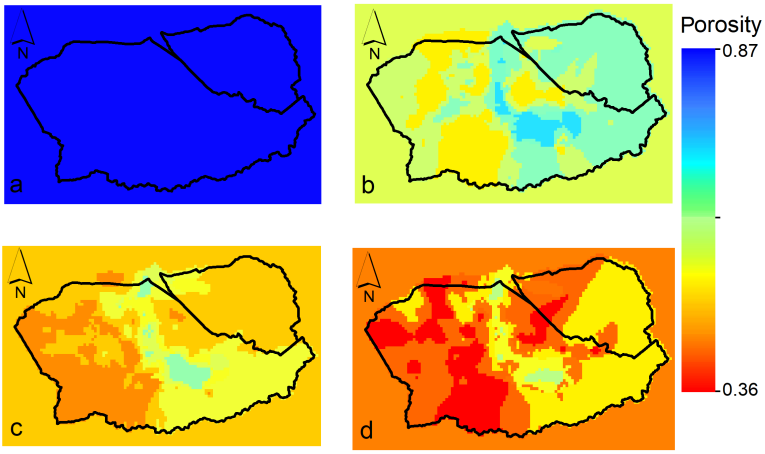

FIGURE 7.3: Porosity parameterization for the different soil layers in the Wüstebach model: (a) the litter layer, (b) mineral soil layer 1, (c) mineral soil layer 2, and (d) mineral soil layer 3.

Similar to Koch et al. (2016), spatial heterogeneity in porosity was considered by grouping the inverse distance weighted interpolation results of the maximum observed soil moisture in the period between May 2010 and May 2013 in the Wüstebach catchment (31 classes; Figure 7.3). To represent lateral flow processes in the catchment, an anisotropy factor of 20 was set for the hydraulic conductivity in soil layer 3 of the Wüstebach catchment (Figure 7.2). The boundary condition at the sides of the modelling domain were set to a constant head of -0.88 m (average observed water depth). This implies that water can flow into and out of the domain along these boundaries depending on the pressure distribution within the model domain. A no-flux boundary condition was used for the bottom of the model domain, as the Devonian shale is assumed to have a very low permeability (Graf et al., 2014b).

The climatic forcing data for the CLM model was prepared for a 69-months-timeframe (1st of January 2010 to 1st of September 2015) and contained hourly input data from on-site and off-site weather stations. On-site climate data included longwave and shortwave radiation. Off-site climate data included hourly precipitation data from Kalterherberg with the Richter correction (Richter, 1995) and hourly wind speed, air pressure, air temperature, air humidity, and vapor pressure from Schöneseiffen (3.5 km east of the Wüstebach). More information about these measurements and the test site are

given in Chapter 3.

7.2.2.2 Parking Lot Test

Three parking lot tests were performed to evaluate the routing response of the Wüstebach stream derived from the 10 m DEM. In all three tests, the porosity and permeability were set close to 0. In the first test with the original DEM, the western stream got stuck at the location of the intersection with the road. Therefore, the DEM was adjusted at this location and two further parking lot test cases were performed with the adjusted DEM. The first test case used an initial positive hydraulic head at the surface (0.52 m), and a second test case used an initial positive hydraulic head at the surface (0.50 m) and a constant incoming precipitation of 0.0000095 m/h (83.22 mm/year).

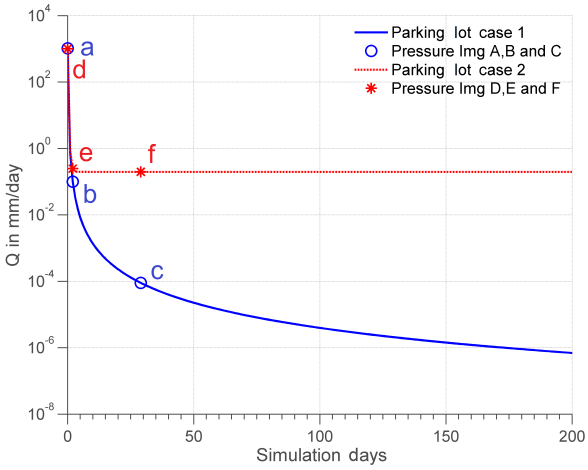

FIGURE 7.4: Discharge [mm/day] at the catchment outlet for the first 200 days of parking lot test case 1 (blue) and parking lot test case 2 (red). The corresponding pressure distribution is shown in Figure 7.5.

The results of both test cases are presented in Figure 7.4 and 7.5. Figure 7.4 shows the course of the discharge [mm/day] at the catchment outlet during the first 200 simulation days, and Figure 7.5 shows the change in surface pressure [m] at simulation day 1 (a and d), 3 (b and e) and 30 (c and f). For the first test case, the discharge decreased exponentially (Figure 7.4) and the surface water was rapidly removed (Figure 7.5a-c). In the second test case,

the discharge first decreased exponentially, but remained at a constant level at late times due to the constant rate of incoming precipitation. Figure 7.4 shows that the surface pressure remained the same after three days (e and f). Overall, the results of these two parking lot tests show that the overland flow routing is successful after some pre-processing of the available DEM.

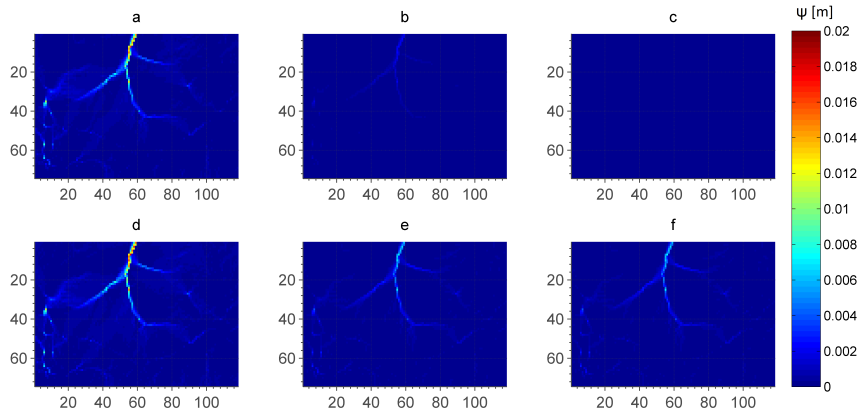

FIGURE 7.5: Pressure head distribution (ψ) at three selected times (day 1, 3 and 30) for parking lot test case 1 (a – c; initial positive head) and 2 (d – f; initial positive head plus constant incoming flux).

7.2.2.3 Local Sensitivity Analysis for Manning's Roughness Coefficient

As already shown in Equation 7.3, the Manning's roughness coefficient (n_m) influences overland flow velocity and thus routing. The Manning's roughness coefficient is typically considered to be a spatially variable parameter that depends on land use type in ParFlow (Baatz et al., 2017). Although it can have a strong influence on simulated discharge, little to no information was provided on the setting of this coefficient in previous modelling studies in the Wüstebach catchment (Fang et al., 2015; Fang et al., 2016; Koch et al., 2016). Additionally, literature n_m values for different vegetation types considerably differ and are highly uncertain (Baatz et al., 2017). Due to the limited amount of information on the Manning's roughness coefficient (n_m) and the homogeneous vegetation within the catchment (before deforestation), it was decided to use a single value for the entire modelling domain. To determine an appropriate value for the Manning's coefficient, a local sensitivity analysis was performed. Four simulations with widely different Manning's coefficients (n_m= 0.001; n_m= 0.0005; n_m= 0.0001; n_m= 0.00005) were made for the meteorological year 2010 using a one-year spin-up period that also used

the meteorological data of 2010.

To analyse the impact of the different n_m values, discharge, actual evapotranspiration, and total soil moisture storage output was analysed. Figure 7.6 shows the results for the spin-up period and the one-year analysis period. The one-year spin-up period was judged to be sufficient as the simulated discharge, actual evapotranspiration, and mean soil moisture at the end of the spin-up period were similar to the values simulated at the end of the one-year analysis period. The results of this sensitivity analysis showed that different Manning's coefficients mainly affected the discharge peaks, but did not largely affect the overall cumulative discharge. In addition, no large differences were observed in actual evapotranspiration and the temporal dynamics of the mean soil moisture at the different reference depths (5, 20 and 50 cm). Due to the low sensitivity of the simulation results to the parameterization of n_m, it was set to the intermediate value of 0.0001 s/m.

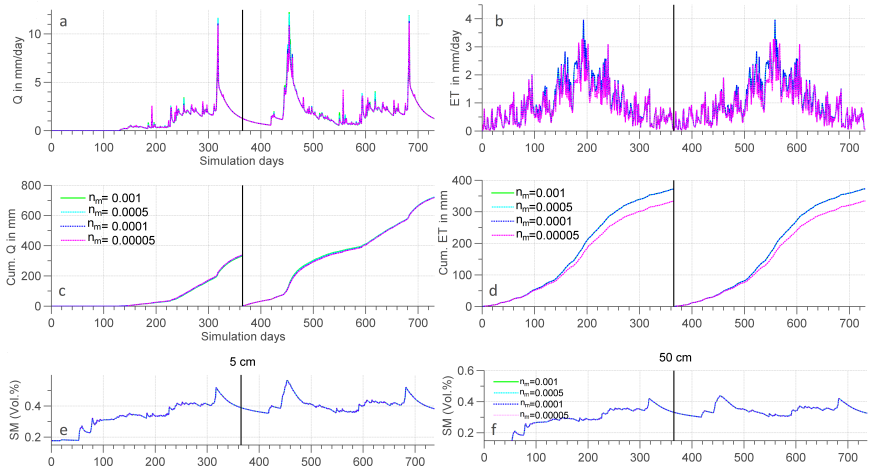

FIGURE 7.6: Simulated (a) discharge, (b) evapotranspiration, (c) cumulative discharge, (d) cumulative evapotranspiration, (e) mean soil moisture at 5 and (f) 50 cm depth for a two-year simulation period (one year of spin-up and a one-year analysis period) with different n_m values (0.001, 0.0005, 0.0001, 0.00005 s/m).

7.2.2.4 Plant Parameterization before the Deforestation

The land use type for the entire model domain was set to "vegetation". For the entire spin-up period and the simulation period before the deforestation,

the PFT of the entire CLM model domain was set to needleleaf evergreen boreal tree with a constant monthly LAI of 5 and a constant monthly SAI of 2. For detailed information about the parameterization of this PFT, the reader is referred to Appendix A. Preliminary simulations for the Wüstebach catchment showed that this PFT parameterization did not result in accurate simulations of the water balance and the partitioning of runoff and evapotranspiration. In particular, there was too much discharge, baseflow, and too little evapotranspiration. Although this may be associated with the simplified soil parameterization with artificially high n_{mvg} values, this seems unlikely because ET_a was also highly underestimated during wet conditions. Even though soil evaporation does depend on soil moisture conditions, the transpiration is only affected by soil conditions during dry conditions. Therefore, it was decided to adjust the parameterization of the PFT.

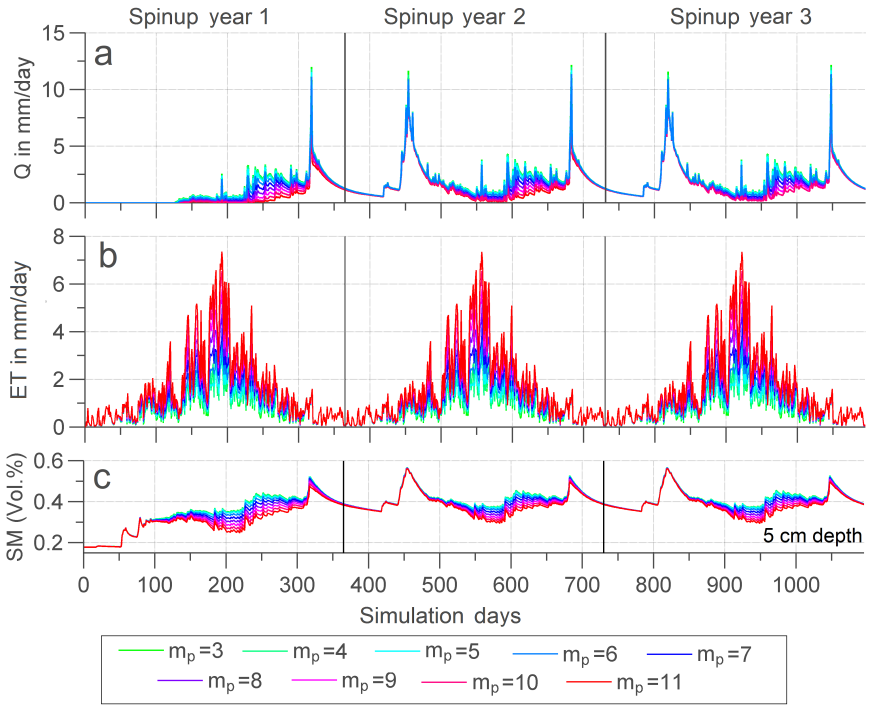

FIGURE 7.7: Simulation results for three years of model spin-up for ParFlow-CLM showing: (a) simulated discharge, (b) actual evapotranspiration and (c) soil moisture at 5 cm depth for different slopes (m_p) in the Ball-Berry equation.

Due to the complexity and long run-time of the ParFlow-CLM model,

global calibration of many model parameters is unfeasible. Therefore, an alternative approach based on literature and local calibration was used. Using a sensitivity analysis, Jefferson et al. (2017) found that the empirical slope (m_p) and intercept (b_p) parameters of the Ball-Berry equation (Equation 7.17) were amongst the most sensitive parameters for simulated transpiration for a range of test cases. As the intercept (b_p) of the Ball-Berry equation (7.17) was set to a fixed and hard-coded value of 2000 μmol CO2 m-2 s-1, this parameter was kept constant. In the following, the Parflow-CLM model was calibrated by varying the value of m_p between 3 and 11 (only considering the positive integers). Figure 7.7 shows the simulated discharge, actual evapotranspiration and soil moisture at 5 cm depth during the spin-up period of three years for the selected range of m_p values. Generally, higher m_p values increased the variability in simulated states and fluxes, and caused lower baseflow and higher maximum evapotranspiration. All models were in equilibrium after two years of spin-up. Figure 7.8 exemplary shows that simulated discharge, evapotranspiration and soil moisture for m_p = 8 were almost identical in the second and third spin-up year. Based on these results, it was decided that a spin-up period of three years was sufficient for the ParFlow-CLM model of the Wüstebach catchment.

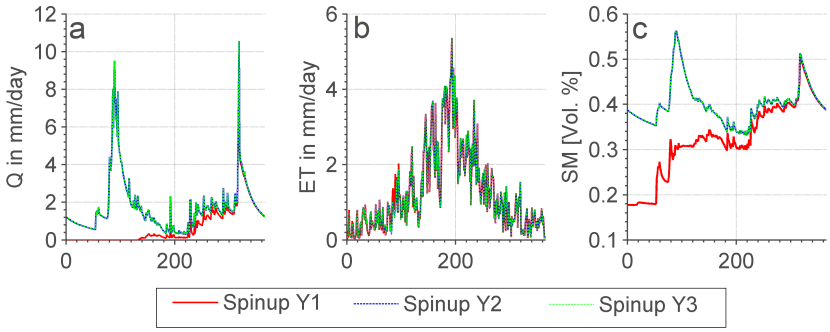

FIGURE 7.8: Simulation results for three years of model spin-up for ParFlow-CLM showing: (a) simulated discharge, (b) actual evapotranspiration and (c) mean soil moisture at 5 cm depth for an exemplary m_p of 8 in the Ball-Berry equation.

To determine the most suitable value for the m_p parameter, the total simulated actual evapotranspiration ($ET_{am,s}$) and discharge (Q_s) for the hydrological years 2011 and 2012 (HY2011, HY2012; September - September) were compared to the measured data. Figure 7.9 shows a two-year time series

of daily and cumulative ($ET_{am,s}$, Q_s and measured actual evapotranspiration ($ET_{am,o}$) and discharge (Q_o) for m_p values ranging from 3 to 11. Clearly, there are some differences in daily discharge and evapotranspiration patterns between the simulations and measurements. For example, not all observed discharge peaks are well-matched by the simulations. It can be seen that the baseflow of the Wüstebach stream is better described by models with higher m_p that lead to an overall lower baseflow.

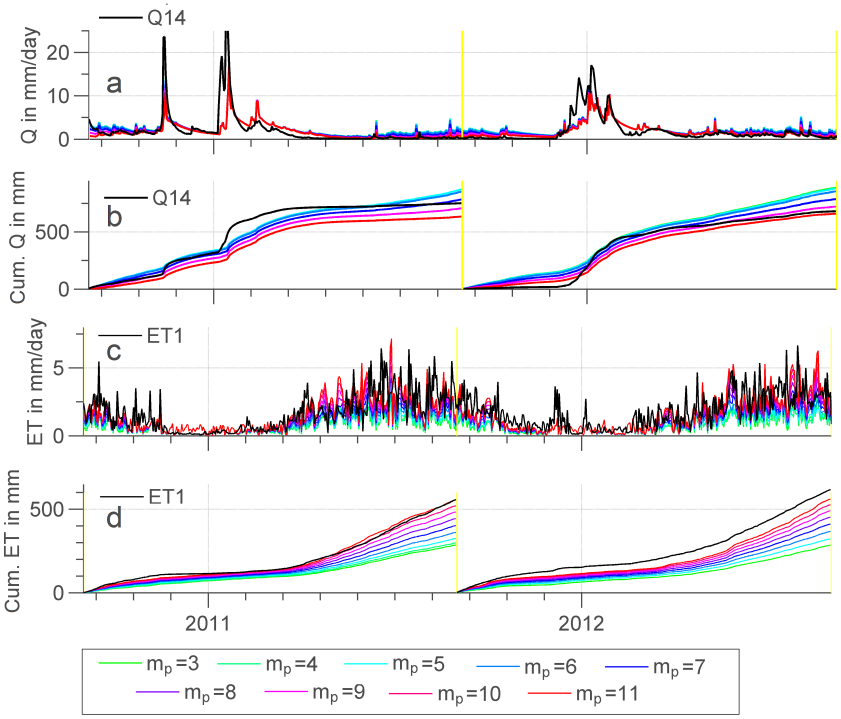

FIGURE 7.9: Simulated and measured discharge and actual evapotranspiration for HY2011 and HY2012 for different values of m_p in the Ball-Berry equation.

The shape of the cumulative $ET_{am,s}$ curve is similar to the cumulative $ET_{am,o}$ curve for all values of m_p, especially for HY2011. For HY2012, cumulative $ET_{am,o}$ is underestimated for all considered values of m_p. Compared to the cumulative Q_o curves, Q_s curves are less steep in the second half of HY2011 because a large discharge event was not well described by the model. Table7.3 compares the annual simulated and measured Q and ET sums for the different m_p parameters. In both hydrological years, an m_p value of 11

generated the smallest differences between $ET_{am,s}$ and $ET_{am,o}$. The differences in simulated and observed discharge were the smallest for m_p values of 9 (HY2011) and 10 (HY2012), but were also small for an m_p value of 11. Overall, the model with an m_p value of 11 produced the smallest (absolute) cumulative differences between measured and simulated discharge and ET_a, and this value was therefore used for all further simulations.

TABLE 7.3: Cumulative $ET_{am,s}$ and $ET_{am,o}$, Q_o and Q_s for HY2011 and HY2012 and the yearly difference between the measurements ($_o$) and simulations ($_s$).

m_p	$\mathbf{ET_{am,s}}$ **HY 2011**	$\delta\mathbf{ET_{am,o}}$	$\mathbf{ET_{am,s}}$ **HY 2012**	$\delta\mathbf{ET_{am,o}}$	$\mathbf{Q_s}$ **HY 2011**	$\delta\mathbf{Q_{am,o}}$	$\mathbf{Q_s}$ **HY 2012**	$\delta\mathbf{Q_o}$	$\sum \mid ET_{am,o} + Q_o \mid$
3	286	-283	286	-322	883	180	889	209	995
4	299	-270	292	-316	873	170	882	202	959
5	325	-244	323	-285	853	150	857	177	856
6	362	-207	368	-240	823	120	822	142	709
7	402	-167	412	-196	785	82	788	108	554
8	444	-125	453	-155	746	43	755	75	398
9	484	-85	491	-117	708	5	723	43	250
10	521	-48	527	-81	671	-32	692	12	173
11	556	-13	561	-47	636	-67	661	-19	147
$ET_{am,o}$ & Q_o	569	-	608	-	703	-	680	-	-

7.2.2.5 Plant Parameterization after the Partial Deforestation

To simulate hydrological processes during the first year after the deforestation, a bare soil parameterization was assigned to the deforested area (Figure 3.3). The parameterization of the reference area remained as described in the previous section. As there is no standard PFT class "bare soil" available in CLM 3.5, a new PFT class was manually added. In this PFT, the monthly LAI and SAI were set to zero so that E_i and T were zero. In the second simulation year after the deforestation, the growth of grass was observed in the catchment and the observed ET_a increased (Chapter 4). Based on personal observations in the catchment, it was decided to leave 50% of the soil bare

for the second year after the deforestation for each grid-cell with deforestation, and to assign the PFT "c3 grass" to the remaining 50%. Monthly SAI and LAI values for this PFT were adapted from Gebler et al. (2017). Appendix A gives a more detailed overview of the different PFT classes and the associated parameterization that were used here.

7.2.3 Model Evaluation

To evaluate the modelling results of the ParFlow-CLM model for the Wüstebach catchment, a five-year dataset including discharge, evapotranspiration and discharge data was used. For the evaluation, daily discharge data from Q14 and ET_{am}, ET_{ad}, and ET_{ad} data from the two eddy covariance stations (ET1 and ET2) were used (for more information see Chapter 3). In addition, soil moisture data from 108 locations (Chapter 3 and Koch et al., 2016) were used to evaluate the predicted spatial and temporal variability of soil moisture. The predictive quality of the discharge and ET_a simulations before and after the deforestation were evaluated using a set of six goodness-of-fit measures that evaluate different aspects of the fit of the model to the data.

The correlation between the modelled and measured data was evaluated using the Pearson correction coefficient (Pearson R), and the total explained variance of the model was described by the coefficient of determination (R^2), which is the squared value of the Pearson R (Legates and McCabe Jr., 1999):

$$R^2 = \left(\frac{\sum_{i=1}^{n}(Obs_i - \bar{Obs})(Sim_i - \bar{Sim})}{\sqrt{\sum_{i=1}^{n}(Obs_i - \bar{Obs})^2}\sqrt{\sum_{i=1}^{n}(Sim_i - \bar{Sim})^2}} \right)^2 \tag{7.17}$$

where *Obs* are the observations and *Sim* the model predictions. To address the skewedness of the discharge data, R^2 scores for log-transformed measurements and simulations were additionally calculated. The Pearson R ranges between -1 (negative correlation) and +1 positive correlation). R^2 ranges between 0 and 1, where 0 resembles a model that does not explain the variance in the dataset at all and 1 suggests that the model is able to explain all of the existing variance in the dataset. The spread of the prediction error is described by the Root Mean Square Error (RMSE):

$$RMSE = \sqrt{\frac{\sum_{i=1}^{n}(Sim_i - Obs_i)^2}{n}} \tag{7.18}$$

which ranges from 0 (no error) to ∞ and depends on the unit of the measurements and the simulations. The bias of the model is characterized by the Mean Bias Error (MBE; range: -∞ - +∞):

$$MBE = \frac{\sum_{i=1}^{n}(Sim_i - Obs_i)}{n} \tag{7.19}$$

Besides looking at goodness-of-fit criteria that describe the fit of a single aspect of the model, two criteria that combine multiple diagnostic components in its score are used to evaluate the Parflow-CLM model: the Nash–Sutcliffe efficiency (NSE; Nash and Sutcliffe, 1970) and the non-parametric Kling-Gupta efficiency (KGE_{np}; Pool et al., 2018). The NSE is a goodness-of-fit criteria that includes correlation, bias and variability measures for the model (Gupta et al., 2009):

$$NSE = 1 - \frac{\sum_{i=1}^{n}(Sim_i - Obs_i)^2}{\sum_{i=1}^{n}(Obs_i - \bar{Obs})^2} \tag{7.20}$$

The NSE score can obtain a value between - ∞ and 1, describing the range between a very poor up to an extremely good fit between the measurements and the simulations. Although this model evaluation criterium has its deficits (e.g Gupta et al., 2009; Pool et al., 2018), it is a widely used measure in hydrology. It was included here to create an opportunity to compare the results of ParFlow-CLM with other modelling studies. To also address the skewedness of the discharge data, the NSE was additionally calculated for log-transformed data and simulations.

The non-parametric Kling-Gupta efficiency (KGE_{np}) is a recently introduced good-ness-of-fit criterium where data linearity, data normality, and the absence of outliers are not a pre-requisite (Pool et al., 2018):

$$KGE_{np} = 1 - \sqrt{(\beta_{np} - 1)^2(\alpha_{np} - 1)^2(R_s - 1)^2} \tag{7.21}$$

where β_{np} is the bias in discharge volume given by:

$$\beta_{np} = \frac{\bar{Sim}}{\bar{Obs}} \tag{7.22}$$

α_{np} is the absolute error of the flow duration curve given by:

$$\alpha_{np} = 1 - \frac{1}{2}\sum_{k=1}^{n}\left|\frac{Sim(I(k))}{n * \bar{Sim}}\frac{Obs(J(k))}{n * \bar{Obs}}\right| \tag{7.23}$$

where $I(k)$ and $J(k)$ represent the sorting of the observations and simulations into the k-th largest flow. Finally, R_s is the Spearman rank correlation coefficient calculated by:

$$R_s = \frac{\sum_{i=1}^{n}(Obs(t) - \bar{Obs})(Sim(t) - \bar{Sim})}{(\sum_{i=1}^{n}(Obs(t) - \bar{Obs})^2) \cdot (\sum_{i=1}^{n}(Sim(t) - \bar{Sim})^2)} \tag{7.24}$$

where (t) represents the rank of the observed and simulated data. Similar to the NSE, the KGE_{np} can also vary between - ∞ (very poor fit) and 1 (perfect fit). All evaluation scores were calculated using Matlab 7.12 (MathWorks, Natick, MA). Clearly, the performance rating of these different model evaluation criteria can be subjective and differs a lot amongst studies and might depend on the applied model, the calibration procedure and its complexity (e.g. Moriasi et al., 2007; Moriasi et al., 2015). To keep the performance rating (PR) in this study as transparent and as uniform as possible (for different types of data and metrics),the scoring system for R^2, NSE and KGE_{np} and Pearson R is presented in Table 7.4. Furthermore, the obtained scores were compared with scores obtained in other modelling studies (e.g. same (type of) model, same study area) to give further meaning to the obtained values.

TABLE 7.4: Model performance rating (PR) of the different evaluation criteria. Performance rating was divided into two groups (NSE and KGE_{np}, and Pearson R and R^2) to adjust the ranges to the characteristics of the evaluation criteria. Mind that no universal performance rating was applied to the RMSE and MBE, due to the variability in the unit and range of the assessed data.

Performance rating	**Unsatisfactory**	**Reasonable, fair**	**Good**	**Very good**
NSE and KGE_{np}	< 0.4	0.4 - 0.6	0.6 - 0.8	0.8 - 1
Pearson R and R^2	< 0.5	0.5 - 0.6	0.6 - 0.8	0.8 - 1

The evaluation of the model performance for the soil moisture data was based on only three of the model evaluation criteria (R^2, Pearson R and RMSE), but was additionally assisted by four different types of visualisation. First, temporal images of spatially averaged soil moisture of the reference and the treated area were generated. Afterwards, spatial correlation plots between soil moisture in the reference area and the treated area before and after the deforestation were evaluated. Third, the relationship between the mean soil moisture <θ> and the associated standard deviation σ(<θ>) before

and after the deforestation was plotted for the treated area, the reference area and the whole catchment. Finally, spatial images of the soil moisture distribution before and after deforestation calculated using ordinary kriging (as described in Section 4.2.4) were evaluated.

7.3 Results and Discussion

7.3.1 Annual Water Balance

Table 7.5 shows all modelled and measured components of the annual water balance for the entire monitoring period. For the period before the deforestation, the model represented the water balance and its components quite well for the first two years that were used for the calibration of the m_p parameter. Here, the difference between modelled and measured Q, ET_a, and the difference in incoming P and Q_s + $ET_{am,s}$ was relatively small (< 10%). The model did not perform as well in HY2013, which was the first year that was not used for calibration, and that included one month after the partial deforestation. In particular, large deviations between the yearly cumulative Q_s and Q_o were observed (>25%). The differences between the catchment-averaged $ET_{am,s}$ and $ET_{am,o}$ were smaller. The deviation in cumulative discharge caused a larger difference between the incoming P and Q_s and $ET_{am,s}$ (12.6 %), which could be caused by a change in storage but may also be associated with in- and outflow at the sides of the modelling domain (Figure 7.2 with constant head boundary conditions. In particular, water can leave the catchment and the modelling domain via the subsurface if there is a negative pressure head (ψ) gradient from the middle of the modelling domain towards the edges.

During the two-year simulation period after the deforestation, the model performed highly variable in terms of the annual water balance. For the first year after deforestation (HY2014), the difference between the yearly cumulative Q_s and Q_o and the yearly cumulative $ET_{am,s}$ and $ET_{am,o}$ were large. Both the yearly cumulative ET_{ad} after deforestation and Q were clearly underestimated by ParFlow-CLM. This resulted in large deviations between the incoming P and Qs + $ET_{am,s}$ (18.3%). The observed large deviation between $ET_{ad,m}$ and $ET_{ad,o}$ might be caused by an underestimation of soil evaporation by CLM 3.5, the slowly developing vegetation and the associated increase in ET_a in the first year that is not represented in the model, or measurement and gap filling errors in the Eddy Covariance dataset. During the second

year after the deforestation (HY2015), the model performed very well and only small deviations (< 5%) between the yearly cumulative Q_s and Q_o and the yearly cumulative $ET_{am,s}$ and $ET_{am,o}$ were found.

TABLE 7.5: Cumulative yearly simulated and measured water balance components for the Wüstebach catchment for HY2011 – HY2015, where Q_o and Q_s are the measured and simulated discharge, $ET_{am,o}$ and $ET_{am,s}$ are the catchment-averaged measured and simulated evapotranspiration, $ET_{af,o}$ and $ET_{af,s}$ are the measured and simulated evapotranspiration for the forested area, and $ET_{ad,o}$ and $ET_{ad,s}$ are the measured and simulated evapotranspiration for the deforested area.

	HY2011	**HY2012**	**HY2013**	**HY2014**	**HY2015**
P	1192	1279	1304	1304	1250
Q_o	703	680	830	898	789
Q_s	636	661	612	645	722
$\lvert Q_s - Q_o \rvert$	67	19	218	253	67
$ET_{am,o}$	569	608	578	510	483
$ET_{am,s}$	556	561	528	420	479
$\lvert ET_{am,s} - ET_{am,o} \rvert$	13	47	50	90	4
$ET_{ad,o}$	-	-	-	312	369
$ET_{ad,s}$	-	-	-	162	307
$\lvert ET_{ad,s} - ET_{ad,o} \rvert$	-	-	-	150	62
$ET_{af,o}$	569	608	578	566	515
$ET_{af,s}$	556	561	528	497	533
$\lvert ET_{af,s} - ET_{af,o} \rvert$	13	47	50	69	18
$ET_{am,o} + Q_o$	1272	1288	1408	1408	1272
$ET_{am,s} + Q_s$	1192	1222	1140	1065	1201

This chapter presents one of the first distributed hydrological modelling studies where all simulated water balance components can be compared to observations. Overall, the water balance and its components were quite well represented by ParFlow-CLM for three out of five hydrological simulation years (HY2011, HY2012, and HY2015). Large annual discharge deviations were observed for HY2013 and HY2014. Earlier reported water balance residuals ($P - (Q_s + ET_{am,s})$) for distributed hydrological modelling studies in the Wüstebach catchment using different models (ParFlow-CLM,

HydroGeoSphere and Mike-SHE) and the (nearby) Rollesbroich catchment (ParFlow-CLM) were of a similar magnitude for HY2011, HY2012, HY2013 and HY2015, but were slightly higher for HY2014 (Fang et al., 2015; Koch et al., 2016; Gebler et al., 2017). Whereas this study found mainly positive water balance residuals (indicating too little water), the residuals for the ParFlow-CLM simulations by Fang et al. (2015), Koch et al. (2016), and Gebler et al. (2017) showed negative residuals (indicating too much water). Positive residuals were reported for HydroGeoSphere and Mike-SHE applications in the Wüstebach catchment (Koch et al., 2016).

7.3.2 Daily Discharge

Figure 7.10 shows daily Q_s and Q_o as a function of time, cumulative daily Q_s - Q_o as a function of time, and a plot of Q^s against Q^o. During the control period, low flow conditions were generally better predicted than high flow conditions. Peak flows were underestimated by the model and the simulated recession of the hydrographs was too slow. Associated evaluation statistics for the five-year period are presented in Table 7.6. The Pearson correlation coefficient ranged between 0.66 and 0.85, indicating an overall good to very good correlation between daily Q_s and Q_o. The R^2 ranged between 0.44 and 0.72 (PR: poor – good), and the log-R^2 was between 0.59 and 0.76 (PR: satisfactory – good), indicating an overall intermediate to good explained variance. The RMSE ranged between 1.72 and 2.74 (mm), NSE values ranged between 0.36 and 0.65 (PR: poor to good) and log-NSE values ranged between 0.53 and 0.69 (PR: reasonable – good). The results indicated worse performance for HY2013 for HY2013 (NSE 0.36 and log-NSE of 0.53; PR: poor to reasonable) and an intermediate to good fit for HY2011 and HY2012. The MBE scores indicate a general negative model bias, indicating that the model generally produces lower Qs values. The obtained KGEnp scores (0.61 – 0.82) indicate a good – very good model performance and show that the model is able to represent the main characteristics of the flow duration curve.

To put the presented scores in perspective, available evaluation scores (R^2, NSE, log-NSE, RMSE) from related modelling studies (Breuer et al., 2009; Cornelissen et al., 2014; Fang et al., 2015; Koch et al., 2016) were compared. The presented R^2 values were very similar to the values presented for the HydroGeoSphere model application in the Wüstebach catchment (Cornelissen

et al., 2014), where R^2 values between 0.58 and 0.77 were obtained. The obtained NSE values for HY2011 and HY2012 and the whole period before the deforestation (B.D.) performed similar or slightly worse than the distributed models TOPLATS and Mike-SHE in the hydrological model intercomparison study by Breuer et al. (2009). Compared to other modelling studies in the Wüstebach catchment, NSE values were generally in the lower to middle range of the reported scores (0.51 and 0.86), and log-NSE scores were in the middle range of the reported values (0.27 – 0.84). RMSE values were in the same range (around 1.73 mm) or slightly higher than the obtained values by Fang et al. (2016).

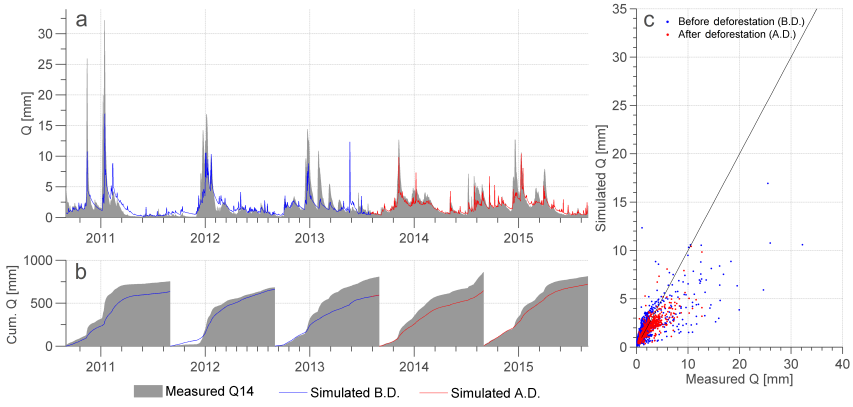

FIGURE 7.10: (a) Simulated and measured daily discharge, (b) simulated and measured cumulative daily discharge and (c) measured versus simulated discharge for the five year simulation period (HY2011 – HY2015), including a three year pre-deforestation period (B.D.) and a two-year post-deforestation period (A.D.).

When comparing scores from HY2011 - HY2013 with yearly evaluation statistics after partial deforestation for HY2014 – HY2015, the model predictions were of similar or higher quality, indicating no loss in predictive quality despite changes in system behaviour (flashier system, higher low flow; see Figure 4.7b). Lower RMSE values and higher log R^2 and log NSE scores for HY2014 and HY2015 indicate an improved discharge performance after the deforestation. Figure 7.10 and negative MBE scores indicate that high flow conditions were still underestimated, which was expected based on the results before deforestation. When comparing the overall periods, the overall model performance of Parflow-CLM is better for the period after the deforestation (A.D.) than the period before the deforestation (B.D.). If the relatively

poor model performance in HY2013 is not considered, the differences between the two evaluation periods is much smaller. Although it would be interesting to compare the performance results during changed conditions with other hydrological modelling studies, this is not possible because most of the existing studies dealing with the hydrological impacts of land use change have been focussed on scenario analysis. Until present, there are no other modelling studies in the temperate zone that (1) have used data from the period before and after the deforestation to validate the predicted changes (2) with a set of performance metrics.

TABLE 7.6: Model evaluation statistics for daily discharge (Q) predictions. An explanation of the evaluation statistics and the calculation of the scores is given in section 7.2.3.

	HY 2011	**HY 2012**	**HY 2013**	**HY 2014**	**HY 2015**	**HY11-15**	**B.D.**	**A.D.**
Pearson R	0.76***	0.85***	0.66***	0.84***	0.80***	0.77***	0.76***	0.81***
R^2	0.58	0.72	0.44	0.7	0.63	0.6	0.58	0.66
Log- R^2	0.74	0.76	0.59	0.78	0.83	0.71	0.69	0.79
RMSE [mm]	2.74	1.72	1.89	1.24	1.32	1.86	2.19	1.25
MBE	-0.32	-0.06	-0.58	-0.59	-0.25	-0.36	-0.33	-0.41
NSE	0.50	0.65	0.36	0.53	0.58	0.53	0.51	0.57
Log-NSE	0.69	0.53	0.57	0.71	0.8	0.67	0.62	0.77
KGE_{np}	0.71	0.78	0.61	0.71	0.82	0.75	0.72	0.77

*** behind the Pearson correlation coefficients indicate p-values < 0.05.

Overall, the model performance for daily discharge was quite similar to other modelling studies that took place in the same catchment or with similarly complex models. While assessing these results, one has to bear in mind that the only calibration that was made was based on yearly ET_a and Q sums for HY2011 and HY2012. This is comes close to the blind prediction concept by Ewen and Parkin (1996) and Bathurst et al. (2004). The ParFlow-CLM model showed very similar model performance before and after partial deforestation. Generally, the performance in HY2013 was worse than in the

other two years due to several underestimated events. This is not only related to simplifications in the modelling approach, but also to potential errors in input data (e.g. precipitation). The model is able to reasonably predict low and intermediate flow conditions, but failed to represent peak flow conditions accurately. The underestimated peak flow explains the generally negative MBE scores, and also explains the gap between the cumulative observed and simulated discharge. This could be related to the adjusted n_{mvg} parameterization that creates a sandier soil with higher infiltration capacity. At the same time, the general soil hydraulic parameterization obtained by Hydrus 1D might be too simplistic.

7.3.3 Actual Evapotranspiration

One of the major innovations of this study is the opportunity to validate spatiotemporal $ET_{a,s}$ values before and after deforestation with available $ET_{a,o}$ data from two eddy covariance stations (ET1 and ET2). In their model-intercomparison study, Breuer et al. (2009) already reported that the most important structural differences in model response were attributed to $ET_{a,s}$, and addressed the importance of a validation dataset with soil-vegetation interactions for different land use types. To investigate the capability of the model to simulate ET_a under forested and changed conditions, the differences in measured and simulated ET_{am} (catchment averaged) ET_{af} (untreated forested area) and ET_{ad} (untreated area) were evaluated for the five-year simulation period (Figure 7.11 and 7.12).

Figure 7.11 shows the simulated and measured ET_a for the entire catchment before and after partial deforestation. Daily $ET_{am,o}$ values after the deforestation were obtained by areal-averaging of the EC data from both stations (ET1 and ET2; for more details, see Chapter **??**). Not only the yearly $ET_{am,s}$ sums were close to $ET_{am,o}$ sums (except for HY2014; Table 7.5; Figure 7.11b), but also the seasonal fluctuations were well represented by ParFlow-CLM (Figure 7.11a and c). Table 7.7 presents model evaluation statistics for $ET_{am,s}$ for HY2011 to HY2015. A high variability in model performance was found for both the period before and after the deforestation. In particular, intermediate to good Pearson correlation coefficients (0.52 - 0.75), high RMSE values (0.91 – 1.24 mm) and poor to intermediate R^2 (0.28 – 0.49) and NSE

scores (-0.36 - +0.46) were found. This indicates that there is a clear correlation between the simulations and measurements, but that daily ET_{am} predictions are not very accurate. The KGE_{np} scores suggest an intermediate to good model performance and a good fit between the that the frequency distribution of $ET_{am,s}$ and $ET_{am,o}$. Compare the obtained KGE_{np} scores for the discharge data with $ET_{am,s}$ scores, the results are not quite as different, as the values are only slightly lower (0.58 – 0.77) indicating a satisfactory to good performance.

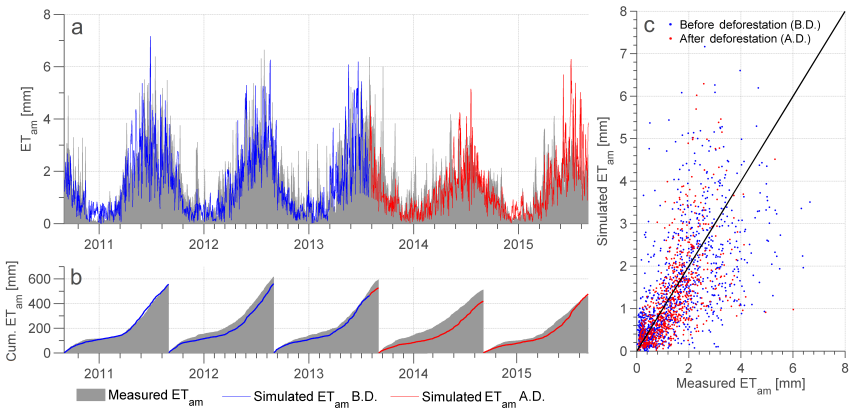

FIGURE 7.11: Visualization of the (a) daily $ET_{am,o}$ and $ET_{am,s}$ values, (b) daily cumulative $ET_{am,o}$ and $ET_{am,s}$ values, and (c) correlation plot between daily $ET_{am,o}$ and $ET_{am,s}$ values for the Wüstebach catchment between HY2011 and HY2015. The blue colour indicates daily $ET_{am,s}$ and cumulative daily $ET_{am,s}$ before the partial deforestation and the red colour indicates daily $ET_{am,s}$ and cumulative $ET_{am,s}$ values after the partial deforestation.

Figure 7.12 shows the daily simulated and measured ET_a of the forested (ET_{af}) and the deforested area (ET_{ad}) for HY2014 and HY2015. The corresponding model evaluation statistics are provided in Table 7.8. For HY2014, $ET_{ad,s}$ and $ET_{af,s}$ were clearly underestimated by the model (Figure 7.12, Table 7.5). This resulted in large negative MBE scores. Cumulative differences between measured and modelled ET_{ad} and ET_{af} were smaller in HY2015. Model predictions for ET_{ad} were generally better compared to ET_{af}. Although the total ET_{ad} sums were too low for the two years after the deforestation, simulated ET_{ad} values were clearly closer to the observations in comparison to the simulation of ET_{af} since the simulations for ET_{ad} resulted in a higher Pearson R and R^2 values. This suggests that the variability in actual

evapotranspiration of the deforested area was more accurately reproduced by the model. Still, larger deviations in absolute ET_{ad} values for HY2014 caused large differences for NSE and KGE_{np} between HY2014 (bad - intermediate) and HY2015 (good).

TABLE 7.7: Model evaluation statistics for daily ET_{am} predictions. An explanation of the evaluation statistics and the calculation of the scores is given in section 7.2.3.

	HY 2011	**HY 2012**	**HY 2013**	**HY 2014**	**HY 2015**	**HY11-15**	**B.D.**	**A.D.**
Pearson R	0.58***	0.75***	0.53***	0.52***	0.70***	0.61***	0.61***	0.62***
R^2	0.34	0.56	0.28	0.27	0.49	0.37	0.38	0.38
RMSE [mm]	1.19	0.91	1.24	0.93	0.95	1.05	1.11	0.96
MBE	0.146	-0.153	-0.149	-0.040	0.182	-0.003	-0.039	0.053
NSE	0.21	0.46	0.05	-0.36	0.14	0.14	0.24	-0.15

*** behind the Pearson correlation coefficients indicate p-values < 0.05.

To put these evaluation scores in perspective, the results were compared with two other CLM and ParFlow-CLM modelling studies (Gebler et al., 2017; Shrestha et al., 2018). ParFlow-CLM model predictions for ET_a of a nearby grassland site produced NSE scores that were generally higher than the modelling results in this study (0.64 - 0.77). Grassland ET_a simulations using CLM3.5 and CLM5.0 by Shrestha et al. (2018) produced even higher NSE scores (0.8 - 0.95). Only the ET_{ad} simulations for HY2015 and HY2014 -HY2015 produced scores that were within the range of the reported NSE scores by Shrestha et al. (2018) and Gebler et al. (2017). One improvement to the CLM model could be a more gradual change in vegetation cover (%) to better simulate grass growth after the deforestation. In the end, the mixture of model results has to be put in context as good results for one flux can be compensated by another. Although the NSE scores for ET_a reported by Gebler et al. (2017) were generally higher, their reported NSE scores for discharge were highly negative. In this study, the reported results were the other way around and did provide intermediate to good Pearson correlation

scores for the discharge simulations, but worse scrores for ET_a.

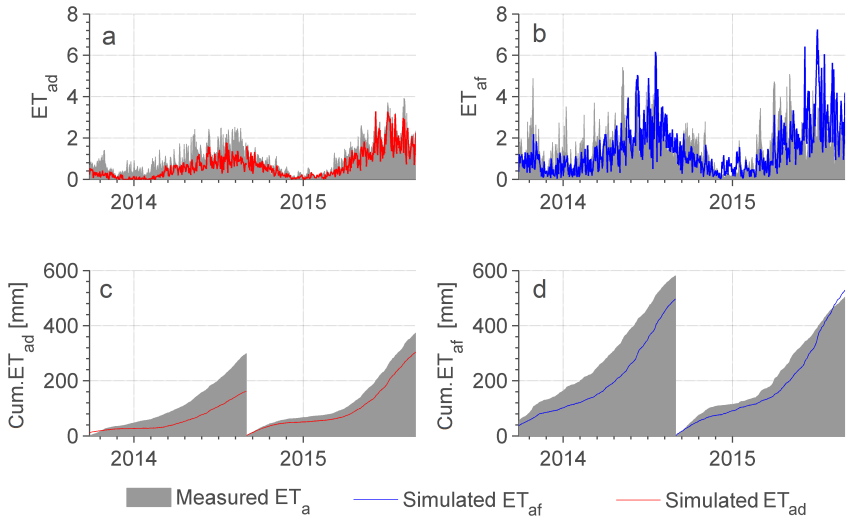

FIGURE 7.12: Daily simulated ET_a (in blue and red) and measured ET_a (in grey) of the forested area (ET_{af}) and deforested area (ET_{ad}) for the Wüstebach catchment in HY2014 – HY2015.

TABLE 7.8: Model evaluation statistics for daily and cumulative ET_{af} and ET_{ad} predictions. An explanation of the evaluation statistics and the calculation of the scores is given in section 7.2.3.

	ET_{ad}			**ET_{af}**		
	HY2014	**HY2015**	**HY14-15**	**HY2014**	**HY2015**	**HY 14-15**
Pearson R	0.84***	0.93***	0.88***	0.4***	0.45***	0.45***
R^2	0.71	0.87	0.78	0.21	0.21	0.2
RMSE	0.56	0.37	0.47	1.08	1.23	1.16
MBE	-0.44	-0.19	-0.31	-0.2	0.07	-0.06
NSE	0.13	0.82	0.61	-0.29	-0.48	-0.38
KGE_{np}	0.47	0.79	0.64	0.53	0.59	0.57

*** behind the Pearson correlation coefficients indicate p-values < 0.05.

To further evaluate the intra-annual model performance for ET_a, the daily ET_{af} and ET_{ad} values and their corresponding evaporative indices are shown

in Figure 7.13. A similar graph for the observed data is provided in Chapter 4 (Figure 4.4). As already apparent from Figure 7.12, the seasonal variability of daily ET_{af} and ET_{ad} were quite similar and daily ET_{af} were generally smaller than daily ET_{ad} values. Nonetheless, there are clear differences between the observed and simulated values. One of the most important differences is that the observed higher ET_{ad} values ($ET_{ad} > ET_{af}$) during the late summer of 2015 (August) were not reproduced by the model, as ET_{ad} was always lower than ET_{af} throughout HY2014 -HY2015. This might indicate that the strategy of the forest to transpire less during heat waves is not adequately represented in the model (e.g Teuling et al., 2010).

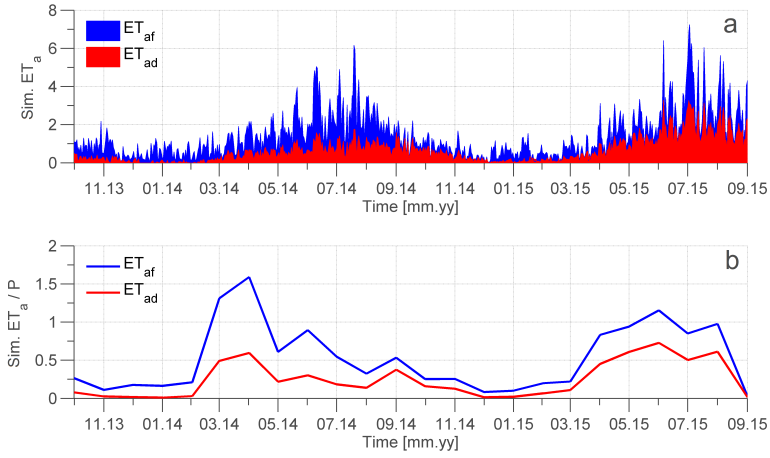

FIGURE 7.13: Daily simulated ET_{af}, ET_{ad} and monthly ET_a/P for the Wüstebach catchment for HY2014 – HY2015.

Overall, the model was capable of reproducing inter-annual evapotranspiration trends, cumulative trends, and annual ET_a sums for different areas in the catchment. The model was able to simulate general annual and monthly trends for the forested and the deforested area (Figure 7.13). The generally lower ET_{ad} values were reasonably reproduced by the model, suggesting that the general effect of partial deforestation on the evapotranspiration in the Wüstebach catchment was adequately predicted. At the same time, this study has shown that the general parameterization of a PFT might not always be suitable, which could also be an explanation for some of the low evaluation scores. If the moisture conditions remain wet enough, the

simulated ET_a is less dependent on simulated soil moisture conditions and depends more strongly on the plant parameterization and the weather conditions. Here, the question is whether the pre-condition PFT parameterization is suitable to represent the vegetation in a catchment, as these CLM parameter sets were originally created for global simulations and might not be specific enough to present the local vegetation conditions in detail. The predictions additionally depend a lot on the user-defined monthly LAI and SAI values, with also need to be correctly estimated in order to get reasonable predictions. The highest NSE scores were obtained for the treated area in HY2015, where the LAI and SAI parameterization of the new grassland area (50% cover) was the same as documented by Gebler et al. (2017).

7.3.4 Soil Moisture

In a final step, the simulated and observed spatio-temporal variability of soil moisture is compared. Figure 7.14 shows time series (HY2011 - HY2015) of predicted and measured area-averaged soil moisture at 5, 20 and 50 cm depth for the reference area (Figure 7.14a – 7.14c) and the treated (deforested) area (Figure 7.14d – 7.14f). At first sight, the model performance for the reference area looks quite similar for the control and treatment period, which indicates that the general model performance for soil moisture was not affected by possible differences in climate conditions between the different hydrological years. Still, there were clear differences between measured and observed soil moisture. The predicted soil moisture at 5 cm depth had shorter wet periods and was too high during the dry summer periods. For the soil moisture at 20 cm depth, the predicted soil moisture conditions were generally too low and the wet periods were drastically underestimated. The general variability of the predicted soil moisture at 50 cm depth was very similar to the measured soil moisture but the predicted soil moisture was lower than average.

The simulated soil moisture for the treated area for HY2011 – HY2015 also underestimated the soil moisture dynamics at 5 and 20 cm depth. The simulation results at 50 cm depth showed better agreement with the measured soil moisture. The simulations at 5 cm depth showed higher deviations after the deforestation. In particular, the increased wetness that was observed for the measured soil moisture was not well reproduced by the model. Although soil moisture conditions in the summer months were partly represented by

the model before deforestation in the treated area, this was not the case anymore after deforestation.

Summary statistics for the modelling results are shown in Table 7.9, and are compared to modelling results by Gebler et al. (2017) and Koch et al. (2016). Generally, the correlation between the modelled and observed soil moisture at all depths is very good and ranges between 0.74 and 0.83, which is very similar to the scores obtained by Gebler et al. (2017) and Koch et al. (2016). The R^2 generally ranges between 0.53 and 0.70 showing moderate to good scores for the explained variance (treated area, 50 cm depth) and the RMSE range between 2.5 – 7.5 vol. %. These scores are within the same range as those reported by Gebler et al. (2017).

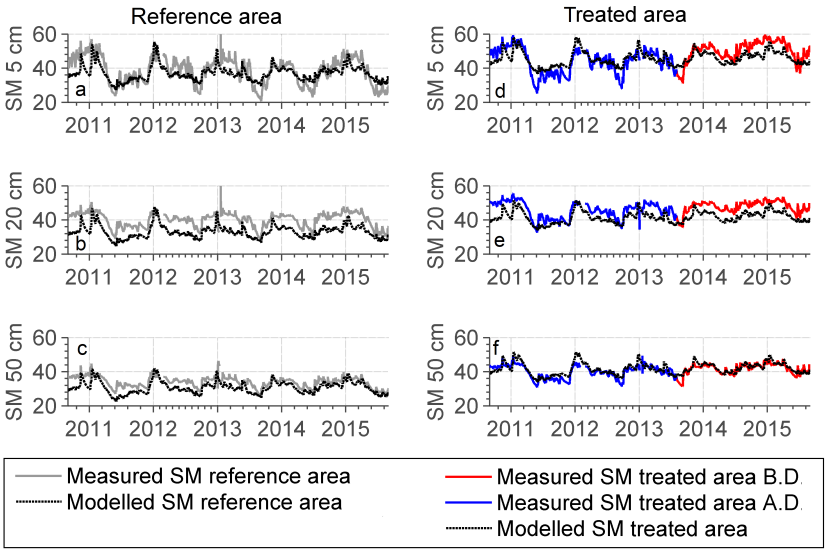

FIGURE 7.14: Simulated and measured daily soil moisture between HY2011 and HY2015 for the reference area (a-c) and the treated area (d and f) at 5 (a and d), 20 (b and e) and 50 (c and f) cm depth. A.D. = after deforestation and B.D. = before deforestation. The measurements during the control period are shown in blue, whereas measurements after deforestation are shown in red.

TABLE 7.9: Model evaluation statistics soil moisture in the reference area and in the treated area for 5,20 and 50 cm depth.

	Ref. area -5 cm	**Treated - 5 cm**	**Ref. area -20 cm**	**Treated -20 cm**	**Ref. area -50 cm**	**Treated -50 cm**
Pearson R	0.74***	0.76***	0.75***	0.78***	0.76***	0.83***
R^2	0.55	0.58	0.56	0.61	0.57	0.70
RMSE [Vol. %]	5.60	5.11	7.51	5.55	4.04	2.46

*** behind the Pearson correlation coefficients indicate p-values < 0.05.

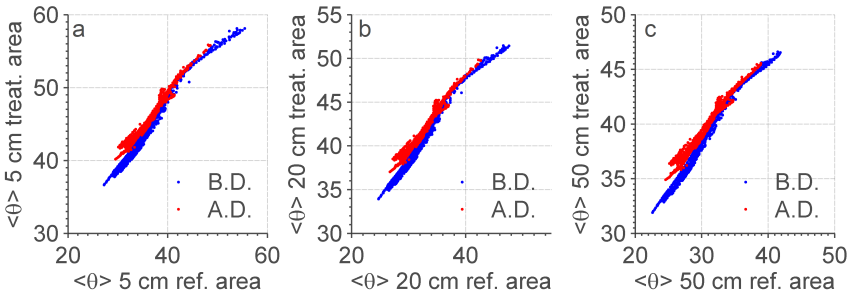

FIGURE 7.15: Areal mean simulated soil moisture for the reference area (ref. area) versus the areal mean simulated soil moisture for the treated area for the period before deforestation (B.D. in blue) and after deforestation (A.D. in red) for (a) 5 cm depth, (b) 20 cm depth, and (c) 50 cm depth.

Figure 7.15 shows the relationship between the simulated mean soil moisture before and after deforestation for the reference and the treated area at 5, 20 and 50 cm depth. Figure 4.9 shows the same relationships for the measured data (5 cm depth and depth-averaged). Similar to the measured data, the treated area was always wetter than the reference area. For all depths, the relationship between the mean soil moisture in the reference and the treated area changed after deforestation, and the deforested area became wetter during the dryer periods. However, the simulated change in this relationship is less pronounced compared to the observed data (Figure 4.9). This is related with the generally smaller simulated soil moisture fluctuations and the

underestimation of observed soil moisture in the summer before the deforestation.

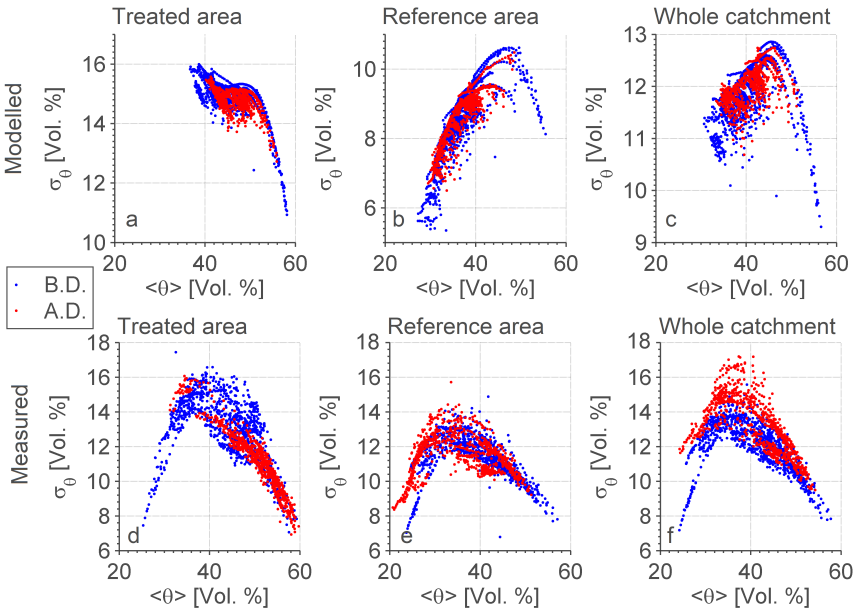

FIGURE 7.16: Modelled and measured σ_θ<θ> relationships before the partial deforestation (B.D.) and after the partial deforestation (A.D.) for the treated area (a and d), the reference area (b and e) and the whole catchment (c and f). Please mind that the vertical axes are not matched to better represent the shape of the soil moisture relationships.

Besides looking at mean soil moisture conditions, it is also important to evaluate the spatial variability in simulated water content. In a first step, the relationship between mean soil water content <θ> and standard deviation σ_θ was used for this. Figure 7.16a-c show the modelled σ_θ<θ> relationships for the treated area, the reference area, and the entire catchment using simulated mean daily soil moisture content. Figure 7.16d-f present the same plots for the observed daily soil moisture data. Generally, the σ_θ<θ> relationships obtained from the simulations are quite different from the observed relationships. Only the position of the maximum standard deviation for the simulations results was similar to the maximum σ_θ for the observed data. However, the simulated data did not accurately represent the dry range. The relationships for the reference area and the entire catchment (c vs. f) look

more similar, but also missed parts of the falling or rising limb. Also, the observed changes in the σ_θ<θ> relationship due to deforestation for the treated area and the entire catchment were not accurately represented by the model. Most importantly, the simulated σ_θ<θ> relationship of the entire catchment did not change after deforestation, whereas the observed curve showed clear differences. In general, only part of the soil variability is presented in the model. For example, the n_{mvg} parameterization was simplified for numerical stability. Previous studies dealing with σ_θ<θ> relationships have argued that variability in n_{mvg} is a key factor determining spatial variability in water content (e.g Qu et al., 2015).

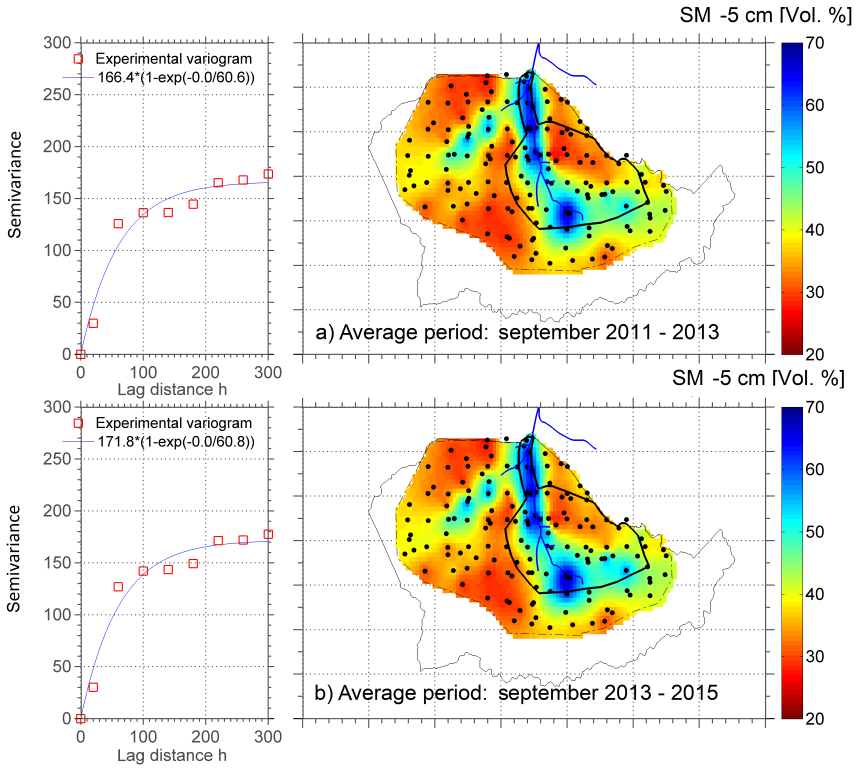

FIGURE 7.17: Experimental variograms and interpolated maps (ordinary kriging) of the simulated mean soil moisture content for (a) HY2012 and HY2013 prior to the deforestation and (b) HY2014 and HY2015 after deforestation. As a reference, the deforested area within the catchment is marked on both maps.

In a final step, observed and simulated spatial soil moisture patterns are

compared directly. Figure 7.17 and 7.18 show spatially interpolated maps of simulated soil moisture at 108 locations. Whereas the observed soil moisture data (Figure 4.11) showed clear changes in soil moisture patterns for HY2012 -HY2013 and HY2014 – HY2015, no clear differences in temporally averaged soil moisture were observed for the model results for HY2012 -HY2013 and HY2014 – HY2015 (Figure 7.17). A similar comparison can be made for the measured (Figure 4.12) and simulated soil moisture for the summer of 2011 and 2014 (Figure 7.18). Although clear changes in soil moisture patterns before and after the deforestation can be observed in this case, the magnitude and spread of the increased soil moisture is not entirely reproduced by the model. Additionally, the change in the correlation lengths that was observed for the measured data was also not reproduced by the model, which is related to the underpredicted magnitude and spread of the soil moisture increase in the treated area. This, in turn, could be related to the relatively homogeneous soil parameterization.

Overall, the simulated soil moisture results showed reasonable to good agreement with the measurement data with a good representation of inter-annual variability, intermediate to good evaluation scores, and a simulated increase in soil wetness after the deforestation. When looking at the spatial images, there are clear similarities in soil moisture patterns between the model and the observations before the deforestation, indicating that the general behaviour of the riparian zone is represented by the model. However, clear differences in patterns become more visible after the deforestation measures. This could be partly improved by changing the Mualem-van Genuchten parameterization (Qu et al., 2015), which could already improve the representation of the soil moisture dynamics before the deforestation (Gebler et al., 2017) and might therewith increase the predictive power after the deforestation.

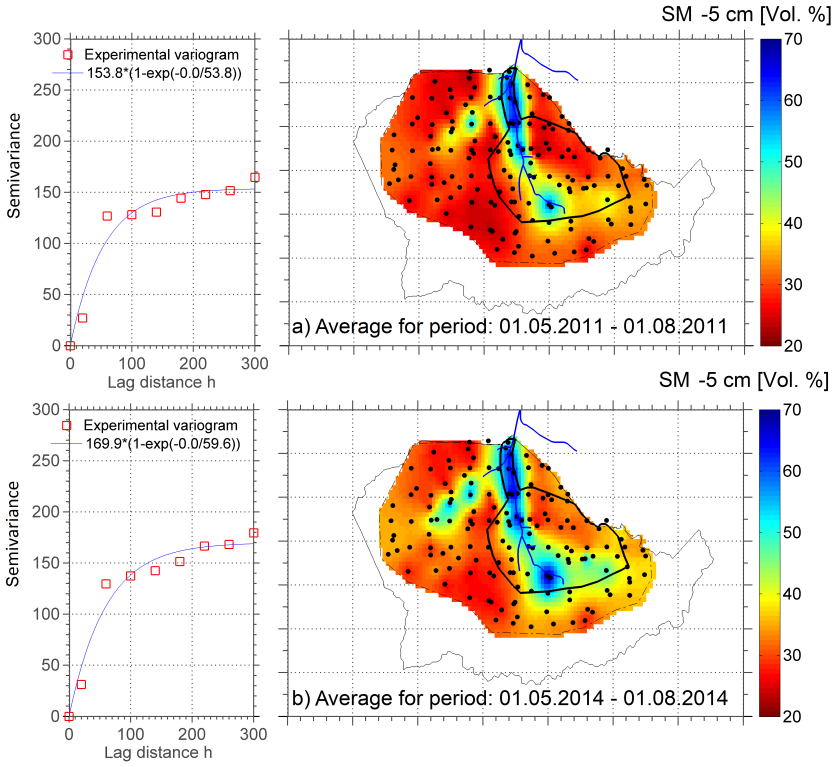

FIGURE 7.18: Experimental variograms and interpolated maps (ordinary kriging) of the simulated mean soil moisture content for (a) summer 2011 prior to the deforestation and (b) summer 2014 after the deforestation. As a reference, the deforested area within the catchment is marked on both maps.

7.4 Conclusions

The aim of this chapter was to evaluate the ability of the ParFlow-CLM model to predict hydrological effects of partial deforestation using the extensive hydrological dataset available for the Wüstebach catchment. The results presented in this chapter show that the ParFlow-CLM model was generally able to reproduce observed discharge, evapotranspiration and soil moisture fluctuations, obtaining mostly reasonable to good evaluation scores. Above all, this chapter provided one of the first approaches to thouroughly validate hydrological deforestation predictions, which showed that ParFlow-CLM was also capable of predicting most of the observed state and flux changes that were caused by the partial deforestation. Discharge simulations showed that

the model was mainly capable of reproducing low and intermediate flow conditions in the catchment for the periods before and after the deforestation. The unique measurement and modelling setup in this study allowed for spatial validation of evapotranspiration data, revealing that model was capable of simulating general evapotranspiration fluctuations and deforestation-related changes in evapotranspiration in the treated area. Most general spatial and temporal soil moisture patterns in the catchment could also be reproduced by the model, and the model also simulated an increase in wetness at the treated area after partial deforestation. However, this study also highlighted some caveats of the model. The global parameterization strategy based on plant functional types does not always accurately represent the vegetation behaviour in local scale studies at the catchment scale. The model was not able to correctly simulate peak flow conditions before and after the deforestation and changes in soil moisture conditions were underestimated. Also, the model was not able to represent the σ_θ<θ> relationships before and after the deforestation. Additionally, forest and grassland evaporative feedback mechanisms to heatwaves were not accurately represented by the model. Part of the caveats could be resolved by improved parameterization strategies for the Mualem-van Genuchten parameters the Mannings coefficient. Overall, this chapter has shown that distributed hydrological models like ParFlow-CLM have a lot of potential in land use change studies.

Chapter 8

Synthesis: Towards an Improved Ecohydrological Understanding of Partial Deforestation Measures

This thesis started with an overview of the current limitations in studies dealing with the hydrological impact of deforestation and the potential contribution of this thesis to the field of hydrology. In this synthesis, the results of this PhD thesis are evaluated in this context and put into a wider scientific and practical context by addressing the following questions:

1. What new knowledge regarding the hydrological effects of deforestation has been obtained from a high-resolution spatiotemporal hydrological dataset?
2. What has been learned from confronting the TerrSysMP model with such a high-resolution spatiotemporal hydrological dataset?

Besides addressing these questions, an outlook to potential future research will be provided.

8.1 New Ecohydrological Insights from the TERENO Wüstebach Dataset

One question that is often asked in catchment hydrological studies is: What is the added value of yet another set of measurements made in a small headwater catchment? As demonstrated in Chapter 2, there are already a large amount of small experimental catchments where hydrological deforestation studies have been performed, but it was also clear that many of these study

areas have their limitations. Modern observatories, such as the TERENO Wüstebach catchment, can overcome part of these limitations and provide new opportunities for modern analysis with a range of new measurement equipment that provide opportunities for new hypothesis testing (e.g. Blöschl et al., 2016). This, in turn, can provide new insights into the (changes in) functioning of different hydrological components within a system and the inter-related feedback mechanisms.

Chapter 4 highlighted that the Wüstebach dataset provides a unique opportunity to investigate changes for different hydrological fluxes after partial deforestation. The elaborate measurement set-up revealed changes in soil moisture patterns and highly dynamic changes in ET_a. Clearly, the combination of local eddy covariance measurements to determine actual evapotranspiration and soil moisture measurements revealed interesting insight into surface-atmosphere interactions. Not only could clear increases in soil moisture due to deforestation be linked to decreases in evapotranspiration, but less intuitive opposite behaviour was also observed. The increase in soil moisture in combination with prolific grass growth caused higher evapotranspiration rates in the deforested area. This example shows that a modern monitoring setup that includes multiple states and fluxes can provide valuable information on the coupling between different hydrological processes and the role of vegetation.

Chapter 5 and Chapter 6 have shown that the extensive soil moisture dataset acquired in the Wüstebach catchment combined with a sensor response time analysis provides valuable insights into the spatiotemporal occurrence of preferential flow in a catchment. In sensor response time analysis, the order of the depth-based sequence of sensor response is used to classify the response into one of the following four classes: (1) non-sequential preferential flow, (2) sequential preferential flow, (3) sequential flow and (4) no flow. Whereas Chapter 5 mainly focussed on the general factors that controlled the spatiotemporal occurrence of preferential flow, Chapter 6 focussed specifically on the effect of partial deforestation on preferential and sequential flow occurrence. Both chapters showed that compared to single-point-in-time observations of preferential flow (e.g. dye tracing), the response time analysis offers much higher spatial and temporal resolution and can help to better understand the underlying governing factors. Chapter 5 demonstrated that given a high precipitation input, preferential flow could occur anywhere

within a forested catchment. Chapter 6 showed the strength of a wireless soil moisture network in combination with planned management practices. This revealed that partial deforestation increased the occurrence of sequential flow and decreased the occurrence of no flow in the affected area. At the same time, no clear changes in preferential occurrence were observed.

Currently, there still is a lot of controversy on the governing factors of preferential flow occurrence, including the effects of vegetation. A comparison of the results obtained in Chapter 5 and 6 with the studies by van Schaik (2009; 2010), Graham and Lin (2011), Hardie et al. (2011; 2013) and Liu and Lin (2015) already shows that the factors that explain the spatiotemporal occurrence of preferential flow are still not fully understood (Beven and Germann, 2013; Jarvis et al., 2016). To improve this understanding, similar sensor response time analyses in different landscape units would be required. A promising example of such an approach was recently presented by Demand et al. (2019). Other limitations of the work presented in this thesis are: (1) the limited sensing volume of the EC-5 and 5-TE soil moisture sensors, (2) the inability to identify flow response during saturated soil moisture conditions and (3) the lack of ability to distinguish vertical bypass flow and lateral flow (Graham and Lin, 2011). Therefore, it is worthwhile to combine sensor response time analysis with more traditional methods for preferential flow analysis (e.g. dye tracing), and water potential sensors. This combination of methods can help to understand how local scale controls affect the sensor response time analysis. At the same time, it can also improve our more general understanding of preferential flow occurrence. In addition, geophysical methods could also provide a valuable resource for a detailed characterization of subsurface hydrological changes due to the available range in temporal and spatial resolution.

Although this thesis has shown that the measurement setup in the Wüstebach catchment offers a lot of potential, a single study site is insufficient to fully understand the effects of deforestation on hydrological processes. Therefore, it is advocated that similar studies should be undertaken in other climatological and geological regions to better understand the coupling between changes in hydrological states and fluxes in relation to land use change. Additionally, the review in Chapter 2 has clearly shown that longer monitoring records are required to reveal more information on the eco-hydrological

resilience of the catchment (e.g. Andréassian, 2004). Hence, it might be worthwhile to repeat the presented analyses with a longer dataset to look at longer-term perspective.

Even if discharge response to rainfall is relatively prompt, the flowing water in the stream can be years to decades old (Kirchner, 2006; McDonnell and Beven, 2014). This illustrates the importance of incorporating both the concept of celerity and velocity in hydrological studies. While flow velocities are defined as "the mass flux of the water itself" (McDonnell and Beven, 2014) and control the age distribution of the water in a system, celerities describe "the speed with which a perturbation to the flow propagates through the flow domain" (McDonnell and Beven, 2014) and determine the discharge response in the system. As indicated in Chapter 3, water quality and water isotope data (pre-deforestation and post-deforestation period) are also available for the Wüstebach catchment. Isotope data include weekly $\delta^{18}O$ and $\delta^{2}H$ isotope data from one precipitation station, 16 stream water sampling locations along the main stream and eight groundwater sites (Stockinger et al., 2014; Bogena et al., 2015). Water chemistry data include water temperature, pH, redox potential, electrical conductivity, major anions and cations. These indicators were measured for 16 stream water sampling locations and eight groundwater sites (Bogena et al., 2015). Water quality changes are frequently observed after deforestation measures (e.g. Findlay et al., 2001; Tetzlaff et al., 2007; Hunter and S. Walton, 2008; Figueiredo et al., 2010; Jacobs, 2018) and provide information on velocity changes in the system. As water chemistry is, however, highly variable in time and space (Neal et al., 2012; Abbott et al., 2018; Isaak et al., 2014; Jacobs, 2018; Dupas et al., 2019) and deforestation measures also have a spatial character, spatially variable changes might be expected. Previous work by Stockinger et al. (2014) has already shown that the transit time of water can also have a high spatial variability. The spatiotemporal water chemistry and isotope dataset of the Wüstebach catchment offers a unique chance to evaluate and combine observed spatiotemporal changes in water quality, celerity and velocity.

Besides looking at opportunities to connect the existing dataset with other available information, new analysis methods should be developed to better extract information contained in this type of spatiotemporal dataset. Existing options that are already applied in hydrological science include empirical orthogonal functions (EOF) analysis (e.g. Graf et al., 2014b; Koch et al., 2016),

wavelet transform coherence analysis (e.g. Graf et al., 2014b; Weigand et al., 2017), and spatial stability analysis (Abbott et al., 2018; Dupas et al., 2019). Both the EOF analysis and the spatial stability analysis can compress spatiotemporal datasets to identify similarities in spatial and temporal patterns. The wavelet transform coherence analysis helps to identify temporally variable correlations between two datasets and existing lag times. In the framework of deforestation and other hydrological land use change studies, these methods could help to identify changes in spatiotemporal relationships and patterns. Other new data analysis methods, arising from neighbouring disciplines, such as TOCSY - Toolboxes for Complex Systems (Wessel et al., 2013), can also provide new opportunities to look at spatiotemporal datasets. The TOCSY toolbox offers a set of innovative nonlinear data analyses methods that can be used to understand changes in nonlinear relationships resulting from land use change.

8.2 New Ecohydrological Insights from TerrSysMP Model Predictions

Within the field of hydrology, many different modelling studies that address land use change effects with a variety of models are available (Dwarakish and Ganasri, 2015, Section 2.6). Still, the question whether these non-stationary changes are accurately predicted by the model remains largely unanswered (Semenova and Beven, 2015; Nijzink et al., 2016). This is mainly due to the lack of data that can thoroughly test existing distributed hydrological models for non-stationary conditions. The five-year long Wüstebach dataset provides a unique opportunity for validating post-deforestation conditions. Obviously, the dataset is highly suitable for multi-criteria evaluation of distributed hydrological models and this was explored for the coupled subsurface-land surface model ParFlow-CLM in Chapter 7.

The results of this chapter showed that ParFlow-CLM was able to reproduce the main features of the discharge, actual evapotranspiration and soil moisture storage before and after deforestation with only minor calibration. Not only was the model able to simulate major trends for catchment-average evapotranspiration, but also the evapotranspiration in the deforested area was reasonably reproduced. Low and intermediate flow conditions were well reproduced by ParFlow-CLM with relatively similar model evaluation

statistics before and after deforestation. In addition, the model was able to simulate the general spatiotemporal soil moisture patterns in the catchment, and an increase in moisture after the deforestation. Overall, Chapter 7 provided new insights into the predictive ability of distributed hydrological models under land use change and showed that ParFlow-CLM has considerable potential for future land use change studies.

While model success informs us about the capabilities of the model, model failures teach us about remaining caveats and possible improvements required to better represent the processes that are taking place within the catchment (e.g Beven, 2018). First of all, there is a need for a procedure to objectively decide on the parameterization of a plant functional type (PFT) for the current state and conditions after land use change. The required calibration of the empirical m_p parameter showed that the global pre-set parameterization of the PFT might not always be suitable for local catchment conditions. CLM 3.5 additionally requires coverage, SAI and LAI information to simulate evapotranspiration, which might not always be available for land use change scenarios. Second, there is a need to improve the modelled soil parameterization, since both peak flow conditions and soil moisture variability were not well represented. For this, different approaches could be tested. The first approach relies on an improved n_{mvg} parameterization, which is expected to decrease infiltration and increase peak flow. A second approach could be a more heterogeneous Mualem-van Genuchten parameterization, which was already successfully implemented by Gebler et al. (2017). In their study, the more advanced parameterization strategy improved the simulation of spatiotemporal soil moisture patterns.

A third, very important, but time-consuming approach would be the implementation of preferential flow and the improvement of the lateral flow representation in ParFlow-CLM. Chapter 5 and 6 already indicated that preferential flow is an important process in the catchment, which is not directly considered by ParFlow-CLM, but could be considered indirectly in the Mualem-van Genuchten parameterization. On the other hand, lateral flow has been artificially incorporated in existing Wüstebach models (Cornelissen et al., 2014; Fang et al., 2015; Koch et al., 2016) by increasing the anisotropy in K_s. However, this could be improved by a more physical representation of the model. Although there is a lot of discussion in the field regarding the importance and implementation of these flow processes (Beven and Germann,

2013; Weiler, 2017), recent findings by Glaser et al. (2019) suggest that the implementation of lateral flow is more important than the implementation of vertical preferential flow for catchment scale models. Besides the proposed improvements for ParFlow-CLM, there are additional research activities that could be initiated to improve land use forecasting with hydrological models. First of all, a repetition of this modelling study for other hydrological models and an ensemble of models (e.g. Huisman et al., 2009; Viney et al., 2009) could inform us about the type of models and modelled processes that are required to successfully represent the hydrological impacts of deforestation. Second, repeating a similar study with state-of-the-art datasets from paired catchment studies or other modern hydrological datasets that contain non-stationary changes could provide more space for intercomparison of performance under different geographic and change conditions. Even though this modelling setup and data evaluation already rigorously tested if the model was "getting the right answers for the right reasons" (Kirchner, 2006) by evaluating the validity of the discharge, evapotranspiration and soil moisture data, isotope and water chemistry information could further asses the validity of the model simulations. This approach would include (1) the implementation of particle tracking into the ParFlow-CLM model and (2) the validating the model simulations with isotope and chemistry data.

Finally, another way to objectively improve hydrological model predictions for stationary and non-stationary conditions is to combine the strengths of the different modelling approaches. Under stationary conditions, machine learning models (e.g. neural networks and deep learning; see Tanty and Desmukh, 2015; Shen, 2018) can outperform well-established physically based and conceptual models (based on performance metrics; e.g. Hsu et al., 1995; Best et al., 2015; Nearing et al., 2018). At the same time, these simulations might not perform very well under non-stationary conditions (e.g. Milly et al., 2008; Milly et al., 2015; Nearing, 2019), and might require information from distributed hydrological models (e.g. physical laws, boundary conditions). Combining the strengths of both worlds could provide a new way forward to address non-stationarity in hydrological science. One approach could be to assess the functional performance of a model to improve the process description in the physically based model with information that is stored within the dataset (Nearing and Gupta, 2015; Ruddell et al., 2019; Bennett et al., 2019). Here, information transfer between the observed and modelled system is compared to identify model structural errors and other

deficiencies in the model, which can be used to improve the model. Another opportunity would be to create multiple neural network models for different states of the non-stationary system to identify differences in process connectivity (described by transfer entropy; Bennett et al., 2019), for example before and after deforestation measures. This information could then help to create either improved distributed hydrological models or aid at generating neural network models that also perform well during non-stationary conditions.

Overall, this thesis has revealed that high resolution spatiotemporal hydrological datasets, such as the Wüstebach dataset, can provide new ecohydrological insights on the functioning of natural and disturbed systems. The combination of the Wüstebach dataset and a coupled distributed hydrological model has shown that models like ParFlow-CLM have a lot of potential to forecast non-stationary conditions.

Appendix A

Reproducibility and Data Availability

A very important criteria in scientific research is reproducibility, which can help to improve the transparency of the research and can aid scientific progress (Hutton et al., 2016). To serve this cause, this appendix provides information on the storage locations of the measurement dataset and the other model files that were used to generate the results that are presented in this thesis. For completeness, It furthermore provides details on the adjusted parameterization of the Plant Functional Types that were used for the ParFlow-CLM simulations.

A.1 Data Availability and GitHub Data Repository

All presented hydrological data of the Wüstebach catchment is freely available from the TERENO data portal: *www.tereno.net*. More information about the dataset can be found in Bogena et al. (2015) and in Chapter 3. In addition, a large dataset with soil chemistry and soil physics data that has also been used in this thesis can be downloaded via the following link: *http://tiny.cc/WueSoilData* and is documented in detail by Gottselig et al. (2017). The input files that are required to run the presented ParFlow-CLM model (TerrSysMP platform) can be downloaded from the following GitHub repository: *http://github.com/IngeWiekenkamp/PhDThesisParFlowCLM*.

A.2 Adjusted Plant Parameterization CLM 3.5

The representation of vegetation in CLM 3.5 is based on patches of "Plant Functional Types" (PFTs), representing the main vegetation types occurring on our planet. For each individual PFT, a large set of parameters is defined

that represent morphological and physical characteristics of the vegetation. In this thesis, I have shown that the standard parameterization of the PFT does not always resemble the hydrological characteristics of the vegetation in a catchment accurately. The adjusted sets of parameters that were used in Chapter 7 are presented in Table A.1 and the monthly LAI and SAI values that were used for this study are given in Table A.2.

TABLE A.1: Parameterization of the Plant Functional Types that were used in this thesis. Parameter names are based on $pft - physiology.c070207.readme$ (CLM 3.5 readme file). The origional needleleaf tree parameterization and the C3 grass parameternzation are based on $pft - physiology.c070207$ (CLM 3.5 input file). The adjusted needleleaf tree parameterization uses only a highler m_p value to generate more evapotranspiration. The bare soil parameterization was generated for this thesis specifically. Values were chosen to set E_i and T to 0.

	Needleleaf tree (origional)	**Needleleaf tree (adjusted)**	**Bare soil**	**C3 grass**
z0mr	0.055	0.055	0.01	0.12
displar	0.67	0.67	0	0.68
dleaf	0.04	0.04	0	0.04
c3psn	1	1	1	1
vcmx25	43	43	17	43
mp	6	11	0.01	9
qe25	0.06	0.06	0.01	0.06
rhol(1)	0.07	0.07	0.001	0.11
rhol(2)	0.35	0.35	0.001	0.58
rhos(1)	0.16	0.16	0.001	0.36
rhos(2)	0.39	0.39	0.001	0.58
taul(1)	0.05	0.05	0.001	0.07
taul(2)	0.1	0.1	0.001	0.25
taus(1)	0.001	0.001	0.001	0.22
taus(2)	0.001	0.001	0.001	0.38
xl	0.01	0.01	0.001	-0.3
roota par	7	7	0	11
rootb par	2	2	0	2
slasun	0.008	0.008	0.0001	0.05
dsladlai	0.001	0.001	0	0
leafcn	40	40	25	25
flnr	0.04	0.04	0.05	0.09
smpso	$-6.6 \cdot 10^4$	$-6.6 \cdot 10^4$	$-5.0 \cdot 10^5$	$-7.4 \cdot 10^4$

TABLE A.1: Parameterization of the Plant Functional Types that were used in this thesis. Parameter names are based on $pft - physiology.c070207.readme$ (CLM 3.5 readme file). The origional needleleaf tree parameterization and the C3 grass parameternzation are based on $pft - physiology.c070207$ (CLM 3.5 input file). The adjusted needleleaf tree parameterization uses only a highler m_p value to generate more evapotranspiration. The bare soil parameterization was generated for this thesis specifically. Values were chosen to set E_i and T to 0.

	Needleleaf tree (origional)	**Needleleaf tree (adjusted)**	**Bare soil**	**C3 grass**
smpsc	$-2.55 \cdot 10^5$	$-2.55 \cdot 10^5$	$-5.01 \cdot 10^5$	$-2.75 \cdot 10^5$
fnitr	0.78	0.78	0.6	0.61
woody	1	1	0	0
lflitcn	80	80	50	50
frootcn	42	42	42	42
livewdcn	50	50	0	0
deadwdcn	500	500	0	0
froot leaf	1	1	1	3
stem leaf	1.5	1.5	0	0
croot stem	0.3	0.3	0	0
flivewd	0.1	0.1	0	0
fcur	1	1	0	0.5
lf flab	0.25	0.25	0.25	0.25
lf fcel	0.5	0.5	0.5	0.5
lf flig	0.25	0.25	0.25	0.25
fr flab	0.25	0.25	0.25	0.25
fr fcel	0.5	0.5	0.5	0.5
fr flig	0.25	0.25	0.25	0.25
dw fcel	0.75	0.75	0.75	0.75
dw flig	0.25	0.25	0.25	0.25
leaf long	6	6	0	1
evergreen	1	1	0	0
stress decid	0	0	0	1
season decid	0	0	0	0
resist	0.12	0.12	0.01	0.12

TABLE A.2: SAI and Parameterization of the three Plant Functional Types that were used in this thesis (C3 grass, needleleaf trees and bare soil)

	LAI Needle-leaf tree	**SAI Needle-leaf tree**	**LAI Bare soil**	**SAI Bare soil**	**LAI C3 Grass**	**SAI C3 Grass**
January	5	2	0	0	0.26	0.26
February	5	2	0	0	0.71	0.71
March	5	2	0	0	1.05	1.05
April	5	2	0	0	1.93	1.93
May	5	2	0	0	2.66	2.66
June	5	2	0	0	2.78	2.78
July	5	2	0	0	2.59	2.59
August	5	2	0	0	2.57	2.57
September	5	2	0	0	2.44	2.44
October	5	2	0	0	1.77	1.77
November	5	2	0	0	0.51	0.51
December	5	2	0	0	0.2	0.2

Bibliography

Abbott, B. W., G. Gruau, J. P. Zarnetske, F. Moatar, L. Barbe, Z. Thomas, O. Fovet, T. Kolbe, S. Gu, A. C. Pierson-Wickmann, P. Davy, and G. Pinay (2018). "Unexpected spatial stability of water chemistry in headwater stream networks". In: *Ecology Letters* 21.2, pp. 296–308. DOI: 10.1111/ele.12897. URL: https://onlinelibrary.wiley.com/doi/abs/10.1111/ele.12897.

Acharya, B. S., T. Halihan, C. B. Zou, and R. E. Will (2017). "Vegetation controls on the spatio-temporal heterogeneity of deep moisture in the unsaturated zone: a hydrogeophysical evaluation". In: *Scientific Reports* 7.1499. DOI: 10.1038/s41598-017-01662-y. URL: http://dx.doi.org/10.1038/s41598-017-01662-y.

Adams, K. N. and A. M. Fowler (2006). "Improving empirical relationships for predicting the effect of vegetation change on annual water yield". In: *Journal of Hydrology* 321.1–4, pp. 90–115. DOI: http://dx.doi.org/10.1016/j.jhydrol.2005.07.049. URL: http://www.sciencedirect.com/science/article/pii/S002216940500380X.

Ahn, K.-H. and V. Merwade (2017). "The effect of land cover change on duration and severity of high and low flows". In: *Hydrological Processes* 31.1, pp. 133–149. DOI: 10.1002/hyp.10981. URL: http://dx.doi.org/10.1002/hyp.10981.

Alaoui, A., U. Caduff, H. H. Gerke, and R. Weingartner (2011). "Preferential flow effects on infiltration and runoff in grassland and forest soils". In: *Vadose Zone Journal* 10.1, pp. 367–377. DOI: 10.2136/vzj2010.0076. URL: https://dl.sciencesocieties.org/publications/vzj/abstracts/10/1/367.

Alila, Y., P. K. Kuraś, M. Schnorbus, and R. Hudson (2009). "Forests and floods: a new paradigm sheds light on age-old controversies". In: *Water Resources Research* 45.8. DOI: 10.1029/2008WR007207. URL: https://doi.org/10.1029/2008WR007207.

Allaire, S. E., S. Roulier, and A. J. Cessna (2009). "Quantifying preferential flow in soils: a review of different techniques". In: *Journal of Hydrology* 378.1, pp. 179–204. DOI: https://doi.org/10.1016/j.jhydrol.2009.

08.013. URL: https://www.sciencedirect.com/science/article/pii/S0022169409004776.

Allen, R. G., L. S. Pereira, D. Raes, and M. Smith (1998). *Crop evapotranspiration: guidelines for computing crop water requirements.* Tech. rep. 56. Rome: Food and Agricultural Organization of the United Nations, p. 300. URL: http://www.fao.org/3/X0490E/X0490E00.htm.

Altdorff, D., C. von Hebel, N. Borchard, J. van der Kruk, H. R. Bogena, H. Vereecken, and J. A. Huisman (2017). "Potential of catchment-wide soil water content prediction using electromagnetic induction in a forest ecosystem". In: *Environmental Earth Sciences* 76.3, pp. 1–11. DOI: https://doi.org/10.1007/s12665-016-6361-3. URL: https://link.springer.com/article/10.1007/s12665-016-6361-3.

Amiro, B. D., A. L. Orchansky, A. G. Barr, T. A. Black, S. D. Chambers, F. S. Chapin Iii, M. L. Goulden, M. Litvak, H. P. Liu, J. H. McCaughey, A. McMillan, and J. T. Randerson (2006). "The effect of post-fire stand age on the boreal forest energy balance". In: *Agricultural and Forest Meteorology* 140, pp. 41–50. DOI: http://dx.doi.org/10.1016/j.agrformet.2006.02.014. URL: http://www.sciencedirect.com/science/article/pii/S0168192306002267.

Andréassian, V. (2004). "Waters and forests: from historical controversy to scientific debate". In: *Journal of Hydrology* 291, pp. 1–27. DOI: http://dx.doi.org/10.1016/j.jhydrol.2003.12.015. URL: http://www.sciencedirect.com/science/article/pii/S0022169403005171.

Andreasen, M., K. H. Jensen, M. Zreda, D. Desilets, H. Bogena, and M. C. Looms (2016). "Modeling cosmic ray neutron field measurements". In: *Water Resources Research* 52.8, pp. 6451–6471. DOI: 10.1002/2015WR018236. URL: https://doi.org/10.1002/2015WR018236.

Anthoni, P. M., M. H. Unsworth, B. E. Law, J. Irvine, D. D. Baldocchi, S. Van Tuyl, and D. Moore (2002). "Seasonal differences in carbon and water vapor exchange in young and old-growth ponderosa pine ecosystems". In: *Agricultural and Forest Meteorology* 111.3, pp. 203–222. DOI: https://doi.org/10.1016/S0168-1923(02)00021-7. URL: http://www.sciencedirect.com/science/article/pii/S0168192302000217.

Archer, N. A. L., M. Bonell, N. Coles, A. M. MacDonald, C. A. Auton, and R. Stevenson (2013). "Soil characteristics and landcover relationships on soil hydraulic conductivity at a hillslope scale: A view towards local flood management". In: *Journal of Hydrology* 497, pp. 208–222. ISSN: 0022-1694.

DOI: https://doi.org/10.1016/j.jhydrol.2013.05.043. URL: http://www.sciencedirect.com/science/article/pii/S0022169413004204.

Armbruster, M., J. Seegert, and K.-H. Feger (2004). "Effects of changes in tree species composition on water flow dynamics – model applications and their limitations". In: *Plant and Soil* 264.1, pp. 13–24. DOI: 10.1023/B:PLSO.0000047716.45245.23. URL: https://doi.org/10.1023/B:PLSO.0000047716.45245.23.

Asbjornsen, H., G. R. Goldsmith, M. S. Alvarado-Barrientos, K. Rebel, F. P. Van Osch, M. Rietkerk, J. Chen, S. Gotsch, C. Tobón, D. R. Geissert, A. Gómez-Tagle, K. Vache, and T. E. Dawson (2011). "Ecohydrological advances and applications in plant–water relations research: a review". In: *Journal of Plant Ecology* 4.1–2, pp. 3–22. DOI: 10.1093/jpe/rtr005. URL: http://dx.doi.org/10.1093/jpe/rtr005.

Ashby, S. F. and R. D. Falgout (1996). "A parallel multigrid preconditioned conjugate gradient algorithm for groundwater flow simulations". In: *Nuclear Science and Engineering* 124.1, pp. 145–159. DOI: 10.13182/NSE96-A24230. URL: https://doi.org/10.13182/NSE96-A24230.

Baatz, D., W. Kurtz, H. J. Hendricks Franssen, H. Vereecken, and S. J. Kollet (2017). "Catchment tomography - an approach for spatial parameter estimation". In: *Advances in Water Resources* 107, pp. 147–159. DOI: https://doi.org/10.1016/j.advwatres.2017.06.006. URL: http://www.sciencedirect.com/science/article/pii/S0309170816302019.

Baatz, R., H. R. Bogena, H. J. Hendricks Franssen, J. A. Huisman, C. Montzka, and H. Vereecken (2015). "An empirical vegetation correction for soil water content quantification using cosmic ray probes". In: *Water Resources Research* 51.4, pp. 2030–2046. DOI: 10.1002/2014wr016443. URL: http://dx.doi.org/10.1002/2014WR016443.

Bachmair, S., M. Weiler, and G. Nützmann (2009). "Controls of land use and soil structure on water movement: lessons for pollutant transfer through the unsaturated zone". In: *Journal of Hydrology* 369.3, pp. 241–252. DOI: https://doi.org/10.1016/j.jhydrol.2009.02.031. URL: http://www.sciencedirect.com/science/article/pii/S0022169409001115.

Bailey, R. G. (1994). *Ecoregions and subregions of the United States (map)*. Ed. by P. E. Avers, T. King, and W. H. McNab. Vol. 1:7,500,000. With supplementary table of map unit descriptions, compiled and edited by W. H. McNab and R. G. Bailey. Washington DC: USDA Forest Service. DOI: https://doi.org/10.2737/RDS-2016-0003. URL: https://www.fs.usda.gov/rds/archive/catalog/RDS-2016-0003.

Baldauf, M., A. Seifert, J. Förstner, D. Majewski, M. Raschendorfer, and T. Reinhardt (2011). "Operational convective-scale numerical weather prediction with the COSMO model: description and sensitivities". In: *Monthly Weather Review* 139.12, pp. 3887–3905. DOI: 10.1175/MWR-D-10-05013.1. URL: https://doi.org/10.1175/MWR-D-10-05013.1.

Baldocchi, D. D. and Y. Ryu (2011). "Chapter 5: A synthesis of forest evaporation fluxes – from days to years – as measured with eddy covariance". In: *Forest hydrology and biogeochemistry: synthesis of past research and future directions*. Ed. by D. F. Levia, D. Carlyle-Moses, and T. Tanaka. Dordrecht: Springer Netherlands, pp. 101–116. DOI: 10.1007/978-94-007-1363-5_5. URL: https://doi.org/10.1007/978-94-007-1363-5_5.

Baldocchi, D. D., B. B. Hincks, and T. P. Meyers (1988). "Measuring biosphere - atmosphere exchanges of biologically related gases with micrometeorological methods". In: *Ecology* 69.5, pp. 1331–1340. DOI: 10.2307/1941631. URL: http://dx.doi.org/10.2307/1941631.

Bargués Tobella, A., H. Reese, A. Almaw, J. Bayala, A. Malmer, H. Laudon, and U. Ilstedt (2014). "The effect of trees on preferential flow and soil infiltrability in an agroforestry parkland in semiarid Burkina Faso". In: *Water Resources Research* 50.4, pp. 3342–3354. DOI: 10.1002/2013wr015197. URL: http://dx.doi.org/10.1002/2013WR015197.

Bathurst, J. C., J. Ewen, G. Parkin, P. E. O'Connell, and J. D. Cooper (2004). "Validation of catchment models for predicting land-use and climate change impacts. 3. Blind validation for internal and outlet responses". In: *Journal of Hydrology* 287.1, pp. 74–94. DOI: https://doi.org/10.1016/j.jhydrol.2003.09.021. URL: http://www.sciencedirect.com/science/article/pii/S0022169403003950.

Bayazit, Mehmetcik (2015). "Nonstationarity of hydrological records and recent trends in trend analysis: a state-of-the-art review". In: *Environmental Processes* 2.3, pp. 527–542. DOI: 10.1007/s40710-015-0081-7. URL: https://doi.org/10.1007/s40710-015-0081-7.

Benegas, L., U. Ilstedt, O. Roupsard, J. Jones, and A. Malmer (2014). "Effects of trees on infiltrability and preferential flow in two contrasting agroecosystems in Central America". In: *Agriculture, Ecosystems and Environment* 183, pp. 185–196. DOI: https://doi.org/10.1016/j.agee.2013.10.027. URL: http://www.sciencedirect.com/science/article/pii/S0167880913003794.

Bennett, A., B. Nijssen, G. Ou, M. Clark, and G. Nearing (2019). "Quantifying process connectivity with transfer entropy in hydrologic models". In:

Water Resources Research 55.6, pp. 4613–4629. DOI: 10.1029/2018wr024555. URL: https://agupubs.onlinelibrary.wiley.com/doi/abs/10.1029/2018WR024555.

Beschta, R. L., M. R. Pyles, A. E. Skaugset, and C. G. Surfleet (2000). "Peakflow responses to forest practices in the western cascades of Oregon, USA". In: *Journal of Hydrology* 233, pp. 102–120. DOI: http://dx.doi.org/10.1016/S0022-1694(00)00231-6. URL: http://www.sciencedirect.com/science/article/pii/S0022169400002316.

Best, A., L. Zhang, T. McMahon, A. Western, and R. Vertessy (2003). *A critical review of paired catchment studies with reference to seasonal flows and climatic variability*. Tech. rep. CSIRO Land and Water Technical Report 25/03, CRC for Catchment Hydrology Technical Report 03/4. Canberra: Murray-Darling Basin Commission and CSIRO. URL: https://publications.csiro.au/rpr/pub?list=BRO&pid=procite:fcdfd12f-dca1-41c0-85ce-d06d0c542e7c.

Best, M. J., G. Abramowitz, H. R. Johnson, A. J. Pitman, G. Balsamo, A. Boone, M. Cuntz, B. Decharme, P. A. Dirmeyer, J. Dong, M. Ek, Z. Guo, V. Haverd, B. J. J. van den Hurk, G. S. Nearing, B. Pak, C. Peters-Lidard, J. A. Santanello, L. Stevens, and N. Vuichard (2015). "The Plumbing of Land Surface Models: Benchmarking Model Performance". In: *Journal of Hydrometeorology* 16.3, pp. 1425–1442. DOI: 10.1175/JHM-D-14-0158.1. eprint: https://doi.org/10.1175/JHM-D-14-0158.1. URL: https://doi.org/10.1175/JHM-D-14-0158.1.

Beven, K. and P. Germann (1982). "Macropores and water flow in soils". In: *Water Resources Research* 18.5, pp. 1311–1325. DOI: 10.1029/WR018i005p01311. URL: http://dx.doi.org/10.1029/WR018i005p01311.

— (2013). "Macropores and water flow in soils revisited". In: *Water Resources Research* 49.6, pp. 3071–3092. DOI: 10.1002/wrcr.20156. URL: http://dx.doi.org/10.1002/wrcr.20156.

Beven, K., H. Cloke, F. Pappenberger, R. Lamb, and N. Hunter (2015). "Hyperresolution information and hyperresolution ignorance in modelling the hydrology of the land surface". In: *Science China Earth Sciences* 58.1, pp. 25–35. DOI: 10.1007/s11430-014-5003-4. URL: http://dx.doi.org/10.1007/s11430-014-5003-4.

Beven, K. J. (2012). *Rainfall-runoff modelling: the primer*. Oxford, USA: John Wiley & Sons Ltd. DOI: 10.1002/9781119951001.

— (2018). "On hypothesis testing in hydrology: why falsification of models is still a really good idea". In: *Wiley Interdisciplinary Reviews: Water* 5.3,

e1278. DOI: 10.1002/wat2.1278. URL: https://onlinelibrary.wiley.com/doi/abs/10.1002/wat2.1278.

Biederman, J. A., A. A. Harpold, D. J. Gochis, B. E. Ewers, D. E. Reed, S. A. Papuga, and P. D. Brooks (2014). "Increased evaporation following widespread tree mortality limits streamflow response". In: *Water Resources Research* 50.7, pp. 5395–5409. DOI: 10.1002/2013wr014994. URL: http://dx.doi.org/10.1002/2013WR014994.

Biederman, J. A., A. J. Somor, A. A. Harpold, E. D. Gutmann, D. D. Breshears, P. A. Troch, D. J. Gochis, R. L. Scott, A. J. H. Meddens, and P. D. Brooks (2015). "Recent tree die-off has little effect on streamflow in contrast to expected increases from historical studies". In: *Water Resources Research* 51.12, pp. 9775–9789. DOI: 10.1002/2015wr017401. URL: http://dx.doi.org/10.1002/2015WR017401.

Binley, A., S. S. Hubbard, J. A. Huisman, A. Revil, D. A. Robinson, K. Singha, and L. D. Slater (2015). "The emergence of hydrogeophysics for improved understanding of subsurface processes over multiple scales". In: *Water Resources Research* 51.6, pp. 3837–3866. DOI: 10.1002/2015WR017016. URL: https://doi.org/10.1002/2015WR017016.

Bittelli, M. (2011). "Measuring soil water content: a review". In: *HortTechnology* 21.3, pp. 293–300. DOI: https://doi.org/10.21273/HORTTECH.21.3.293. URL: https://journals.ashs.org/horttech/view/journals/horttech/21/3/article-p293.xml.

Blonquist, J. M., S. B. Jones, and D. A. Robinson (2005). "Standardizing characterization of electromagnetic water content sensors: part 2. evaluation of seven sensing systems". In: *Vadose Zone Journal* 4.4, pp. 1059–1069. DOI: 10.2136/vzj2004.0141. URL: http://vzj.geoscienceworld.org/content/4/4/1059.abstract.

Blöschl, G., A. P. Blaschke, M. Broer, C. Bucher, G. Carr, X. Chen, A. Eder, M. Exner-Kittridge, A. Farnleitner, A. Flores-Orozco, P. Haas, P. Hogan, A. Kazemi Amiri, M. Oismüller, J. Parajka, R. Silasari, P. Stadler, P. Strauss, M. Vreugdenhil, W. Wagner, and M. Zessner (2016). "The hydrological open air laboratory (HOAL) in Petzenkirchen: a hypothesis-driven observatory". In: *Hydrology and Earth System Sciences* 20.1, pp. 227–255. DOI: 10.5194/hess-20-227-2016. URL: https://www.hydrol-earth-syst-sci.net/20/227/2016/.

Blöschl, G. and M. Sivapalan (1995). "Scale issues in hydrological modelling: a review". In: *Hydrological Processes* 9.3-4, pp. 251–290. DOI: 10.1002/hyp.3360090305. URL: http://dx.doi.org/10.1002/hyp.3360090305.

Blöschl, G., M. Sivapalan, T. Wagener, A. Viglione, and H. Savenije, eds. (2013). *Runoff prediction in ungauged basins: synthesis across processes, places and scales*. Cambridge University Press. ISBN: 1107067553. DOI: https://doi.org/10.1017/CBO9781139235761.

Bogena, H., R. Kunkel, T. Puetz, H. Vereecken, E. Krueger, S. Zacharias, P. Dietrich, U. Wollschlaeger, H. Kunstmann, H. Papen, H. P. Schmid, J. C. Munch, E. Priesack, M. Schwank, O. Bens, A. Brauer, E. Borg, and I. Hajnsek (2012). "TERENO - Long-term monitoring network for terrestrial environmental research". In: *Hydrologie und Wasserbewirtschaftung* 56.3, pp. 138–143.

Bogena, H., H.-J. Hendricks Franssen, C. Montzka, and H. Vereecken (2017). "Chapter 11: A blueprint for a distributed terrestrial ecosystem research infrastructure". In: *Terrestrial ecosystem research infrastructures: challenges and oppurtunities*. Ed. by A. Chabbi and H. W. Loescher. CRC Press, pp. 279–302. DOI: 10.1201/9781315368252-12. URL: http://dx.doi.org/10.1201/9781315368252-12.

Bogena, H. R., J. A. Huisman, C. Oberdörster, and H. Vereecken (2007). "Evaluation of a low-cost soil water content sensor for wireless network applications". In: *Journal of Hydrology* 344.1–2, pp. 32–42. DOI: http://dx.doi.org/10.1016/j.jhydrol.2007.06.032. URL: http://www.sciencedirect.com/science/article/pii/S0022169407003514.

Bogena, H. R., J. A. Huisman, R. Baatz, H. J. Hendricks Franssen, and H. Vereecken (2013). "Accuracy of the cosmic-ray soil water content probe in humid forest ecosystems: the worst case scenario". In: *Water Resources Research* 49.9, pp. 5778–5791. DOI: 10.1002/wrcr.20463. URL: http://dx.doi.org/10.1002/wrcr.20463.

Bogena, H. R., R. Bol, N. Borchard, N. Brüggemann, B. Diekkrüger, C. Drüe, J. Groh, N. Gottselig, J. A. Huisman, A. Lücke, A. Missong, B. Neuwirth, T. Pütz, M. Schmidt, M. Stockinger, W. Tappe, L. Weihermüller, I. Wiekenkamp, and H. Vereecken (2015). "A terrestrial observatory approach for the integrated investigation of the effects of deforestation on water, energy, and matter fluxes". In: *Sci. China: Earth Sci.* 58.1, pp. 61–75. DOI: 10.1007/s11430-014-4911-7. URL: https://link.springer.com/article/10.1007/s11430-014-4911-7.

Bogena, H.R., M. Herbst, J.A. Huisman, U. Rosenbaum, A. Weuthen, and H. Vereecken (2010). "Potential of wireless sensor networks for measuring soil water content variability". In: *Vadose Zone Journal* 9.4, pp. 1002–

1013. DOI: 10.2136/vzj2009.0173. URL: https://www.soils.org/publications/vzj/abstracts/9/4/1002.

Bogena, H.R., C. Montzka, J.A. Huisman, A. Graf, M. Schmidt, M. Stockinger, C. von Hebel, H.J. Hendricks Franssen, J. van der Kruk, W. Tappe, A. Lücke, R. Baatz, R. Bol, J. Groh, T. Pütz, J. Jakobi, R. Kunkel, J. Sorg, and H. Vereecken (2018). "The TERENO-Rur hydrological observatory: a multiscale multi-compartment research platform for the advancement of hydrological science". In: *Vadose Zone Journal* 17.1, pp. 1–22. DOI: 10.2136/vzj2018.03.0055. URL: http://dx.doi.org/10.2136/vzj2018.03.0055.

Bol, R., A. Lücke, W. Tappe, S. Kummer, M. Krause, S. Weigand, T. Pütz, and H. Vereecken (2015). "Spatio-temporal variations of Dissolved Organic Matter in a German forested mountainous headwater catchment". In: *Vadose Zone Journal* 14.4. DOI: 10.2136/vzj2015.01.0005. URL: http://vzj.geoscienceworld.org/content/14/4/vzj2015.01.0005.abstract.

Borchardt, H. (2012). "Impact of pleistocene cover-beds on discharge : the anthropogenic influenced Wüstebach-river (nationalpark Eifel) as an example". Thesis. Aachen, Techn. Hochsch. URL: http://publications.rwth-aachen.de/record/210381?ln=de.

Bormann, H., L. Breuer, T. Gräff, and J. A. Huisman (2007). "Analysing the effects of soil properties changes associated with land use changes on the simulated water balance: a comparison of three hydrological catchment models for scenario analysis". In: *Ecological Modelling* 209.1, pp. 29–40. DOI: http://dx.doi.org/10.1016/j.ecolmodel.2007.07.004.

Bormann, H., L. Breuer, T. Gräff, J. A. Huisman, and B. Croke (2009). "Assessing the impact of land use change on hydrology by ensemble modelling (LUCHEM) IV: Model sensitivity to data aggregation and spatial (re-)distribution". In: *Advances in Water Resources* 32.2, pp. 171–192. DOI: http://dx.doi.org/10.1016/j.advwatres.2008.01.002. URL: http://www.sciencedirect.com/science/article/pii/S0309170808000067.

Bosch, J. M. and J. D. Hewlett (1982). "A review of catchment experiments to determine the effect of vegetation changes on water yield and evapotranspiration". In: *Journal of Hydrology* 55.1-4, pp. 3–23. DOI: http://dx.doi.org/10.1016/0022-1694(82)90117-2. URL: http://www.sciencedirect.com/science/article/pii/0022169482901172.

Bouten, W. (1995). "Soil water dynamics of the Solling spruce stand, calculated with the forhyd simulation package". In: *Ecological Modelling* 83.1–2, pp. 67–75. DOI: http://dx.doi.org/10.1016/0304-3800(95)00085-A.

Bouten, W., P. J. F. Swart, and E. De Water (1991). "Microwave transmission, a new tool in forest hydrological research". In: *Journal of Hydrology* 124.1, pp. 119–130. DOI: http://dx.doi.org/10.1016/0022-1694(91)90009-7. URL: http://www.sciencedirect.com/science/article/pii/0022169491900097.

Bouten, W., T. J. Heimovaara, and A. Tiktak (1992). "Spatial patterns of throughfall and soil water dynamics in a Douglas fir stand". In: *Water Resources Research* 28.12, pp. 3227–3233. DOI: 10.1029/92wr01764. URL: http://dx.doi.org/10.1029/92WR01764.

Brath, A., A. Montanari, and G. Moretti (2006). "Assessing the effect on flood frequency of land use change via hydrological simulation (with uncertainty)". In: *Journal of Hydrology* 324.1, pp. 141–153. DOI: https://doi.org/10.1016/j.jhydrol.2005.10.001. URL: http://www.sciencedirect.com/science/article/pii/S0022169405004816.

Breuer, L. and J. A. Huisman (2009). "Assessing the impact of land use change on hydrology by ensemble modeling (LUCHEM)". In: *Advances in Water Resources* 32.2, pp. 127–128. DOI: http://dx.doi.org/10.1016/j.advwatres.2008.10.010. URL: www.sciencedirect.com/science/article/pii/S0309170808001875.

Breuer, L., J. A. Huisman, and H.-G. Frede (2006). "Monte Carlo assessment of uncertainty in the simulated hydrological response to land use change". In: *Environmental Modeling and Assessment* 11.3, pp. 209–218. DOI: 10.1007/s10666-006-9051-9. URL: http://dx.doi.org/10.1007/s10666-006-9051-9.

Breuer, L., J. A. Huisman, P. Willems, H. Bormann, A. Bronstert, B. F. W. Croke, H. G. Frede, T. Gräff, L. Hubrechts, A. J. Jakeman, G. Kite, J. Lanini, G. Leavesley, D. P. Lettenmaier, G. Lindström, J. Seibert, M. Sivapalan, and N. R. Viney (2009). "Assessing the impact of land use change on hydrology by ensemble modeling (LUCHEM). I: Model intercomparison with current land use". In: *Advances in Water Resources* 32.2, pp. 129–146. DOI: http://dx.doi.org/10.1016/j.advwatres.2008.10.003.

Bronstert, A., D. Niehoff, and G. Bürger (2002). "Effects of climate and land-use change on storm runoff generation: present knowledge and modelling capabilities". In: *Hydrological Processes* 16.2, pp. 509–529. DOI: 10.1002/hyp.326. URL: https://doi.org/10.1002/hyp.326.

Brown, A. E., L. Zhang, T. A.McMahon, A. W.Western, and R. A. Vertessy (2005). "A review of paired catchment studies for determining changes in

water yield resulting from alterations in vegetation". In: *Journal of Hydrology* 310.1–4, pp. 28–61. DOI: http://dx.doi.org/10.1016/j.jhydrol.2004.12.010. URL: http://www.sciencedirect.com/science/article/pii/S0022169404005906.

Brown, A. E., A. W. Western, T. A. McMahon, and L. Zhang (2013). "Impact of forest cover changes on annual streamflow and flow duration curves". In: *Journal of Hydrology* 483.0, pp. 39–50. DOI: http://dx.doi.org/10.1016/j.jhydrol.2012.12.031. URL: http://www.sciencedirect.com/science/article/pii/S0022169412011146.

Bruijnzeel, L. A. (1990). *Hydrology of moist tropical forests and effects of conversion: a state of knowledge review*. Faculty of Earth Sciences, Free University Amsterdam, The Netherlands. URL: https://unesdoc.unesco.org/ark:/48223/pf0000097405.

Bultot, F., G. L. Dupriez, and D. Gellens (1990). "Simulation of land use changes and impacts on the water balance - A case study for Belgium". In: *Journal of Hydrology* 114.3–4, pp. 327–348. DOI: http://dx.doi.org/10.1016/0022-1694(90)90064-5. URL: http://www.sciencedirect.com/science/article/pii/0022169490900645.

Burton, T. A. (1997). "Effects of basin-scale timber harvest on water yield and peak streamflow". In: *Journal of the American Water Resources Association* 33.6, pp. 1187–1196. DOI: 10.1111/j.1752-1688.1997.tb03545.x. URL: http://dx.doi.org/10.1111/j.1752-1688.1997.tb03545.x.

Calder, I. R. (1990). *Evaporation in the uplands*. Vol. Institute of Hydrology, Wallingford, UK. Wiley and Sons.

— (1991). "Implications and assumptions in using the 'total counts' and convection-dispersion equations for tracer flow measurements - With particular reference to transpiration measurements in trees". In: *Journal of Hydrology* 125.1, pp. 149–158. DOI: http://dx.doi.org/10.1016/0022-1694(91)90088-Y. URL: http://www.sciencedirect.com/science/article/pii/002216949190088Y.

Chandler, K. R. and N. A. Chappell (2008). "Influence of individual oak (Quercus robur) trees on saturated hydraulic conductivity". In: *Forest Ecology and Management* 256.5, pp. 1222–1229. DOI: https://doi.org/10.1016/j.foreco.2008.06.033. URL: http://www.sciencedirect.com/science/article/pii/S0378112708005239.

Chen, L., L. Wang, Y. Ma, and P. Liu (2015). "Overview of ecohydrological models and systems at the watershed scale". In: *IEEE Systems Journal*

9.3, pp. 1091–1099. DOI: 10.1109/JSYST.2013.2296979. URL: https://ieeexplore.ieee.org/document/6782450.

Choudhury, B. (1999). "Evaluation of an empirical equation for annual evaporation using field observations and results from a biophysical model". In: *Journal of Hydrology* 216.1–2, pp. 99–110. DOI: http://dx.doi.org/10.1016/S0022-1694(98)00293-5. URL: http://www.sciencedirect.com/science/article/pii/S0022169498002935.

Clarke, R. T. (2007). "Hydrological prediction in a non-stationary world". In: *Hydrology and Earth System Sciences* 11.1, pp. 408–414. DOI: 10.5194/hess-11-408-2007. URL: https://www.hydrol-earth-syst-sci.net/11/408/2007/.

Clenciala, E., J. Kucera, M. G. Ryan, and A. Lindroth (1998). "Water flux in boreal forest during two hydrologically contrasting years; species specific regulation of canopy conductance and transpiration". In: *Ann. For. Sci.* 55.1-2, pp. 47–61. DOI: 10.1051/forest:19980104. URL: https://doi.org/10.1051/forest:19980104.

Condon, L. E. and R. M. Maxwell (2015). "Evaluating the relationship between topography and groundwater using outputs from a continental-scale integrated hydrology model". In: *Water Resources Research* 51.8, pp. 66–02–6621. DOI: 10.1002/2014WR016774. URL: https://doi.org/10.1002/2014WR016774.

— (2017). "Systematic shifts in Budyko relationships caused by groundwater storage changes". In: *Hydrology and Earth System Sciences* 21.2, pp. 1117–1135. DOI: 10.5194/hess-21-1117-2017. URL: https://www.hydrol-earth-syst-sci.net/21/1117/2017/.

Cornelissen, T., B. Diekkrüger, and H. Bogena (2013). "Using HydroGeoSphere in a forested catchment: how does spatial resolution influence the simulation of spatio-temporal soil moisture variability?" In: *Procedia Environmental Sciences* 19, pp. 198–207. DOI: http://dx.doi.org/10.1016/j.proenv.2013.06.022. URL: http://www.sciencedirect.com/science/article/pii/S1878029613002922.

Cornelissen, T., B. Diekkrüger, and H. R. Bogena (2014). "Significance of scale and lower boundary condition in the 3D simulation of hydrological processes and soil moisture variability in a forested headwater catchment". In: *Journal of Hydrology* 516, pp. 140–153. DOI: https://doi.org/10.1016/j.jhydrol.2014.01.060. URL: www.sciencedirect.com/science/article/pii/S0022169414000821.

Creed, I. F., A. T. Spargo, J. A. Jones, J. M. Buttle, M. B. Adams, F. D. Beall, E. G. Booth, J. L. Campbell, D. Clow, K. Elder, M. B. Green, N. B. Grimm, C. Miniat, P. Ramlal, A. Saha, S. Sebestyen, D. Spittlehouse, S. Sterling, M. W. Williams, R. Winkler, and H. Yao (2014). "Changing forest water yields in response to climate warming: results from long-term experimental watershed sites across North America". In: *Global Change Biology* 20.10, pp. 3191–3208. DOI: 10.1111/gcb.12615. URL: http://dx.doi.org/10.1111/gcb.12615.

Crooks, S. and H. Davies (2001). "Assessment of land use change in the Thames catchment and its effect on the flood regime of the river". In: *Physics and Chemistry of the Earth, Part B: Hydrology, Oceans and Atmosphere* 26.7, pp. 583–591. DOI: https://doi.org/10.1016/S1464-1909(01)00053-3. URL: https://www.sciencedirect.com/science/article/pii/S1464190901000533.

D'Almeida, C., C. J. Vörösmarty, G. C. Hurtt, J. A. Marengo, S. L. Dingman, and B. D. Keim (2007). "The effects of deforestation on the hydrological cycle in Amazonia: a review on scale and resolution". In: *International Journal of Climatology* 27.5, pp. 633–647. DOI: 10.1002/joc.1475. URL: http://dx.doi.org/10.1002/joc.1475.

Danielson, R.E. and P.L. Sutherland (1986). "Porosity". In: *Methods of soil analysis, part 1, Physical and mineralogical methods*. Ed. by A. Klute. Madison, Wisconsin: Am. Soc. Agr., 443—461.

De Roo, A., M. Odijk, G. Schmuck, E. Koster, and A. Lucieer (2001). "Assessing the effects of land use changes on floods in the meuse and oder catchment". In: *Physics and Chemistry of the Earth, Part B: Hydrology, Oceans and Atmosphere* 26.7–8, pp. 593–599. DOI: http://dx.doi.org/10.1016/S1464-1909(01)00054-5. URL: http://www.sciencedirect.com/science/article/pii/S1464190901000545.

DeFries, R. and K. N. Eshleman (2004). "Land-use change and hydrologic processes: a major focus for the future". In: *Hydrological Processes* 18.11, pp. 2183–2186. DOI: 10.1002/hyp.5584. URL: http://dx.doi.org/10.1002/hyp.5584.

Dekker, S. C. (2000). "Modelling and monitoring forest evapotranspiration. behaviour, concepts and parameters". Thesis. University of Amsterdam, the Netherlands. URL: https://www.researchgate.net/publication/46656485_Modelling_and_Monitoring_Forest_Evapotranspiration_Behaviour_Concepts_and_Parameters.

Demand, D., T. Blume, and M. Weiler (2019). "Relevance and controls of preferential flow at the landscape scale". In: *Hydrology and Earth System Sciences Discussions* 2019, pp. 1–37. DOI: 10.5194/hess-2019-80. URL: https://www.hydrol-earth-syst-sci-discuss.net/hess-2019-80/.

Devi, G. K., B. P. Ganasri, and G. S. Dwarakish (2015). "A review on hydrological models". In: *Aquatic Procedia* 4, pp. 1001–1007. DOI: http://dx.doi.org/10.1016/j.aqpro.2015.02.126. URL: http://www.sciencedirect.com/science/article/pii/S2214241X15001273.

D'Odorico, P., K. Caylor, G. S. Okin, and T. M. Scanlon (2007). "On soil moisture – vegetation feedbacks and their possible effects on the dynamics of dryland ecosystems". In: *Journal of Geophysical Research: Biogeosciences* 112.G4. DOI: 10.1029/2006jg000379. URL: http://dx.doi.org/10.1029/2006JG000379.

Donohue, R. J., M. L. Roderick, and T. R. McVicar (2007). "On the importance of including vegetation dynamics in Budyko's hydrological model". In: *Hydrology and Earth System Sciences* 11.2, pp. 983–995. DOI: 10.5194/hess-11-983-2007. URL: https://www.hydrol-earth-syst-sci.net/11/983/2007/.

Doppler, T., M. Honti, U. Zihlmann, P. Weisskopf, and C. Stamm (2014). "Validating a spatially distributed hydrological model with soil morphology data". In: *Hydrology and Earth System Sciences* 18.9, pp. 3481–3498. DOI: 10.5194/hess-18-3481-2014. URL: https://www.hydrol-earth-syst-sci.net/18/3481/2014/.

Dore, S., M. Montes-Helu, T. Kolb, B. Hungate, G. Koch, and S. Hart (2012). "Forest thinning increases ecosystem carbon sequestration during drought". In: *Global Change Biology* 18, 3171—3185.

Dorigo, W. A., A. Xaver, M. Vreugdenhil, A. Gruber, A. Hegyiová, A. D. Sanchis-Dufau, D. Zamojski, C. Cordes, W. Wagner, and M. Drusch (2013). "Global automated quality control of in situ soil moisture data from the International Soil Moisture Network". In: *Vadose Zone Journal* 12.3. DOI: 10.2136/vzj2012.0097. URL: https://dl.sciencesocieties.org/publications/vzj/abstracts/12/3/vzj2012.0097.

Douglass, J. E. and W. T. Swank (1975). "Effects of management practices on water quality and quantity: Coweeta Hydrologic Laboratory, North Carolina". In: *Municipal watershed management symposium proceedings*. USDA Forest Service Gen. Tech. Report NE-13, Northeastern Forest Experimental Station, pp. 1–13. URL: http://coweeta.uga.edu/publications/1040.pdf.

Droppo, J. G. and H. L. Hamilton (1973). "Experimental variability in the determination of the energy balance in a deciduous forest". In: *Journal of Applied Meteorology* 12.5, pp. 781–791. DOI: 10.1175/1520-0450(1973)012<0781:evitdo>2.0.co;2. URL: https://doi.org/10.1175/1520-0450(1973)012<0781:EVITDO>2.0.CO.

Drüe, C., A. Graf, G. Heinemann, and T. Pütz (2012). "Observation of atmosphere - forest exchange processes at the new TERENO site Wüstebach". In: *20th Symposium on Boundary Layers and Turbulence*. Vol. Boston, Mass. 9–13 Jul, AMS (American Meteorological Society).

Dunn, S. M. and R. Mackay (1995). "Spatial variation in evapotranspiration and the influence of land use on catchment hydrology". In: *Journal of Hydrology* 171.1, pp. 49–73. DOI: http://dx.doi.org/10.1016/0022-1694(95)02733-6. URL: http://www.sciencedirect.com/science/article/pii/0022169495027336.

Dupas, R., C. Minaudo, and B. Abbott (2019). "Stability of spatial patterns in water chemistry across temperate ecoregions". In: *Environmental Research Letters* 14.7, p. 074015. DOI: 10.1088/1748-9326/ab24f4. URL: https://iopscience.iop.org/article/10.1088/1748-9326/ab24f4.

Dwarakish, G. S. and B. P. Ganasri (2015). "Impact of land use change on hydrological systems: a review of current modeling approaches". In: *Cogent Geoscience* 1.1, p. 1115691. DOI: 10.1080/23312041.2015.1115691. URL: http://dx.doi.org/10.1080/23312041.2015.1115691.

Dwersteg, D. (2012). "Spatial and temporal variability of soil CO_2 efflux in a spruce-dominated forest in the Eifel National Park, Germany." PhD thesis. Bonn, Germany: Friedrich-Wilhelms-University Bonn. URL: http://hss.ulb.uni-bonn.de/2012/2823/2823.htm.

Dyer, A. J. (1961). "Measurements of evaporation and heat transfer in the lower atmosphere by an automatic eddy-correlation technique". In: *Quarterly Journal of the Royal Meteorological Society* 87.373, pp. 401–412. DOI: 10.1002/qj.49708737311. URL: http://dx.doi.org/10.1002/qj.49708737311.

Ebel, B. A. and B. B. Mirus (2014). "Disturbance hydrology: challenges and opportunities". In: *Hydrological Processes* 28.19, pp. 5140–5148. DOI: 10.1002/hyp.10256. URL: http://dx.doi.org/10.1002/hyp.10256.

Eckhardt, K., L. Breuer, and H.-G. Frede (2003). "Parameter uncertainty and the significance of simulated land use change effects". In: *Journal of Hydrology* 273.1–4, pp. 164–176. DOI: http://dx.doi.org/10.1016/S0022-

1694(02)00395-5. URL: http://www.sciencedirect.com/science/article/pii/S0022169402003955.

Edwards, W. R. N. (1986). "Precision weighing lysimetry for trees, using a simplified tared-balance design". In: *Tree Physiology* 1.2, pp. 127–144. DOI: https://doi.org/10.1093/treephys/1.2.127. URL: http://citeseerx.ist.psu.edu/viewdoc/download?doi=10.1.1.897.9976&rep=rep1&type=pdf.

Ehret, U., H. V. Gupta, M. Sivapalan, S. V. Weijs, S. J. Schymanski, G. Blöschl, A. N. Gelfan, C. Harman, A. Kleidon, T. A. Bogaard, D. Wang, T. Wagener, U. Scherer, E. Zehe, M. F. P. Bierkens, G. Di Baldassarre, J. Parajka, L. P. H. van Beek, A. van Griensven, M. C. Westhoff, and H. C. Winsemius (2014). "Advancing catchment hydrology to deal with predictions under change". In: *Hydrology and Earth System Sciences* 18.2, pp. 649–671. DOI: 10.5194/hess-18-649-2014. URL: http://www.hydrol-earth-syst-sci.net/18/649/2014/.

Elfert, S. and H. Bormann (2010). "Simulated impact of past and possible future land use changes on the hydrological response of the Northern German lowland 'Hunte' catchment". In: *Journal of Hydrology* 383.3–4, pp. 245–255. DOI: http://dx.doi.org/10.1016/j.jhydrol.2009.12.040.

Etmann, M. (2009). "Dendrologische Aufnahmen im Wassereinzugsgebiet Oberer Wüstebach anhand verschiedener Mess- und Schätzverfahren". Thesis. University of Münster. URL: http://juser.fz-juelich.de/record/10505.

Ewen, J. and G. Parkin (1996). "Validation of catchment models for predicting land-use and climate change impacts. 1. Method". In: *Journal of Hydrology* 175.1–4, pp. 583–594. DOI: http://dx.doi.org/10.1016/S0022-1694(96)80026-6. URL: http://www.sciencedirect.com/science/article/pii/S0022169496800266.

Fang, Z., H. Bogena, S.n Kollet, J. Koch, and H. Vereecken (2015). "Spatio-temporal validation of long-term 3D hydrological simulations of a forested catchment using empirical orthogonal functions and wavelet coherence analysis". In: *Journal of Hydrology* 529, Part 3, pp. 1754–1767. DOI: http://dx.doi.org/10.1016/j.jhydrol.2015.08.011. URL: http://www.sciencedirect.com/science/article/pii/S0022169415005703.

Fang, Z., H. Bogena, S. Kollet, and H. Vereecken (2016). "Scale dependent parameterization of soil hydraulic conductivity in 3D simulation of hydrological processes in a forested headwater catchment". In: *Journal of Hydrology* 536, pp. 365–375. DOI: https://doi.org/10.1016/j.jhydrol.

2016.03.020. URL: http://www.sciencedirect.com/science/article/pii/S0022169416301251.

Farjad, B., A. Gupta, S. Razavi, M. Faramarzi, and J. D. Marceau (2017). "An integrated modelling system to predict hydrological processes under climate and land-use/cover change scenarios". In: *Water* 9.10. DOI: 10.3390/w9100767. URL: https://www.mdpi.com/2073-4441/9/10/767.

Farley, K. A., E. G. Jobbágy, and R. B. Jackson (2005). "Effects of afforestation on water yield: a global synthesis with implications for policy". In: *Global Change Biology* 11.10, pp. 1565–1576. DOI: 10.1111/j.1365-2486.2005.01011.x. URL: http://dx.doi.org/10.1111/j.1365-2486.2005.01011.x.

Fatichi, S., E. R. Vivoni, F. L. Ogden, V. Y. Ivanov, B. Mirus, D. Gochis, C. W. Downer, M. Camporese, J. H. Davison, B. Ebel, N. Jones, J. Kim, G. Mascaro, R. Niswonger, P. Restrepo, R. Rigon, C. Shen, M. Sulis, and D. Tarboton (2016). "An overview of current applications, challenges, and future trends in distributed process-based models in hydrology". In: *Journal of Hydrology* 537, pp. 45–60. DOI: https://doi.org/10.1016/j.jhydrol.2016.03.026. URL: http://www.sciencedirect.com/science/article/pii/S0022169416301317.

Feng, H. (2016). "Individual contributions of climate and vegetation change to soil moisture trends across multiple spatial scales". In: *Scientific Reports* 6, p. 32782. DOI: 10.1038/srep32782. URL: http://dx.doi.org/10.1038/srep32782.

Fenicia, F., H. H. G. Savenije, and Y. Avdeeva (2009). "Anomaly in the rainfall-runoff behaviour of the Meuse catchment. Climate, land-use, or land-use management?" In: *Hydrology and Earth System Sciences* 13.9, pp. 1727–1737. DOI: 10.5194/hess-13-1727-2009. URL: https://www.hydrol-earth-syst-sci.net/13/1727/2009/.

Figueiredo, R. O., D. Markewitz, E. A. Davidson, A. E. Schuler, O. dos S. Watrin, and P. de Souza Silva (2010). "Land-use effects on the chemical attributes of low-order streams in the eastern Amazon". In: *Journal of Geophysical Research: Biogeosciences* 115.G4. DOI: 10.1029/2009JG001200. URL: https://agupubs.onlinelibrary.wiley.com/doi/abs/10.1029/2009JG001200.

Filoso, S., M. O. Bezerra, K. C. B. Weiss, and M. A. Palmer (2017). "Impacts of forest restoration on water yield: a systematic review". In: *PLOS ONE* 12.8, e0183210. DOI: 10.1371/journal.pone.0183210. URL: http://www.ncbi.nlm.nih.gov/pmc/articles/PMC5560669/.

Findlay, S., J. M. Quinn, C. W. Hickey, G. Burrell, and M. Downes (2001). "Effects of land use and riparian flowpath on delivery of dissolved organic carbon to streams". In: *Limnology and Oceanography* 46.2, pp. 345–355. DOI: 10.4319/lo.2001.46.2.0345. URL: https://aslopubs.onlinelibrary.wiley.com/doi/abs/10.4319/lo.2001.46.2.0345.

Flury, M., H. Flühler, W. A. Jury, and J. Leuenberger (1994). "Susceptibility of soils to preferential flow of water: a field study". In: *Water Resources Research* 30.7, pp. 1945–1954. DOI: 10.1029/94wr00871. URL: http://dx.doi.org/10.1029/94WR00871.

Foken, T. (2008). *Micrometeorology*. Ed. by C. J. Nappo. Berlin, Heidelberg: Springer Science and Business Media.

Foken, T., M. Aubinet, J. J. Finnigan, M. Y. Leclerc, M. Mauder, and K. T. P. U (2011). "Results of a panel discussion about the energy balance closure correction for trace gases". In: *Bulletin of the American Meteorological Society* 92.4, ES13–ES18. DOI: doi:10.1175/2011BAMS3130.1. URL: http://journals.ametsoc.org/doi/abs/10.1175/2011BAMS3130.1.

Garré, S., M. Javaux, J. Vanderborght, and H. Vereecken (2011). "Three-dimensional electrical resistivity tomography to monitor root zone water dynamics". In: *Vadose Zone Journal* 10.1, pp. 412–424. DOI: https://doi.org/10.2136/vzj2010.0079. URL: https://dl.sciencesocieties.org/publications/vzj/abstracts/10/1/412.

Gasper, F., K. Goergen, P. Shrestha, M. Sulis, J. Rihani, M. Geimer, and S. Kollet (2014). "Implementation and scaling of the fully coupled Terrestrial Systems Modeling Platform (TerrSysMP v1.0) in a massively parallel supercomputing environment – a case study on JUQUEEN (IBM Blue Gene/Q)". In: *Geosci. Model Dev.* 7.5, pp. 2531–2543. DOI: 10.5194/gmd-7-2531-2014. URL: https://www.geosci-model-dev.net/7/2531/2014/.

Gebler, S., H. J. Hendricks Franssen, S. J. Kollet, W. Qu, and H. Vereecken (2017). "High resolution modelling of soil moisture patterns with TerrSysMP: a comparison with sensor network data". In: *Journal of Hydrology* 547, pp. 309–331. DOI: https://doi.org/10.1016/j.jhydrol.2017.01.048. URL: http://www.sciencedirect.com/science/article/pii/S0022169417300586.

Geris, J., D. Tetzlaff, J. McDonnell, and C. Soulsby (2015). "The relative role of soil type and tree cover on water storage and transmission in northern headwater catchments". In: *Hydrological Processes* 29.7, pp. 1844–1860. DOI: 10.1002/hyp.10289. URL: http://dx.doi.org/10.1002/hyp.10289.

Germann, P. F. and D. Hensel (2006). "Poiseuille flow geometry inferred from velocities of wetting fronts in soils". In: *Vadose Zone Journal* 5.3, pp. 867–876. DOI: 10.2136/vzj2005.0080. URL: https://www.soils.org/publications/vzj/abstracts/5/3/867.

Ghasemizade, M. and M. Schirmer (2013). "Subsurface flow contribution in the hydrological cycle: lessons learned and challenges ahead—a review". In: *Environmental Earth Sciences* 69.2, pp. 707–718. DOI: 10.1007/s12665-013-2329-8. URL: http://dx.doi.org/10.1007/s12665-013-2329-8.

Ghestem, M., R. C. Sidle, and A. Stokes (2011). "The influence of plant root systems on subsurface flow: implications for slope stability". In: *BioScience* 61.11, pp. 869–879. DOI: 10.1525/bio.2011.61.11.6. URL: http://bioscience.oxfordjournals.org/content/61/11/869.abstract.

Gilfedder, M., D. W. Rassam, M. P. Stenson, I. D. Jolly, G. R. Walker, and M. Littleboy (2012). "Incorporating land-use changes and surface–groundwater interactions in a simple catchment water yield model". In: *Environmental Modelling and Software* 38, pp. 62–73. DOI: http://dx.doi.org/10.1016/j.envsoft.2012.05.005. URL: http://www.sciencedirect.com/science/article/pii/S1364815212001600.

Gioli, B., F. Miglietta, B. De Martino, R. W. A. Hutjes, H. A. J. Dolman, A. Lindroth, M. Schumacher, M. J. Sanz, G. Manca, A. Peressotti, and E. J. Dumas (2004). "Comparison between tower and aircraft-based eddy covariance fluxes in five European regions". In: *Agricultural and Forest Meteorology* 127.1, pp. 1–16. DOI: https://doi.org/10.1016/j.agrformet.2004.08.004. URL: http://www.sciencedirect.com/science/article/pii/S0168192304001911.

Glaser, B., C. Jackisch, L. Hopp, and J. Klaus (2019). "How meaningful are plot-scale observations and simulations of preferential flow for catchment models?" In: *Vadose Zone Journal* 18:180146. DOI: 10.2136/vzj2018.08.0146.

Goovaerts, P. (1998). "Geostatistical tools for characterizing the spatial variability of microbiological and physico-chemical soil properties". In: *Biology and Fertility of Soils* 27.4, pp. 315–334. DOI: 10.1007/s003740050439. URL: http://dx.doi.org/10.1007/s003740050439.

Gottselig, N., R. Bol, V. Nischwitz, H. Vereecken, W. Amelung, and E. Klumpp (2014). "Distribution of Phosphorus-containing fine colloids and nanoparticles in stream water of a forest catchment". In: *Vadose Zone Journal* 13.7. DOI: 10.2136/vzj2014.01.0005. URL: http://dx.doi.org/10.2136/vzj2014.01.0005.

Gottselig, N., I. Wiekenkamp, L. Weihermüller, N. Brüggemann, A. E. Berns, H. R. Bogena, N. Borchard, E. Klumpp, A. Lücke, A. Missong, T. Pütz, H. Vereecken, J. A. Huisman, and R. Bol (2017). "A three-dimensional view on soil biogeochemistry: a dataset for a forested headwater catchment". In: *Journal of Environmental Quality*. Journal of Environmental Quality 46.1, pp. 210–218. DOI: 10.2134/jeq2016.07.0276. URL: http://www.cifor.org/nc/online-library/browse/view-publication/publication/6371.html.

Graf, A., J. Werner, M. Langensiepen, A. van de Boer, M. Schmidt, M. Kupisch, and H. Vereecken (2013). "Validation of a minimum microclimate disturbance chamber for net ecosystem flux measurements". In: *Agricultural and Forest Meteorology* 174-175, pp. 1–14. DOI: https://doi.org/10.1016/j.agrformet.2013.02.001. URL: http://www.sciencedirect.com/science/article/pii/S0168192313000269.

Graf, A., A. van de Boer, A. Moene, and H. Vereecken (2014a). "Intercomparison of methods for the simultaneous estimation of zero-pane displacement and aerodynamic roughness length from single-level eddy-covariance data". In: *Boundary-Layer Meteorology* 151.2, pp. 373–387. DOI: 10.1007/s10546-013-9905-z. URL: http://dx.doi.org/10.1007/s10546-013-9905-z.

Graf, A., H. R. Bogena, C. Drüe, H. Hardelauf, T. Pütz, G. Heinemann, and H. Ver-eecken (2014b). "Spatiotemporal relations between water budget components and soil water content in a forested tributary catchment". In: *Water Resources Research* 50.6, pp. 4837–4857. DOI: 10.1002/2013wr014516. URL: http://dx.doi.org/10.1002/2013WR014516.

Graham, C. B. and H. S. Lin (2011). "Controls and frequency of preferential flow occurrence: a 175-event analysis". In: *Vadose Zone Journal* 10.3, pp. 816–831. DOI: 10.2136/vzj2010.0119. URL: https://dl.sciencesocieties.org/publications/vzj/abstracts/10/3/816.

Grant, Kirsten N., Merrin L. Macrae, and Genevieve A. Ali (2019). "Differences in preferential flow with antecedent moisture conditions and soil texture: Implications for subsurface P transport". In: *Hydrological Processes* 33.15, pp. 2068–2079. DOI: 10.1002/hyp.13454. URL: https://onlinelibrary.wiley.com/doi/abs/10.1002/hyp.13454.

Green, K. C. and Y. Alila (2012). "A paradigm shift in understanding and quantifying the effects of forest harvesting on floods in snow environments". In: *Water Resources Research* 48.10. DOI: 10.1029/2012wr012449. URL: http://dx.doi.org/10.1029/2012WR012449.

Greve, A. K., M. S. Andersen, and R. I. Acworth (2012). "Monitoring the transition from preferential to matrix flow in cracking clay soil through changes in electrical anisotropy". In: *Geoderma* 179–180.0, pp. 46–52. DOI: http://dx.doi.org/10.1016/j.geoderma.2012.02.003. URL: http://www.sciencedirect.com/science/article/pii/S0016706112000778.

Greve, P., B. Orlowsky, B. Mueller, J. Sheffield, M. Reichstein, and S. I. Seneviratne (2014). "Global assessment of trends in wetting and drying over land". In: *Nature Geoscience* 7.10, pp. 716–721. DOI: 10.1038/ngeo2247. URL: http://dx.doi.org/10.1038/ngeo2247.

Guo, L. and H. S. Lin (2016). "Critical zone research and observatories: current status and future perspectives". In: *Vadose Zone Journal* 15.9. DOI: doi:10.2136/vzj2016.06.0050. URL: http://dx.doi.org/10.2136/vzj2016.06.0050.

Guo, L., J. Chen, and H. Lin (2014). "Subsurface lateral preferential flow network revealed by time-lapse ground-penetrating radar in a hillslope". In: *Water Resources Research* 50.12, pp. 9127–9147. DOI: 10.1002/2013wr014603. URL: http://dx.doi.org/10.1002/2013WR014603.

Gupta, H. V., H. Kling, K. K. Yilmaz, and G. F. Martinez (2009). "Decomposition of the mean squared error and NSE performance criteria: implications for improving hydrological modelling". In: *Journal of Hydrology* 377.1, pp. 80–91. DOI: https://doi.org/10.1016/j.jhydrol.2009.08.003. URL: http://www.sciencedirect.com/science/article/pii/S0022169409004843.

Guswa, A. J., K. A. Brauman, C. Brown, P. Hamel, B. L. Keeler, and S. S. Stratton Sayre (2014). "Ecosystem services: challenges and opportunities for hydrologic modeling to support decision making". In: *Water Resources Research* 50.5, pp. 4535–4544. DOI: 10.1002/2014wr015497. URL: http://dx.doi.org/10.1002/2014WR015497.

Hardie, M. (2011). "Effect of antecedent soil moisture on infiltration and preferential flow in texture contrast soils". Thesis. the University of Tasmania. URL: https://eprints.utas.edu.au/13007/.

Hardie, M., S. Lisson, R. Doyle, and W. Cotching (2013). "Determining the frequency, depth and velocity of preferential flow by high frequency soil moisture monitoring". In: *Journal of contaminant hydrology* 144.1, pp. 66–77. DOI: 10.1016/j.jconhyd.2012.10.008. URL: https://www.ncbi.nlm.nih.gov/pubmed/23159761.

Harper, W. C. (1969). "Changes in storm hydrographs due to clear-cut logging of coastal watersheds". Masters Thesis. Oregon State University. URL: https://ir.library.oregonstate.edu/downloads/5138jj028.

Hawtree, D., J. P. Nunes, J. J. Keizer, R. Jacinto, J. Santos, M. E. Rial-Rivas, A. K. Boulet, F. Tavares-Wahren, and K. H. Feger (2015). "Time series analysis of the long-term hydrologic impacts of afforestation in the Águeda watershed of north-central Portugal". In: *Hydrology and Earth System Sciences* 19.7, pp. 3033–3045. DOI: 10.5194/hess-19-3033-2015. URL: https://www.hydrol-earth-syst-sci.net/19/3033/2015/.

Hebel, C. von, S. Rudolph, A. Mester, J. A. Huisman, P. Kumbhar, H. Vereecken, and J. van der Kruk (2014). "Three-dimensional imaging of subsurface structural patterns using quantitative large-scale multiconfiguration electromagnetic induction data". In: *Water Resources Research* 50.3, pp. 2732–2748. ISSN: 1944-7973. DOI: 10.1002/2013wr014864. URL: http://dx.doi.org/10.1002/2013WR014864.

Heijmans, M. M. P. D., W. J. Arp, and F. S. Chapin (2004a). "Carbon dioxide and water vapour exchange from understory species in boreal forest". In: *Agricultural and Forest Meteorology* 123.3, pp. 135–147. ISSN: 0168-1923. DOI: https://doi.org/10.1016/j.agrformet.2003.12.006. URL: http://www.sciencedirect.com/science/article/pii/S0168192303002995.

— (2004b). "Controls on moss evaporation in a boreal black spruce forest". In: *Global Biogeochemical Cycles* 18.2. DOI: 10.1029/2003GB002128. URL: https://doi.org/10.1029/2003GB002128.

Hewlett, J. D. and L. Pienaar (1973). "Design and analysis of the catchment experiment". In: *Proceedings a symposium on use of small watersheds in determining effects of forest land use on water quality*. Lexington, KY. URL: http://cwt33.ecology.uga.edu/publications/2164.pdf.

Hewlett, J.D. (1961). *Station Paper No 132: Soil Moisture as a Source of Base Flow from Steep Mountain Watersheds*. Southeastern Forest Experiment Station: U.S. Department of Agriculture. URL: https://books.google.de/books?id=eszmnAAACAAJ.

Hibbert, A. R. (1967). "Forest treatment effects on water yield". In: *International Symposium on Forest Hydrology*. Ed. by W. E. Sopper and H. W. Lull. Pergamon, pp. 527–543.

Hillman, G. R. and J. P. Verschuren (1988). "Simulation of the effects of forest cover, and its removal, on subsurface water". In: *Water Resources Research* 24.2, pp. 305–314. DOI: 10.1029/WR024i002p00305. URL: https://agupubs.onlinelibrary.wiley.com/doi/abs/10.1029/WR024i002p00305.

Hirano, T., K. Suzuki, and R. Hirata (2017). "Energy balance and evapotranspiration changes in a larch forest caused by severe disturbance during an early secondary succession". In: *Agricultural and Forest Meteorology* 232, pp. 457–468. DOI: http://dx.doi.org/10.1016/j.agrformet.2016.10.003. URL: http://www.sciencedirect.com/science/article/pii/S016819231630394X.

Hornbeck, J. W., R. S. Pierce, and C. A. Federer (1970). "Streamflow changes after forest clearing in New England". In: *Water Resources Research* 6.4, pp. 1124–1132. DOI: 10.1029/WR006i004p01124. URL: http://dx.doi.org/10.1029/WR006i004p01124.

Hornbeck, J. W., M. B. Adams, E. S. Corbett, E. S. Verry, and J. A. Lynch (1993). "Long-term impacts of forest treatments on water yield: a summary for northeastern USA". In: *Journal of Hydrology* 150.2–4, pp. 323–344. DOI: http://dx.doi.org/10.1016/0022-1694(93)90115-P. URL: http://www.sciencedirect.com/science/article/pii/002216949390115P.

Hornbeck, J. W., C. W. Martin, and C. Eagar (1997). "Summary of water yield experiments at Hubbard Brook Experimental Forest, New Hampshire". In: *Canadian Journal of Forest Research* 27.12, pp. 2043–2052. DOI: 10.1139/x97-173. URL: https://doi.org/10.1139/x97-173.

Hsu, K.-l., H. V. Gupta, and S. Sorooshian (1995). "Artificial neural network modeling of the rainfall-runoff process". In: *Water Resources Research* 31.10, pp. 2517–2530. DOI: 10.1029/95WR01955. URL: https://agupubs.onlinelibrary.wiley.com/doi/abs/10.1029/95WR01955.

Huisman, J. A., L. Breuer, and H. G. Frede (2004). "Sensitivity of simulated hydrological fluxes towards changes in soil properties in response to land use change". In: *Physics and Chemistry of the Earth, Parts A/B/C* 29.11–12, pp. 749–758. DOI: http://dx.doi.org/10.1016/j.pce.2004.05.012. URL: http://www.sciencedirect.com/science/article/pii/S147470650400107X.

Huisman, J. A., L. Breuer, H. Bormann, A. Bronstert, B. F. W. Croke, H. G. Frede, T. Gräff, L. Hubrechts, A. J. Jakeman, G. Kite, J. Lanini, G. Leavesley, D. P. Lettenmaier, G. Lindström, J. Seibert, M. Sivapalan, N. R. Viney, and P. Willems (2009). "Assessing the impact of land use change on hydrology by ensemble modeling (LUCHEM) III: Scenario analysis". In: *Advances in Water Resources* 32.2, pp. 159–170. DOI: http://dx.doi.org/10.1016/j.advwatres.2008.06.009. URL: http://www.sciencedirect.com/science/article/pii/S0309170808001085.

Hundecha, Y. and A. Bárdossy (2004). "Modeling of the effect of land use changes on the runoff generation of a river basin through parameter regionalization of a watershed model". In: *Journal of Hydrology* 292.1–4 , pp. 281–295. DOI: http://dx.doi.org/10.1016/j.jhydrol.2004.01.002. URL: http://www.sciencedirect.com/science/article/pii/\linebeakS0022169404000125.

Hunter, H. and R. S. Walton (2008). "Land-use effects on fluxes of suspended sediment, nitrogen and phosphorus from a river catchment of the Great Barrier Reef, Australia". In: *Journal of Hydrology* 356, pp. 131–146. DOI: 10.1016/j.jhydrol.2008.04.003. URL: https://www.sciencedirect.com/science/article/pii/S0022169408001765.

Hurkmans, R. T. W. L., W. Terink, R. Uijlenhoet, E. J. Moors, P. A. Troch, and P. H. Verburg (2009). "Effects of land use changes on streamflow generation in the Rhine basin". In: *Water Resources Research* 45.6. DOI: 10.1029/2008WR007574. URL: https://doi.org/10.1029/2008WR007574.

Hutton, C., T. Wagener, J. Freer, D. Han, C. Duffy, and B. Arheimer (2016). "Most computational hydrology is not reproducible, so is it really science?" In: *Water Resources Research* 52.10, pp. 7548–7555. DOI: 10.1002/2016wr019285. URL: http://dx.doi.org/10.1002/2016WR019285.

Ingwersen, J., K. Steffens, P. Högy, K. Warrach-Sagi, D. Zhunusbayeva, M. Poltoradnev, R. Gäbler, H. D. Wizemann, A. Fangmeier, V. Wulfmeyer, and T. Streck (2011). "Comparison of Noah simulations with eddy covariance and soil water measurements at a winter wheat stand". In: *Agricultural and Forest Meteorology* 151.3, pp. 345–355. ISSN: 0168-1923. DOI: http://dx.doi.org/10.1016/j.agrformet.2010.11.010. URL: http://www.sciencedirect.com/science/article/pii/S0168192310003114.

Isaak, D., E. Peterson, J. Ver Hoef, S. Wenger, J. Falke, C. E. Torgersen, C. Sowder, E. Steel, M.-J. Fortin, C. Jordan, A. Ruesch, N. Som, and P. Monestiez (2014). "Applications of spatial statistical network models to stream data". In: *Wiley Interdisciplinary Reviews - Water* 1. DOI: 10.1002/wat2.1023. URL: https://onlinelibrary.wiley.com/doi/abs/10.1002/wat2.1023.

Isik, S., L. Kalin, J. E. Schoonover, P. Srivastava, and G. B. Lockaby (2013). "Modeling effects of changing land use/cover on daily streamflow: an artificial neural network and curve number based hybrid approach". In: *Journal of Hydrology* 485, pp. 103–112. DOI: https://doi.org/10.1016/j.jhydrol.2012.08.032. URL: http://www.sciencedirect.com/science/article/pii/S0022169412007111.

ISO 10694 (1995). *Soil Quality – Determination of Organic and Total Carbon after Dry Combustion (Elementary Analysis)*.

Ivanov, V. Y., S. Fatichi, G. D. Jenerette, J. F. Espeleta, P. A. Troch, and T. E. Huxman (2010). "Hysteresis of soil moisture spatial heterogeneity and the "homogenizing" effect of vegetation". In: *Water Resources Research* 46.9, W09521. DOI: 10.1029/2009wr008611. URL: http://dx.doi.org/10.1029/2009WR008611.

Iwema, J., R. Rosolem, R. Baatz, T. Wagener, and H. R. Bogena (2015). "Investigating temporal field sampling strategies for site-specific calibration of three soil moisture–neutron intensity parameterisation methods". In: *Hydrology and Earth System Sciences* 19.7, pp. 3203–3216. DOI: 10.5194/hess-19-3203-2015. URL: https://www.hydrol-earth-syst-sci.net/19/3203/2015/.

Jackson, B. M., H. S. Wheater, N. R. McIntyre, J. Chell, O. J. Francis, Z. Frogbrook, M. Marshall, B. Reynolds, and I. Solloway (2008). "The impact of upland land management on flooding: insights from a multiscale experimental and modelling programme". In: *Journal of Flood Risk Management* 1.2, pp. 71–80. DOI: 10.1111/j.1753-318X.2008.00009.x. URL: http://dx.doi.org/10.1111/j.1753-318X.2008.00009.x.

Jacobs, S. R. (2018). "Assessing the impact of land use on water and nutrient fluxes in the South-West Mau, Kenya". eng. PhD thesis. Gießen: Justus-Liebig-Universität. URL: http://geb.uni-giessen.de/geb/volltexte/2018/13606.

James, S. E., M. Pärtel, S. D. Wilson, and D. A. Peltzer (2003). "Temporal heterogeneity of soil moisture in grassland and forest". In: *Journal of Ecology* 91.2, pp. 234–239. DOI: 10.1046/j.1365-2745.2003.00758.x. URL: http://dx.doi.org/10.1046/j.1365-2745.2003.00758.x.

Jarvis, N., J. Koestel, and M. Larsbo (2016). "Understanding preferential flow in the vadose zone: recent advances and future prospects". In: *Vadose Zone Journal* 15.12. DOI: 10.2136/vzj2016.09.0075. URL: http://dx.doi.org/10.2136/vzj2016.09.0075.

Jarvis, N. J. (2007). "A review of non-equilibrium water flow and solute transport in soil macropores: principles, controlling factors and consequences for water quality". In: *European Journal of Soil Science* 58.3, pp. 523–546. DOI: 10.1111/j.1365-2389.2007.00915.x. URL: http://dx.doi.org/10.1111/j.1365-2389.2007.00915.x.

Jarvis, P. G. and J. B. Stewart (1979). "The ecology of even-aged forest plantations". In: *Evaporation of water from plantation forest*. Ed. by E. D. Ford, D.

C. Malcolm, and J. Atterson. Cambridge, Institute of Terrestrial Ecology, pp. 327–350.

Jasechko, S., Z. D. Sharp, J. J. Gibson, S. J. Birks, Y. Yi, and P. J. Fawcett (2013). "Terrestrial water fluxes dominated by transpiration". In: *Nature* 496.7445, pp. 347–350. DOI: https://doi.org/10.1038/nature11983. URL: http://europepmc.org/abstract/MED/23552893.

Jayawickreme, D. H., R. L. Van Dam, and D. W. Hyndman (2008). "Subsurface imaging of vegetation, climate, and root-zone moisture interactions". In: *Geophysical Research Letters* 35.18, p. L18404. DOI: 10.1029/2008gl034690. URL: http://dx.doi.org/10.1029/2008GL034690.

— (2010). "Hydrological consequences of land-cover change: quantifying the influence of plants on soil moisture with time-lapse electrical resistivity". In: *Geophysics* 75.4, WA43–WA50. DOI: 10.1190/1.3464760. URL: http://library.seg.org/doi/abs/10.1190/1.3464760.

Jefferson, J. L. (2016). "Exploring sensitivities of latent heat parameterizations using a coupled, integrated hydrologic model". Thesis. Golden, Colorado: Colorado School of Mines.

Jefferson, J. L. and R. M. Maxwell (2015). "Evaluation of simple to complex parameterizations of bare ground evaporation". In: *Journal of Advances in Modeling Earth Systems* 7.3, pp. 1075–1092. DOI: 10.1002/2014ms000398. URL: http://dx.doi.org/10.1002/2014MS000398.

Jefferson, Jennifer L., Reed M. Maxwell, and Paul G. Constantine (2017). "Exploring the sensitivity of photosynthesis and stomatal resistance parameters in a land surface model". In: *Journal of Hydrometeorology* 18.3, pp. 897–915. DOI: 10.1175/jhm-d-16-0053.1. URL: http://journals.ametsoc.org/doi/abs/10.1175/JHM-D-16-0053.1.

Jin, Z., L. Guo, H. Lin, Y. Wang, Y. Yu, G. Chu, and J. Zhang (2018). "Soil moisture response to rainfall on the Chinese Loess Plateau after a long-term vegetation rehabilitation". In: *Hydrological Processes* 32, pp. 1738–1754. DOI: https://doi.org/10.1002/hyp.13143. URL: https://onlinelibrary.wiley.com/doi/abs/10.1002/hyp.13143.

Johnson, M. S. and J. Lehmann (2006). "Double-funneling of trees: stemflow and root-induced preferential flow". In: *Écoscience* 13.3, pp. 324–333. DOI: 10.2980/i1195-6860-13-3-324.1. URL: https://doi.org/10.2980/i1195-6860-13-3-324.1.

Johnson, R. (1998). "The forest cycle and low river flows: a review of UK and international studies". In: *Forest Ecology and Management* 109.1–3, pp. 1–7.

DOI: http://dx.doi.org/10.1016/S0378-1127(98)00231-X. URL: http://www.sciencedirect.com/science/article/pii/S037811279800231X.

Jones, J. A. and G. E. Grant (1996). "Peak flow responses to clear-cutting and roads in small and large basins, Western Cascades, Oregon". In: *Water Resources Research* 32.4, pp. 959–974. DOI: 10.1029/95WR03493. URL: http://dx.doi.org/10.1029/95WR03493.

— (2001). "Comment on "Peak flow responses to clear-cutting and roads in small and large basins, Western Cascades, Oregon: a second opinion" by R. B. Thomas and W. F. Megahan". In: *Water Resources Research* 37.1, pp. 175–178. DOI: 10.1029/2000WR900276. URL: http://dx.doi.org/10.1029/2000WR900276.

Jones, J. A. and D. A. Post (2004). "Seasonal and successional streamflow response to forest cutting and regrowth in the northwest and eastern United States". In: *Water Resources Research* 40.5. DOI: 10.1029/2003wr002952. URL: http://dx.doi.org/10.1029/2003WR002952.

Jost, G., H. Schume, and H. Hager (2004). "Factors controlling soil water-recharge in a mixed European beech(Fagus sylvatica L.)–Norway spruce [Picea abies (L.) Karst.] stand". In: *European Journal of Forest Research* 123.2, pp. 93–104. DOI: 10.1007/s10342-004-0033-7. URL: http://dx.doi.org/10.1007/s10342-004-0033-7.

Julich, Stefan, Raphael Benning, Dorit Julich, and Karl-Heinz Feger (2017). "Quantification of Phosphorus Exports from a Small Forested Headwater-Catchment in the Eastern Ore Mountains, Germany". In: *Forests* 8.6. ISSN: 1999-4907. DOI: 10.3390/f8060206. URL: https://www.mdpi.com/1999-4907/8/6/206.

Jung, I. W., H. Chang, and H. Moradkhani (2011). "Quantifying uncertainty in urban flooding analysis considering hydro-climatic projection and urban development effects". In: *Hydrology and Earth System Sciences* 15.2, pp. 617–633. DOI: 10.5194/hess-15-617-2011. URL: http://www.hydrol-earth-syst-sci.net/15/617/2011/.

Jung, M., M. Reichstein, P. Ciais, S. I. Seneviratne, J. Sheffield, M. L. Goulden, G. Bonan, A. Cescatti, J. Chen, R. de Jeu, A. J. Dolman, W. Eugster, D. Gerten, D. Gianelle, N. Gobron, J. Heinke, J. Kimball, B. E. Law, L. Montagnani, Q. Mu, B. Mueller, K. Oleson, D. Papale, A. D. Richardson, O. Roupsard, S. Running, E. Tomelleri, N. Viovy, U. Weber, C. Williams, E. Wood, S. Zaehle, and K. Zhang (2010). "Recent decline in the global

land evapotranspiration trend due to limited moisture supply". In: *Nature* 467.7318, pp. 951–954. DOI: 10.1038/nature09396. URL: http://dx.doi.org/10.1038/nature09396.

Keune, J., F. Gasper, K. Goergen, A. Hense, P. Shrestha, M. Sulis, and S. Kollet (2016). "Studying the influence of groundwater representations on land surface - atmosphere feedbacks during the European heat wave in 2003". In: *Journal of Geophysical Research: Atmospheres* 121.22, pp. 13,301–13,325. DOI: 10.1002/2016JD025426. URL: https://doi.org/10.1002/2016JD025426.

Keune, J., M. Sulis, S. Kollet, S. Siebert, and Y. Wada (2018). "Human water use impacts on the strength of the continental sink for atmospheric water". In: *Geophysical Research Letters* 45.9, pp. 4068–4076. DOI: 10.1029/2018gl077621. URL: https://agupubs.onlinelibrary.wiley.com/doi/abs/10.1029/2018GL077621.

Kim, J. G., S.-G. Park, M.-J. Yi, and J.-H. Kim (2010). "Tracing solute infiltration using a combined method of dye tracer test and electrical resistivity tomography in an undisturbed forest soil profile". In: *Hydrological Processes* 24.21, pp. 2977–2982. DOI: 10.1002/hyp.7711. URL: http://dx.doi.org/10.1002/hyp.7711.

Kirchner, J. W. (2006). "Getting the right answers for the right reasons: Linking measurements, analyses, and models to advance the science of hydrology". In: *Water Resources Research* 42.3. DOI: 10.1029/2005WR004362. URL: https://agupubs.onlinelibrary.wiley.com/doi/abs/10.1029/2005WR004362.

Koch, J., T. Cornelissen, Z. Fang, H. R. Bogena, B. Diekkrüger, S. Kollet, and S. Stisen (2016). "Inter-comparison of three distributed hydrological models with respect to seasonal variability of soil moisture patterns at a small forested catchment". In: *Journal of Hydrology* 533, pp. 234–249. DOI: https://doi.org/10.1016/j.jhydrol.2015.12.002. URL: http://www.sciencedirect.com/science/article/pii/S0022169415009415.

Koestel, J. and H. Jorda (2014). "What determines the strength of preferential transport in undisturbed soil under steady-state flow?" In: *Geoderma* 217–218.0, pp. 144–160. DOI: http://dx.doi.org/10.1016/j.geoderma.2013.11.009. URL: http://www.sciencedirect.com/science/article/pii/S0016706113004242.

Kokkonen, T. S. and A. J. Jakeman (2002). "Chapter 14: Structural effects of landscape and land use on streamflow response". In: *Developments in Environmental Modelling*. Ed. by M. B. Beck. Vol. 22. Elsevier, pp. 303–321.

DOI: https://doi.org/10.1016/S0167-8892(02)80015-X. URL: http://www.sciencedirect.com/science/article/pii/S016788920280015X.

Kollet, S., M. Sulis, R. M. Maxwell, C. Paniconi, M. Putti, G. Bertoldi, E. T Coon, E. Cordano, S. Endrizzi, and E. Kikinzon (2017). "The integrated hydrologic model intercomparison project, IH-MIP2: A second set of benchmark results to diagnose integrated hydrology and feedbacks". In: *Water Resources Research* 53.1, pp. 867–890. ISSN: 1944-7973.

Kollet, S. J. and R. M. Maxwell (2006). "Integrated surface–groundwater flow modeling: a free-surface overland flow boundary condition in a parallel groundwater flow model". In: *Advances in Water Resources* 29.7, pp. 945–958. DOI: http://dx.doi.org/10.1016/j.advwatres.2005.08.006. URL: http://www.sciencedirect.com/science/article/pii/S0309170805002101.

Kollet, Stefan J. and Reed M. Maxwell (2008). "Capturing the influence of groundwater dynamics on land surface processes using an integrated, distributed watershed model". In: *Water Resources Research* 44.2, W02402. ISSN: 1944-7973. DOI: 10.1029/2007wr006004. URL: http://dx.doi.org/10.1029/2007WR006004.

Korres, W., T. G. Reichenau, P. Fiener, C. N. Koyama, H. R. Bogena, T. Cornelissen, R. Baatz, M. Herbst, B. Diekkrüger, H. Vereecken, and K. Schneider (2015). "Spatio-temporal soil moisture patterns – a meta-analysis using plot to catchment scale data". In: *Journal of Hydrology* 520, pp. 326–341. DOI: http://dx.doi.org/10.1016/j.jhydrol.2014.11.042. URL: http://www.sciencedirect.com/science/article/pii/S0022169414009627.

Köppen, W. P. (1884). "Die Wärmezonen der Erde, nach der Dauer der heissen, gemässigten und kalten Zeit und nach der Wirkung der Wärme auf die organische Welt betrachtet". In: *Meteorologische Zeitschrif* 1, pp. 215–226.

Krause, S., J. Jacobs, and A. Bronstert (2007). "Modelling the impacts of land-use and drainage density on the water balance of a lowland–floodplain landscape in northeast Germany". In: *Ecological Modelling* 200.3, pp. 475–492. DOI: https://doi.org/10.1016/j.ecolmodel.2006.08.015.

Krysanova, V. and J. G. Arnold (2008). "Advances in ecohydrological modelling with SWAT - a review". In: *Hydrological Sciences Journal* 53.5, pp. 939–947. DOI: 10.1623/hysj.53.5.939. URL: https://doi.org/10.1623/hysj.53.5.939.

Kurtz, W., G. He, S. J. Kollet, R. M. Maxwell, H. Vereecken, and H. J. Hendricks Franssen (2016). "TerrSysMP–PDAF (version 1.0): a modular high-performance data assimilation framework for an integrated land surface–subsurface model". In: *Geoscientific Model Development* 9.4, pp. 1341–1360. DOI: 10.5194/gmd-9-1341-2016. URL: https://www.geosci-model-dev.net/9/1341/2016/.

Lahmer, W., B. Pfützner, and A. Becker (2001). "Assessment of land use and climate change impacts on the mesoscale". In: *Physics and Chemistry of the Earth, Part B: Hydrology, Oceans and Atmosphere* 26.7, pp. 565–575. DOI: http://dx.doi.org/10.1016/S1464-1909(01)00051-X. URL: http://www.sciencedirect.com/science/article/pii/S146419090100051X.

Lal, Rattan (2008). "Carbon sequestration". In: *Philosophical Transactions of the Royal Society B: Biological Sciences* 363.1492, pp. 815–830. DOI: 10.1098/rstb.2007.2185. eprint: https://royalsocietypublishing.org/doi/pdf/10.1098/rstb.2007.2185. URL: https://royalsocietypublishing.org/doi/abs/10.1098/rstb.2007.2185.

Lane, P. N. J., A. E. Best, K. Hickel, and L. Zhang (2005). "The response of flow duration curves to afforestation". In: *Journal of Hydrology* 310.1, pp. 253–265. DOI: https://doi.org/10.1016/j.jhydrol.2005.01.006. URL: http://www.sciencedirect.com/science/article/pii/S0022169405000077.

Lavigne, M.-P., A. N. Rousseau, R. Turcotte, A.-M. Laroche, J.-P. Fortin, and J.-P. Villeneuve (2004). "Validation and use of a semidistributed hydrological modeling system to predict short-term effects of clear-cutting on a watershed hydrological regime". In: *Earth Interactions* 8.3, pp. 1–19. DOI: 10.1175/1087-3562(2004)008<0001:VAUOAS>2.0.CO;2. URL: https://doi.org/10.1175/1087-3562(2004)008<0001:VAUOAS>2.0.CO.

Lawrence, D. M., P. E. Thornton, K. W. Oleson, and G. B. Bonan (2007). "The partitioning of evapotranspiration into transpiration, soil evaporation, and canopy evaporation in a GCM: impacts on land–atmosphere interaction". In: *Journal of Hydrometeorology* 8.4, pp. 862–880. DOI: 10.1175/jhm596.1. URL: https://doi.org/10.1175/JHM596.1.

Legates, D. R. and G. J. McCabe Jr. (1999). "Evaluating the use of "goodness-of-fit" measures in hydrologic and hydroclimatic model validation". In: *Water Resources Research* 35.1, pp. 233–241. DOI: 10.1029/1998WR900018. URL: https://agupubs.onlinelibrary.wiley.com/doi/abs/10.1029/1998WR900018.

Lehmkuhl, F., D. Loibl, and H. Borchardt (2010). "Geomorphological map of the Wüstebach (Nationalpark Eifel, Germany)—an example of human impact on mid-European mountain areas". In: *Journal of Maps* 6.1, pp. 520–530. DOI: 10.4113/jom.2010.1118. URL: http://dx.doi.org/10.4113/jom.2010.1118.

LeMone, M. A., F. Chen, J. G. Alfieri, M. Tewari, B. Geerts, Q. Miao, R. L. Grossman, and R. L. Coulter (2007). "Influence of land cover and soil moisture on the horizontal distribution of sensible and latent heat fluxes in Southeast Kansas during IHOP 2002 and CASES 97". In: *Journal of Hydrometeorology* 8.1, pp. 68–87. DOI: 10.1175/jhm554.1. URL: http://dx.doi.org/10.1175/JHM554.1.

Li, H., Y. Zhang, J. Vaze, and B. Wang (2012). "Separating effects of vegetation change and climate variability using hydrological modelling and sensitivity-based approaches". In: *Journal of Hydrology* 420–421.0, pp. 403–418. DOI: http://dx.doi.org/10.1016/j.jhydrol.2011.12.033.

Lin, H. (2006). "Temporal stability of soil moisture spatial pattern and subsurface preferential flow pathways in the Shale Hills Catchment". In: *Vadose Zone Journal* 5.1, pp. 317–340. DOI: 10.2136/vzj2005.0058. URL: http://dx.doi.org/10.2136/vzj2005.0058.

— (2010). "Linking principles of soil formation and flow regimes". In: *Journal of Hydrology* 393.1–2, pp. 3–19. ISSN: 0022-1694. DOI: http://dx.doi.org/10.1016/j.jhydrol.2010.02.013. URL: http://www.sciencedirect.com/science/article/pii/S0022169410000831.

Lin, H. and X. Zhou (2008). "Evidence of subsurface preferential flow using soil hydrologic monitoring in the Shale Hills catchment". In: *European Journal of Soil Science* 59.1, pp. 34–49. DOI: 10.1111/j.1365-2389.2007.00988.x. URL: http://dx.doi.org/10.1111/j.1365-2389.2007.00988.x.

Liu, H., J. T. Randerson, J. Lindfors, and F. S. Chapin (2005). "Changes in the surface energy budget after fire in boreal ecosystems of interior Alaska: an annual perspective". In: *Journal of Geophysical Research: Atmospheres* 110.D13. DOI: 10.1029/2004JD005158. URL: https://doi.org/10.1029/2004JD005158.

Liu, H. P. and H. Lin (2015). "Frequency and control of subsurface preferential flow occurrence in the Shale Hills catchment: from pedon to catchment scales". In: *Soil Science Society of America Journal* 79.2, pp. 362–377. DOI: 10.2136/sssaj2014.08.0330. URL: https://dl.sciencesocieties.org/publications/sssaj/abstracts/79/2/362.

Liu, Q., T. R. McVicar, Z. Yang, R. J. Donohue, L. Liang, and Y. Yang (2016). "The hydrological effects of varying vegetation characteristics in a temperate water-limited basin: Development of the dynamic Budyko- Choudhury- Porporato (dBCP) model". In: *Journal of Hydrology* 543, Part B, pp. 595–611. DOI: https://doi.org/10.1016/j.jhydrol.2016.10.035.

Long, D., L. Longuevergne, and B. R. Scanlon (2014). "Uncertainty in evapotranspiration from land surface modeling, remote sensing, and GRACE satellites". In: *Water Resources Research* 50.2, pp. 1131–1151. DOI: 10.1002/2013WR014581. URL: https://doi.org/10.1002/2013WR014581.

Ma, L., C. He, H. Bian, and L. Sheng (2016). "MIKE SHE modeling of ecohydrological processes: merits, applications, and challenges". In: *Ecological Engineering* 96, pp. 137–149. DOI: https://doi.org/10.1016/j.ecoleng.2016.01.008. URL: http://www.sciencedirect.com/science/article/pii/S0925857416300088.

Manzoni, Stefano, Gabriel Katul, and Amilcare Porporato (Dec. 2009). "Analysis of soil carbon transit times and age distributions using network theories". In: *J. Geophys. Res* 114. DOI: 10.1029/2009JG001070.

Martini, E., U. Werban, S. Zacharias, M. Pohle, P. Dietrich, and U. Wollschläger (2017). "Repeated electromagnetic induction measurements for mapping soil moisture at the field scale: validation with data from a wireless soil moisture monitoring network". In: *Hydrology and Earth System Sciences* 21.1, pp. 495–513. DOI: 10.5194/hess-21-495-2017. URL: https://www.hydrol-earth-syst-sci.net/21/495/2017/.

Matalas, N. C. (1998). "Note on the assumption of hydrologic stationarity". In: *Global Change and Water Resources Management* Water Resources Update No 112. edited by K. Schilling and E. Stakhiv, Univ. Counc. on Water Resour., Carbondale, Ill., pp. 64–72.

Mauder, M. and T. Foken (2011). *Documentation and instruction manual of the eddy-covariance software package TK3*. Vol. 46. Bayreuth: Univ., Abt. Mikrometeorologie. URL: https://epub.uni-bayreuth.de/342/.

Mauder, M., M. Cuntz, C. Drüe, A. Graf, C. Rebmann, H. P. Schmid, M. Schmidt, and R. Steinbrecher (2013). "A strategy for quality and uncertainty assessment of long-term eddy-covariance measurements". In: *Agricultural and Forest Meteorology* 169, pp. 122–135. DOI: http://dx.doi.org/10.1016/j.agrformet.2012.09.006. URL: http://www.sciencedirect.com/science/article/pii/S0168192312002808.

Maxwell, R. M. (2013). "A terrain-following grid transform and preconditioner for parallel, large-scale, integrated hydrologic modeling". In: *Advances in Water Resources* 53, pp. 109–117. DOI: 10.1016/j.advwatres.2012.10.001. URL: www.sciencedirect.com/science/article/pii/S0309170812002564.

Maxwell, R. M. and L. E. Condon (2016). "Connections between groundwater flow and transpiration partitioning". In: *Science* 353.6297, p. 377. DOI: 10.1126/science.aaf7891. URL: http://science.sciencemag.org/content/353/6297/377.abstract.

Maxwell, R. M., M. Putti, S. Meyerhoff, J.-O. Delfs, I. M. Ferguson, V. Ivanov, J. Kim, O. Kolditz, S. J. Kollet, and M. Kumar (2014). "Surface-subsurface model intercomparison: a first set of benchmark results to diagnose integrated hydrology and feedbacks". In: *Water Resources Research* 50.2, pp. 1531–1549. DOI: https://doi.org/10.1002/2013WR01372. URL: https://agupubs.onlinelibrary.wiley.com/doi/full/10.1002/2013WR013725.

Maxwell, R. M., L. E. Condon, and S. J. Kollet (2015). "A high-resolution simulation of groundwater and surface water over most of the continental US with the integrated hydrologic model ParFlow v3". In: *Geoscientific Model Development* 8.3, pp. 923–937. DOI: https://doi.org/10.5194/gmd-8-923-2015. URL: https://www.geosci-model-dev.net/8/923/2015/.

McCulloch, J. S. G. (2007). "All our yesterdays: a hydrological retrospective". In: *Hydrology and Earth System Sciences* 11.1, pp. 3–11. DOI: 10.5194/hess-11-3-2007. URL: http://www.hydrol-earth-syst-sci.net/11/3/2007/.

McDonnell, J. J. and K. Beven (2014). "Debates—The future of hydrological sciences: a (common) path forward? A call to action aimed at understanding velocities, celerities and residence time distributions of the headwater hydrograph". In: *Water Resources Research* 50.6, pp. 5342–5350. DOI: 10.1002/2013WR015141. URL: https://agupubs.onlinelibrary.wiley.com/doi/abs/10.1002/2013WR015141.

McGrath, G. S., C. Hinz, M. Sivapalan, J. Dressel, T. Pütz, and H. Vereecken (2010). "Identifying a rainfall event threshold triggering herbicide leaching by preferential flow". In: *Water Resources Research* 46.2, W02513. DOI: 10.1029/2008wr007506. URL: http://dx.doi.org/10.1029/2008WR007506.

McGuinness, J. L. and L. L. Harrold (1971). "Reforestation influences on small watershed streamflow". In: *Water Resources Research* 7.4, pp. 845–852. DOI: 10.1029/WR007i004p00845.

McMinn, J. W. and J. D. Hewlett (1975). "First-year yield increase after forest cutting: an alternative model". In: *Journal of Forestry*. URL: http://cwt33.ecology.uga.edu/publications/684.pdf.

Milly, P. C. D., J. Betancourt, M. Falkenmark, R. M. Hirsch, Z. W. Kundzewicz, D. P. Lettenmaier, and R. J. Stouffer (2008). "Stationarity is dead: whither water management?" In: *Science* 319.5863, pp. 573–574. DOI: 10.1126/science.1151915. URL: https://science.sciencemag.org/content/319/5863/573.

Milly, P. C. D., J. Betancourt, M. Falkenmark, R. M. Hirsch, Z. W. Kundzewicz, D. P. Lettenmaier, R. J. Stouffer, M. D. Dettinger, and V. Krysanova (2015). "On critiques of "stationarity is dead: whither water management?"" In: *Water Resources Research* 51.9, pp. 7785–7789. DOI: 10.1002/2015wr017408. URL: https://agupubs.onlinelibrary.wiley.com/doi/full/10.1002/2015WR017408.

Missong, A., R. Bol, S. Willbold, J. Siemens, and E. Klumpp (2016). "Phosphorus forms in forest soil colloids as revealed by liquid-state 31P-NMR". In: *Journal of Plant Nutrition and Soil Science* 179.2, pp. 159–167. DOI: doi:10.1002/jpln.201500119. URL: https://onlinelibrary.wiley.com/doi/abs/10.1002/jpln.201500119.

Montes-Helu, M. C., T. Kolb, S. Dore, B. Sullivan, S. C. Hart, G. Koch, and B. A. Hungate (2009). "Persistent effects of fire-induced vegetation change on energy partitioning and evapotranspiration in ponderosa pine forests". In: *Agricultural and Forest Meteorology* 149.3, pp. 491–500. DOI: https://doi.org/10.1016/j.agrformet.2008.09.011. URL: http://www.sciencedirect.com/science/article/pii/S016819230800258X.

Moore, C. J. (1986). "Frequency response corrections for eddy correlation systems". In: *Boundary-Layer Meteorology* 37.1, pp. 17–35. DOI: 10.1007/bf00122754. URL: http://dx.doi.org/10.1007/BF00122754.

Moore, G. W., J. A. Jones, and B. J. Bond (2011). "How soil moisture mediates the influence of transpiration on streamflow at hourly to interannual scales in a forested catchment". In: *Hydrological Processes* 25.24, pp. 3701–3710. DOI: 10.1002/hyp.8095. URL: http://dx.doi.org/10.1002/hyp.8095.

Moriasi, D., J. Arnold, M. Van Liew, R. Bingner, R. D. Harmel, and T. Veith (2007). "Model evaluation guidelines for systematic quantification of accuracy in watershed simulations". In: *Transactions of the ASABE* 50.3, pp. 885–900. DOI: 10.13031/2013.23153. URL: http://citeseerx.ist.psu.edu/viewdoc/download?doi=10.1.1.532.2506&rep=rep1&type=pdf.

Moriasi, Daniel, Margaret Gitau, Naresh Pai, and Prasad Daggupati (Dec. 2015). "Hydrologic and Water Quality Models: Performance Measures and Evaluation Criteria". In: *Transactions of the ASABE (American Society of Agricultural and Biological Engineers)* 58, pp. 1763–1785. DOI: 10.13031/trans.58.10715.

Morán-Tejeda, E., J. Zabalza, K. Rahman, A. Gago-Silva, J. I. López-Moreno, S. Vicente-Serrano, A. Lehmann, C. L. Tague, and M. Beniston (2015). "Hydrological impacts of climate and land-use changes in a mountain watershed: uncertainty estimation based on model comparison". In: *Ecohydrology* 8.8, pp. 1396–1416. DOI: 10.1002/eco.1590. URL: http://dx.doi.org/10.1002/eco.1590.

Moysey, S. M. J. and Z. Liu (2012). "Can the onset of macropore flow be detected using electrical resistivity measurements?" In: *Soil Science Society of America Journal* 76.1, pp. 10–17. DOI: 10.2136/sssaj2010.0413. URL: https://www.soils.org/publications/sssaj/abstracts/76/1/10.

Nandakumar, N. and R. G. Mein (1997). "Uncertainty in rainfall—runoff model simulations and the implications for predicting the hydrologic effects of land-use change". In: *Journal of Hydrology* 192.1, pp. 211–232. DOI: http://dx.doi.org/10.1016/S0022-1694(96)03106-X. URL: http://www.sciencedirect.com/science/article/pii/S002216949603106X.

Nash, J. E. and J. V. Sutcliffe (1970). "River flow forecasting through conceptual models part 1 — a discussion of principles". In: *Journal of Hydrology* 10.3, pp. 282–290. DOI: https://doi.org/10.1016/0022-1694(70)90255-6. URL: http://www.sciencedirect.com/science/article/pii/0022169470902556.

Neal, C., B. Reynolds, P. Rowland, D. Norris, J. W. Kirchner, M. Neal, D. Sleep, A. Lawlor, C. Woods, S. Thacker, H. Guyatt, C. Vincent, K. Hockenhull, H. Wickham, S. Harman, and L. Armstrong (2012). "High-frequency water quality time series in precipitation and streamflow: from fragmentary signals to scientific challenge". In: *Science of The Total Environment* 434, pp. 3–12. DOI: https://doi.org/10.1016/j.scitotenv.2011.10.072. URL: http://www.sciencedirect.com/science/article/pii/S0048969711013751.

Nearing, G. (2019). *Machine learning and information theory for model benchmarking and process diagnostics*. Spring Cyberseminar Series CUASI 2019. URL: https://www.cuahsi.org/uploads/cyberseminars/Grey_Nearing_-_PDF_-_Cyberseminar.pdf.

Nearing, G. S. and H. V. Gupta (2015). "The quantity and quality of information in hydrologic models". In: *Water Resources Research* 51.1, pp. 524–538. DOI: 10.1002/2014WR015895. URL: https://agupubs.onlinelibrary.wiley.com/doi/abs/10.1002/2014WR015895.

Nearing, G. S., B. L. Ruddell, M. P. Clark, B. Nijssen, and C. Peters-Lidard (2018). "Benchmarking and process diagnostics of land models". In: *Journal of Hydrometeorology* 19.11, pp. 1835–1852. DOI: 10.1175/JHM-D-17-0209.1. URL: https://doi.org/10.1175/JHM-D-17-0209.1.

Neumann R., B. and Z. G. Cardon (2012). "The magnitude of hydraulic redistribution by plant roots: a review and synthesis of empirical and modeling studies". In: *New Phytologist* 194.2, pp. 337–352. DOI: 10.1111/j.1469-8137.2012.04088.x. URL: https://doi.org/10.1111/j.1469-8137.2012.04088.x.

Niehoff, D., U. Fritsch, and A. Bronstert (2002). "Land-use impacts on storm-runoff generation: scenarios of land-use change and simulation of hydrological response in a meso-scale catchment in SW-Germany". In: *Journal of Hydrology* 267.1–2, pp. 80–93. DOI: http://dx.doi.org/10.1016/S0022-1694(02)00142-7. URL: http://www.sciencedirect.com/science/article/pii/S0022169402001427.

Nijland, W., M. van der Meijde, E. A. Addink, and S. M. de Jong (2010). "Detection of soil moisture and vegetation water abstraction in a Mediterranean natural area using electrical resistivity tomography". In: *CATENA* 81.3, pp. 209–216. DOI: http://dx.doi.org/10.1016/j.catena.2010.03.005. URL: http://www.sciencedirect.com/science/article/pii/S0341816210000408.

Nijzink, R., C. Hutton, I. Pechlivanidis, R. Capell, B. Arheimer, J. Freer, D. Han, T. Wagener, K. McGuire, H. Savenije, and M. Hrachowitz (2016). "The evolution of root-zone moisture capacities after deforestation: a step towards hydrological predictions under change?" In: *Hydrology and Earth System Sciences* 20.12, pp. 4775–4799. DOI: 10.5194/hess-20-4775-2016. URL: http://www.hydrol-earth-syst-sci.net/20/4775/2016/.

Oberdörster, C., J. Vanderborght, A. Kemna, and H. Vereecken (2010). "Investigating preferential flow processes in a forest soil using time domain reflectometry and electrical resistivity tomography". In: *Vadose Zone Journal* 9.2, pp. 350–361. DOI: 10.2136/vzj2009.0073. URL: https://dl.sciencesocieties.org/publications/vzj/abstracts/9/2/350.

Oki, T. and S. Kanae (2006). "Global hydrological cycles and world water resources". In: *Science* 313.5790, p. 1068. DOI: 10.1126/science.1128845.

URL: http://science.sciencemag.org/content/313/5790/1068.abstract.

Oleson, K. W., G. Y. Niu, Z. L. Yang, D. M. Lawrence, P. E. Thornton, P. J. Lawrence, R. Stöckli, R. E. Dickinson, G. B. Bonan, S. Levis, A. Dai, and T. Qian (2008). "Improvements to the Community Land Model and their impact on the hydrological cycle". In: *Journal of Geophysical Research: Biogeosciences* 113.G1. DOI: 10.1029/2007jg000563. URL: http://dx.doi.org/10.1029/2007JG000563.

Olson, D. M., E. Dinerstein, E. D. Wikramanayake, N. D. Burgess, G. V. N. Powell, E. C. Underwood, J. A. D'Amico, I. Itoua, H. E. Strand, J. C. Morrison, C. J. Loucks, T. F. Allnutt, T. H. Ricketts, Y. Kura, J. F. Lamoreux, W. W. Wettengel, P. Hedao, and K. R. Kassem (2001). "Terrestrial ecoregions of the world: a new map of life on Eath: A new global map of terrestrial ecoregions provides an innovative tool for conserving biodiversity". In: *BioScience* 51.11, pp. 933–938. DOI: 10.1641/0006-3568(2001)051[0933:teotwa]2.0.co;2. URL: http://dx.doi.org/10.1641/0006-3568(2001)051[0933:TEOTWA]2.0.CO.

Ott, B. and S. Uhlenbrook (2004). "Quantifying the impact of land-use changes at the event and seasonal time scale using a process-oriented catchment model". In: *Hydrology and Earth System Sciences* 8.1, pp. 62–78. DOI: 10.5194/hess-8-62-2004. URL: https://www.hydrol-earth-syst-sci.net/8/62/2004/.

Oudin, L., V. Andréassian, J. Lerat, and C. Michel (2008). "Has land cover a significant impact on mean annual streamflow? An international assessment using 1508 catchments". In: *Journal of Hydrology* 357.3–4, pp. 303–316. DOI: http://dx.doi.org/10.1016/j.jhydrol.2008.05.021.

Pan, Y., S. Weill, P. Ackerer, and F. Delay (2015). "A coupled stream flow and depth-integrated subsurface flow model for catchment hydrology". In: *Journal of Hydrology* 530, pp. 66–78. DOI: https://doi.org/10.1016/j.jhydrol.2015.09.044. URL: http://www.sciencedirect.com/science/article/pii/S0022169415007271.

Pathiraja, S., L. Marshall, A. Sharma, and H. Moradkhani (2016). "Detecting non-stationary hydrologic model parameters in a paired catchment system using data assimilation". In: *Advances in Water Resources* 94, pp. 103–119. DOI: https://doi.org/10.1016/j.advwatres.2016.04.021.

Patric, J. H. (1973). *Deforestation effects on soil moisture, streamflow, and water balance in the central Appalachians*. Tech. rep. Res. Pap. NE-259. Upper Darby, PA: U.S. Department of Agriculture, Forest Service, Northeastern Forest

Experiment Station., p. 12. URL: https://www.fs.usda.gov/treesearch/pubs/23635.

Patric, J. H. and K. G. Reinhart (1971). "Hydrologic effects of deforesting two mountain watersheds in West Virginia". In: *Water Resources Research* 7.5, pp. 1182–1188.

Peel, M. C. and G. Blöschl (2011). "Hydrological modelling in a changing world". In: *Progress in Physical Geography* 35.2, pp. 249–261. DOI: 10.1177/0309133311402550. URL: http://journals.sagepub.com/doi/abs/10.1177/0309133311402550.

Pilgrim, D. H., I. Cordery, and B. C. Baron (1982). "Effects of catchment size on runoff relationships". In: *Journal of Hydrology* 58.3, pp. 205–221. DOI: http://dx.doi.org/10.1016/0022-1694(82)90035-X. URL: http://www.sciencedirect.com/science/article/pii/002216948290035X.

Ponton, S., L. B. Flanagan, K. P. Alstad, B. G. Johnson, K. A. I. Morgenstern, N. Kljun, T. A. Black, and A. G. Barr (2006). "Comparison of ecosystem water-use efficiency among Douglas-fir forest, aspen forest and grassland using eddy covariance and carbon isotope techniques". In: *Global Change Biology* 12.2, pp. 294–310. DOI: 10.1111/j.1365-2486.2005.01103.x. URL: https://doi.org/10.1111/j.1365-2486.2005.01103.x.

Pool, S., M. Vis, and J. Seibert (2018). "Evaluating model performance: towards a non-parametric variant of the Kling-Gupta efficiency". In: *Hydrological Sciences Journal* 63. DOI: 10.1080/02626667.2018.1552002. URL: https://www.tandfonline.com/doi/full/10.1080/02626667.2018.1552002.

Price, K., C. R. Jackson, and A. J. Parker (2010). "Variation of surficial soil hydraulic properties across land uses in the southern Blue Ridge Mountains, North Carolina, USA". In: *Journal of Hydrology* 383.3–4, pp. 256–268. DOI: http://dx.doi.org/10.1016/j.jhydrol.2009.12.041. URL: http://www.sciencedirect.com/science/article/pii/S002216940900835X.

Qi, S., G. Sun, Y. Wang, S. G. McNulty, and J. A. Moore Myers (2009). "Streamflow response to climate and landuse changes in a coastal watershed in North Carolina". In: *American Society of Agricultural and Biological Engineers* 52.3, pp. 739–749. URL: https://www.fs.usda.gov/treesearch/pubs/33551.

Qu, W., H. R. Bogena, J. A. Huisman, J. Vanderborght, M. Schuh, E. Priesack, and H. Vereecken (2015). "Predicting subgrid variability of soil water content from basic soil information". In: *Geophysical Research Letters*

42.3, pp. 789–796. DOI: 10.1002/2014gl062496. URL: http://dx.doi.org/10.1002/2014GL062496.

Quilbé, R., A. N. Rousseau, J. S. Moquet, S. Savary, S. Ricard, and M. S. Garbouj (2008). "Hydrological responses of a watershed to historical land use evolution and future land use scenarios under climate change conditions". In: *Hydrology and Earth System Sciences* 12.1, pp. 101–110. DOI: 10.5194/hess-12-101-2008. URL: https://www.hydrol-earth-syst-sci.net/12/101/2008/.

Rabbel, I., B. Diekkrüger, H. Voigt, and B. Neuwirth (2016). "Comparing ΔT(max) determination approaches for Granier-based sapflow estimations". In: *Sensors (Basel, Switzerland)* 16.12, p. 2042. URL: https://www.ncbi.nlm.nih.gov/pubmed/27916949.

Rabbel, I., H. Bogena, B. Neuwirth, and B. Diekkrüger (2018). "Using sap flow data to parameterize the Feddes water stress model for Norway spruce". In: *Water* 10.3, p. 279. DOI: 10.3390/w10030279. URL: https://www.mdpi.com/2073-4441/10/3/279.

Rahman, A. S. M. M. (2015). "Influence of subsurfac hydrodynamics on the lower atmoshpere at the catchment scale". Thesis. University of Bonn, Germany. URL: http://hss.ulb.uni-bonn.de/2015/4209/4209.pdf.

Rahman, M., M. Sulis, and S. J. Kollet (2014). "The concept of dual-boundary forcing in land surface-subsurface interactions of the terrestrial hydrologic and energy cycles". In: *Water Resources Research* 50.11, pp. 8531–8548. DOI: 10.1002/2014wr015738. URL: http://dx.doi.org/10.1002/2014WR015738.

Rannik, Ü., N. Altimir, J. Raittila, T. Suni, A. Gaman, T. Hussein, T. Hölttä, H. Lassila, M. Latokartano, A. Lauri, A. Natsheh, T. Petäjä, R. Sorjamaa, H. Ylä-Mella, P. Keronen, F. Berninger, T. Vesala, P. Hari, and M. Kulmala (2002). "Fluxes of carbon dioxide and water vapour over Scots pine forest and clearing". In: *Agricultural and Forest Meteorology* 111.3, pp. 187–202. DOI: https://doi.org/10.1016/S0168-1923(02)00022-9. URL: http://www.sciencedirect.com/science/article/pii/S0168192302000229.

Ranzi, R., M. Bochicchio, and B. Bacchi (2002). "Effects on floods of recent afforestation and urbanisation in the Mella River (Italian Alps)". In: *Hydrology and Earth System Sciences* 6.2, pp. 239–254. DOI: 10.5194/hess-6-239-2002. URL: https://www.hydrol-earth-syst-sci.net/6/239/2002/.

Rebmann, C., N. Arriga, M. Aurela, L. Hörtnagl, A. Ibrom, L. Merbold, S. Metzger, M., Pavelka, M. Roland, H. P. Schmid, and J. P. Tuovinen (2018).

"ICOS ecosystem protocol for flux station site setup including complementary measurements". In: *International agrophysics* 32.4, pp. 471–494. DOI: 10.1515/intag-2017-0044. URL: https://publikationen.bibliothek.kit.edu/1000088745.

Renner, M., K. Brust, K. Schwärzel, M. Volk, and C. Bernhofer (2014). "Separating the effects of changes in land cover and climate: a hydro-meteorological analysis of the past 60 yr in Saxony, Germany". In: *Hydrology and Earth System Sciences* 18.1, pp. 389–405. DOI: 10.5194/hess-18-389-2014. URL: http://www.hydrol-earth-syst-sci.net/18/389/2014/.

Richter, D. (1995). *Ergebnisse methodischer Untersuchungen zur Korrektur des systematischen Meßfehlers des Hellmann-Niederschlagsmessers*. German. Berichte des Deutschen Wetterdienstes. Offenbach am Main: Selbstverl. des Dt. Wetterdienstes. URL: https://katalog.ub.uni-leipzig.de/Record/0-272612669.

Richter, F. (2008). "Bodenkarte zur Standorterkundung. Verfahren Quellgebiet Wüstebachtal (Forst)." In: *Geological Survey North Rhine-Westphalia, Krefeld, Germany*.

Richter, K.-G. and G. A. Schultz (1987). "Modelling the influence of land use change on flood flows". In: *Water for the Future: Hydrology in Perspective*. Vol. 164. IAHS Publ., pp. 381–391. URL: http://hydrologie.org/redbooks/a164/iahs_164_0381.pdf.

Robinson, D., H. Abdu, I. Lebron, and S. Jones (2012). "Imaging of hill-slope soil moisture wetting patterns in a semi-arid oak savanna catchment using time-lapse electromagnetic induction". In: *Journal of Hydrology* 416–417, pp. 39–49. DOI: 10.1016/j.jhydrol.2011.11.034. URL: https://www.sciencedirect.com/science/article/pii/S0022169411008195?via%3Dihub.

Rodriguez-Iturbe, I. (2000). "Ecohydrology: a hydrologic perspective of climate-soil-vegetation dynamics". In: *Water Resources Research* 36.1, pp. 3–9. DOI: 10.1029/1999WR900210. URL: https://doi.org/10.1029/1999WR900210.

Rogger, M., M. Agnoletti, A. Alaoui, J. C. Bathurst, G. Bodner, M. Borga, V. Chaplot, F. Gallart, G. Glatzel, J. Hall, J. Holden, L. Holko, R. Horn, A. Kiss, S. Kohnová, G. Leitinger, B. Lennartz, J. Parajka, R. Perdigão, S. Peth, L. Plavcová, J. N. Quinton, M. Robinson, J. L. Salinas, A. Santoro, J. Szolgay, S. Tron, J. J. H. van den Akker, A. Viglione, and G. Blöschl (2017). "Land-use change impacts on floods at the catchment scale – challenges and opportunities for future research". In: *Water Resources Research* 53.7,

pp. 1–11. DOI: 10.1002/2017wr020723. URL: http://dx.doi.org/10.1002/2017WR020723.

Roosmalen, L. van, T. O. Sonnenborg, and K. H. Jensen (2009). "Impact of climate and land use change on the hydrology of a large-scale agricultural catchment". In: *Water Resources Research* 45.7, pp. 1–18. DOI: 10.1029/2007wr006760. URL: http://dx.doi.org/10.1029/2007WR006760.

Rosenbaum, U., J. A. Huisman, A. Weuthen, H. Vereecken, and H. R. Bogena (2010). "Sensor-to-sensor variability of the ECH2O EC-5, TE, and 5TE sensors in dielectric liquids". In: *Vadose Zone Journal* 9.1, pp. 181–186. DOI: 10.2136/vzj2009.0036. URL: https://www.soils.org/publications/vzj/abstracts/9/1/181.

Rosenbaum, U., H. R. Bogena, M. Herbst, J. A. Huisman, T. J. Peterson, A. Weuthen, A. W. Western, and H. Vereecken (2012). "Seasonal and event dynamics of spatial soil moisture patterns at the small catchment scale". In: *Water Resources Research* 48.10, W10544. DOI: 10.1029/2011wr011518. URL: http://dx.doi.org/10.1029/2011WR011518.

Ruddell, B. L., D. T. Drewry, and G. S. Nearing (2019). "Information theory for model diagnostics: structural error is indicated by trade-off between functional and predictive performance". In: *Water Resources Research* 55, pp. 1–21. DOI: 10.1029/2018WR023692. URL: https://agupubs.onlinelibrary.wiley.com/doi/abs/10.1029/2018WR023692.

Sahin, V. and M. J. Hall (1996). "The effects of afforestation and deforestation on water yields". In: *Journal of Hydrology* 178.1, pp. 293–309. DOI: http://dx.doi.org/10.1016/0022-1694(95)02825-0. URL: http://www.sciencedirect.com/science/article/pii/0022169495028250.

Salemi, L. F., J. D. Groppo, R. Trevisan, J. Marcos de Moraes, W. de Paula Lima, and L. A. Martinelli (2012). "Riparian vegetation and water yield: a synthesis". In: *Journal of Hydrology* 454–455, pp. 195–202. DOI: http://dx.doi.org/10.1016/j.jhydrol.2012.05.061. URL: http://www.sciencedirect.com/science/article/pii/S0022169412004647.

Savenije, H. H. G. and M. Hrachowitz (2017). "HESS Opinions "Catchments as meta-organisms – a new blueprint for hydrological modelling"". In: *Hydrology and Earth System Sciences* 21.2, pp. 1107–1116. DOI: 10.5194/hess-21-1107-2017. URL: http://www.hydrol-earth-syst-sci.net/21/1107/2017/.

Schaefli, B., C. J. Harman, M. Sivapalan, and S. J. Schymanski (2011). "HESS Opinions: Hydrologic predictions in a changing environment: behavioral modeling". In: *Hydrology and Earth System Sciences* 15.2, pp. 635–646. DOI:

10.5194/hess-15-635-2011. URL: http://infoscience.epfl.ch/record/165030.

Schaik, N. L. M. B. van (2009). "Spatial variability of infiltration patterns related to site characteristics in a semi-arid watershed". In: *Catena* 78.1, pp. 36–47. DOI: http://dx.doi.org/10.1016/j.catena.2009.02.017. URL: http://www.sciencedirect.com/science/article/pii/S0341816209000381.

— (2010). "The role of macropore flow from plot to catchment scale : a study in a semi-arid area". PhDThesis. Utrecht: University of Utrecht, p. 174. URL: https://www.hydrology.nl/images/docs/dutch/2010.01.08_Loes_van_Schaik.pdf.

Schilling, K. E., P. W. Gassman, C. L. Kling, T. Campbell, M. K. Jha, C. F. Wolter, and J. G. Arnold (2014). "The potential for agricultural land use change to reduce flood risk in a large watershed". In: *Hydrological Processes* 28.8, pp. 3314–3325. DOI: 10.1002/hyp.9865. URL: https://doi.org/10.1002/hyp.9865.

Schmid, H. P. (1997). "Experimental design for flux measurements: matching scales of observations and fluxes". In: *Agricultural and Forest Meteorology* 87.2, pp. 179–200. DOI: http://dx.doi.org/10.1016/S0168-1923(97)00011-7. URL: http://www.sciencedirect.com/science/article/pii/S0168192397000117.

Schnorbus, Markus and Younes Alila (2004). "Forest harvesting impacts on the peak flow regime in the Columbia mountains of southeastern British Columbia: an investigation using long-term numerical modeling". In: *Water Resources Research* 40.5. DOI: 10.1029/2003WR002918. URL: https://doi.org/10.1029/2003WR002918.

Schume, H., G. Jost, and H. Hager (2004). "Soil water depletion and recharge patterns in mixed and pure forest stands of European beech and Norway spruce". In: *Journal of Hydrology* 289.1, pp. 258–274. DOI: https://doi.org/10.1016/j.jhydrol.2003.11.036. URL: http://www.sciencedirect.com/science/article/pii/S0022169403004797.

Scott, D. F. and W. Lesch (1996). "The effects of riparian clearing and clearfelling of an indigenous forest on streamflow, stormflow and water quality". In: *South African Forestry Journal* 175.1, pp. 1–14. URL: http://dx.doi.org/10.1080/00382167.1996.9629886.

Sebestyen, S. D. and E. S. Verry (2011). "Effects of watershed experiments on water chemistry at the Marcell Experimental Forest". In: *Peatland biogeochemistry and watershed hydrology*. Ed. by K. Randall, S. D. Sebestyen, E. S.

Verry, and K. Brooks. Taylor and Francis Group, LLC, pp. 433–458. URL: https://www.fs.usda.gov/treesearch/pubs/37984.

Semenova, O. and K. Beven (2015). "Barriers to progress in distributed hydrological modelling". In: *Hydrological Processes* 29.8, pp. 2074–2078. DOI: 10.1002/hyp.10434. URL: http://dx.doi.org/10.1002/hyp.10434.

Senatore, A., G. Mendicino, D. J. Gochis, W. Yu, D. N. Yates, and H. Kunstmann (2015). "Fully coupled atmosphere-hydrology simulations for the central Mediterranean: impact of enhanced hydrological parameterization for short and long time scales". In: *Journal of Advances in Modeling Earth Systems* 7.4, pp. 1693–1715. DOI: 10.1002/2015MS000510. URL: https://doi.org/10.1002/2015MS000510.

Seneviratne, S. I., T. Corti, E. L. Davin, M. Hirschi, E. B. Jaeger, I. Lehner, B. Orlowsky, and A. J. Teuling (2010). "Investigating soil moisture–climate interactions in a changing climate: a review". In: *Earth-Science Reviews* 99.3–4, pp. 125–161. DOI: http://dx.doi.org/10.1016/j.earscirev.2010.02.004. URL: http://www.sciencedirect.com/science/article/pii/S0012825210000139.

Shen, C. (2018). "A transdisciplinary review of deep learning research and its relevance for water resources scientists". In: *Water Resources Research* 54.11, pp. 8558–8593. DOI: 10.1029/2018WR022643. URL: https://agupubs.onlinelibrary.wiley.com/doi/abs/10.1029/2018WR022643.

Shrestha, P., M. Sulis, M. Masbou, S. Kollet, and C. Simmer (2014). "A scale-consistent terrestrial systems modeling platform based on COSMO, CLM, and ParFlow". In: *Monthly Weather Review* 142.9, pp. 3466–3483. DOI: 10.1175/mwr-d-14-00029.1. URL: http://journals.ametsoc.org/doi/abs/10.1175/MWR-D-14-00029.1.

Shrestha, P., M. Sulis, C. Simmer, and S. Kollet (2015). "Impacts of grid resolution on surface energy fluxes simulated with an integrated surface-groundwater flow model". In: *Hydrology and Earth System Sciences* 19.10, pp. 4317–4326. DOI: 10.5194/hess-19-4317-2015. URL: https://www.hydrol-earth-syst-sci.net/19/4317/2015/.

— (2018). "Effects of horizontal grid resolution on evapotranspiration partitioning using TerrSysMP". In: *Journal of Hydrology* 557, pp. 910–915. DOI: 10.1016/j.jhydrol.2018.01.024. URL: https://www.sciencedirect.com/science/article/pii/S0022169418300246.

Siriwardena, L., B. L. Finlayson, and T. A. McMahon (2006). "The impact of land use change on catchment hydrology in large catchments: the Comet River, Central Queensland, Australia". In: *Journal of Hydrology* 326.1–4,

pp. 199–214. DOI: https://doi.org/10.1016/j.jhydrol.2005.10.030. URL: http://www.sciencedirect.com/science/article/pii/S0022169405005639.

Sivakumar, B. (2017). "Characteristics of hydrologic systems". In: *Chaos in Hydrology: Bridging Determinism and Stochasticity*. Dordrecht: Springer NL, pp. 29–62. ISBN: 978-90-481-2552-4. DOI: 10.1007/978-90-481-2552-4_2. URL: https://doi.org/10.1007/978-90-481-2552-4_2.

Sivapalan, M. (2003). "Process complexity at hillslope scale, process simplicity at the watershed scale: is there a connection?" In: *Hydrological Processes* 17.5, pp. 1037–1041. DOI: 10.1002/hyp.5109. URL: http://dx.doi.org/10.1002/hyp.5109.

Sivapalan, Murugesu, Hubert H. G. Savenije, and Günter Blöschl (2012). "Socio-hydrology: A new science of people and water". In: *Hydrological Processes* 26.8, pp. 1270–1276. ISSN: 0885-6087. DOI: 10.1002/hyp.8426. URL: https://doi.org/10.1002/hyp.8426.

Skøien, J. O., G. Blöschl, and A. W. Western (2003). "Characteristic space scales and timescales in hydrology". In: *Water Resources Research* 39.10. DOI: http://dx.doi.org/10.1029/2002WR001736. URL: https://agupubs.onlinelibrary.wiley.com/doi/full/10.1029/2002WR001736.

Smith, D. M. and S. J. Allen (1996). "Measurement of sap flow in plant stems". In: *Journal of Experimental Botany* 47.12, pp. 1833–1844. DOI: 10.1093/jxb/47.12.1833. URL: http://dx.doi.org/10.1093/jxb/47.12.1833.

Smith, E. P. (2002). "BACI design [Volume 1] ". In: *Encyclopedia of Environmetrics*. Ed. by A. H. El-Shaarawi and W. W. Piegorsch. John Wiley and Sons, pp. 141–148.

Snedecor, G. W. and W. G. Cochran (1989). *Statistical methods*. 8th edition. AmeIowa State University Press. ISBN: 0813815614. URL: https://trove.nla.gov.au/work/10694367?q&sort=holdings+desc&_=1567098398156&versionId=28403945.

Srivastava, P. K. (2017). "Satellite soil moisture: review of theory and applications in water resources". In: *Water Resources Management* 31.10, pp. 1–16. DOI: 10.1007/s11269-017-1722-6. URL: https://link.springer.com/article/10.1007/s11269-017-1722-6.

Stednick, J. D. (1996). "Monitoring the effects of timber harvest on annual water yield". In: *Journal of Hydrology* 176.1, pp. 79–95. DOI: http://dx.doi.org/10.1016/0022-1694(95)02780-7. URL: http://www.sciencedirect.com/science/article/pii/0022169495027807.

Steppeler, J., G. Doms, U. Schttler, H. W. Bitzer, A. Gassmann, U. Damrath, and G. Gregoric (2003). "Meso-gamma scale forecasts using the nonhydrostatic model LM". In: *Meteorology and Atmospheric Physics* 82.1-4, pp. 75–96. DOI: 10.1007/s00703-001-0592-9. URL: https://link.springer.com/article/10.1007/s00703-001-0592-9.

Sterling, S. M., A. Ducharne, and J. Polcher (2012). "The impact of global land-cover change on the terrestrial water cycle". In: *Nature Climate Change* 3, p. 385. DOI: 10.1038/nclimate1690. URL: http://dx.doi.org/10.1038/nclimate1690.

Stockinger, M. P., H. R. Bogena, A. Luecke, B. Diekkrueger, M. Weiler, and H. Ver-eecken (2014). "Seasonal soil moisture patterns: controlling transit time distributions in a forested headwater catchment". In: *Water Resources Research* 50.6, pp. 5270–5289. ISSN: 0043-1397. DOI: 10.1002/2013wr014815. URL: <GotoISI>://WOS:000340430400041.

Stockinger, M. P., A. Lücke, J. J. McDonnell, B. Diekkrüger, H. Vereecken, and H. R. Bogena (2015). "Interception effects on stable isotope driven streamwater transit time estimates". In: *Geophysical Research Letters* 42.13, pp. 5299–5308. DOI: 10.1002/2015GL064622. URL: https://doi.org/10.1002/2015GL064622.

Stockinger, M. P., H. R. Bogena, A. Lücke, B. Diekkrüger, T. Cornelissen, and H. Vereecken (2016). "Tracer sampling frequency influences estimates of young water fraction and streamwater transit time distribution". In: *Journal of Hydrology* 541, pp. 952–964. DOI: 10.1016/j.jhydrol.2016.08.007. URL: http://www.sciencedirect.com/science/article/pii/S0022169416304863.

Stockinger, M. P., H. R. Bogena, A. Lücke, C. Stumpp, and H. Vereecken (2019). "Time variability and uncertainty in the fraction of young water in a small headwater catchment". In: *Hydrology and Earth System Sciences* 23.10, pp. 4333–4347. DOI: 10.5194/hess-23-4333-2019. URL: https://www.hydrol-earth-syst-sci.net/23/4333/2019/.

Stoy, P. C., G. G. Katul, M. Siqueira, J.-Y. Juang, K. A. Novick, H. R. McCarthy, C.. A. Oishi, J. M. Uebelherr, H.-S. Kim, and R. Oren (2006). "Separating the effects of climate and vegetation on evapotranspiration along a successional chronosequence in the southeastern US". In: *Global Change Biology* 12.11, pp. 2115–2135. DOI: 10.1111/j.1365-2486.2006.01244.x. URL: https://onlinelibrary.wiley.com/doi/abs/10.1111/j.1365-2486.2006.01244.x.

Sulis, M., J. L. Williams, P. Shrestha, M. Diederich, C. Simmer, S. J. Kollet, and R. M. Maxwell (2017). "Coupling groundwater, vegetation, and atmospheric processes: a comparison of two integrated models". In: *Journal of Hydrometeorology* 18.5, pp. 1489–1511. DOI: 10.1175/jhm-d-16-0159.1. URL: https://journals.ametsoc.org/doi/abs/10.1175/JHM-D-16-0159.1.

Sulis, M., J. Keune, P. Shrestha, C. Simmer, and S. J. Kollet (2018). "Quantifying the impact of subsurface-land surface physical processes on the predictive skill of subseasonal mesoscale atmospheric simulations". In: *Journal of Geophysical Research: Atmospheres* 123.17, pp. 9131–9151. DOI: 10.1029/2017JD028187. URL: https://doi.org/10.1029/2017JD028187.

Sun, G., H. Riekerk, and N. B. Comerford (1998). "Modeling the hydrologic impacts of forest harvesting on Florida Flatwoods". In: *Journal of the American Water Resources Association* 34.4, pp. 843–854. DOI: 10.1111/j.1752-1688.1998.tb01520.x. URL: https://doi.org/10.1111/j.1752-1688.1998.tb01520.x.

Sun, G., A. Noormets, J. Chen, and S. G. McNulty (2008). "Evapotranspiration estimates from eddy covariance towers and hydrologic modeling in managed forests in Northern Wisconsin, USA". In: *Agricultural and Forest Meteorology* 148, pp. 257–267. URL: https://www.fs.usda.gov/treesearch/pubs/29056.

Sun, G., P. V. Caldwell, and S. G. McNulty (2015). "Modelling the potential role of forest thinning in maintaining water supplies under a changing climate across the conterminous United States". In: *Hydrological Processes* 29.24, pp. 5016–5030. DOI: 10.1002/hyp.10469. URL: http://dx.doi.org/10.1002/hyp.10469.

Susha Lekshmi, S. U., D. N. Singh, and M. Shojaei Baghini (2014). "A critical review of soil moisture measurement". In: *Measurement* 54, pp. 92–105. DOI: https://doi.org/10.1016/j.measurement.2014.04.007. URL: http://www.sciencedirect.com/science/article/pii/S0263224114001651.

Swank, W. T., C. E. Johson, B. Moldan, and J. Cerny (1994). "Small catchment research in the evaluation and development of forest management practices". In: *Biogeochemistry of small catchments: a tool for environmental research*. Ed. by B. Moldan and J. Cerny. John Wiley and Sons Ltd, pp. 383–408.

Swank, W. T., J. M. Vose, and K. J. Elliott (2001). "Long-term hydrologic and water quality responses following commercial clearcutting of mixed

hardwoods on a southern Appalachian catchment". In: *Forest Ecology and Management* 143.1, pp. 163–178. DOI: https://doi.org/10.1016/S0378-1127(00)00515-6. URL: https://www.sciencedirect.com/science/article/pii/S0378112700005156.

Swift, L. W. and W. T. Swank (1981). "Long term responses of streamflow following clearcutting and regrowth / Réactions à long terme du débit des cours d'eau après coupe et repeuplement". In: *Hydrological Sciences Bulletin* 26.3, pp. 245–256. DOI: 10.1080/02626668109490884. URL: http://dx.doi.org/10.1080/02626668109490884.

Tague, C. and L. Band (2001). "Simulating the impact of road construction and forest harvesting on hydrologic response". In: *Earth Surface Processes and Landforms* 26.2, pp. 135–151. DOI: 10.1002/1096-9837(200102)26:2<135::AID-ESP167>3.0.CO;2-J. URL: https://doi.org/10.1002/1096-9837(200102)26:2<135::AID-ESP167>3.0.CO.

Tanty, Rakesh and Tanweer S. Desmukh (2015). "Application of artificial neural network in hydrology- a review". In: *International Journal of Engineering Research & Technology* 4.6, pp. 184–188. DOI: http://dx.doi.org/10.17577/IJERTV4IS060247. URL: https://www.ijert.org/application-of-artificial-neural-network-in-hydrology-a-review.

Tetzlaff, D., I. A. Malcolm, and C. Soulsby (2007). "Influence of forestry, environmental change and climatic variability on the hydrology, hydrochemistry and residence times of upland catchments". In: *Journal of Hydrology* 346.3–4, pp. 93–111. DOI: http://dx.doi.org/10.1016/j.jhydrol.2007.08.016. URL: http://www.sciencedirect.com/science/article/pii/S0022169407004647.

Teuling, A. J. (2007). "Soil moisture dynamics and land surface-atmosphere interaction". Thesis. University of Wageningen. URL: http://edepot.wur.nl/24257.

Teuling, A. J. and P. A. Troch (2005). "Improved understanding of soil moisture variability dynamics". In: *Geophysical Research Letters* 32.5. DOI: 10.1029/2004gl021935. URL: http://dx.doi.org/10.1029/2004GL021935.

Teuling, A. J., S. I. Seneviratne, C. Williams, and P. A. Troch (2006). "Observed timesca-les of evapotranspiration response to soil moisture". In: *Geophysical Research Letters* 33.23. DOI: 10.1029/2006gl028178. URL: http://dx.doi.org/10.1029/2006GL028178.

Teuling, A. J., M. Hirschi, A. Ohmura, M. Wild, M. Reichstein, P. Ciais, N. Buchmann, C. Ammann, L. Montagnani, A. D. Richardson, G. Wohlfahrt,

and S. I. Seneviratne (2009). "A regional perspective on trends in continental evaporation". In: *Geophysical Research Letters* 36.2. DOI: 10.1029/2008GL036584. URL: https://doi.org/10.1029/2008GL036584.

Teuling, A. J., S. I. Seneviratne, R. Stockli, M. Reichstein, E. Moors, P. Ciais, S. Luyssaert, B. van den Hurk, C. Ammann, C. Bernhofer, E. Dellwik, D. Gianelle, B. Gielen, T. Grunwald, K. Klumpp, L. Montagnani, C. Moureaux, M. Sottocornola, and G. Wohlfahrt (2010). "Contrasting response of European forest and grassland energy exchange to heatwaves". In: *Nature Geosci* 3.10, pp. 722–727. DOI: 10.1038/NGEO950. URL: https://www.nature.com/articles/ngeo950.

Teuling, A. J., A. F. Van Loon, S. I. Seneviratne, I. Lehner, M. Aubinet, B. Heinesch, C. Bernhofer, T. Grünwald, H. Prasse, and U. Spank (2013). "Evapotranspiration amplifies European summer drought". In: *Geophysical Research Letters* 40.10, pp. 2071–2075. DOI: 10.1002/grl.50495. URL: https://doi.org/10.1002/grl.50495.

The Nature Conservancy (2009). *Global ecoregions, major habitat types, biogeographical realms and The Nature Conservancy terrestrial assessment units as of december 14, 2009*. Online. URL: http://maps.tnc.org/files/metadata/TerrEcos.xml.

Thomas, F. M., A. Rzepecki, A. Lücke, I. Wiekenkamp, I. Rabbel, T. Pütz, and B. Neuwirth (2018). "Growth and wood isotopic signature of Norway spruce (Picea abies) along a small-scale gradient of soil moisture". In: *Tree Physiology* 38.12, pp. 1855–1870. DOI: 10.1093/treephys/tpy100. URL: http://dx.doi.org/10.1093/treephys/tpy100.

Thomas, R. B. and W. F. Megahan (1998). "Peak flow responses to clear-cutting and roads in small and large basins, Western Cascades, Oregon: a second opinion". In: *Water Resources Research* 34.12, pp. 3393–3403. DOI: 10.1029/98wr02500. URL: http://dx.doi.org/10.1029/98WR02500.

— (2001). "Reply to "Comment on 'Peak flow responses to clear-cutting and roads in small and large basins, Western Cascades, Oregon: A Second Opinion' by R. B. Thomas and W. F. Megahan"". In: *Water Resources Research* 37.1, pp. 181–183. DOI: 10.1029/2000WR900277. URL: http://dx.doi.org/10.1029/2000WR900277.

Thompson, S. E., C. J. Harman, P. Heine, and G. G. Katul (2010). "Vegetation - infiltration relationships across climatic and soil type gradients". In: *Journal of Geophysical Research: Biogeosciences* 115.G2. DOI: 10.1029/2009JG001134. URL: https://doi.org/10.1029/2009JG001134.

Todini, E. (2007). "Hydrological catchment modelling: past, present and future". In: *Hydrology and Earth System Sciences* 11.1, pp. 468–482. DOI: 10.5194/hess-11-468-2007. URL: https://www.hydrol-earth-syst-sci.net/11/468/2007/.

Trenberth, K. E., P. D. Jones, P. Ambenje, R. Bojariu, D. Easterling, A. Klein Tank, D. Parker, F. Rahimzadeh, J. A. Renwick, M. Rusticucci, B. Soden, and P. Zhai (2007). "IPCC fourth assessment report: climate change 2007. working group I: the physical science basis." In: Cambridge: Cambridge University Press. Chap. Observations: surface and atmospheric climate change observations: surface and atmospheric climate change observations: surface and atmospheric climate change observations: surface and atmospheric climate change, pp. 235–336. URL: https://www.ipcc.ch/report/ar4/wg1/.

Troendle, C. A. and R. M. King (1985). "The effect of timber harvest on the fool creek watershed, 30 years later". In: *Water Resources Research* 21.12, pp. 1915–1922. DOI: 10.1029/WR021i012p01915. URL: http://dx.doi.org/10.1029/WR021i012p01915.

Valcke, S. (2013). "The OASIS3 coupler: a European climate modelling community software". In: *Geoscientific Model Development* 6.2, pp. 373–388. DOI: 10.5194/gmd-6-373-2013. URL: https://www.geosci-model-dev.net/6/373/2013/.

Valler, V and A. Graf (2015). "Kammermessungen zu CO2-Fluss und Verdunstung auf der entfichteten Fläche, Presentation on the annual meeting on research in the National Park Eifel, Monschau-Hoefen, Germany, 2015-01-15". Presentation. (Chamber measurements on CO2 flux and evapotranspiration on the deforested area, in German language).

Van Dijk, A., A. F. Moene, and H. A. R. De Bruin (2004). "The principles of surface flux physics: theory, practice and description of the ECPACK library". In: *Wageningen : Meteorology and Air Quality (MAQ) (Internal Report 2004/1)* . P. 96.

Van Haveren, B. P. (1988). "A reevaluation of the Wagon Wheel Gap forest watershed experiment". In: *Forest Science* 34.1, pp. 208–214. DOI: 10.1093/forestscience/34.1.208. URL: http://dx.doi.org/10.1093/forestscience/34.1.208.

Van Loon, A. F. (2015). "Hydrological drought explained". In: *Wiley Interdisciplinary Reviews: Water* 2.4, pp. 359–392. DOI: 10.1002/wat2.1085. URL: http://dx.doi.org/10.1002/wat2.1085.

VanShaar, J. R., I. Haddeland, and D. P. Lettenmaier (2002). "Effects of land-cover changes on the hydrological response of interior Columbia River basin forested catchments". In: *Hydrological Processes* 16.13, pp. 2499–2520. DOI: 10.1002/hyp.1017. URL: http://dx.doi.org/10.1002/hyp.1017.

Velde, Y. van der, N. Vercauteren, F. Jaramillo, S. C. Dekker, G. Destouni, and S. W. Lyon (2014). "Exploring hydroclimatic change disparity via the Budyko framework". In: *Hydrological Processes* 28.13, pp. 4110–4118. DOI: 10.1002/hyp.9949. URL: http://dx.doi.org/10.1002/hyp.9949.

Vellinga, O. S., B. Gioli, J. A. Elbers, A. A. M. Holtslag, P. Kabat, and R. W. A. Hutjes (2010). "Regional carbon dioxide and energy fluxes from airborne observations using flight-path segmentation based on landscape characteristics". In: *Biogeosciences* 7.4, pp. 1307–1321. DOI: 10.5194/bg-7-1307-2010. URL: https://www.biogeosciences.net/7/1307/2010/.

Vereecken, H., T. Kamai, T. Harter, R. Kasteel, J. Hopmans, and J. Vanderborght (2007). "Explaining soil moisture variability as a function of mean soil moisture: a stochastic unsaturated flow perspective". In: *Geophysical Research Letters* 34.22. DOI: 10.1029/2007gl031813. URL: http://dx.doi.org/10.1029/2007GL031813.

Vereecken, H., J. A. Huisman, H. Bogena, J. Vanderborght, J. A. Vrugt, and J. W. Hopmans (2008). "On the value of soil moisture measurements in vadose zone hydrology: a review". In: *Water Resources Research* 44.4, W00D06. DOI: 10.1029/2008wr006829. URL: http://dx.doi.org/10.1029/2008WR006829.

Vereecken, H., S. Kollet, and C. Simmer (2010). "Patterns in soil – vegetation – atmosphere systems: monitoring, modeling, and data assimilation". In: *Vadose Zone Journal* 9.4, pp. 821–827. DOI: 10.2136/vzj2010.0122. URL: https://doi.org/10.2136/vzj2010.0122.

Vereecken, H., J. A. Huisman, H. J. Hendricks Franssen, N. Brüggemann, H. R. Bogena, S. Kollet, M. Javaux, J. van der Kruk, and J. Vanderborght (2015). "Soil hydrology: recent methodological advances, challenges, and perspectives". In: *Water Resources Research* 51.4, pp. 2616–2633. DOI: 10.1002/2014wr016852. URL: http://dx.doi.org/10.1002/2014WR016852.

Vesala, T., T. Suni, Ü. Rannik, P. Keronen, T. Markkanen, S. Sevanto, T. Grönholm, S. Smolander, M. Kulmala, H. Ilvesniemi, R. Ojansuu, A. Uotila, J. Levula, A. Mäkelä, J. Pumpanen, P. Kolari, L. Kulmala, N. Altimir, F. Berninger, E. Nikinmaa, and P. Hari (2005). "Effect of thinning on surface fluxes in a boreal forest". In: *Global Biogeochemical Cycles* 19.2. DOI: 10.1029/2004GB002316. URL: https://doi.org/10.1029/2004GB002316.

Vincke, C., N. Breda, A. Granier, and F. Devillez (2005a). "Evapotranspiration of a declining Quercus robur (L.) stand from 1999 to 2001. I. Trees and forest floor daily transpiration". In: *Annals of Forest Science* 62.6, pp. 503–512. DOI: 10.1051/forest:2005060. URL: https://doi.org/10.1051/forest:2005055.

Vincke, C., A. Granier, N. Breda, and F. Devillez (2005b). "Evapotranspiration of a declining Quercus robur (L.) stand from 1999 to 2001. II. Daily actual evapotranspiration and soil water reserve". In: *Annals of Forest Science* 62.7, pp. 615–623. DOI: 10.1051/forest:2005060. URL: https://doi.org/10.1051/forest:2005060.

Viney, N. R., H. Bormann, L. Breuer, A. Bronstert, B. F. W. Croke, H. Frede, T. Gräff, L. Hubrechts, J. A. Huisman, A. J. Jakeman, G. W. Kite, J. Lanini, G. Leavesley, D. P. Lettenmaier, G. Lindström, J. Seibert, M. Sivapalan, and P. Willems (2009). "Assessing the impact of land use change on hydrology by ensemble modelling (LUCHEM) II: Ensemble combinations and predictions". In: *Advances in Water Resources* 32.2, pp. 147–158. DOI: http://dx.doi.org/10.1016/j.advwatres.2008.05.006. URL: http://www.sciencedirect.com/science/article/pii/S0309170808000882.

Vivoni, E. R., J. C. Rodríguez, and C. J. Watts (2010). "On the spatiotemporal variability of soil moisture and evapotranspiration in a mountainous basin within the North American monsoon region". In: *Water Resources Research* 46.2, W02509. DOI: 10.1029/2009wr008240. URL: http://dx.doi.org/10.1029/2009WR008240.

Wagener, T., M. Sivapalan, P. A. Troch, B. L. McGlynn, C. J. Harman, H. V. Gupta, P. Kumar, P. S. C. Rao, N. B. Basu, and J. S. Wilson (2010). "The future of hydrology: an evolving science for a changing world". In: *Water Resources Research* 46.5, W05301. DOI: 10.1029/2009wr008906. URL: http://dx.doi.org/10.1029/2009WR008906.

Wahl, N. A., B. Wöllecke, O. Bens, and R. F. Hüttl (2005). "Can forest transformation help reducing floods in forested watersheds? Certain aspects on soil hydraulics and organic matter properties". In: *Physics and Chemistry of the Earth, Parts A/B/C* 30.8–10, pp. 611–621. DOI: http://dx.doi.org/10.1016/j.pce.2005.07.013. URL: http://www.sciencedirect.com/science/article/pii/S1474706505000628.

Waichler, S. R., B. C. Wemple, and M. S. Wigmosta (2005). "Simulation of water balance and forest treatment effects at the H.J. Andrews Experimental Forest". In: *Hydrological Processes* 19.16, pp. 3177–3199. DOI: 10.1002/hyp.5841. URL: https://doi.org/10.1002/hyp.5841.

Wang, C., S. Wang, B. Fu, and L. Zhang (2016). "Advances in hydrological modelling with the Budyko framework: a review". In: *Progress in Physical Geography* 40.3, pp. 409–430. DOI: 10.1177/0309133315620997. URL: https://journals.sagepub.com/doi/abs/10.1177/0309133315620997.

Wang, K. and R. E. Dickinson (2012). "A review of global terrestrial evapotranspiration: observation, modeling, climatology, and climatic variability". In: *Reviews of Geophysics* 50.2. DOI: 10.1029/2011rg000373. URL: http://dx.doi.org/10.1029/2011RG000373.

Wang, L., S. P. Good, and K. K. Caylor (2014). "Global synthesis of vegetation control on evapotranspiration partitioning". In: *Geophysical Research Letters* 41.19, pp. 6753–6757. DOI: 10.1002/2014gl061439. URL: http://dx.doi.org/10.1002/2014GL061439.

Wang, S., M. Pan, Q. Mu, X. Shi, J. Mao, C. Brümmer, R.l S. Jassal, P. Krishnan, J. Li, and T. A. Black (2015a). "Comparing evapotranspiration from eddy covariance measurements, water budgets, remote sensing, and land surface models over Canada". In: *Journal of Hydrometeorology* 16.4, pp. 1540–1560. DOI: 10.1175/jhm-d-14-0189.1. URL: http://journals.ametsoc.org/doi/abs/10.1175/JHM-D-14-0189.1.

Wang, T., T. E. Franz, V. A. Zlotnik, J. You, and M. D. Shulski (2015b). "Investigating soil controls on soil moisture spatial variability: numerical simulations and field observations". In: *Journal of Hydrology* 524, pp. 576–586. DOI: http://dx.doi.org/10.1016/j.jhydrol.2015.03.019. URL: http://www.sciencedirect.com/science/article/pii/S0022169415001900.

Ward, P. J., H. Renssen, J. C. J. H. Aerts, R. T. van Balen, and J. Vandenberghe (2008). "Strong increases in flood frequency and discharge of the river Meuse over the late Holocene: impacts of long-term anthropogenic land use change and climate variability". In: *Hydrology and Earth System Sciences* 12.1, pp. 159–175. DOI: 10.5194/hess-12-159-2008. URL: https://www.hydrol-earth-syst-sci.net/12/159/2008/.

Wattenbach, M., F. Hattermann, R. Weng, F. Wechsung, V. Krysanova, and F. Badeck (2005). "A simplified approach to implement forest eco-hydrological properties in regional hydrological modelling". In: *Ecological Modelling* 187.1, pp. 40–59. DOI: https://doi.org/10.1016/j.ecolmodel.2005.01.026. URL: http://www.sciencedirect.com/science/article/pii/S0304380005000402.

Wattenbach, M., M. Zebisch, F. Hattermann, P. Gottschalk, H. Goemann, P. Kreins, F. Badeck, P. Lasch, F. Suckow, and F. Wechsung (2007). "Hydrological impact assessment of afforestation and change in tree-species composition – a regional case study for the federal state of Brandenburg (Germany)". In: *Journal of Hydrology* 346.1, pp. 1–17. DOI: http://dx.doi.org/10.1016/j.jhydrol.2007.08.005. URL: http://www.sciencedirect.com/science/article/pii/S002216940700443X.

Webster, J. R., S. W. Golladay, E. F. Benfield, J. L. Meyer, W. T. Swank, and J. B. Wallace (1992). "Catchment disturbance and stream response: an overview of stream research at Coweeta Hydrologic Laboratory". In: *River conservation and management* 15, pp. 232–253.

Wei, L., J. Dong, M. Gao, and X. Chen (2017). "Factors controlling temporal stability of surface soil moisture: a watershed-scale modeling study". In: *Vadose Zone Journal* 16. DOI: 10.2136/vzj2016.12.0132. URL: https://dl.sciencesocieties.org/publications/vzj/abstracts/16/10/vzj2016.12.0132.

Weigand, S., R. Bol, B. Reichert, A. Graf, I. Wiekenkamp, M. Stockinger, A. Luecke, W. Tappe, H. Bogena, T. Puetz, W. Amelung, and H. Vereecken (2017). "Spatiotemporal analysis of Dissolved Organic Carbon and Nitrate in waters of a forested catchment using wavelet analysis". In: *Vadose Zone Journal* 16.3. DOI: 10.2136/vzj2016.09.0077.

Weiler, M. (2017). "Macropores and preferential flow–a love-hate relationship". In: *Hydrological Processes* 31.1, pp. 15–19. DOI: 10.1002/hyp.11074. URL: https://doi.org/10.1002/hyp.11074.

Weill, S., A. Mazzia, M. Putti, and C. Paniconi (2011). "Coupling water flow and solute transport into a physically-based surface–subsurface hydrological model". In: *Advances in Water Resources* 34.1, pp. 128–136. DOI: https://doi.org/10.1016/j.advwatres.2010.10.001. URL: http://www.sciencedirect.com/science/article/pii/S030917081000182X.

Wessel, N., N. Marwan, J. F. Krämer, and J. Kurths (2013). "TOCSY - Toolboxes for modelling of dynamical systems and time series". In: *Biomedizinische Technik. Biomedical engineering*. DOI: 10.1515/bmt-2013-4180.

Western, A. (1998). "The Tarrawarra data set: soil moisture patterns, soil characteristics, and hydrological flux measurements". In: *Water Resources Research* 34.10, pp. 2765–2768. DOI: 10.1029/98WR01833. URL: https://doi.org/10.1029/98WR01833.

Western, A. W., S.-L. Zhou, R. B. Grayson, T. A. McMahon, G. Blöschl, and D. J. Wilson (2004). "Spatial correlation of soil moisture in small catchments and its relationship to dominant spatial hydrological processes". In: *Journal of Hydrology* 286.1–4, pp. 113–134. DOI: http://dx.doi.org/10.1016/j.jhydrol.2003.09.014. URL: http://www.sciencedirect.com/science/article/pii/S0022169403003809.

Wiekenkamp, I., J. A. Huisman, H.R. Bogena, H.S. Lin, and H. Vereecken (2016). "Spatial and Temporal Occurrence of Preferential Flow in a Forested Headwater Catchment". In: *Journal of Hydrology* 534, pp. 139–149. DOI: http://dx.doi.org/10.1016/j.jhydrol.2015.12.050.

Wijesekara, G. N., A. Gupta, C. Valeo, J. G. Hasbani, Y. Qiao, P. Delaney, and D. J. Marceau (2012). "Assessing the impact of future land-use changes on hydrological processes in the Elbow river watershed in southern Alberta, Canada". In: *Journal of Hydrology* 412–413, pp. 220–232. DOI: https://doi.org/10.1016/j.jhydrol.2011.04.018. URL: http://www.sciencedirect.com/science/article/pii/S0022169411002587.

Wiken, E. B. (1986). "Terrestrial ecozones of Canada." Ecological Land Classification Series No. 19. URL: http://sis.agr.gc.ca/cansis/nsdb/ecostrat/hierarchy.html.

Wilk, J., L. Andersson, and V. Plermkamon (2001). "Hydrological impacts of forest conversion to agriculture in a large river basin in northeast Thailand". In: *Hydrological Processes* 15.14, pp. 2729–2748. DOI: 10.1002/hyp.229. URL: http://dx.doi.org/10.1002/hyp.229.

Williams, C. A., M. Reichstein, N. Buchmann, D. Baldocchi, C. Beer, C. Schwalm, G. Wohlfahrt, N. Hasler, C. Bernhofer, T. Foken, D. Papale, S. Schymanski, and K. Schaefer (2012). "Climate and vegetation controls on the surface water balance: synthesis of evapotranspiration measured across a global network of flux towers". In: *Water Resources Research* 48.6, W06523. DOI: 10.1029/2011wr011586. URL: http://dx.doi.org/10.1029/2011WR011586.

Williams, C. A., M. K. Vanderhoof, M. Khomik, and B. Ghimire (2014). "Post-clearcut dynamics of carbon, water and energy exchanges in a midlatitude temperate, deciduous broadleaf forest environment". In: *Global Change Biology* 20.3, pp. 992–1007. DOI: 10.1111/gcb.12388. URL: http://dx.doi.org/10.1111/gcb.12388.

Wilson, K., A. Goldstein, E. Falge, M. Aubinet, D. Baldocchi, P. Berbigier, C. Bernhofer, R. Ceulemans, H. Dolman, and C. Field (2002). "Energy balance closure at FLUXNET sites". In: *Agricultural and Forest Meteorology*

113.1, pp. 223–243. DOI: https://doi.org/10.1016/S0168-1923(02)00109-0. URL: https://www.sciencedirect.com/science/article/pii/S0168192302001090.

Wilson, Kell B., Paul J. Hanson, Patrick J. Mulholland, Dennis D. Baldocchi, and Stan D. Wullschleger (2001). "A comparison of methods for determining forest evapotranspiration and its components: sap-flow, soil water budget, eddy covariance and catchment water balance". In: *Agricultural and Forest Meteorology* 106.2, pp. 153–168. ISSN: 0168-1923. DOI: http://dx.doi.org/10.1016/S0168-1923(00)00199-4. URL: http://www.sciencedirect.com/science/article/pii/S0168192300001994.

Wohlleben, C. (2014). "Auswirkungen anthropogener Eingriffe auf das System Waldboden, gemessen anhand ausgewählter Bodeneigenschaften, im Untersuchungsgebiet Wüstebach". Master Thesis. University of Bonn, Germany.

Wu, B., I. Wiekenkamp, Y. Sun, A. S. Fisher, R. Clough, N. Gottselig, H. Bogena, T. Pütz, N. Brüggemann, H. Vereecken, and R. Bol (2017). "A dataset for three-dimensional distribution of 39 elements including plant nutrients and other metals and metalloids in the soils of a forested headwater catchment". In: *Journal of Environmental Quality* 46.6, pp. 1510–1518. DOI: 10.2134/jeq2017.05.0193. URL: http://dx.doi.org/10.2134/jeq2017.05.0193.

Yang, Yang, Ole Wendroth, and Riley J. Walton (2016). "Temporal dynamics and stability of spatial soil matric potential in two land use systems". In: *Vadose Zone Journal* 15.8. DOI: 10.2136/vzj2015.12.0157. URL: http://dx.doi.org/10.2136/vzj2015.12.0157.

Yu, X., A. Lamačová, C. Duffy, P. Krám, J. Hruška, T. White, and G. Bhatt (2015). "Modelling long-term water yield effects of forest management in a Norway spruce forest". In: *Hydrological Sciences Journal* 60.2, pp. 174–191. DOI: 10.1080/02626667.2014.897406. URL: http://dx.doi.org/10.1080/02626667.2014.897406.

Zacharias, S., H. R. Bogena, L. Samaniego, M. Mauder, R. Fuß, T. Pütz, M. Frenzel, M. Schwank, C. Baessler, K. Butterbach-Bahl, O. Bens, E. Borg, A. Brauer, P. Dietrich, I. Hajnsek, G. Helle, R. Kiese, H. Kunstmann, S. Klotz, J. C. Munch, H. Papen, E. Priesack, H. P. Schmid, R. Steinbrecher, U. Rosenbaum, G. Teutsch, and H. Vereecken (2011). "A network of terrestrial environmental observatories in Germany". In: *Vadose Zone Journal* 10.3, pp. 955–973. DOI: 10.2136/vzj2010.0139. URL: http://vzj.geoscienceworld.org/content/10/3/955.abstract.

Zégre, N. P. (2008). "Local and downstream effects of contemporary forest harvesting on streamflow and sediment yield". PhD thesis. Oregon State University. ISBN: 1109043015. URL: https://ir.library.oregonstate.edu/concern/graduate_thesis_or_dissertations/df65vb33j.

Zhang, H., W. Kurtz, S. Kollet, H. Vereecken, and H.-J. Hendricks Franssen (2018). "Comparison of different assimilation methodologies of groundwater levels to improve predictions of root zone soil moisture with an integrated terrestrial system model". In: *Advances in Water Resources* 111, pp. 224–238. DOI: https://doi.org/10.1016/j.advwatres.2017.11.003. URL: http://www.sciencedirect.com/science/article/pii/S0309170817304888.

Zhang, L., W. R. Dawes, and G. R. Walker (2001). "Response of mean annual evapotranspiration to vegetation changes at catchment scale". In: *Water Resources Research* 37.3, pp. 701–708. DOI: 10.1029/2000wr900325. URL: http://dx.doi.org/10.1029/2000WR900325.

Zhang, W., S. An, Z. Xu, J. Cui, and Q. Xu (2011). "The impact of vegetation and soil on runoff regulation in headwater streams on the east Qinghai–Tibet Plateau, China". In: *CATENA* 87.2, pp. 182–189. DOI: https://doi.org/10.1016/j.catena.2011.05.020. URL: http://www.sciencedirect.com/science/article/pii/S034181621100110X.

Zhang, Y., J. L. Peña-Arancibia, T. R. McVicar, F. H. S. Chiew, J. Vaze, C. Liu, X. Lu, H. Zheng, Y. Wang, Y. Y. Liu, D. G. Miralles, and M. Pan (2016). "Multi-decadal trends in global terrestrial evapotranspiration and its components". In: *Scientific Reports* 6.19124. DOI: 10.1038/srep19124. URL: http://dx.doi.org/10.1038/srep19124.

Zhao, Ying, Tang, Graham, Zhu, Takagi, and Lin (2012). "Hydropedology: Synergistic Integration of Soil Science and Hydrology." In: ed. by H.S. Lin. Academic Press, Elsevier B.V. Chap. Hydropedology in the ridge and valley: soil moisture patterns and preferential flow dynamics in two contrasting landscapes, 381–411.

Zhou, G., X. Wei, X. Chen, P. Zhou, X. Liu, Y. Xiao, G. Sun, D. F. Scott, S. Zhou, L. Han, and Y. Su (2015). "Global pattern for the effect of climate and land cover on water yield". In: *Nature Communications* 6, p. 5918. DOI: 10.1038/ncomms6918. URL: http://dx.doi.org/10.1038/ncomms6918.

Zucco, G., L. Brocca, T. Moramarco, and R. Morbidelli (2014). "Influence of land use on soil moisture spatial–temporal variability and monitoring". In: *Journal of Hydrology* 516, pp. 193–199. DOI: http://dx.doi.org/10.

1016/j.jhydrol.2014.01.043. URL: http://www.sciencedirect.com/science/article/pii/S0022169414000651.

Band / Volume 505
Towards a new real-time irrigation scheduling method: observation, modelling and their integration by data assimilation
D. Li (2020), viii, 94 pp
ISBN: 978-3-95806-492-8

Band / Volume 506
Modellgestützte Analyse kosteneffizienter CO_2-Reduktionsstrategien
P. M. Lopion (2020), XIV, 269 pp
ISBN: 978-3-95806-493-5

Band / Volume 507
Integration of Renewable Energy Sources into the Future European Power System Using a Verified Dispatch Model with High Spatiotemporal Resolution
C. Syranidou (2020), VIII, 242 pp
ISBN: 978-3-95806-494-2

Band / Volume 508
Solar driven water electrolysis based on silicon solar cells and earth-abundant catalysts
K. Welter (2020), iv, 165 pp
ISBN: 978-3-95806-495-9

Band / Volume 509
Electric Field Assisted Sintering of Gadolinium-doped Ceria
T. P. Mishra (2020), x, 195 pp
ISBN: 978-3-95806-496-6

Band / Volume 510
Effect of electric field on the sintering of ceria
C. Cao (2020), xix, 143 pp
ISBN: 978-3-95806-497-3

Band / Volume 511
Techno-ökonomische Bewertung von Verfahren zur Herstellung von Kraftstoffen aus H_2 und CO_2
S. Schemme (2020), 360 pp
ISBN: 978-3-95806-499-7

Band / Volume 512
Enhanced crosshole GPR full-waveform inversion to improve aquifer characterization
Z. Zhou (2020), VIII, 136 pp
ISBN: 978-3-95806-500-0

Band / Volume 513
Time-Resolved Photoluminescence on Perovskite Absorber Materials for Photovoltaic Applications
F. Staub (2020), viii, 198 pp
ISBN: 978-3-95806-503-1

Band / Volume 514
Crystallisation of Oxidic Gasifier Slags
J. P. Schupsky (2020), III, 127, XXII pp
ISBN: 978-3-95806-506-2

Band / Volume 515
Modeling and validation of chemical vapor deposition for tungsten fiber reinforced tungsten
L. Raumann (2020), X, 98, XXXVIII pp
ISBN: 978-3-95806-507-9

Band / Volume 516
Zinc Oxide / Nanocrystalline Silicon Contacts for Silicon Heterojunction Solar Cells
H. Li (2020), VIII, 135 pp
ISBN: 978-3-95806-508-6

Band / Volume 517
Iron isotope fractionation in arable soil and graminaceous crops
Y. Xing (2020), X, 111 pp
ISBN: 978-3-95806-509-3

Band / Volume 518
Geophysics-based soil mapping for improved modelling of spatial variability in crop growth and yield
C. Brogi (2020), xxi, 127 pp
ISBN: 978-3-95806-510-9

Band / Volume 519
Measuring and modelling spatiotemporal changes in hydrological response after partial deforestation
I. Wiekenkamp (2020), xxxvii, 276 pp
ISBN: 978-3-95806-512-3

Energie & Umwelt / Energy & Environment
Band / Volume 519
ISBN 978-3-95806-512-3

Mitglied der Helmholtz-Gemeinschaft

JÜLICH
Forschungszentrum